Universitat de Lleida

Plasma and Cerebrospinal Fluid Lipidomic Signature of Alzheimer's Disease Diagnosis and Progression

Faridé Dakterzada

http://hdl.handle.net/10803/687483

Universitat de Lleida

TESI DOCTORAL

Plasma and Cerebrospinal Fluid Lipidomic Signature of Alzheimer's Disease Diagnosis and Progression

Faridé Dakterzada

Memòria presentada per optar al grau de Doctor per la Universitat de Lleida

Programa de Doctorat en Salut

Directors

Gerard Piñol Ripoll; Reinald Pamplona Gras

Tutor

Gerard Piñol Ripoll

2022

Dr. Gerard Piñol Ripoll, director i tutor, i Dr. Reinald Pamplona Gras, director de la tesi doctoral titulada:

"Plasma and Cerebrospinal Fluid Lipidomic Signature of Alzheimer's Disease Diagnosis and Progression"

Presentada per Faridé Dakterzada Sedaghat, INFORMEN

Que els treballs de recerca d'aquesta tesi han estat finançats a través del projecte PERIS 2019 SLT008/18/00050 de la Generalitat de Catalunya, departament de Salut a Dr. Gerard Piñol Ripoll.

Que el projecte relacionat amb aquest treball de la tesi té l'aprovació del comitè d'ètica del Hospital Arnau de Vilanova (CEIC-1374).

Que la Faridé Dakterzada Sedaghat ha rebut suport econòmic de l'Agència de Gestió d'Ajuts Universitari i de Recerca (AGAUR) i el Fons Social Europeu (FI-B100153) per realitzar aquesta tesi.

Que aquesta tesi ha rebut una beca per a la seva revisió lingüística per part de l'Institut de Llengües de la Universitat de Lleida (convocatòria 2022).

Així mateix considerem que la mateixa reuneix les condicions formals i científiques per tal de poder ser defensada davant el tribunal de tesi corresponent i, si s'escau, obtenir el grau de doctor per la Universitat de Lleida.

Signats pels directors i tutor,

Dr. Gerard Piñol Ripoll
Director i tutor

Dr. Reinald Pamplona Gras
Director

Lleida, juliol de 2022

Agraïment

Estic molt agraïda de totes les persones que m'han ajudat o acompanyat en el camí per realitzar aquesta tesi.

Moltíssimes gràcies, Dr. Gerard Piñol i Dr. Reinal Pamplona, per enriquir els meus coneixements, i ampliar i aprofundir la meva mirada científica. Ha estat una gran experiència estar sota la vostra supervisió i compartir amb vosaltres l'entusiasme i les ganes d'aprendre.

Moltes gràcies, Dr. Piñol, per confiar en mi i donar-me tota la llibertat que pot desitjar una investigadora per ser independent, per donar-me coneixements clínics que de ben segur han estat entre els més útils que he rebut aquests últims anys. Moltes gràcies per la teva paciència i entendre la meva situació familiar.

Moltes gràcies, Dr. Pamplona, per la teva manera de ser: positiu i pacient. Moltes gràcies per compartir els teus coneixements amb mi i ajudar-me a escriure amb "més literatura".

Moltes gràcies, Dra. Alba Naudí. Encara que vam estar juntes durant poc temps, sempre t'he admirat per ser tan valenta i seguir el camí dels teus somnis.

Estic molt agraïda a l'equip del Servei de Lipidòmica per analitzar les dades crues de lipidòmica i identificar les masses i a l'equip del Servei de Biobanc per la gestió de les mostres.

Moltes gràcies, David Argilés, pel cop de mà que em vas donar durant el temps que vaig treballar al laboratori de Fisiopatologia metabòlica.

Moltes gràcies, Dr. Purroy i totes les noies del Neurosciencies clíniques: Leila, Glòria, Coral i Cris. Moltes gràcies per generar conjuntament un ambient de treball agradable en el laboratori.

La meva gratitud a tots els pacients que ens van confiar i proporcionar la seva mostra: sense ells i elles no hauríem pogut dur a terme aquest treball.

Finalment, mil gràcies als amors de la meva vida: Ramon, Ariana i Sam. No hauria pogut acabar la tesi sense el suport i la col·laboració del meu marit, Ramon, que em va estimular a continuar els estudis. Moltes gràcies, Ariana i Sam, per donar-me alegria i energia per tirar endavant.

Moltes gràcies a tots i totes.

Table of contents

ABSTRACT

Abstract

Objectives: To determine plasma and cerebrospinal fluid (CSF) lipids and oxidative protein damage markers associated with the diagnosis of Alzheimer's disease (AD) and mild cognitive impairment (MCI), pathological hallmarks of AD, progression and rate of progression from MCI to AD.

Methods: CSF and plasma lipidome and oxidative protein damage markers were determined by chromatography coupled to mass spectrometry for 290 subjects (104 AD, 92 MCI, and 94 control subjects).

Main results: CSF levels of hexacosanoic acid (C26:0), ceramide (Cer(d38:4)), and phosphatidylethanolamine (PE(40:0)) were associated with pathological levels of Aβ42 in CSF, while sphingomyelin (SM(30:1)) was associated with pathological levels of phosphorylated tau (Ptau). Regarding MCI to AD progression, CSF levels of cholesteryl ester (CE(11D3:1)) and docosahexaenoic acid (DHA) were associated with the risk of progression. Ether triglyceride (TG(O-52:2)) was the lipid that most affected time to progression.
In plasma, oleic acid (OA) was associated with reduced risk of MCI and AD vs control, while vaccenic acid was associated with increased risk. SM(36:0), SM(40:1) and diglyceride (DG(44:3)) were the lipids most associated with pathological levels of Aβ42, while TG(O-60:10) was associated with pathological levels of Ptau. Fatty acid ester of hydroxy fatty acid (FAHFA(34:0)) and ether phosphatidylcholine (PC(O-34:3)) were lipids associated with pathological levels of total tau (Ttau). Regarding plasma lipids most associated with progression from MCI to AD, our analysis detected OA, plasmalogen (PE(P-36:4)), and three TGs (TG(64:1), TG(46:0), and TG(O-62:7)). Furthermore, TG(O-62:7) was the lipid that most affected time to progression. We found no association between oxidative protein damage markers and diagnosis, AD pathological hallmarks, or progression from MCI to AD.

Conclusions: Central and peripheral lipid alterations are involved, as a cause or consequence, in the development of AD pathology, MCI to AD progression, and could affect time to progression. Neutral lipids could play an important role in pathological processes of AD progression and, affect time to progression.

Key words: Alzheimer's disease, mild cognitive impairment, progression, lipidomics, fatty acid, lipid, protein oxidative damage, plasma, cerebrospinal fluid

Resum

Objectius: Determinar el lipidoma plasmàtic i del líquid cefalorraquidi (LCR) i el dany oxidatiu proteic associat al diagnòstic de malaltia d'Alzheimer (MA) i deteriorament cognitiu lleu (DCL), la patologia de la MA, la progressió i la velocitat de la progressió de DCL a MA.

Mètodes: Es va determinar el lipidoma plasmàtic i del LCR i els marcadors de dany oxidatiu proteic amb tècniques de cromatografia combinada amb espectrometria de masses per 290 individus (104 amb MA, 92 amb DCL i 94 subjectes control).

Resultats principals: El contingut d'àcid hexacosanoic (C26:0), ceramida (Cer(d38:4)) i fosfatidiletanolamina (PE(40:0)) al LCR es van associar amb la presència de nivells patològics d'Aβ42 i els nivells d'esfingomielina (SM(30:1)) es van associar amb fosfotau (Ptau). Pel que fa a la progressió de la malaltia, els nivells d'èster de colesterol (CE(11D3:1)) i d'àcid docosahexaenoic (DHA) al LCR es van associar amb el risc de progressió. El lípid que més va afectar el temps d'aquesta progressió va ser èter triglicèrid (TG(O-52:2)).
A nivell plasmàtic, l'àcid oleic (AO) es va associar amb menor risc del DCL i la MA vs control, mentre que l'àcid vaccènic es va associar amb major risc. SM(36:0), SM(40:1) i diglicèrid (DG(44:3)) van ser els lípids més associats amb la presència de nivells patològics d'Aβ42 al LCR, mentre que TG(O-60:10) es va associar a nivells patològics de Ptau. En relació a Tau total (Ttau), l'àcid gras esterificat a àcid gras hidroxilat (FAHFA(34:0)) i èter fosfatidilcolina (PC(O-34:3)) van ser els lípids identificats significativament associats. Pel que fa als lípids plasmàtics que més s'associen amb la progressió del DCL a la MA, es va detectar AO, plasmalogen (PE(P-36:4)) i tres TGs (TG(64:1), TG(46:0), i TG(O-62:7)). A més, el TG(O-62:7) va ser el lípid que més va afectar el temps de la progressió. No vam trobar cap associació entre els marcadors de dany oxidatiu i el diagnòstic, els marcadors patològics de la MA o la progressió del DCL a la MA.

Conclusions: Les alteracions lipídiques centrals i perifèriques estan implicades, com a causa o conseqüència, en el desenvolupament de la patologia de la MA i la progressió del DCL a la MA. Els lípids neutres podrien tenir un paper important en els processos patològics de la progressió de la malaltia i, afectar la velocitat de la seva progressió.

Paraules clau: malaltia d'Alzheimer, deteriorament cognitiu lleu, progressió, lipidòmica, àcid gras, lípid, dany oxidatiu proteic, plasma, líquid cefalorraquidi

Resumen

Objetivos: Determinar el lipidoma plasmático y del líquido cefalorraquídeo (LCR) y el daño oxidativo proteico asociado con el diagnóstico de enfermedad de Alzheimer (EA) y deterioro cognitivo leve (DCL), la patología de la EA, la progresión y la velocidad de progresión de DCL a EA.

Métodos: Se determinó el lipidoma plasmático y de LCR y los marcadores de daño oxidativo proteico por técnicas de cromatografía acoplada a espectrometría de masas para 290 individuos (104 con EA, 92 con DCL y 26 sujetos control).

Resultados principales: Los niveles de ácido hexacosanoico (C26:0), ceramida (Cer(d38:4)) y fosfatidiletanolamina (PE(40:0)) en LCR se asociaron con la presencia de los niveles patológicos de Aβ42 y los niveles de esfingomielina (SM(30:1)) se asociaron con fosfotau (Ptau). Con respecto a la progresión de la enfermedad, los niveles de éster de colesterol (CE(11D3:1)) y de ácido docosahexaenoico en LCR se asociaron con el riesgo de progresión. El lípido que más afectó el tiempo de esta progresión fue éter triglicérido (TG(O-52:2)).
A nivel plasmático, el ácido oleico (AO) se asoció con menor riesgo del DCL y la EA frente al control, mientras que el ácido vaccénico se asoció con mayor riesgo. SM(36:0), SM(40:1) y diglicérido (DG(44:3)) fueron los lípidos más asociados con la presencia de niveles patológicos de Aβ42 en LCR, mientras que TG(O-60:10) se asoció con los niveles patológicos de Ptau. En relación a tau total (Ttau), el ácido graso esterificado a ácido graso hidroxilado (FAHFA(34:0)) y éter fosfatidilcolina (PC(O-34:3)) fueron los lípidos identificados significativamente asociados. En cuanto a los lípidos plasmáticos que más se asocian con la progresión del DCL a la EA, se detectó AO, plasmalógeno (PE(P-36:4)) y tres TGs (TG(64:1), TG(46) :0), y TG(O-62:7)). Además, TG(O-62:7) fue el lípido que más afectó la velocidad de progresión. No encontramos asociación entre los marcadores de daño oxidativo y el diagnóstico, los marcadores patológicos de la EA o la progresión del DCL a la EA.

Conclusiones: Las alteraciones de los lípidos centrales y periféricos estan implicados, como causa o consecuencia, en el desarrollo de la patología de la EA y la progresión del DCL a la EA. Los lípidos neutros podrían desempeñar un papel importante en los procesos patológicos de la progresión de la enfermedad y, afectar la velocidad de su progresión.

Palabras clave: enfermedad de Alzheimer, deterioro cognitivo leve, progresión, lipidómica, ácido graso, lípido, daño oxidativo proteico, plasma, líquido cefalorraquídeo

Abbreviations

A

AA	Arachidonic acid
AASA	Aminoadipic semialdehyde
AChE	Acetylcholinesterase
ACL	Average chain length
AD	Alzheimer's disease
ADAM10	A disintegrin and metalloproteinase 10
AGE	Advanced glycoxidation end products
AI	Anti-inflammatory index
AICD	APP intracellular C-terminal domain
ALE	Advanced lipoxidation end products
ALS	Autophagy-lysosome system
APLPs	APP/APP-like proteins
APOE	Apolipoprotein E
APP	Amyloid precursor protein
AUC	Area under the curve
Aβ	Amyloid beta protein
Aβ38	Amyloid beta 1-38
Aβ40	Amyloid beta 1-40
Aβ42	Amyloid beta 1-42

B

BACE1	β-site APP-cleaving enzyme 1
BBB	Blood brain barrier
BHT	Butylated hydroxytoluene

C

cAMP	Cyclic adenosine monophosphate
CE	Cholesteryl ester
CEL	Carboxyethyl lysine
Cer	Ceramide
CERAD	Consortium to Establish a Registry for Alzheimer’s disease
CJD	Creutzfeldt-Jakob disease
CL	Cardiolipin
CML	Carboxymethyl lysine
CSF	Cerebrospinal fluid
CTF	C-terminal fragment
CTL	Control

D

DBI	Double bond index
DG	Diglyceride

DGLA	Dihomo-γ-linoleic acid
DHA	Docosahexaenoic acid
DMN	Default mode network
DSM-IV	Diagnostic and statistical manual of mental disorders, 4th edition
DTPAC	Diethylenetriaminepentaacetic acid

E

EA	Stearic acid
EDTA	Ethylenediaminetetraacetic acid
EEG	Electroencephalogram
EET	Epoxyeicosatrienoic acid
ELISA	Enzyme-linked immunosorbent assay
EOAD	Early-onset Alzheimer's disease
EPA	Eicosapentaenoic acid
ER	Endoplasmic reticulum

F

FA	Fatty acid
FAHFA	Fatty acid ester of hydroxy fatty acid
FAME	Fatty acid methyl ester
FDA	Food and Drug Administration
FDG	^{18}Fluorodeoxyglucose
FDR	False discovery rate
FID	Flame ionization detector
fMRI	Functional magnetic resonance imaging
FRET	Fluorescence resonance energy transfer
FTD	Frontotemporal dementia

G

GC	Gas chromatography
GC-FID	Gas chromatography with flame ionization detector
GC-MS	Gas chromatography coupled to mass spectrometry
GDS	Global dementia scale
GL	Glycerolipids
GPL	Glycerophospholipid
GSA	Glutamic semialdehyde
GSK3β	Glycogen synthase kinase-3 beta
GWAS	Genome-wide association studies

H

HACA	6-hydroxy-2-aminocaproic acid
HAVA	5-hydoxy-2-aminovaleric acid
HCl	Hydrochloric acid
HDL	High-density lipoprotein

HDL-C	High-density lipoprotein cholesterol
HexCer	Hexosylceramide
HPLC	High performance liquid chromatography
HPLC-MS	High performance liquid chromatography coupled to mass spectrometry

I

IDE	Insulin degrading enzyme
IFN-α	Interferon alpha
IL-1β	Interleukin 1 beta

L

LA	Linoleic acid
LC-PUFAs	Long-chain polyunsaturated fatty acids
LD	Lipid droplet
LDL-C	Low-density lipoprotein cholesterol
LNA	Linolenic acid
LOAD	Late-onset Alzheimer's disease
LOOH	Lipid hydroperoxides
LRP	Low-density lipoprotein receptor-related protein
LTD	Long-term depression
LTP	Long term potentiation

M

m/s	Mass-to-charge ratio
MAP	Microtubule-associated protein
MAPT	Microtubule-associated protein tau
MCI	Mild cognitive impairment
MDA	Malondialdehyde
MDAL	Malondialdehyde lysine
MG	Monoglyceride
MMSE	Mini-mental state examination
MRI	Magnetic resonance imaging
MS	Mass spectrometry
MS/MS	Tandem mass spectrometry
MTBE	Methyl tert-butyl ether
MUFA	Monounsaturated fatty acid

N

NEP	Neprilysin
NfL	Neurofilament light
NFT	Neurofibrillary tangles
Ng	Neurogranin
NIA-AA	National Institute on Aging and Alzheimer’s Association
NINCDS-ADRDA	National Institute of Neurological and Communicative Disorders and Stroke and the Alzheimer Disease and Related Disorders Association

NMDA	N-methyl-D-aspartate

O

OA	Oleic acid
OR	Odd ratio

P

PA	Phosphatidic acid
PC	Phosphatidylcholine
PC(O)	Ether-linked phosphatidylcholine (alkyl-acylphosphatidylcholine)
PC(P)	Phosphatidylcholine plasmalogen (alkenyl-acylphosphatidylcholine)
PCA	Principal component analysis
PCR	Polymerase chain reaction
PE	Phosphatidylethanolamine
PE(O)	Ether-linked phosphatidylethanolamine (alkyl-acylphosphatidylethanolamine)
PE(P)	Phosphatidylethanolamine plasmalogen (alkenyl-acylphosphatidylethanolamine)
PET	Positron emission tomography
PHF	Paired helical filaments
PI	Phosphatidylinositol
PL	Phospholipid
PLD	Phospholipase D
PLS-DA	Partial least squares-discriminant analysis
PPARα	Peroxisome proliferator-activated receptor-alpha
PR	Prenol lipid
PS	Phosphatidylserine
PSEN1	Presenilin subunit 1
PSEN2	Presenilin subunit 2
Ptau	Hyperphosphorylated tau
PUFA	Polyunsaturated fatty acid
PUFA n-3	Polyunsaturated fatty acids from n-6 series
PUFA n-6	Polyunsaturated fatty acid from n-3 series

R

RAGE	Advanced glycation end products
RNS	Reactive nitrogen species
ROC	Receiver operating characteristic
ROS	Reactive oxygen species
RT	Retention time

S

S1P	Sphingosine 1-phosphate
sAPPα	Soluble APP fragment cleaved by α-secretase

sAPPβ	Soluble APP fragment cleaved by β-secretase
SCFA	Short-chain fatty acid
SFA	Saturated fatty acid
SIM	Selected ion-monitoring
SiMoA	Single molecule array
SM	Sphingomyelin
SMase	Sphingomyelinase
sMRI	Structural magnetic resonance imaging
SOD1	Superoxide dismutase 1
SP	Sphingolipid
SphK	Sphingosine kinase
SPL	Sphingosine 1-phosphate lyase
ST	Sterol lipids
SV2A	Synaptic vesicle glycoprotein 2A

T

TAG	Triacylglycerol
TC	Total cholesterol
TCA	Trichloroacetic acid
TFA	Trans fatty acid
TG	Triglyceride
TG(O)	Ether-linked triglyceride
TNF-α	Tumor necrotic factor alpha
TOF	Time of flight
TREM2	Triggering receptor expressed on myeloid cells 2
Ttau	Total tau

U

UFA	Unsaturated fatty acid
UHPLC	Ultra-high performance liquid chromatograph

V

VA	Vaccenic acid
VLCFA	Very long chain fatty acid
VLDL	Very low-density lipoproteins

Others

αCTF	C-terminal fragment cleaved by α-secretase
βCTF	C-terminal fragment cleaved by β-secretase
3-NT	3-nitrotyrosine
4-HNE	4-hydroxynonenal

INTRODUCTION

1. Introduction

1.1. Alzheimer's disease: a brief history and definition

In 1907, Alois Alzheimer – a German psychiatrist and neuropathologist– reported the results of an autopsy on a 55-year-old woman who had died from a progressive behavioral and cognitive disorder. He reported the presence of some distinctive pathologies in the patient's brain: first, an abnormal tangle of fibrils, which we now know are composed of hyperphosphorylated and cleaved forms of the microtubule-associated protein tau. Second, "minute military foci" that were caused by "the deposition of a special substance in the cortex". This special substance was later known to be the aggregates of amyloid beta (Aβ) protein. Third, the presence of "adipose saccules" inside glia, which mentions the dysregulation of lipid metabolism. Fourth, growth on the endothelia without infiltration (Stelzmann et al., 1995). However, the relationship between the amount of neuritic Aβ plaques in the brain of elderly subjects and the risk of dementia was not established until 1968 (Blessed et al., 1968).

Alzheimer's disease (AD) is the most common cause of dementia. Dementia is a general term for the loss of cognitive functions—thinking, remembering, problem solving, reasoning, and speaking—and behavioral abilities beyond what might be expected as a result of normal aging. AD is a progressive neurodegenerative disease that is typically characterized by initial memory impairment that can ultimately affect behavior, speech, visuospatial orientation and the motor system. The increasing decline in these mental capacities affects a person's ability to perform everyday activities and finally leads to their complete loss of independence, disability, and death. However, AD patients with atypical symptoms are not rare. Importantly, other forms of dementia, such as Lewy body dementia or vascular dementia may cause the same symptoms as AD. Therefore, in 2018 the National Institute on Aging and Alzheimer's Association (NIA-AA) defined AD, independently of the clinical symptoms, as a biological construct. Based on this definition, AD refers to the presence of aggregates of Aβ and tau proteins in the brain that can be demonstrated by biomarkers in living people or during post-mortem examination (Jack et al., 2018).

1.2. AD epidemiology

AD accounts for 60-70% of all dementia cases. In a period of 16 years, from 1990 to 2016, the number of persons with dementia increased more than twice, from 20.2 to 43.8 million worldwide. In this period, the number of deaths due to dementia increased by 148%, and in 2016 dementia was the fifth highest cause of death (2.4 million) after ischemic heart disease, chronic obstructive pulmonary disease, intracerebral hemorrhage, and ischemic stroke. However, dementia is the second cause of death in persons aged over 70 years after ischemic heart disease. The prevalence of dementia is higher in women than in men (27 million vs 16.8 million in 2016) (Nichols et al., 2019). In a more recent analysis, the global prevalence of dementia was estimated at 57.4 million cases in 2019. This number was expected to increase to 152.8 million cases in 2050. Moreover, nearly 10 million new cases of dementia are reported each year (Nichols et al., 2022).

AD is divided in two subtypes based on age of onset: early-onset AD (EOAD) and late-onset AD (LOAD). In EOAD, the age of onset of symptoms is before 65 years, typically between 40 and 60 years. EOAD is mainly attributed to genetic mutations and causes a rare familial form of AD. This subtype accounts for 5–10% of all AD cases and its annual prevalence and incidence for people between the ages of 45 and 64 are approximately 24.2/100,000 and 6.3/100,000, respectively. However, the age of onset of LOAD, which is the most common form of AD and is studied in the present thesis, is mainly after the age of 65 years. LOAD has a prevalence of approximately 3.9% worldwide and an estimated annual incidence of nearly 7.5 per 1000 individuals above the age of 60 (Ayodele et al., 2021). This subtype seems to be driven by a complex interaction between genetic and environmental factors. Overall, more than 90% of AD cases appear to be sporadic late-onset. Age is the most important risk factor for this subtype of AD. However, there are some genetic factors that increase the risk of sporadic AD, such as genes that are implicated in innate immunity, cholesterol metabolism and endosomal vesicle recycling pathways, but having the apolipoprotein E ε4 allele (APOE ε4) is the strongest genetic risk factor for LOAD (Guerreiro & Hardy, 2014).

1.3. AD risk factors

1.3.1. Non-modifiable risk factors

1.3.1.1. Age

Advanced age is the strongest risk factor of AD. The vast majority of patients with AD are older than 65 years. With advancing age, the risk of developing AD reaches 19% in individuals 75-84 years of age and this prevalence reaches to 30-35% for those older than 85 years. The age-specific incidence rates for AD demonstrate a doubling of incidence for approximately every six additional years of life, which indicates an exponentially higher risk with increasing age. Although AD is developed in older people, it is not a normal process of aging (Armstrong et al., 2019).

1.3.1.2. Sex

The incidence of AD is higher in women than in men. Currently, two-thirds of AD patients are females, and postmenopausal women comprise over 60% of these patients. This increased incidence in women may be attributed to women's higher longevity compared to men. However, there is emerging evidence that suggests there may be gender-specific biological differences beyond longevity alone. For example, the female sex hormone, estrogen, has been shown to have neuroprotective effects and its reduction during menopause transition has been related to a greater risk of AD-brain alterations in middle-aged peri- and postmenopausal women compared to men of a similar age. In addition, it has been shown that AD risk is higher in women harboring the APOE ε4 allele compared to men. Other possible conditions that may contribute to an increased risk of AD development in women are suffering from higher rates of obesity, diabetes, depression and having lower levels of education and performing fewer intellectual and physical activities (Rahman et al., 2019; Viña et al., 2010).

1.3.1.3. Genetic risk factors

The vast majority of AD cases are not genetically inherited although some genes may act as risk factors. EOAD is mainly attributed to genetic mutations in the amyloid

precursor protein (APP), presenilin 1 (PSEN1) and presenilin 2 (PSEN2) genes that cause a rare familial form of the disease. In EOAD, symptoms develop before the age of 60, and may appear in persons aged between 30 and 40 years (Gomez et al., 2020).

Down syndrome is another genetic risk factor for EOAD. This genetic disorder is the result of an extra copy of chromosome 21 or a part thereof. This chromosome codes APP, and as a result people with Down syndrome have overexpression of the Aβ1-42 (Aβ42) protein, that may be the main cause for presenting classic pathological features of AD prematurely. By the age of 40, the brains of almost all individuals with Down syndrome have significant levels of Aβ plaques and tau tangles. It is estimated that about 50% of people with Down syndrome who are in their 60s have AD (Gomez et al., 2020).

In the case of LOAD, no specific gene has been found as a direct cause of the disease. However, more than 40 genes/loci have been related to the risk of LOAD (Bellenguez et al., 2020). The main genetic risk factors associated with LOAD that were identified by genome-wide association studies (GWAS) or sequencing studies are shown in ***Table 1***.

Inheritance of the APOE ε4 allele is the strongest genetic risk factor for LOAD. APOE is involved in the transport and metabolism of fats, especially cholesterol. Human APOE exists as three common isoforms – ε2, ε3, and ε4 –which have a worldwide frequency of 8.4%, 77.9%, and 13.7%, respectively. Relative to the prevalent ε3/ε3 genotype, carriers with one copy of the ε4 allele have a nearly 3.7-fold increased risk of developing AD, while those with two copies have a 12-fold increased risk. The ε2 allele appears to be protective [odds ratio (OR) = 0.4] relative to the ε3/ε3 genotype. In addition to increased risk for AD, the APOE ε4 allele has also been associated with an earlier age of disease onset. The frequency of the ε4 allele increases to approximately 40% in patients with AD (T.-P. V. Huynh et al., 2017; C. C. Liu et al., 2013).

1.3.2. Modifiable risk factors

As mentioned earlier, the vast majority of AD cases are not inherited genetically. Although advancing age is one of the main risk factors for LOAD, several modifiable risk factors also increase the risk of AD development. The modifiable risk factors can be divided in two groups: (1) Comorbidities, such as vascular diseases, type II diabetes,

traumatic brain injury, and depression; and (2) Lifestyle, such as physical activity, sleep disturbances, alcohol consumption, smoking, and diet (Edwards et al., 2019).

Table 1. The main genetic risk factors associated with LOAD.

Locus	Protein	Main biological role
APOE ε4	Apolipoprotein E	Lipid metabolism and transport (Serrano-Pozo et al., 2021)
SORL1	Sortilin-related receptor 1	Role in intracellular sorting and trafficking of proteins (Barthelson et al., 2020)
CLU	Clusterin (Apolipoprotein J)	Molecular chaperone (Rodríguez-Rivera et al., 2021)
PICALM	Phosphatidylinositol binding clathrin assembly protein	Involvement in clathrin-mediated endocytosis and autophagy (Tebar et al., 1999)
CR1	Complement component (3b/4b) receptor 1	Regulation of complement activation (Dunkelberger & Song, 2009)
BIN1	Bridging integrator 1	Clathrin-mediated endocytosis and endocytic recycling (Tan et al., 2013)

1.3.2.1. Comorbidities

1.3.2.1.1. Vascular diseases

The neurovascular control system has a pivotal role in maintaining the activity and integrity of the brain by assuring constant blood flow. Alterations to this vascular system mediated by vascular diseases, such as hypertension, hypercholesterolemia or heart diseases, contribute to a reduction in cerebral perfusion leading to brain dysfunction, cognitive impairment, and, in combination with other factors, contribute to the neuropathology of AD. While vascular diseases may result in Aβ deposition and affect the onset of age symptoms, Aβ may itself trigger cardiovascular degeneration (Armstrong et al., 2019; Edwards et al., 2019).

1.3.2.1.2. Type II diabetes

Patients with type II diabetes are at nearly a 60% greater risk of developing AD compared to non-diabetic individuals. This risk can be attributed to the vascular problems suffered by these patients, however, direct and indirect links between pathophysiological

alterations of diabetes and pathological processes of AD have been evidenced. For example, irregular insulin levels can disrupt the cholinergic system, which is compromised in both diabetes and AD. In addition, insulin degrading enzyme (IDE) degrades both insulin and Aβ and, therefore, hyperinsulinemia can lead to reduced Aβ clearance (Edwards et al., 2019).

1.3.2.1.3. Traumatic brain injury

Traumatic brain injury may activate multiple cell death pathways leading to synapse loss and eventually neuronal death. Neurodegenerative processes initiated by brain injury may trigger the development of memory problems that may then turn into AD. The overall risk of dementia in individuals with a history of traumatic brain injury was estimated at being 24% higher than for individuals without a history of such brain injury (Blennow et al., 2016).

1.3.2.1.4. Depression

Depression is one of the common symptoms seen in patients with AD. A strong association between depression and AD onset has been evidenced. Neurotransmitters like dopamine and serotonin may have a central role in the conversion of depression into AD because these two neurotransmitters play a pivotal role in the development of depression and AD pathology. Serotonin is involved in controlling mood, social behavior, and memory, whereas, dopamine, regulates reward-motivated behavior and motor functions (Demir et al., 2019).

1.3.2.2. Lifestyle

1.3.2.2.1. Physical inactivity

Physical activity reduces the risk for cardiovascular diseases and, therefore, may indirectly decrease the risk of dementia. In addition, clinical evidence indicates that physical exercise may help preserve cognition and maintain the brain's neuroplasticity. Moreover, physical activity has been shown to positively affect cognitive symptoms in mild cognitive impairment (MCI) and AD patients and slow down the rate of cognitive decline. In animal models, physical activity was able to decrease the load of amyloid

aggregates and have a positive effect on synaptic plasticity, hippocampal shrinkage, and memory formation (Edwards et al., 2019).

1.3.2.2.2. Sleep disturbances

Sleep homeostasis is important to many brain functions. During sleep, toxic substances that have been accumulated throughout the day are removed from the brain. Sleep disturbances such as insomnia, sleep fragmentation, and sleep-disordered breathing have been associated with an increased risk of developing AD. A reduced quality of sleep also increases the rate of cognitive decline in patients with AD. It has been demonstrated that sleep increases the rate of Aβ clearance in the brain through the glymphatic system. Increased light input during the sleep-wake cycle have been seen to increase the amount of insoluble tau and lead to memory impairment because continuous light input suppresses the production of melatonin, the hormone that regulates the body's circadian rhythm (Edwards et al., 2019; Targa et al., 2021).

1.3.2.2.3. Alcohol consumption

Heavy alcohol consumption has been related to cognitive impairment and risk of AD development and progression in various studies (Topiwala et al., 2017). In contrast, mild consumption of alcoholic beverages has demonstrated beneficial effects against AD by decreasing amyloid burden, reducing mortality, and lowering the risk of dementia. Some alcoholic beverages such as red wine contain polyphenols that can inhibit amyloid aggregation and have other beneficial effects including the reduction of oxidative stress, inflammation, and the regulation of protein homeostasis (Dhouafli et al., 2018). Possibly, to determine the effect of alcohol as a protector or inducer of AD dementia, the amount, length of consumption, period of consumption (early or late life), and type of alcoholic beverages (fermented or distilled drinks) should be taken into consideration.

1.3.2.2.4. Smoking

Smoking is related to an increased risk of cardiovascular diseases which, as mentioned, are risk factors for AD. Additionally, smoking leads to cognitive impairment and a faster decline in verbal memory and slower visual search speeds. In animal models, exposure

to cigarette smoke increased amyloid deposition, induced tau hyperphosphorylation, and exacerbated the inflammatory response in a dose-dependent manner (Moreno-Gonzalez et al., 2013). However, other studies present contradictory results (Nordberg et al., 2002).

1.3.2.2.5. Diet

Studies have shown that a low intake of saturated fatty acids and high consumption of vegetables, legumes, fruits, cereals, fish and unsaturated fatty acids (Mediterranean diet) may have a protective effect against AD. A high fat-diet increases the risk of developing obesity, diabetes and cardiovascular diseases and, therefore, may promote the development of cognitive deficits and AD (Gardener et al., 2012). A high-glycemic regimen, including sugar and carbohydrates, correlates with an increment in Aβ accumulation before AD manifests clinically (Taylor et al., 2017). However, other studies have found no significant association between dietary patterns, including the Mediterranean diet, and the risk of dementia (Akbaraly et al., 2019).

1.4. Clinical manifestations

Clinically, AD is defined as a progressive neurologic disorder that manifests with a continuous decline in thinking, behavioral and social skills and affects a person's ability to function independently. The early signs of the disease include forgetting recent events or conversations. This occurs because the first neurons to be damaged are in brain regions involved in forming new memories, including the entorhinal cortex and hippocampus. As neurons in other parts of the brain become damaged, individuals manifest other difficulties. The most common symptoms of AD are:

- Episodic memory loss with the preservation of the historical memory
- Difficulties in planning or solving problems.
- Challenges with completing routine tasks at home, at work or at leisure.
- Temporal-spatial disorientation.
- Difficulty in understanding visual images and spatial relationships.
- Trouble with words when speaking or writing.

- Misplacing objects and losing the ability to retrace steps.
- Decreased or poor judgment.
- Withdrawal from social activities or work.
- Alterations in mood and personality, including depression and apathy.
- Increased anxiety, agitation and sleep disturbances.

The time at which the symptoms advance from mild to severe varies between individuals. In general, there is an average evolutionary course of 10 to 12 years after diagnosis, during which cognitive and functional abilities decline. Impairment progresses to such an extent that an independent person with occasional episodes of memory loss, such as forgetting familiar words or the location of everyday objects (MCI due to AD) gradually becomes a completely dependent person who needs help with basic activities of daily living, such as bathing, dressing, eating and using the bathroom; around-the-clock care. When patients have difficulty moving, they are more vulnerable to infections, that are often a contributing factor to the death of the persons suffering AD (Gaugler et al., 2016).

1.5. Diagnosis

The current diagnostic criteria for AD and MCI due to AD (from now on, MCI) were published in 2011 by the NIA-AA (Albert et al., 2011; G. M. McKhann et al., 2011). Based on these criteria, AD can mainly be diagnosed based on clinical criteria, and if available, biomarkers can increase the degree of certainty.

1.5.1a. Core clinical criteria for the diagnosis of MCI

MCI is diagnosed when there is

- Cognitive concern that reflects a change in cognition reported by patient or informant or clinician
- Objective evidence of impairment in one or more cognitive domains, typically including memory
- Preservation of independence in functional abilities
- No evidence of dementia

And when feasible:

- Ruling out vascular, traumatic, medical causes of cognitive decline
- Providing evidence of longitudinal decline in cognition
- Reporting a history consistent with AD genetic factors (Albert et al., 2011)

1.5.1b. Core clinical criteria for AD diagnosis

AD is diagnosed when there are cognitive or behavioral symptoms that:

- Interfere with functionality at work or when conducting habitual activities
- Are lower than previous levels of functioning and performing
- Cannot be explained by major psychiatric disorders
- Progress gradually over months to years, not sudden over hours or days
- Have been worsened by report or observation
- Implicate at least two domains of cognition. For example, deficits in memory – the most common syndromic presentation of AD–, language deficits, visuospatial problems, or executive dysfunction (G. M. McKhann et al., 2011).

1.5.2. Cognitive tests

The cognitive performance of individuals is evaluated using cognitive assessment tests during an office visit. Some of the most used tests include:

- The Mini-Mental State Examination (MMSE). This is used to estimate the severity of cognitive impairment and to follow the course of cognitive changes in an individual over time. It consists of 30 questions and takes about 10 minutes to complete. The MMSE examines functions including orientation, short-term memory, attention and ability to solve problems, language, comprehension and motors skills (Folstein et al., 1975).
- The Montreal Cognitive Assessment also consists of 30 questions. This questionnaire assesses short-term memory recall, visuospatial abilities, multiple aspects of executive functions, attention, concentration, working memory, language, reasoning, and orientation. Studies have shown that the Montreal cognitive assessment is more reliable for identifying dementia, and better at

identifying early-stage dementia or mild cognitive impairment (Nasreddine et al., 2005).

- The Alzheimer's Disease Assessment Scale-Cognitive Subscale (ADAS-Cog) is a brief neuropsychological assessment tool used to assess the severity of cognitive symptoms of dementia. It is one of the most widely used cognitive scales in clinical trials and is considered to be the "gold standard" for assessing treatments for dementia. This cognitive test consists of a word recall task, naming objects and fingers, following commands, constructional praxis, ideational praxis, orientation, a word recognition task, remembering test directions, spoken language, comprehension, and word-finding difficulty (Connor & Sabbagh, 2008).

1.5.3. Biomarkers

Evidence of AD pathophysiological processes can be measured by CSF analysis and imaging. The major AD biomarkers, based on the 2011 diagnostic criteria, can be divided into two classes based on the biology they measure.

(1) Biomarkers of Aβ pathology
   - Low CSF Aβ42
   - Positive amyloid positron emission tomography (PET) imaging

(2) Biomarkers of neurodegeneration
   - Elevated CSF tau (Total tau (Ttau) and hyperphosphorylated tau (Ptau))
   - Reduced ^{18}fluorodeoxyglucose (FDG) uptake on PET in the temporo–parietal cortex
   - Disproportionate atrophy in structural magnetic resonance imaging (sMRI) in the medial, basal, and lateral temporal lobe, and in the medial parietal cortex (G. M. McKhann et al., 2011)

In 2018, the NIA-AA published a research framework in which AD was defined as a biological instead of a syndromal construct. The research framework focuses on the diagnosis of AD using biomarkers and its intended use was for observational and interventional research, not routine clinical care. The objective of these new criteria was

to generate a common language that would help investigators to create and test hypotheses about the interactions among different pathologic pathways and cognitive manifestations. In this framework, biomarkers are grouped into three categories based on the pathologic process each one measures:

(1) Biomarkers of Aβ pathology (A)
   - Low CSF Aβ42
   - Positive amyloid PET imaging

(2) Biomarkers of pathologic tau (T)
   - High CSF Ptau
   - Positive Tau PET

(3) Biomarkers of neurodegeneration (N)
   - Elevated CSF Ttau
   - Reduced FDG uptake on PET in temporo–parietal cortex
   - Disproportionate atrophy on sMRI in medial, basal, and lateral temporal lobe, and medial parietal cortex (Jack et al., 2018)

Therefore, based on these criteria, AD –refers to Aβ42 plaques and aggregation of pathologic tau– is defined by both abnormal biomarkers of Aβ and pathologic tau in living persons. By contrast, biomarkers of neurodegeneration are not specific for AD but rather nonspecific indicators of neuronal injury that are shared across a variety of etiologies, such as cerebrovascular injury. Binarizing each of three biomarker groups based on their cutoff (+/-) results in eight possible biomarker profiles (***Table 2***) (Jack et al., 2018).

1.6. Treatment

Currently there is no treatment to cure the AD or prevent its progression. However, there are some interventions that have been shown to be effective in delaying cognitive and functional decline and minimizing complications associated with the disease. In this

sense, AD must be approached from different aspects: pharmacologic and non-pharmacologic.

Table 2. Possible biomarker profiles based on biomarkers of amyloid pathology (A), tau pathology (T), and neurodegeneration (N).

AT(N) profiles	Biomarker category	
A-T-(N)-	Normal AD biomarker	
A+T-(N)-	AD pathologic change	AD continuum
A+T+(N)-	AD	
A+T+(N)+	AD	
A+T-(N)+	AD and accompanying non-AD pathologic change	
A-T+(N)-	Non-AD pathologic change	
A-T-(N)+	Non-AD pathologic change	
A-T+(N)+	Non-AD pathologic change	

1.6.1. Pharmacologic interventions

The pharmacological medication used for AD is indicated in the dementia phase. Based on their action mechanism they are divided into two groups: (1) Acetylcholinesterase (AChE) inhibitors, such as donepezil, galantamine and rivastigmine; and (2) non-competitive N-methyl-D-aspartate (NMDA) receptor antagonists, such as memantine.

AD patients have reduced levels of neurotransmitter acetylcholine in the brain. Acetylcholine is believed to be important for memory and cognition. Cholinesterase inhibitors block the action of the enzyme cholinesterase, which is responsible for breaking down acetylcholine and, therefore, increases the levels of acetylcholine in the synaptic cleft. These medications have demonstrated a modest effect on AD symptoms such as cognition and behavioral symptom (Briggs et al., 2016).

Neuronal excitotoxicity, resulting from a dysfunction of glutamatergic neurotransmission, is hypothesized to be involved in the etiology of AD. Memantine is a non-competitive antagonist of glutamatergic NMDA receptors. By binding to the NMDA receptor with a higher affinity than Mg2+ ions, memantine is able to block the prolonged influx of Ca2+ ions and the resultant neuronal excitotoxicity. The use of memantine is indicated for moderate to severe AD and, like AChE inhibitors, has shown to modestly ameliorate cognition, the performance of daily living activities, and psychological and behavioral symptoms (Briggs et al., 2016).

1.6.2. Non-pharmacological interventions

There is growing evidence that cognitive interventions in people with MCI and dementia produce changes in the pattern of brain activation, suggesting that they may increase cognitive reserve and produce neurobiological changes. In addition, the absence of side effects makes them an appropriate option also as a preventive treatment. However, it has not yet been clarified whether these changes are only temporary for the duration of the intervention, or if they are sustainable. Non-drug interventions include memory training, mental and social stimulation, and physical exercise and multimodal programs (Epperly et al., 2017).

1.7. AD pathophysiology

The etiology of AD is multifactorial. Many pathological processes, including abnormal protein aggregation, inflammation, lipid dysregulation, mitochondrial dysfunction and oxidative stress, among others, have been demonstrated to play an active role in the development of this disease. However, the accumulation of extracellular abnormally folded Aβ protein known as amyloid plaques, intracellular aggregations of Ptau protein known as neurofibrillary tangles (NFT), and neurodegeneration are considered the main pathological hallmarks of AD (Jack et al., 2018).

1.7.1. Amyloid pathology

Aβ denotes peptides of 37-42 amino acids that are produced from cleavage of APP by beta and gamma secretases. The slightly longer forms of Aβ, particularly Aβ42, are more hydrophobic and fibrillogenic, and are the main component of amyloid plaques in the brain. Aβ after production is degraded within the brain, or transported out into the periphery. The amount of Aβ that accumulates as plaques within the brain is determined by the interplay between production, degradation and clearance of this peptide (Murphy & Levine, 2010).

1.7.1.1. Amyloid precursor protein processing (Aβ production)

APP is proteolyzed in at least two manners, the non-amyloidogenic processing pathway (nearly 90%) and the potentially amyloidogenic pathway (about 10%) (***Figure 1***). In non-amyloidogenic processing, APP is processed directly by α-secretase and then γ-secretase. α-secretase cleaves APP in the middle of the Aβ sequence generating a soluble APP fragment (APPsα) and a membrane-bound C-terminal fragment of APP (αCTF). αCTF can be subsequently cleaved by γ-secretase producing the p3 fragment (Aβ17-40/42). APP situated in the synaptic membrane can be reinternalized into another endosomal compartment containing β and γ-secretases. The cleavage of APP by β-secretase results in the secretion of APPsβ, and a membrane-bound C-terminal fragment of APP (βCTF). The proteolytic activity of γ-secretase on βCTF generates numerous different Aβ species of different lengths (Aβ37, 38, 39, 40 or 42; the two latter being most common) which are then released into the extracellular space following vesicle recycling or degraded in lysosomes. The Aβ produced either is released to the extracellular space or binds to the molecules of the plasma membrane. The binding of Aβ to ganglioside GM1 in the membrane strongly favors Aβ aggregation. Therefore, Aβ is present in different forms in extracellular space, from soluble monomer and oligomeric conformations to insoluble febril deposits. Investigation has suggested that small soluble species of the Aβ peptide are the most toxic to neuronal cells. Several pathogenic mutations that are associated with EOAD alter secretase processing of APP, leading to increased production of Aβ and/or to a change in the ratio of Aβ peptides.

In addition to Aβ peptides, cleavage of α/βCTFs releases an intracellular C-terminus domain (AICD). "A disintegrin and metalloproteinase" 10 (ADAM10) is the major α-secretase in the human brain, whereas β-site APP-cleaving enzyme 1 (BACE1) is the major β-secretase. γ-Secretase is a multi-subunit enzyme in which the presenilin subunits (PSEN1 and PSEN2) play a catalytic role. Mutations in *PSEN*1 and *PSEN*2 and their substrate, *APP*, are the genetic cause of early onset familial AD (Bergström et al., 2016; O'Brien & Wong, 2011).

1.7.1.2. Aβ degradation and clearance

Aβ can be degraded inside the neurons by ubiquitin-proteasome system or autophagy-lysosome system. It also can be degraded by enzymes such as neprilysin (NEP) and IDE or microglial phagocytosis in the extracellular space. However, a significant amount of Aβ remains undegraded. This undegraded Aβ is transported across the blood brain barrier (BBB) into the circulation. The low-density lipoprotein receptor-related protein (LRP) on the abluminal (brain) side, and the receptor for advanced glycation end products (RAGE) on the luminal (blood) side contribute to the exchange of soluble Aβ across the BBB. Disruption of this mechanism increases the amount of Aβ that remains in the brain, leading to its ultimate accumulation (Xin et al., 2018). It has been shown that in patients with AD, LRP expression is decreased and RAGE increased, highlighting the importance of Aβ clearance in the reduction of plaque burden. In blood, Aβ is mainly bound to soluble LRP and this union may act as a peripheral sink for blood Aβ that may be relevant to the metabolism of Aβ in the brain. Hepatic LRP can assist in Aβ degradation via enzymes such as NEP and IDE (***Figure 2***). Extensive evidence indicates that Aβ clearance plays a more pivotal role in the process of Aβ accumulation in the AD brain rather than Aβ production (D. Wang et al., 2021; Xin et al., 2018).

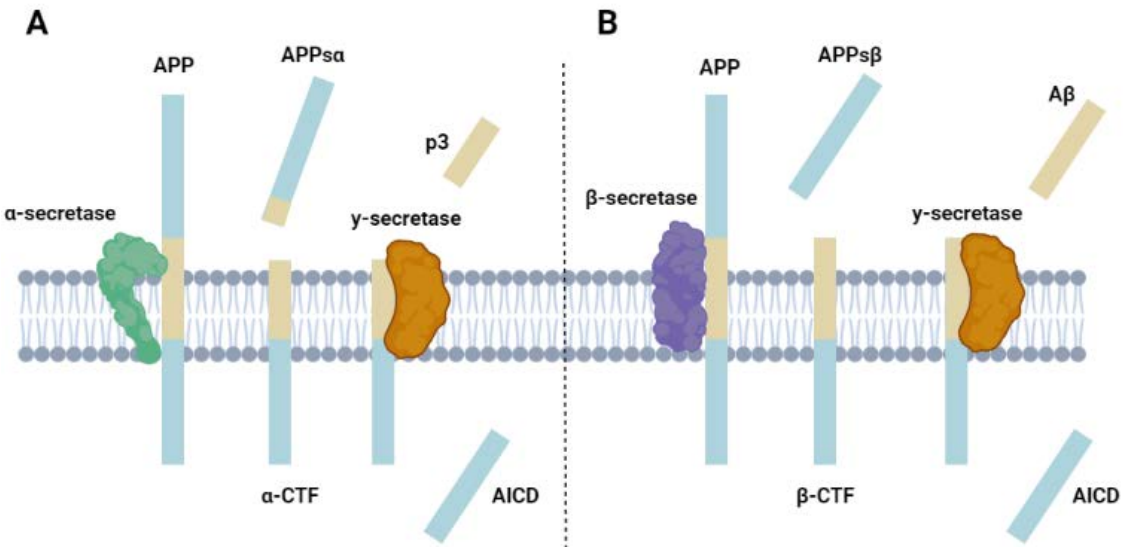

Figure 1. Sequential cleavage of the amyloid precursor protein (APP) by non-amyloidogenic (A) and amyloidogenic (B) pathways. (A) In non-amyloidogenic pathway, APP is cleaved by α-secretase followed by γ-secretase. (B) Amyloidogenic processing of APP involves cleavage by β-secretase followed by γ-secretase. Both pathways produce soluble ectodomians (APPsα and APPsβ) and identical intracellular C-terminal fragments (AICD). Created with BioRender.com.

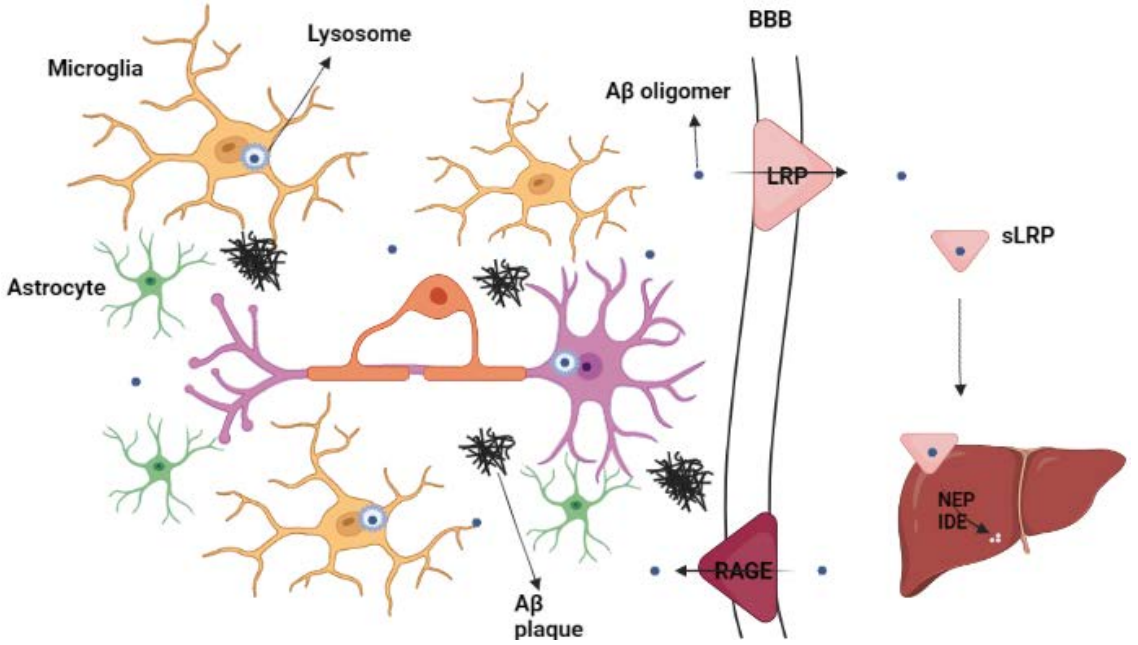

Figure 2. Amyloid beta (Aβ) degradation and clearance. Aβ can be degraded inside neurons by lysosomes or can be eliminated from the extracellular space by microglia or it can be released to the circulation. A balance between receptor for advanced glycation end products (RAGE) and low-density lipoprotein receptor-related protein (LRP) regulates Aβ clearance through transport across the blood-brain barrier (BBB). LRP shuttles Aβ across the BBB into the blood and RAGE is responsible for Aβ influx. Soluble LRP (sLRP) and hepatic LRP contribute to the degradation of Aβ via Aβ-degrading enzymes such as neprilysin (NEP) and insulin degrading enzyme (IDE). Created with BioRender.com.

1.7.1.3. Mechanisms of Aβ toxicity

Aβ peptides form a heterogeneous and polymorphic population during their aggregation. It has been demonstrated that the neurotoxic effects of Aβ are manifested by soluble and diffusive Aβ oligomers. Based on the existing evidence, these species execute their neurotoxicity via the following mechanisms:

1) *Interactions with membranes and membrane receptors*: Aβ species can interact with membrane and membrane-bound synaptic receptors, and consequently, disrupt membrane microenvironments. Both *in vivo* and *in vitro* studies have suggested an interaction between Aβ soluble species and lipid rafts which are membrane microdomains rich in cholesterol, GM1-ganglioside sphingolipids, and synaptic receptors. Animal studies have proposed that Aβ dimers can accumulate at lipid rafts and increase the local Aβ concentration and thus seed Aβ aggregation and plaque formation. Considering that lipid rafts are centers of signal transduction, accumulation of Aβ oligomers at those sites could disrupt signal transduction. In addition, interaction of Aβ oligomers with synaptic receptors could lead to aberrant release of neurotransmitters, promote the internalization of oligomers through the endocytic pathway and consequently damage the intracellular system, and initiate the activity of nitric oxide synthase. Perforation of the membrane can be another mechanism by which Aβ exerts its toxicity toward cells. Aβ oligomers have been shown to directly interact with membranes forming pores and cause ion dysregulation. Finally, all of these disruptions could lead to apoptosis, synapse loss, and loss of connectivity (***Figure 3***) (S. J. C. Lee et al., 2017; Sengupta et al., 2016).
2) *Damage to intracellular organelles and signaling pathways*: After cleavage from APP, extracellular Aβ can internalize into neurons by endocytosis. Additionally, it can be produced intracellularly by the processing of APP present at the organellar membranes, such as mitochondria, endoplasmic reticulum (ER), trans-Golgi network, endosomes, autophagosomes, and lysosomes. The intracellular toxic effects of Aβ can be caused by mitochondrial damage, calcium ion dyshomeostasis, elevated ER stress, altered proteolysis, and the induction of apoptosis (***Figure 3***) (S. J. C. Lee et al., 2017; Reiss et al., 2018).

3) *Cell-to-cell transmission and propagation of neuropathology*: Mouse and primate studies have demonstrated the ability of Aβ to seed plaque formation and spread in the brain. This prion property of Aβ soluble species could be a molecular mechanism whereby Aβ pathology may spread in the brain, however, far more evidence is required to confirm and understand this mechanism (***Figure 3***) (S. J. C. Lee et al., 2017; Sengupta et al., 2016).

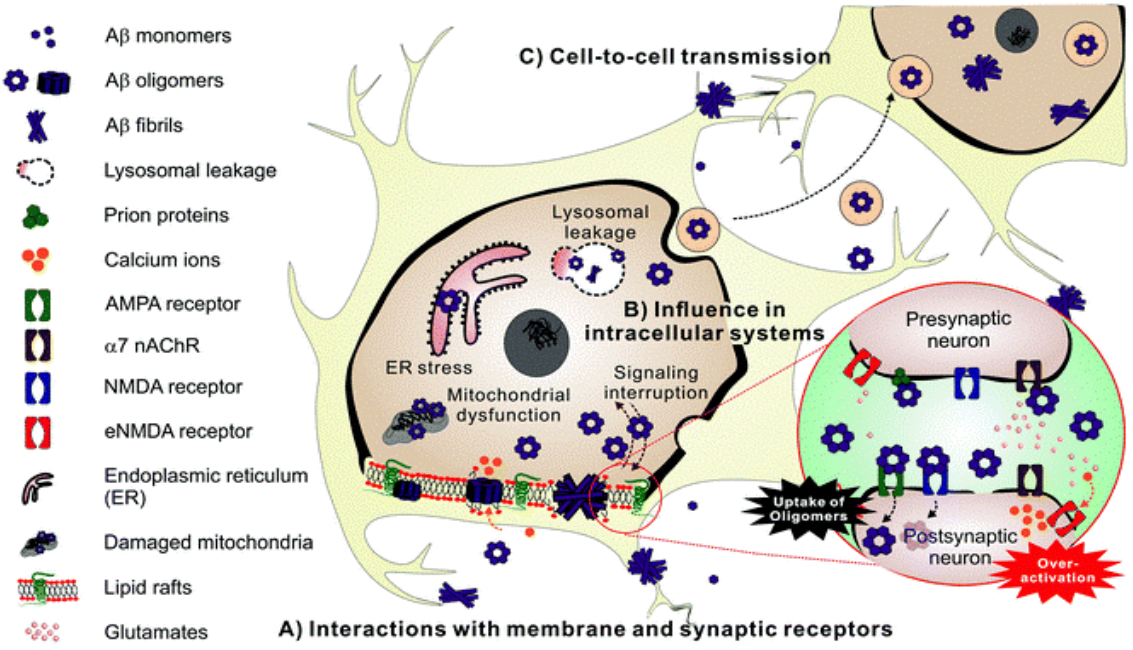

Figure 3. Suggested mechanisms for amyloid beta (Aβ) toxicity. (A) Interaction of Aβ soluble species with membrane and its receptors can disrupt membrane microenvironments. (B) Intracellular Aβ can damage organelles and interfere with signal transduction. (C) Cell-to-cell transmission of Aβ oligomers could play a part in the propagation of neuropathology. From "The Role of Amyloid-β Oligomers in Toxicity, Propagation, and Immunotherapy", by Sengupta U, Nilson AN, Kayed R. *EBioMedicine* 2016; 6:42-49 (doi:10.1016/j.ebiom.2016.03.035). Under the Creative Commons BY-NC-ND license (http://creativecommons.org/licenses/by-nc-nd/4.0/).

1.7.2. Tau pathology

The second pathological hallmark of AD is the presence of NFTs containing Ptau. Tau is the major microtubule associated protein (MAP) of a normal mature neuron. The gene for tau is located on chromosome 17 and alternative splicing of its pre-mRNA results in six isoforms of this molecule. The only established function of tau is interaction with tubulin proteins and helping with their assembly into microtubules and stabilization of

microtubule structure (Hill et al., 2020). However, other functions, such as protecting DNA from oxidative damage and heat shock have also been related to tau (Sultan et al., 2011). The biological activity of tau is regulated by its degree of phosphorylation (***Figure 4***). In a normal brain, tau contains 2–3 moles of phosphate per mole of the protein, the optimal amount for its interaction with tubulin and the promotion of microtubule assembly. The cytosolic Ptau from an AD brain, however, contains 5 to 9 moles of phosphate per mole of the protein (Iqbal et al., 2010). Among more than 80 tau phosphorylation sites, there are some that are exclusively phosphorylated in AD brains (Martin et al., 2013).

Apart from stabilizing microtubules, recently several other functions for this molecule have been revealed in adults. In fact, tau exhibits different functions in different subcellular compartments. In axons, in addition to the role in reorganization of the cytoskeleton, it may have a role in axonal transport, axonal elongation and maturation (neurite formation). Dendritic tau may be involved in the regulation of synaptic plasticity. In the neuronal nuclei, tau seems to play a part in maintaining the integrity of genomic DNA, nuclear RNA, and cytoplasmic RNA. Moreover, tau may be involved in the regulation of neuronal activity, neurogenesis, iron export and long-term depression (LTD) (Y. Wang & Mandelkow, 2016).

Despite intense investigation, the trigger of tau pathology and tau-mediated neurodegeneration in AD remains unclear. The human tau gene can mutate, but none of these mutations has been related to AD. Evidence points to calcium dysregulation, due to stress, head injury or age-related loss of regulatory proteins involved in Ca2+ homeostasis, as a possible initiator of tau pathology. Increased concentration of Ca2+ in cytosol may increase cyclic adenosine monophosphate (cAMP)-protein kinase A activation and, consequently, lead to phosphorylation of tau at S214 that may increase tau susceptibility for further phosphorylation. Protein kinase A inhibits glycogen synthase kinase-3 beta (GSK3β), the main kinase that phosphorylates tau, when cytosolic calcium levels are normal. However, when there are sufficiently high levels of cytosolic Ca2+, protease calpain can be activated and cleave kinase GSK3β to its functional state that consequently, would initiate hyperphosphorylation of pS214Tau at key sites for fibrillation (Arnsten et al., 2021). In short, an imbalance between tau kinase

and phosphatase activities results in the abnormal phosphorylation of tau and thereby contributes to tau pathology initiation. Microtubule-released monomeric tau proteins interact to each other via disulfide bonds or hexapeptide motifs. These interactions move them toward conformational changes from an unfolded, disordered structure to a new beta-sheet-rich and aggregation-competent structure (***Figure 4***). The hyperphosphorylation of tau converts it to a toxic molecule that does not bind to tubulin or promote microtubule assembly, but instead it disrupts microtubule assembly and also sequesters the normal tau and other microtubule-associated proteins (MAP1 A/B and MAP2). This destructive activity has been attributed to non-fibrillized Ptau, while tau polymerized into neurofibrillary tangles is apparently inert. In fact, the self-assembly of the abnormal tau into tangles of paired helical filaments (PHF), is likely a self-defense strategy of neurons to avoid the toxic effects of non-fibrillized Ptau (Hill et al., 2020; Iqbal et al., 2010).

Though necessary, hyperphosphorylation of tau seems to be insufficient for tau aggregation because this process occurs during animal hibernation and in anesthesia-induced hypothermia, but does not lead to tau aggregation. Moreover, it has been demonstrated that phosphorylation of tau occurs many years before the presence of NFTs (Barthélemy et al., 2020). On the other hand, polyanionic cofactors can induce tau aggregation, *in vitro*, regardless of phosphorylation. Thus, unknown cofactors may trigger tau aggregation in the AD brain, whereas phosphorylation may accelerate aggregation in an indirect manner (Y. Wang & Mandelkow, 2016). Moreover, tau undergoes other post-translational modifications including ubiquitination, oxidation, nitration, acetylation, proteolytic cleavage, and glycation, but it is unclear which are causes and which are consequences of the disease process (Alquezar et al., 2021).

1.7.3. Neurodegeneration

Progressive neurodegeneration is the pathological feature of AD that is more closely associated with the progression of cognitive impairment than other pathological characteristics. The neurodegenerative process is initially characterized by synaptic damage followed by neuronal loss.

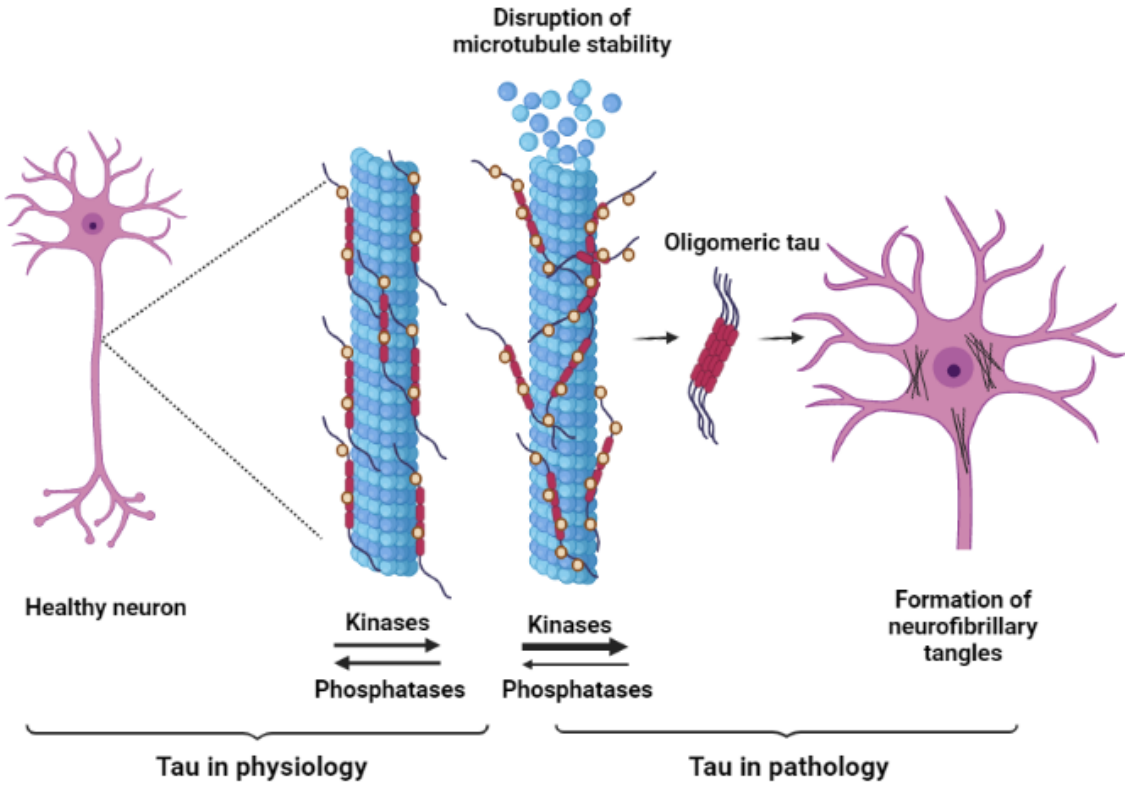

Figure 4. Tau in physiology and pathology. Under physiological conditions, tau is bound to microtubules. A balance between activities of kinases and phosphatases regulates the binding of tau to the microtubules and contributes to the maintenance of microtubule stability. Increased kinase activity under pathological conditions can lead to hyperphosphorylation of tau and the release of this molecule from the microtubules. These events can lead to microtubule instability and aggregation of tau protein, a process that starts with the aggregation of monomers to form oligomers with β-sheet-rich structures and highly toxic properties. Subsequently, oligomers aggregate further into larger constructs and, finally, into neurofibrillary tangles (NFTs). Created with BioRender.com.

Modifications of synaptic transmission, also known as synaptic plasticity, is the major mechanism whereby the neural activity generated by an experience modifies neural circuit function and thereby modifies subsequent thoughts, feelings, and behavior. Synaptic plasticity specifically refers to the ability of synapses to modify their strength or efficacy of synaptic transmission at preexisting synapses in an activity-dependent manner. This ability plays a central role in the capacity of the brain to produce new memories (Citri & Malenka, 2007). In addition, synaptic density is regulated by dynamic gain and loss processes, which are essential for the accurate functioning of a healthy brain. Synaptic dysfunction as a result of neuronal injury is a non-specific pathological hallmark of AD. Epidemiological studies show that there is a strong correlation between synapse failure and cognitive impairment in AD, suggesting a causal role for diminishing

synaptic integrity in the etiology of AD. Importantly, synaptic loss precedes neuronal loss because synaptic density is influenced by an interplay between processes of degeneration and atrophy, and those of maintenance and compensation. Therefore, alterations in synaptic levels can take place before apparent neurodegeneration and should not be considered to uniformly decrease over the course of the disease (Jackson et al., 2019).

Mounting evidence indicates that the route of synaptic damage may be multifocal (***Figure 5***). Both Aβ and tau soluble species have been shown to exert toxic effects on synaptic terminals. Soluble oligomers of Aβ, rather than plaques themselves, may affect normal synaptic functions by inhibiting LTP or facilitating LTD of excitatory synapses and, as a result, contribute to cognitive dysfunction in AD (Z. X. Wang et al., 2016). Other possible mechanisms through which neurotoxic Aβ species might lead to synaptic damage and neurodegeneration include the formation of pore-like structures and the disturbance of the intraneuronal ionic balance, inducing mitochondrial and lysosomal dysfunction, and alterations in signaling pathways related to synaptic plasticity, neuronal cell death, and neurogenesis (Crews & Masliah, 2010).

While there is no evidence to suggest that NFT directly affect synaptic failure, soluble, non-aggregated forms of tau may be causally related to synaptic dysfunction. Tau species, as explained earlier, are able to propagate trans-synaptically between neurons in the AD brain, suggesting a close link between tau pathology progression and synaptic function. Another possible mechanism whereby tau can affect synaptic deficits is tau–induced impairment in axonal transport that affects the accessibility of synapses to organelles that are essential for their proper functioning, such as mitochondria. Moreover, pathological tau species detached from the microtubule can often be translocated from the axon to the somatodendritic compartments and into spines, where it may interfere with synaptic function (Forner et al., 2017; Jackson et al., 2019).

Inflammatory responses resulting from Aβ and tau pathologies may also have a significant effect on the disruption of synaptic terminals. The presence of misfolded proteins in the AD brain can activate an innate immune response. Genome-wide association studies have shown that genes implicated in innate immunity are among AD

risk factors. For example, genetic mutations in triggering receptor expressed on myeloid cells 2 (TREM2) have been shown to significantly increase the risk of AD. TREM2, among other functions, is involved in the phagocytic clearance of neuronal debris. Abnormally increased synaptic pruning by activated microglia has been shown to contribute to a reduction in synaptic density and synapse loss in animal models. Furthermore, pro-inflammatory cytokines such as tumor necrosis factor alpha (TNF-α) and interleukin 1 beta (IL-1β) released from activated microglia can have direct excitotoxic effects on synapses (***Figure 5***). Therefore, neurodegeneration probably occurs as a result of the interplay between several pathological processes including Aβ pathology, tau pathology, and inflammation, among others. In conclusion, a loss of inter-neuronal connectivity may be a final common biological process linking protein pathologies to disease symptoms (Jackson et al., 2019).

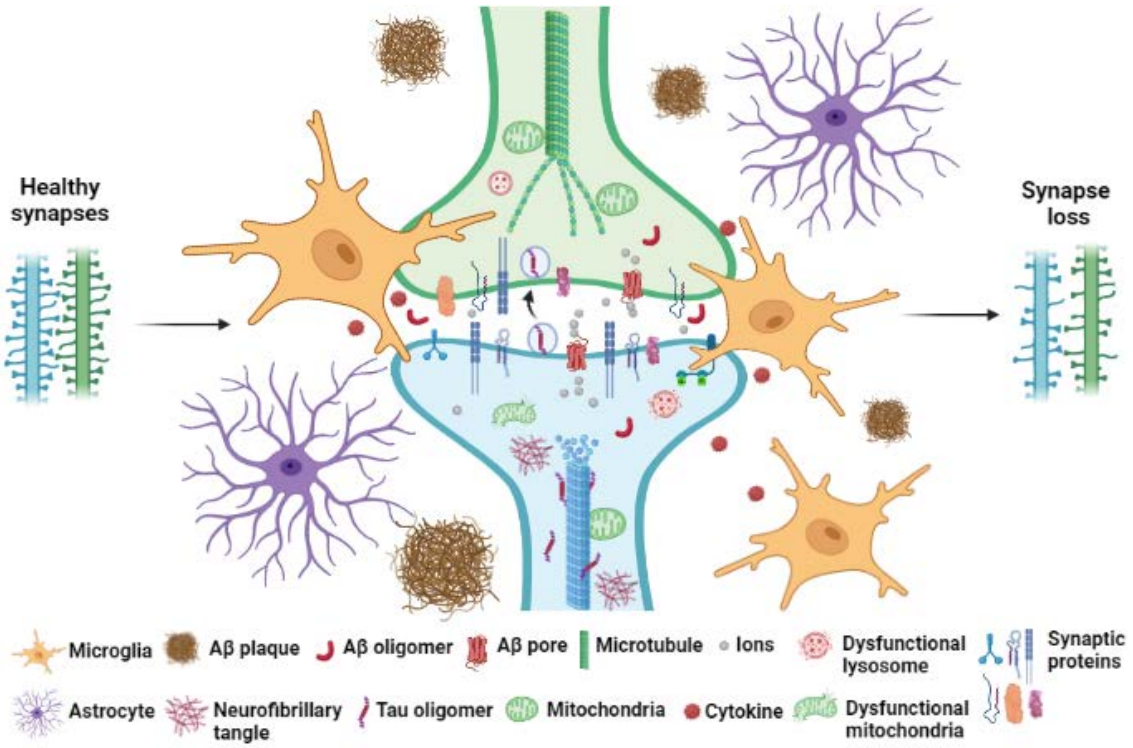

Figure 5. Proposed pathophysiological processes underlying synaptic loss. Amyolid beta (Aβ) oligomers can inhibit long-term potentiation (LTP) or facilitate long-term depression (LTD) of excitatory synapses. In addition, by formation of pore-like stuctures in the membrane, Aβ can disturb the intraneuronal ionic balance and lead to organelle dysfunction. Impairment of axonal transport mediated by tau pathology can limit the accessibility of synapses to organelles, such as mitochondria. Finally, inflammatory responses resulting from Aβ and tau pathologies, including abnomal synpatic pruning and cytokine release, may have a significant effect on the disruption of synaptic terminals. Created with Biorender.com.

1.8. Amyloid cascade hypothesis and its contributors

Several hypotheses have been proposed in order to explain the causative pathophysiology of AD such as Aβ hypothesis, tau hypothesis, oxidative stress hypothesis, and inflammation hypothesis. Aβ cascade hypothesis is the most documented and dominant model. According to this hypothesis, the imbalance between the production and clearance of Aβ peptides occurs very early and is often an initiating factor in AD (Selkoe & Hardy, 2016). In dominantly inherited forms of AD– presence of mutations in the APP, PSEN1 or PSEN2 genes–, there is an increase in Aβ42 production throughout life, while in the sporadic form of the disease there is mainly a failure of the Aβ clearance mechanism that gradually raises Aβ42 levels in the brain. In both conditions, Aβ42 accumulates and oligomerizes in limbic and associated cortices. It has been documented that small oligomeric species of Aβ can enter the lipid bilayer and perturb the biophysical properties of the membrane and the activity of several membrane-associated proteins. These alterations, especially in lipid rafts can lead to the release of some lipid mediators and cause lipoxidation and eventually the activation of cell death processes. In addition, the gradual deposition of Aβ42 and formation of diffuse plaques consequently lead to the activation of microglia and astrocytes that in turn produce and release proinflammatory cytokines, including IL-1β, TNF-α, and interferon alpha (IFN-α). These cytokines can stimulate the nearby astrocyte–neurons to produce further amounts of Aβ42 oligomers. On the other hand, the interaction of Aβ with the lipid rafts can affect the conformation of this protein and induce its aggregation. Altered neuronal ionic homeostasis and oxidative damage also contribute to this scenario. Metal ions such as zinc, iron and copper have been found in amyloid plaques. They can bind Aβ and thus modulate the aggregation process. Furthermore, amyloid aggregates with entrapped redox-active metal ions such as copper ions are more toxic because they can produce reactive oxygen species (ROS) and consequently aggravate the pathological processes. In fact, oxidative stress cannot only contribute to Aβ plaque formation, but can also reduce the clearance of this protein by oxidizing the proteins that contribute to this process. Finally, altered kinase/phosphatase activities lead to the hyperphosphorylation of microtubule associated protein tau, its dislocation from microtubules and the disruption of microtubule trafficking machinery. Ptau

aggregates in the intracellular space form NFTs. Consequently, widespread synaptic dysfunction and neuronal death with attendant neurotransmitter deficits occurs (Kumar et al., 2015; Selkoe & Hardy, 2016).

Although the amyloid hypothesis remains the best defined and most widely accepted view, all of the other pathological processes, including tau, oxidative stress, inflammation and lipid dysregulation, are present from preclinical stages of the disease and may participate actively in the initiation of the disease.

1.9. AD and lipid dysregulation

Lipids are an important class of biomolecules that are involved in many vital cellular processes including their role as building blocks of cell membrane, cell signaling, and energy storage among others. The brain is the most lipid-rich organ after adipose tissue. More than half of the dry brain weight is composed of membrane lipids. Long-chain polyunsaturated fatty acids (LC-PUFAs), such as docosahexaenoic acid (DHA) and arachidonic acid (AA), account for 25–30% of the total fatty acids (FAs) in the human brain. Lipid dysregulation has been reported in many pathologies, including neurodegenerative diseases (Kao et al., 2020). As mentioned earlier, the evidence for the dysregulation of lipid metabolism in AD was present from the first description of the disease by Alois Alzheimer. He noted the existence of some lipid droplets (LDs) inside glia (Stelzmann et al., 1995), suggesting aberrant lipid metabolism. However, little attention was paid to this pathological event until recently, probably because of a lack of tools for the study of lipids.

The link between lipid homeostasis and pathogenesis of AD is strong because: First, harboring APOE ε4 allele is the strongest genetic risk factor for sporadic AD. APOE is mainly expressed in astrocytes and microglia and is responsible for phospholipid and cholesterol transport. It expresses as three major isoforms, APOE ε2, APOE ε3, and APOE ε4. APOE ε4 binds to very low-density lipoproteins (VLDLs) which are large and triglyceride-rich, while APOE ε2 and APOE ε3 preferentially bind to small, phospholipid-rich high-density lipoproteins (HDLs). The frequency of the ε4 allele is increased to approximately 40% in patients with AD (Chew et al., 2020). It has been suggested that

APOE is involved in both Aβ aggregation and clearance. Data from human studies and basic research strongly associate the APOE genotype and cerebral amyloid plaque accumulation with the eventual development of AD (T.-P. V. Huynh et al., 2017). APOE may influence Aβ clearance through modulation of Aβ transport across BBB to the blood circulation and modulation of Aβ intra- and extracellular degradation by astrocytes and microglia (Serrano-Pozo et al., 2021). Evidence that APOE greatly affects AD risk via participating in Aβ pathology is strong, however, there is a large body of literature that supports the role of Aβ-independent APOE in AD pathogenesis. For example, APOE ε4 has a lower affinity for lipids than APOE ε2 and APOE ε3. This low affinity may limit central nervous system transport of lipids that is needed for neuronal remodeling and repair, organelle biogenesis, and synaptogenesis, the fundamental processes in maintaining neuronal plasticity (Mahley, 2016).

Second, lipids– especially those organized in lipid rafts– regulate the trafficking and processing of APP, proteolytic activity of BACE1 and presenilins, and are implicated in Aβ aggregation. Lipid rafts are dynamic structures within cell membranes that play crucial roles in vesicle trafficking, intracellular transport and signal transduction. Lipid rafts are enriched in cholesterol, sphingolipids (SPs) and gangliosides. Changes in the composition of lipid rafts affects APP processing. For example, reducing membrane cholesterol affects the activity of BACE1 and γ-secretase and consequently leads to decreased Aβ production. Furthermore, the introduction of a glycosylphosphatidylinositol anchor, a targeting motif for lipid raft localization, into BACE1 sequence strongly promotes amyloidogenic processing of APP. SPs are also directly involved in APP metabolism, for example, ceramide regulates BACE1-mediated processing of APP probably by the formation of ceramide-enriched platforms and the enhancement of BACE1 stability in cells. Inhibition of sphingomyelinase (SMase), the enzyme that mediates the conversion of sphingomyelin (SM) to ceramide, inhibits γ-secretase activity and leads to a reduction in Aβ secretion (Chew et al., 2020; Paolo & Kim, 2012). Cerebral lipid peroxidation was found to be an early event in AD. It has been suggested that both lipid homeostasis and oxidation state are important for APP processing. When there is a high concentration of oxidized lipids, APP processing may shift from a non-amyloidogenic to an amyloidogenic pathway (Chew et al., 2020). Aβ

peptide harbor a sequence with SP-binding properties that may be potentially important for the aggregation, internalization and intracellular sorting of this peptide. Gangliosides, other lipids abundant in the lipid rafts, are primary modulators of Aβ aggregation. It has been demonstrated that the binding of Aβ to gangliosides GM1 alters the conformation from random coils to β-sheet structures. Thus, membrane GM1 may act as a seed for Aβ aggregation (Paolo & Kim, 2012).

In addition to the aforementioned reasons, the results of numerous biochemical, physiological, and genetic analyses also point to the fundamental role of lipids in AD pathogenesis. Moreover, lipids are involved in blood-brain barrier function, myelination, membrane remodeling, receptor signaling, inflammation, oxidation, and energy balance, all functions that make them central molecules in AD pathological processes (Chew et al., 2020; Hussain et al., 2019). In spite of strong links between AD and lipid dysregulation, our knowledge about the mechanistic role of lipids in AD pathology is in its infancy and little is known about how lipids might participate in pathological processes of AD progression. Hopefully, the recent development of methods for the analysis of lipids and their combination with bioinformatics will have greatly accelerated the study of this class of molecules and future research will uncover the role of lipid dyshomeostasis in all aspects of AD pathology.

1.9.1. Lipidomics

Lipidomics is the science of the large-scale determination of individual lipid species. It emerged in 2003 and has greatly advanced in recent years, largely due to the development of mass spectrometry (MS). MS is the analytical technology in which molecules are ionized to generate cations or anions. Then ions are separated according to their mass/charge (m/z) ratio by a mass analyzer and, finally, a detector determines the species and quantity of each ion. In order to increase the efficiency of the separation of the molecules in a sample, MS is normally coupled to a chromatographic unit. High performance liquid chromatography coupled to MS (HPLC-MS) is one of the most commonly used techniques for the study of lipids (Züllig et al., 2020). A typical workflow for the lipidomic analysis of biological samples includes sample preparation, the

separation of molecules by chromatographic methods, the acquisition of the m/z ratio of the molecules by MS-based analysis, and data processing (***Figure 6***).

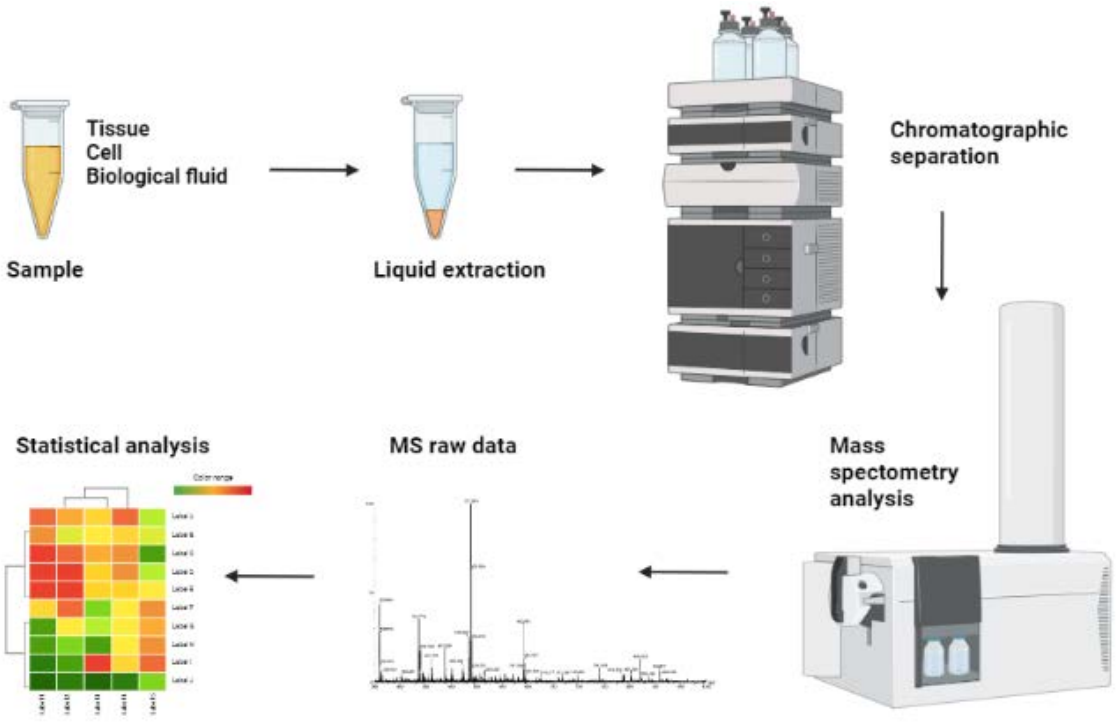

Figure 6. A typical lipidomic workflow consists of lipid extraction, the separation of molecules by chromatographic methods, measurement of the mass-to-charge ratio (m/z) of the molecules, and statistical analysis and interpretation. Created with BioRender.com.

1.9.2. Lipid categories and their link to AD

Lipids can be classified in eight categories: (1) Fatty acids (FA), (2) Glycerolipids (GL), (3) Glycerophospholipids or phospholipids (GPL, PL), (4) Sphingolipids (SP), (5) Sterol lipids (ST), (6) Prenol lipids (PR), (7) Saccharolipids (SL), and (8) Polyketides (PK) (***Figure 7***). The two latter categories are not discussed here because they are not relevant to human cellular functions and structure.

1.9.2.1. Fatty acids

FAs are a diverse group of molecules synthesized by chain-elongation of acetyl coenzyme A. Their structure is composed of a hydrocarbon chain (hydrophobic end) that terminates with a carboxylic acid group (Hydrophilic end) (***Figure 7***). FAs are essentially

found in the structure of GLs and PLs. The carbon chain, typically between four and 24 carbons long, may contain no double bond (saturated FA, SFA), only one double bond (monounsaturated FA, MUFA) or two or more double bonds (Polyunsaturated FA, PUFA). The brain is highly enriched in LC-PUFAs, such as DHA (22:6 (n-3)) and AA (20:4 (n-6)). In the brain, PUFAs are mainly incorporated into PLs of the membranes where they affect membrane fluidity, signal transduction, gene transcription, inflammatory response, and protect against apoptosis (Kao et al., 2020).

Omega-6 (n-6) FAs such as AA– released by enzymatic activity of phospholipases from the membrane PLs– are precursors of many inflammatory mediators including prostaglandins, thromboxanes, leukotrienes, lipoxins, resolvins, and eoxins (Kao et al., 2020; Layé et al., 2018) (***Figure 8***). Inflammation plays a central role in the pathogenesis of AD. It is well documented that patients with AD suffer from a disruption in the equilibrium of anti-inflammatory and pro-inflammatory pathways that results in neuroinflammation (Kinney et al., 2018). Patients with MCI and AD showed higher levels of AA but lower levels of linoleic acid (LA) (AA precursor) compared to healthy controls. Activation of the AA cascade leads to an increase in Aβ and causes impairment in working memory induced by IL-1β (Kao et al., 2020).

On the other hand, Omega-3 (n-3) FAs such as DHA and eicosapentaenoic acid (EPA) released from membrane PLs are precursors of some anti-inflammatory and bioactive mediators. Indeed, omega-3 PUFAs upregulate lipid mediators involved in the resolution of inflammation and downregulate expression of inflammatory gene, such as those of cytokine or enzymes involved in the synthesis of eicosanoids (***Figure 8***). Epidemiological and observational studies suggest that higher omega-3 PUFA levels in blood are associated with lower proinflammatory cytokine production and reduced risk of cognitive decline and dementia (Kao et al., 2020; Lacombe et al., 2018; Layé et al., 2018). DHA-rich dietary supplementation of patients with AD led to a reduced release of proinflammatory cytokines from blood mononuclear leukocytes (Vedin et al., 2008). *In vitro* studies suggest that DHA protective activity on neuroinflammation may result from its direct effect on microglia. Interestingly, DHA is able to increase Aβ phagocytosis by human microglia and reduce proinflammatory responses (Layé et al., 2018).

Short-chain FAs (SCFAs), five carbon or less, including valeric acid and isovaleric acid, isobutyric acid and butyric acid, propionic acid, acetic acid, and formic acid are produced in the colon from bacterial metabolism of dietary fibers. Animal studies suggest that SCFAs may attenuate clinical and pathological features of AD by serving as an energy source, modulating neuro-inflammatory processes or normalizing aberrant histone deacetylation (Silva et al., 2020).

1.9.2.2. Glycerolipids

Glycerolipids consist of a glycerol backbone esterified with one (monoglyceride, MG), two (diglyceride, DG), or three FAs (Triglyceride, TG) (***Figure 7***). MG and DG are elevated in the frontal cortex and plasma of patients with AD. Brain monoacylglycerol lipase is the main enzyme in the hydrolysis of the endocannabinoid 2-arachidonoylglycerol (2-AG) to AA and glycerol. Inactivation of monoacylglycerol lipase in AD animal models exerted anti-inflammatory and neuroprotective effects, reduced Aβ production and accumulation, and improved cognitive skills (Pihlaja et al., 2015; J. Zhang & Chen, 2018). Inside the cells, TGs are found in LDs. LDs are spherical lipid monolayer organelles that store intracellular neutral lipid such as TGs and cholesteryl esters (CEs) after their production in ER. LDs have been shown to be source of energy substrates, lipid signaling molecules, and membrane infrastructure materials. An increase in LDs has been reported during inflammation (both as a cause and as an effect), oxidative stress (in order to reduce lipid peroxidation damage) and starvation (for use as an energy source). In the brain, the subventricular zone, frontal cortex, hippocampus, olfactory bulbs, and hypothalamus have been shown to accumulate LDs (Farmer et al., 2020). Impairments in neurogenesis in AD have been associated with the accumulation of LDs with a high concentration of oleic acid-rich TGs in ependymal cells of the forebrain neural stem cell niche (Hamilton et al., 2015).

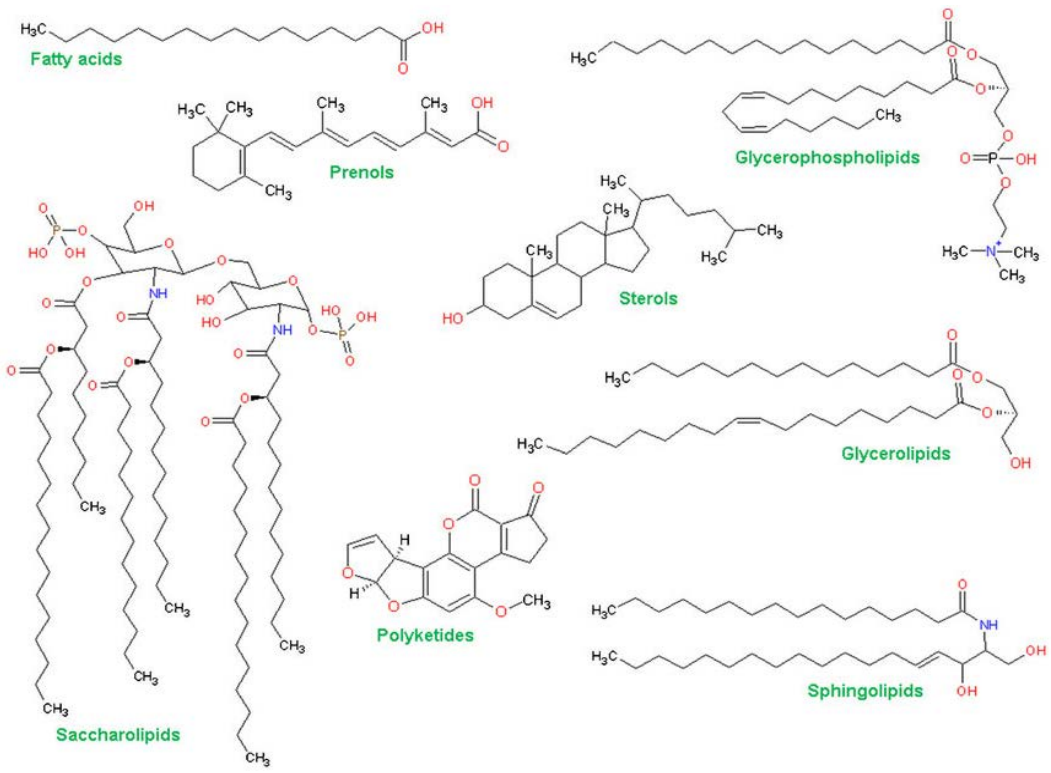

Figure 7. Eight categories of lipids according to the International Lipids Classification and Nomenclature Committee. For each category, one representative structure is illustrated. From "Lipidomics from sample preparation to data analysis: a primer", by Züling T, Trötzmüller M, Köfeler H. Anal Bioanal Chem 2020; 412: 2191–2209 (2020). https://doi.org/10.1007/s00216-019-02241-y. Under the Creative Commons CC BY license.

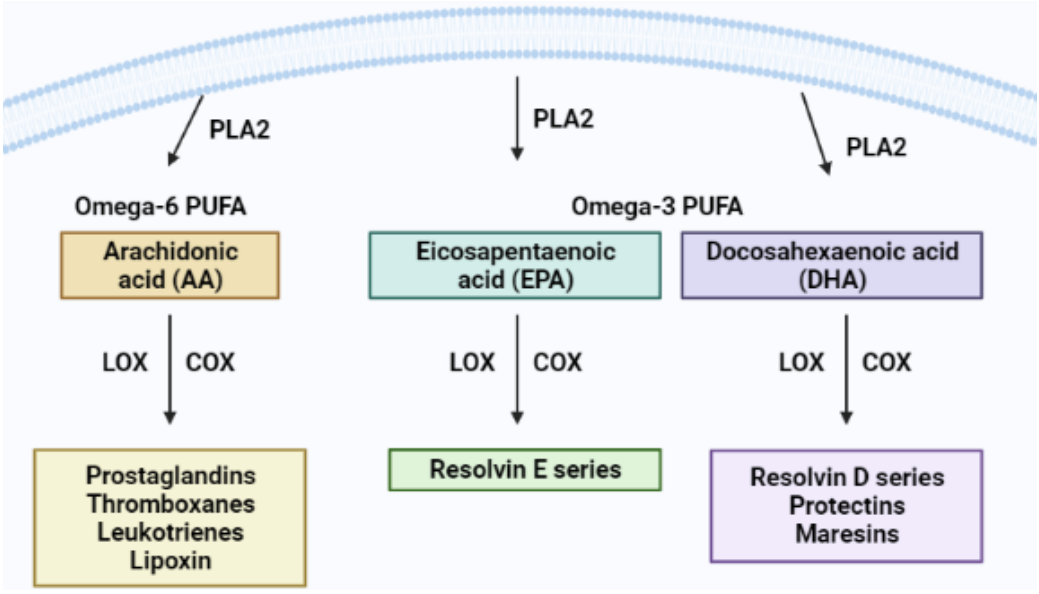

Figure 8. Long-chain polyunsaturated fatty acids (LC-PUFAs) are precursor of proinflammatory and anti-inflammatory lipid mediators. AA, DHA, and EPA released from the membrane phospholipids by the enzymatic activity of phospholipase A2 (PLA2) can be metabolized into various lipid mediators essential for eliciting immune responses or for the resolution of inflammation. This conversion is mainly mediated via activity of the enzymes lipoxygenase (LOX) and cyclooxygenase (COX). Created with BioRender.com.

1.9.2.3. Glycerophospholipids

GPLs or PLs structurally consist of a glycerol backbone in which the first two carbon atoms are bonded to two FAs and a phosphorylated functional group ester-linked to the third carbon (***Figure 7***). PLs are mainly present in the cell membrane. Phosphatidylethanolamine (PE), predominantly in the form of ethanolamine plasmalogen (PE(P)), is the major PL that constitutes more than 35% of total phospholipids in the human brain. Phosphatidylcholine (PC) accounts for nearly 32% of PLs in the human brain. However, PE(P) content is 10-fold higher than choline plasmalogens (PC(P)) in the brain (Su et al., 2019). An increasing number of studies have documented a direct link between PE(P) deficiency and AD. Reduction in PE(P) has been reported in post-mortem brain tissue, CSF, plasma, serum and red blood cells in AD. In the case of brain tissue, the decrease was observed especially in sites vulnerable to neurodegeneration such as the hippocampus, temporal cortex and frontal cortex, but not the cerebellum. A correlation between the reduction of PE(P) in gray matter and disease severity was also observed (Han et al., 2001). It is also not clear whether the reduction of PE(P) in AD is the cause or the consequence of the disease, although both may be the case.

1.9.2.4. Sphingolipids

SPs are essential components of all mammalian tissues, and are highly abundant in the nervous tissue. They are composed of a sphingoid base to which an FA may be attached through an amide bond and a polar head group at the primary hydroxyl (***Figure 7***). According to the polar head group, there are two major classes of SPs: phosphosphingolipids, such as SM, and glycosphingolipids such as cerebrosides and gangliosides. SPs are the major structural components of cellular membranes and together with cholesterol and PLs form lipid rafts where they play important roles in signal transduction and cell recognition. In addition, certain SP metabolites– known as bioactive molecules– such as sphingosine, sphingosine 1-phosphate (S1P), ceramide and ceramide 1-phosphate act as intra- or inter-cellular messengers. They are involved in a variety of important cellular processes such as proliferation, differentiation,

inflammation, apoptosis, autophagy, calcium signaling, and immune responses (Hannun & Obeid, 2017).

SM is the most abundant SP in the brain and is highly enriched in myelin sheaths. Metabolomic assays in AD brains linked an increase in SMs with the severity of AD pathology and an increased risk of cognitive impairment (Varma et al., 2018). However, studies in this regard are inconsistent.

Ceramides play an important role as second messengers of lipids. They have role in inflammation and neuronal apoptosis. Lipidomic studies found increased ceramide levels in AD brains, CSF and serum. Higher baseline plasma concentration of certain ceramides was associated with an increased risk of AD and cognitive decline. Ceramides and AD pathology may have a bidirectional effect on each other as studies showed that ceramide may modulate the function of enzymes implicated in APP processing and, on the other hand, Aβ may increase SMase activity and increase ceramide levels (Kao et al., 2020). Furthermore, ceramides trigger exosome secretion in neural cells, a process that plays an active role in Aβ aggregation and AD progression. SMase-deficient 5XFAD (a mouse model with 5 familial AD mutations) compared to 5XFAD AD model mice showed reduced exosome secretion and AD pathology including reduced glial cell activation, total Aβ plaque deposition, and tau phosphorylation and improved cognitive function (Dinkins et al., 2016).

S1P is another bioactive SP that is produced from the hydrolysis of ceramide and sphingosine by sphingosine kinases (SphKs). S1P is a pro-survival signaling mediator and shows decreased levels in the AD brain. Analysis of the entorhinal cortex of AD patients revealed decreased expression of SphK1 and increased expression of S1P lyase–enzyme that degrades S1P – that were related to the Aβ accumulation in these regions (Ceccom et al., 2014).

Gangliosides are a subclass of glycosphingolipids in which the polar head group at the primary hydroxyl consists of an oligosaccharide chain linked to one or more sialic acids. Under physiological conditions, soluble Aβ oligomers express a high affinity to gangliosides-containing lipid rafts. Studies have shown that gangliosides, especially

GM1, can play role as a seeding place and modulate Aβ aggregation and cytotoxicity (Hong et al., 2014).

1.9.2.5. Sterol lipids

Cholesterol is the major sterol lipid in humans and other animals. Brain cholesterol is originated from de novo biosynthesis because the BBB blocks the entrance of any lipoprotein from blood to the brain. Cholesterol and cholesterol esters play important roles in amyloidogenesis. Membrane cholesterol is mainly present in lipid rafts where APP processing enzymes exert their function. It has been shown that high cholesterol influences APP processing in various ways including regulating all types of APP proteolytic secretases, i.e. α-, β-, and γ-secretase. Cholesterol also mediates Aβ metabolism in many aspects, including its fibrillation, transportation, degradation, and clearance processes (Paolo & Kim, 2012). Although the vast majority of animal studies link hypercholesterolemia to increased Aβ load and neurotoxicity (Kao et al., 2020; Paolo & Kim, 2012), epidemiological studies have demonstrated controversial results. For example, a population-based study found a significant association between hypercholesterolemia and hypertension in midlife and the risk of AD in later life (Kivipelto et al., 2001), while in the Framingham Heart Study, hypercholesterolemia was associated with better cognitive function. Based on a recent meta-analysis, Low-density lipoprotein cholesterol (LDL-C) levels affect the development of AD, whereas, the influence of high-density lipoprotein cholesterol (HDL-C), total cholesterol (TC), and TGs, on AD risk was not significant (Sáiz-Vazquez et al., 2020).

Unlike cholesterol, its oxidized metabolites named oxysterols, such as 24S-hydroxycholesterol (24S-OHC) and 27-hydroxycholesterol (27-OHC), are able to pass through the BBB and are increasingly recognized as having pivotal roles in AD. Oxysterols may indirectly affect Aβ clearance by modifying BBB transporters resulting in alterations in lipoprotein content (Gosselet et al., 2014).

APOE mediates the transport of cholesterols and PLs in the brain. As mentioned earlier, harboring APOE ε4 allele is the major genetic risk factor for AD, highlighting the importance of lipid metabolism, especially cholesterol, in the pathogenesis of AD.

Vitamin D is a fat-soluble vitamin that is predominantly synthesized from cholesterol in the skin under exposure to sunlight. Due to the role of vitamin D in neurodevelopment, calcium homeostasis, the biosynthesis of neurotransmitters and neurotrophic factors, and anti-inflammatory properties, it has been proposed that vitamin D deficiency may play a central role in AD progression (Anjum et al., 2018). Several observational and longitudinal studies have demonstrated a significant association between low serum vitamin D and impaired cognition (Byrn & Sheean, 2019). In addition, several meta-analyses have demonstrated a significant association between vitamin D deficiency and dementia and AD (Chai et al., 2019; Sommer et al., 2017).

1.9.2.6. Prenol lipids

PRs are synthesized from the five-carbon-unit precursors isopentenyl diphosphate and dimethylallyl diphosphate. Carotenoids (tetraterpenoids) are an important class of these lipids. They are precursors of vitamin A and have antioxidant properties. Another important class contains quinones and hydroquinones. Vitamin E and K are examples of this class.

AD patients compared to controls had significantly lower levels of vitamin A in serum. In animal models, the disruption of the retinoid signaling pathway increased Aβ deposition in the brain (Kao et al., 2020). In addition, eight-week intraperitoneal administration of vitamin A to transgenic animals reduced cerebral tau phosphorylation and Aβ plaques. Treated animals also showed decreased activation of microglia and astrocytes, attenuated neuronal degeneration, and improved spatial learning and memory compared to the control animals (Ding et al., 2008).

Vitamin E also has antioxidant properties. The antioxidant capacity results from the presence of a hydroxyl group on the aromatic ring that quenches free radicals through hydrogen atom donation. Vitamin E is present at high concentrations in the brain and in the retina. It protects unsaturated FAs of the membrane from oxidative damage. Many case-control studies have reported diminished vitamin E levels in AD patients. However, prospective studies have shown inconsistent results regarding the use of vitamin E and the risk of AD development. In addition, the majority of clinical trials have failed to

demonstrate any benefit of vitamin E regarding delay in the onset or progression of AD (Browne et al., 2019).

1.10. AD and oxidative stress

Oxidative stress is caused by an imbalance between the production of ROS and reactive nitrogen species (RNS) and the capacity of the body to detoxify them. ROS (e.g. $OH^{\cdot}$, $O_2^{\cdot}$-, H_2O_2) and RNS (e.g., $NO^{\cdot}$, ONOO) are highly reactive. They are inevitable by-products of metabolism that are mainly produced in the mitochondria. ROS and RNS represent a double-edged sword in biological systems. They can play essential roles, for example, as signaling agents, under carefully regulated conditions, while their excessive amounts can damage cells since they are capable of oxidizing all major biomolecules, including nucleic acids, proteins and lipids. The high rate of oxygen consumption and energy demand make the brain especially susceptible to oxidative damage. In addition, elevated levels of PUFAs– which can be easily attacked by free radicals–, high levels of redox transition metal ions, and very low levels of antioxidants are other factors that increase brain susceptibility to oxidative damage (Misrani et al., 2021).

Oxidative stress is considered to play an important role in the pathogenesis of AD. Progressive impairment of mitochondrial function has been considered as the primary cause of ROS generation in aging and AD. On the other hand, the mitochondria are themselves a major target of oxidative and nitrosative damage (Cheignon et al., 2018).

Oxidative stress could be involved in the production of Aβ by the disruption of membrane integrity and altering the functionality of the membrane proteins, including APP processing enzymes (Muche et al., 2017). On the other hand, Aβ oligomers can enter the membrane bilayer and initiate lipid peroxidation of the membrane followed by intracellular oxidation of other molecules. Oxidative stress could be involved in the clearance of Aβ by oxidizing proteins participating in the efflux of Aβ from the brain, such as LRP1. Oxidation of LRP1 and its reduced activity has been evidenced in AD hippocampus (Owen et al., 2010).

Tau protein could also be a target for oxidative stress in AD. Oxidative stress can promote tau phosphorylation and conformational changes that may favor fibril

assembly. These are early events in AD, since the appearance of modified tau in neurofibrillary tangles appears essentially before the maturation of tau inclusion. Furthermore, because of the role of tau in the protection of genomic DNA and of cytoplasmic and nuclear RNA towards oxidative stress, tau alteration would lead to increased DNA and RNA oxidation (Cheignon et al., 2018; Violet et al., 2014).

Glucose hypometabolism is an early pathological event of AD. Oxidative stress can modify proteins involved in glycolysis and ATP production leading to their reduced or diminished function. Several proteins directly involved in glucose metabolism and ATP synthesis including fructose biphosphate aldolase, triose phosphate isomerase, glyceraldehyde phosphate dehydrogenase, phosphoglucose mutase, enolase, pyruvate kinase have been reported to be inactivated by oxidation in the AD brain (Butterfield & Halliwell, 2019; Perluigi et al., 2009).

Memory deficits are a clinical hallmark of AD and MCI due to AD. These altered functions largely originate from synaptic dysfunction. Extensive *in vivo* and *in vitro* studies support a direct relationship between oxidative stress and synaptic dysfunction in AD (Tönnies & Trushina, 2017). Previous studies have shown that small oligomeric species of Aβ can easily enter the neuronal lipid bilayer and provoke lipid peroxidation, and perhaps other forms of oxidative damage in synaptic membranes. Lipid peroxidation in synaptic membranes can affect the activity of NMDA receptors. These receptors, in coordination with AMPA receptors, regulate excitatory synaptic transmission and plasticity in the brain playing an essential role in learning and memory. Mitochondria at synapses provide ATP and buffer Ca2+ concentration, both fundamental processes for neurotransmission and generation of membrane potential along the axon. Lipid peroxidation can affect mitochondrial membranes leading to diminished dynamic and function of this organelle. In addition, destabilization of microtubule machinery by detached Ptau alters mitochondria trafficking and their synaptic docking. Translocation of tau to dendritic spines may also affect NMDA receptor destabilization, excitotoxicity, and increased oxidative stress that contribute to synaptic dysfunction (Butterfield & Halliwell, 2019; Cenini & Voos, 2019; Tönnies & Trushina, 2017).

Metal ions, especially Cu2+, Fe3+ and Mn2+, play a pivotal role in oxidative stress. They are involved in the production and defense of oxidative damage. For example, Cu2+ and

Fe3+ can be reduced to Cu1+ or Fe2+ by glutathione or ascorbate and can then react with O_2 or H_2O_2 to form superoxide and hydroxyl radicals, respectively. On the other hand, the same metal ions also play role in the catalytic core of antioxidant enzymes, like Fe3+ in catalase or Cu2+ in superoxide dismutase 1, where they destroy H_2O_2 and the superoxide anion (O_2-), respectively. Therefore, the control of metal ions metabolism, in terms of concentration, storage, transport, and incorporation into active sites is highly important. Free or loosely bound Cu2+ and Fe3+ are very efficient catalysts of ROS production. In addition, they can bind to other biomolecules and disrupt their function, which could also contribute to exacerbating oxidative stress. Accumulation of Cu, Zn and Fe ions in the amyloid plaques of AD patients is well documented and highlights metal ion dysregulation in AD (Cheignon et al., 2018).

1.10.1. Oxidative stress measurement

ROS including peroxides, superoxide, hydroxyl radicals, singlet oxygen, and alpha-oxygen can be measured in live cells using fluorescent dye-based assays. However, their measurement in tissue and biofluid samples is difficult because of their unstable nature. Indirectly, oxidative stress can be evaluated by measuring the levels of oxidative stress-modified macromolecules that are more stable than ROS and RNS.

1.10.1.1. DNA damage markers

Oxidative damage to DNA can produce nearly 20 DNA adducts. 8-hydroxydeoxyguanosine (8-OHdG) is probably the most commonly used DNA damage marker for oxidative stress. It can be measured in biological fluids, cells and tissue by enzyme-linked immunosorbent assay (ELISA), ligation-mediated polymerase chain reaction, chromatographic and chromatography-mass spectrometry methods (Dabrowska & Wiczkowski, 2017).

1.10.1.2. Lipid peroxidation markers

Lipid peroxidation is described as a process under which oxidants such as free radicals attack unsaturated lipids containing carbon-carbon double bond(s). This process produces lipid hydroperoxides (LOOH) as the primary products and some secondary

aldehyde products, such as malondialdehyde (MDA), propanal, hexanal, 4-hydroxynonenal (4-HNE), and 8-isoprostane. The aldehyde end products can be measured by ELISA, colorimetric/fluorometric methods, chromatographic and chromatography-mass spectrometry methods, and several derivatization-based strategies in biological fluids, cell and tissue (Niki, 2014).

1.10.1.3. Protein oxidation/nitration markers

Oxidative damage to proteins can be produced either by the direct modification of amino acids by ROS and RNS or indirectly as a consequence of glycoxidation or lipoxidation. The highly reactive intermediate species generated during glycoxidation and lipoxidation can attack proteins and modify them. Depending on the origin of reactive species, modified proteins are denoted either as advanced glycoxidation end products (AGE) or advanced lipoxidation end products (ALE). Although all amino acids can be oxidized, several amino acids such as cysteine, methionine, and lysine are more prone to oxidative changes. Aminoadipic semialdehyde (AASA) and glutamic semialdehyde (GSA) are examples for direct oxidation of amino acids (***Figure 9***) (Kehm et al., 2021).

Carboxymethyl lysine (CML) is the most prominent and one of the most abundant AGEs *in vivo*. CML is mainly a product of both glycoxidation and lipoxidation. These oxidative processes lead to the production of highly reactive carbonyl compound glyoxal that in turn can attack lysine of the proteins and modify it to CML. MDA is another reactive carbonyl species that is formed during lipid peroxidation. MDA lysine (MDAL) can be measured in tissue or biological fluids as a marker of ALE. Methylglyoxal is a highly reactive carbonyl compound produced during carbohydrate oxidation and glycolysis. It can also modify lysine residue of the proteins and form carboxyethyl lysine (CEL) that can be quantified as a marker of AGE (***Figure 9***). 4-HNE is another marker of ALE that can cause modifications on cysteine, histidine and lysine. 3-nitrotyrosine (3-NT) is formed by nitration of tyrosine through nitrogen dioxide. 3-NT is used as a marker of protein nitration. Protein oxidation markers can be detected or quantified using spectroscopic, immunohistochemistry, chromatographic or chromatography-MS methods (Kehm et al., 2021).

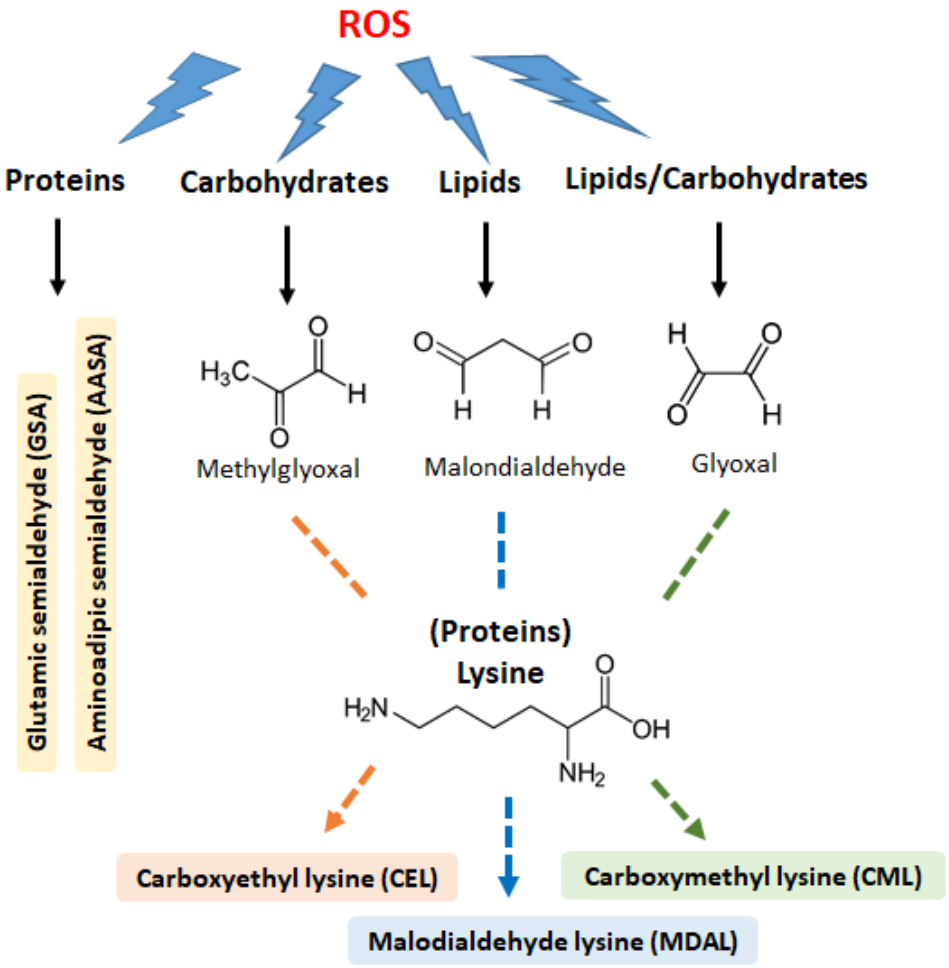

Figure 9. Protein oxidation via direct or indirect pathways. Direct oxidative damage to amino acids form markers, such as AASA or GSA, while indirect protein oxidation followed by glycoxidation or lipid peroxidation generates advanced glycation end products (e.g., CEL and CML) and advanced lipoxidation end products (e.g., MDAL and CML).

1.11. AD progression and the rate of progression

The underlying pathophysiological process of AD and its clinical symptomatology are best conceptualized as a continuum. Clinically, after a long preclinical period that may last over twenty years, patients begin to encounter cognitive problems that are greater than expected for an individual's age and level of education, while they preserve their functionality. These patients are classified as patients with MCI. With the passage of time (this time is highly variable between patients), the patient's cognitive decline progresses and will affect their functionality in performing routine daily life activities (AD, first stages) and finally, their cognitive deficits will progress to such an extent that they will not be able to perform the simplest tasks (AD, last stages). On the other hand,

the specific pathological events associated with the disease also progress gradually. However, pathological progression is not synchronized with clinical progression. Both amyloid and tau pathologies– as principal neuropathological changes of AD– start many years before detectable clinical manifestations and reach their peaks in the asymptomatic phase of the disease, especially in the case of Aβ pathology (***Figure 10***). In fact, these pathologies have shown very poor correlation with clinical progression in AD patients (Sperling et al., 2011). Therefore, they cannot be direct causative actors of cognitive dysfunction. Neurodegeneration is another pathological hallmark of AD. Studies have shown a good correlation between decline in cognition and increase in markers of neuronal injury in CSF and plasma. These markers are released in biological fluids after synaptic damage and neuronal death (Jack et al., 2018) (***Figure 10***).

From the clinical point of view, MCI patients with memory problems (amnestic MCI) are at high risk of progressing to AD dementia. However, for those who progress to AD, the rate of progression is not the same, with some having a faster course than others. The rate of progression to AD is the result of complex mechanisms interacting with each other. Heterogeneity in the speed of disease progression may be affected by disease and patient characteristics. Until now, research has mainly focused on discovering the risk factors for the disease and the probability of developing AD regarding certain risk factors. However, our knowledge about the factors that may affect the disease trajectory is highly limited (Melis et al., 2019). Studies have related patients' neuropsychological levels and neuropsychiatric symptoms with the rate of progression, in which lower baseline level and symptom burden were associated with more rapid decline (Koskas et al., 2017; Tchalla et al., 2018). However, the molecular mechanisms underlying this heterogeneity are not well understood.

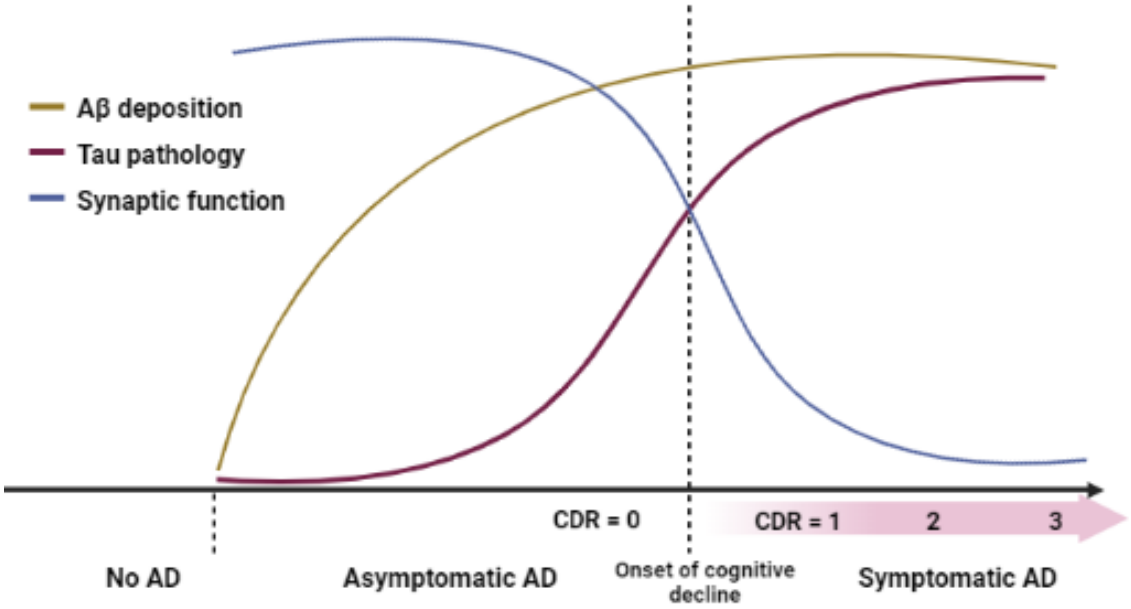

Figure 10. Timing of the main pathological hallmarks of AD. Amyloid and tau pathologies are highly developed upon cognitive impairment onset. However, synaptic dysfunction, although it begins in the preclinical stage, progresses during the symptomatic phase in a good correlation with cognitive decline (cognitive decline is shown as Clinical Dementia rating (CDR) 0 to 3, where 0 means no impairment and 3 means highly impaired). Created with BioRender.com.

1.12. Biomarkers of AD, progression and rate of progression

Traditionally, AD was diagnosed based on the history of the disease, the pattern of cognitive impairments, and additional assessments including blood tests and structural imaging of the brain to rule out non-neurodegenerative causes of the symptoms (G. McKhann et al., 1984). In the past decade, the definition of AD was changed and clinicians and investigators now base diagnoses on biological measures (biomarkers) specific for each neurological alteration of the disease. Although these biomarkers are now used by researchers in their diagnostic criteria, many academic memory clinics also use them in routine practice to help with patient assessment and management (Frisoni et al., 2017).

As explained earlier, from the neuropathological point of view AD is characterized by: (a) extracellular accumulation of Aβ42 protein in the form of plaques; (b) intracellular neurofibrillary tangles composed of aggregations of Ptau protein; and (c) neurodegeneration, especially in the medial temporal lobe structures and the temporo-

parietal association cortices. The most established biomarkers (for use in clinics and investigation) for the detection and measurement of neuropathological hallmarks of AD are detailed below.

1.12.1. Biomarkers of amyloid pathology

1.12.1.1. Aβ positron emission tomography (Aβ-PET)

Amyloid pathology can be measured directly by intravenous injection of PET probes, such as ^{18}F-florbetapir, ^{18}F-flutemetamol, and ^{18}F-florbetaben, that can bind amyloid in senile plaques. These probes are retained in cortical regions of AD brain compared to healthy brains and have shown a good correlation with amyloid pathology burden at autopsy (Morbelli & Bauckneht, 2018).

1.12.1.2. CSF Aβ

Indirectly, amyloidosis can be measured by quantification of Aβ42 in CSF. Patients with Aβ pathology have decreased concentrations of Aβ42 in their CSF due to the sequestration of this protein in senile plaques in the brain. CSF Aβ42 concentrations show high concordance with plaque burden at autopsy and PET brain scans (Lashley et al., 2018).

Aβ40 and Aβ38 are shorter forms of Aβ that are also produced by APP processing mediated by actions of β-secretase and γ-secretase. Aβ40 is the most abundant Aβ peptide in CSF. It is hypothesized that CSF concentration of Aβ42, in addition to the amyloid pathology status, depends on the total amount of CSF Aβ peptides. Therefore, the use of the CSF Aβ42/Aβ40 ratio instead of Aβ42 has been preferred. It has been shown that use of CSF Aβ42/Aβ40 improves predictive accuracy of amyloid plaque burden in MCI patients, improves discrimination of AD from other forms of dementia, and enhances the concordance between CSF and PET amyloid pathology (Dakterzada et al., 2021; Lewczuk et al., 2017).

LC-MS/MS detection is recognized as a reference method for Aβ measurement in CSF by the Joint Committee for Traceability in Laboratory Medicine (JCTLM). However, this method needs expensive, advanced and sophisticated equipment that limits its clinical utility (Korecka et al., 2020).

Immunoassay methods using antibodies specific to Aβ42 and Aβ40 are the most used methods for the measurement of amyloid peptides in CSF. Immunoassay methods have demonstrated good sensitivity (≃ 0.90) and specificity (≃ 0.78) when compared to Aβ-PET. The specificity of immunoassay tests was increased (≃ 0.87) when the Aβ42/Aβ40 ratio is used instead of Aβ42 measures (Janelidze et al., 2017). These tests can be conducted manually or by automated platforms, although the latter may reduce inter- and intra-laboratory inconsistencies (Dakterzada et al., 2021).

1.12.1.3. Blood Aβ

The concentration of AD core biomarkers in blood is much lower than CSF. Until recently, it was not possible to quantify these biomarkers in blood because of the low detection limit of the existing immunoassays (picomolar concentration, 10^{-12} M). However, over the past few years, ultrasensitive technologies such as single molecule array (SiMoA), immunoprecipitation mass spectrometry (IP–MS), immunomagnetic reduction–superconducting quantum interference (MagQu), and the interdigitated microelectrode sensor system have been developed. These technologies provide new opportunities for the measurement of AD biomarkers in blood. SiMoA, in this regard, has attracted much attention. It is able to detect proteins in plasma or serum in sub-femtomolar (< 10^{-16} M) concentrations. The detection system is based on the capturing of analyte by target-specific antibodies that are coupled to paramagnetic particles. In contrast to conventional immunoassays, in SiMoA technology each immune complex is confined to femtoliter-sized wells, which restricts the diffusion of the signal and increases the sensitivity. In spite of this great advantage, i.e., extreme sensitivity, the best diagnostic cut-points for plasma Aβ42 had a sensitivity and specificity of 52% and 78%, respectively, for detecting elevated brain amyloid via Aβ-PET or CSF Aβ. The use of the Aβ42/Aβ40 ratio ameliorated these parameters to a sensitivity of 76-78% and a specificity of 75-76%. In addition, contradictory results were observed after plasma levels of Aβ42 and the Aβ42/Aβ40 ratio measured by SiMoA were compared to other recently developed technologies. Furthermore, studies have reported increased plasma Aβ42 and Aβ42/Aβ40 levels measured by the SiMoA after vascular disease conditions, such as white matter lesions, cerebral microbleeds, hypertension, diabetes, and ischemic heart

disease. Therefore, additional research is required to determine the degree to which other comorbidities affect plasma amyloid levels. Today, kits for measuring Aβ40, Aβ42 in serum or plasma are available, but their use is restricted to investigation purposes (D. Li & Mielke, 2019).

1.12.2. Biomarkers of Tau pathology

1.12.2.1. Tau-PET

PET probes, such as ^{18}F-AV1451, have been developed to bind to tau aggregates in the AD brain. Tau-PET has shown excellent diagnostic performance for distinguishing AD from other neurodegenerative disorders such as vascular dementia or frontotemporal dementia and, recently, have also shown utility for predicting cognitive decline across the clinical spectrum of AD (Ossenkoppele et al., 2021).

1.12.2.2. CSF Ptau

Abnormal hyperphosphorylated and truncated tau proteins are the major constituents of NFTs. Tangle-containing neurons release Ptau in CSF. Increase in CSF Ptau can be measured by immunoassay methods using antibodies that specifically recognize phosphorylated tau epitopes. Currently, CSF Ptau is the most specific biomarker for AD because other tauopathies, such as FTD, progressive supranuclear palsy or Pick's disease, do not show increased concentration of Ptau in CSF, at least not to such an extent as occurs in AD (Lashley et al., 2018).

1.12.2.3. Blood Ptau

As in the case of Aβ, investigation-restricted SiMoA Kits for measurement of Ptau in plasma are also available. In recent studies, Ptau levels have been shown to be the plasmatic biomarker that best correlates with amyloid levels in the brain and it has been shown to be reduced after treatment with monoclonal antibodies against amyloid. Therefore, it seems that it has a promising future at the plasma level (Budd Haeberlein et al., 2022).

1.12.3. Biomarkers of neurodegeneration

Neuronal injury is the pathological feature of AD that is more closely associated with the onset of cognitive impairment than other pathological characteristics. Neurodegeneration can be characterized by neuronal death and brain shrinkage and synaptic dysfunction that precedes phenotypic alterations of the brain.

1.12.3.1. Biomarkers of synaptic loss

Loss of synapses or decreased synaptic density is an early sign of neurodegeneration and it occurs before bulk neurodegeneration. Decreased synaptic density in the neocortex and limbic regions is already present in the pre-dementia stage of the disease. Synapse loss correlates strongly with cognitive decline along the AD continuum because cognitive performance depends on accurate synaptic function. Therefore, longitudinal evaluation of biomarkers of synaptic dysfunction could be useful for monitoring progression in AD. Furthermore, as synapses are responsible for cognitive functions, measures of synapse density are fundamentally important to assess responses to disease-modifying treatments (Colom-Cadena et al., 2020; Smailovic & Jelic, 2019; Young et al., 2020).

1.12.3.1.1. SV2A PET

Synaptic density can be measured directly through the labeling of synaptic vesicle glycoprotein 2A (SV2A) with [^{11}C]UCB-J PET. A reduction of approximately 40% of SV2A signal was observed in the hippocampus in AD cases compared to cognitively healthy controls (Chen et al., 2018). This biomarker, as a direct measure of synapse density, has the potential for use as a strong indicator of brain degeneration and cognitive status. However, the use of this PET ligand to measure synapse loss longitudinally in AD is not yet well established. In addition, the exact function of SV2A, its role in AD and the properties of several other available radioligands have yet to be elucidated (Colom-Cadena et al., 2020).

1.12.3.1.2. Quantitative electroencephalogram

Synaptic activity can be monitored directly using electroencephalography (EEG). EEG measures voltage fluctuations resulting from synaptic function, i.e., summated

excitatory and inhibitory postsynaptic potentials, in cortical pyramidal neuronal dendrites with a high time resolution. Therefore, EEG directly reflects the functioning of the brain synapses. In quantitative EEG, the digital EEG signals are recorded, processed, transformed, and analyzed using complex mathematical algorithms. Quantitative EEG abnormalities in patients with AD have been widely described and have been shown to be sensitive to disease progression and correlate with CSF biomarkers. Across the AD clinical continuum, EEG shows distinct alterations in spectral power indicating a gradual, diffuse slowing of brain electrical activity (Smailovic & Jelic, 2019).

1.12.3.1.3. FDG-PET

The level and pattern of brain metabolic activity can be measured using PET imaging. FDG is an artificial analogue of glucose. Considering that glucose is the brain's main source of energy and synaptic transmission is the most energy-demanding process in neurons, FDG-PET imaging is considered an indirect measure of synaptic function. FDG mimics glucose and crosses the BBB, and its uptake by neurons is a marker of brain metabolism (healthy synapses). Neurodegeneration in special brain regions causes brain hypometabolism in regions that can be visualized as a result of reduced uptake of the tracer (FDG). In AD, hypometabolism normally precedes visible atrophy and is usually seen in the temporoparietal, posterior cingulate and medial temporal cortices. FDG hypometabolism has been shown to parallel cognitive function along the trajectory of preclinical, prodromal, and diagnosed AD. However, higher levels of cognitive reserve attenuate the strength of these correlations and AD patients with high brain reserve can be severely hypometabolic, but clinically mild. In addition, decreased uptake can be caused by other problems, such as reduced cerebrovascular circulation or metabolic disorders like diabetes, rather than neuronal injury (Johnson et al., 2012; Young et al., 2020).

1.12.3.1.4. Functional MRI (fMRI)

fMRI measures brain activity by detecting changes associated with blood flow. This method relies on the fact that when an area is in use, blood flow to the region increases. Since brain functionality depends on accurate synaptic activity, alterations in

functionality of the brain are considered a measure of synaptic functionality. The default mode network (DMN) is a network of functionally interacting brain regions that is active in resting state when a person is not focused on the outside world and is deactivated during active, externally directed tasks. Anatomically, DMN is composed of the medial prefrontal cortex, posterior cingulate cortex/precuneus and angular gyrus (Buckner & DiNicola, 2019). In AD, several fMRI studies have revealed altered connectivity in the DMN. Importantly, the observed connectivity changes follow the trajectory of neuropathology defined by Braak and Braak[1], which first affects the medial temporal lobe, followed by posterolateral cortical regions and, in the latest stages, the frontal cortex. These previous findings highlight the potential of task-based fMRI as a biomarker of disease progression. However, there is a great deal of inconsistency in fMRI studies and sensitivity and reliability of different fMRI tasks within-subject and across cohorts still need to be established. In addition, this technique requires the active collaboration of the patient, which is normally difficult to achieve in patients with cognitive problems (Young et al., 2020).

1.12.3.1.5. CSF neurogranin

Fragments of neurogranin (Ng), a dendritic protein involved in LTP, are increased in CSF of AD patients, whereas full-length Ng is decreased in post-mortem brain tissues. Increase in CSF concentration of Ng was correlated with the severity of cognitive decline, brain atrophy, and glucose hypometabolism in the prodromal stages of the disease. This protein can be quantified in CSF using immunoassay methods. Other synaptic proteins including synaptosomal-associated protein 25 (SNAP25) and Ras-related protein (RAB3A), and a number of other proteins also show promise as CSF biomarkers of synaptic damage and loss. However, they should be characterized in more independent studies (Colom-Cadena et al., 2020).

[1] Braak and Braak is a staging system for neurofibrillary changes in the brain. Six stages of disease propagation can be distinguished with respect to the location of the tangle-bearing neurons and the severity of changes (transentorhinal stages I-II: preclinical AD; limbic stages III-IV: incipient AD; neocortical stages V-VI: fully developed AD) (Braak & Braak, 1995).

1.12.3.1.6. Blood biomarkers of synaptic loss

Blood-based biomarkers of synaptic damage are not yet available. Ng can be measured in plasma, but plasma concentration of Ng does not correlate with its CSF concentration suggesting its extracerebral origin in plasma (Colom-Cadena et al., 2020).

1.12.3.2. Biomarkers of neuronal death

Neuronal death and loss of brain volume can be measured directly using structural magnetic resonance imaging (sMRI) or indirectly by the measurement of proteins released into CSF following neuronal injury.

1.12.3.2.1. Structural MRI (sMRI)

sMRI is a non-invasive technique for the study of the structure and pathology-mediated alterations in the anatomy of the brain. In clinical practice, sMRI is mainly used to exclude other brain pathologies that may justify cognitive impairment, such as tumors or brain lesions and to visualize the pattern of atrophy that may help, to some extent, differentiate between different neurodegenerative diseases. Patients with AD mainly have degeneration in the medial temporal lobe (Johnson et al., 2012) (***Figure 11***). In clinical trials, the use of sMRI extends since monitoring longitudinal rates of atrophy can be used for tracking the progression of the disease, which is important when testing the effectiveness of new therapies. In addition, although volume loss in AD appears later than synaptic dysfunction, hippocampal changes can be detected before symptoms and can be used as a biomarker for trials targeting preclinical stages. Recently, high resolution sMRI has allowed volumetry of hippocampal and extrahippocampal subfields that may help earlier and more accurate diagnosis (Young et al., 2020).

1.12.3.2.2. CSF Ttau and neurofilament light

Measurement of Ttau and neurofilament light (NfL) in CSF can be used to evaluate neurodegeneration. These structural proteins are mainly located in axons and released into CSF after neuronal death. Immunoassay methods are normally used for the measurement of these proteins in CSF. Ttau is measured using antibodies against mid-

domain tau epitopes that are not phosphorylated. CSF concentrations of these proteins have demonstrated a good correlation with cognitive decline in AD (Jack et al., 2018).

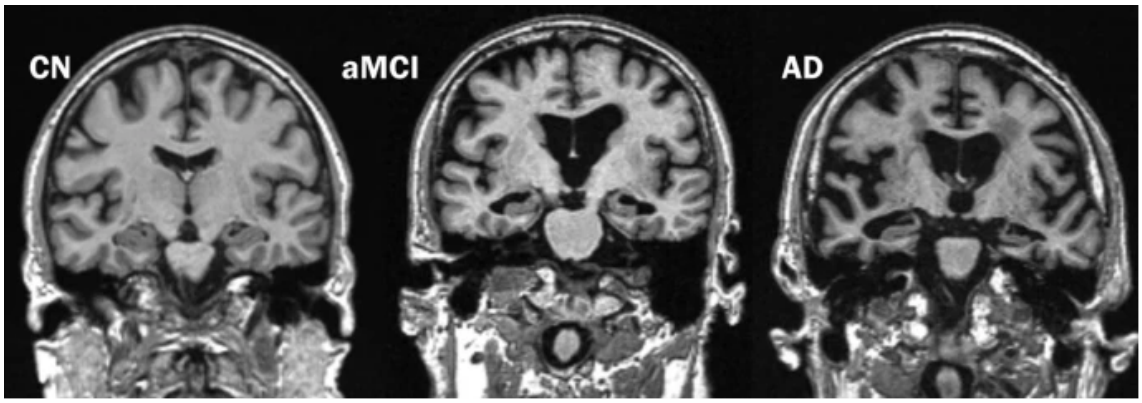

Figure 11. Structural MRI images of an older cognitively normal (CN) subject, an amnestic mild cognitive impairment (aMCI) patient, and an Alzheimer's disease (AD) patient show progressive atrophy in the medial temporal lobe. From "Role of structural MRI in Alzheimer's disease", by Vemuri P and Jack CR. Alz Res Therapy 2020; 2, 23. https://doi.org/10.1186/alzrt47. Under the Creative Commons Public Domain Mark 1.0.

1.12.3.2.3. Blood Ttau and NfL

Ttau and NfL can be measured in blood using SiMoA Kits. The SiMoA Ttau assay measures mid regions of tau protein isoforms. Tau protein isoforms in the blood are different from those in the CSF since they are present in full-length instead of truncated forms that compose the majority of CSF tau. This difference suggests that most plasma tau comes from peripheral sources rather than the brain. Generally, studies suggest that measurement of plasma Ttau is more useful in patients already suffering AD than in patients with MCI or those in preclinical stages of the disease. Unlike Ttau, multiple studies have reported that serum and plasma NfL concentrations show a modest correlation with their concentration in the CSF (0.569 in the Alzheimer's Disease Neuroimaging Initiative and 0.590 in the Mayo Clinic Study of Aging) (D. Li & Mielke, 2019). ***Figure 12*** illustrates the most studied molecular and imaging biomarkers that are used for the measurement of the main pathological hallmarks of AD.

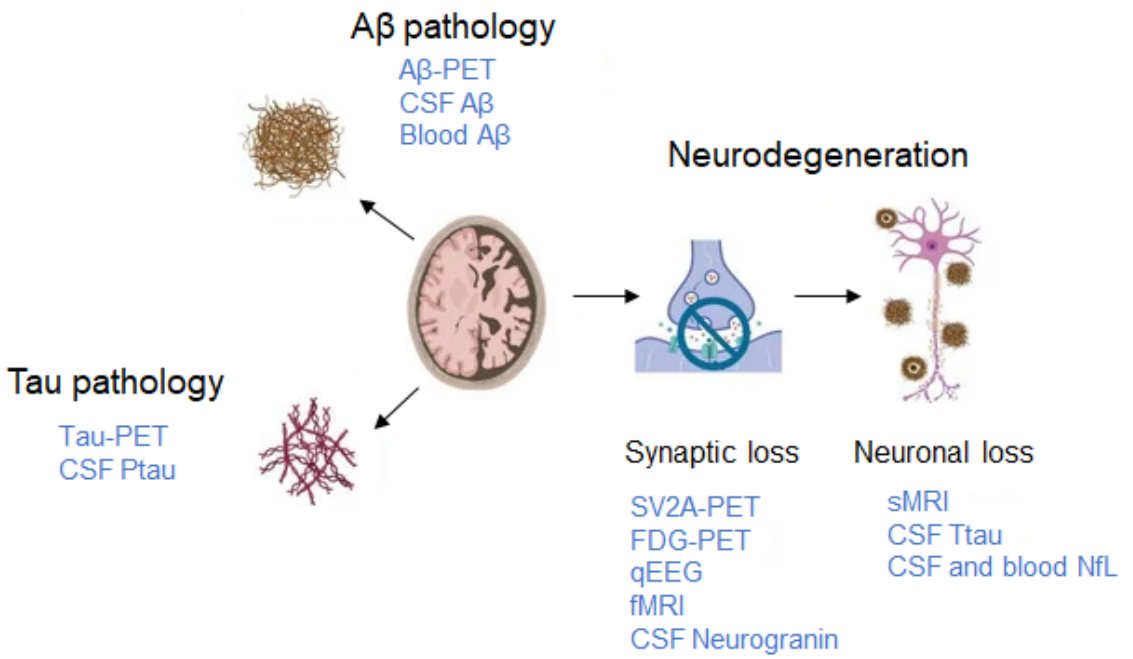

Figure 12. Molecular and imaging biomarkers for the measurement of three main pathological hallmarks of Alzheimer's disease. Adapted from "Molecular and Imaging Biomarkers in Alzheimer's Disease: A Focus on Recent Insights", by Villa C, Lavitrano M, Salvatore E, Combi R. *J. Pers. Med.* 2020, *10*, 61. https://doi.org/10.3390/jpm10030061. Under the Creative Commons CC BY License.

1.12.4. Problems with biomarkers of AD progression

As mentioned earlier, the markers that measure neurodegeneration have demonstrated a good correlation with cognitive decline in AD. Therefore, their use would be valuable for monitoring and predicting progression in the AD continuum. However, these biomarkers have some important limitations that should be taken into consideration. First, a lack of specificity toward neuronal damage due to AD is the major drawback of the existing biomarkers of neurodegeneration. Other neurodegenerative diseases and pathological conditions have also caused alterations in these biomarkers. For example, an increase in CSF Ttau and NfL has also been observed in Creutzfeldt-Jakob disease, frontotemporal dementia, and vascular dementia and after stroke and traumatic brain injury (Jack et al., 2018). An increase in CSF Ng is not specific to AD either and has been reported for other types of dementia (Willemse et al., 2021). For imaging techniques, such as sMRI or FDG-PET, an overlap between the patterns of structural changes produced following different neurodegeneration diseases is not uncommon. In addition,

atypical phenotypes of AD including visual, language, or behavioral presentations in which neurodegeneration starts from regions other than medial temporal lobe may lead to misdiagnosis (Young et al., 2020). Second, the majority of biomarkers of neurodegeneration are obtained via invasive methods that limit their sequential use needed for monitoring progression and for evaluating the effectiveness of new therapies in clinical trials. For example, Ttau, the most established molecular marker of neurodegeneration, is measured in CSF. Measurement in blood, in this case, could be a choice but there is not a good correlation between blood and CSF concentrations of Ttau. PET imaging techniques are also invasive techniques in which a radiolabeled substance is injected intravenously into a patient. Some other non-invasive imaging techniques, such as EEG and fMRI, are not still well established and the results of previous studies have shown inconsistencies that should be overcome before their routine use in clinical trials or settings. Third, imaging techniques are expensive and need specialized technicians, which further limits their repeated use required for monitoring progression. Therefore, searching for reliable, safer biomarkers with high prognostic value is an urgent and important issue.

1.12.5. Biomarkers of rate of progression

Rates of progression in the AD continuum (i.e., preclinical stage to MCI, MCI to AD, and AD first stage to more advanced stages) are variable and dynamic between individuals. The mechanisms that undergo this heterogeneity in progression rate are not well understood and, so far, no biomarker is established for the prediction of the rate of cognitive decline in AD. This is an important issue not only regarding the communication of prognoses in clinical care, but also studies have demonstrated a strong association between the rate of cognitive decline and mortality in AD patients (Hui et al., 2003). Moreover, understanding the physiopathological processes underlying this variability is of utmost importance because of the great potential benefits for the development of effective therapeutic approaches to slow down the rate of progression.

HYPOTHESIS AND OBJECTIVES

2. Hypothesis

Central and peripheral lipid dysregulation and oxidative stress are involved in the development of AD pathology, progression from MCI to AD, and affect time to progression in MCI patients.

3. Objectives

1. To study the impact of lipids and oxidative stress detected in CSF and plasma on the development of AD and MCI.
2. To explore the impact of lipids and oxidative stress identified in CSF and plasma on pathological hallmarks of AD (i.e., amyloid deposition, tau pathology, and neurodegeneration).
3. To investigate whether lipids and oxidative stress markers detected in CSF and plasma can affect progression and rate of progression from MCI to AD.
4. To assess whether alterations of lipid species and markers of oxidative stress in CSF and plasma can serve as prognostic biomarkers of progression and rate of progression from MCI to AD.

MATERIALS AND METHODS

4. Materials and methods

4.1. Study population

The subjects were recruited from a sample of outpatients who visited the cognitive disorders unit of Hospital Universitari Santa Maria de Lleida from June 2014 to December 2016. In addition, we were kindly provided with 74 plasma samples of healthy subjects by Dr. José Luís Cantero from Universidad Pablo de Olavide, Sevilla. The diagnosis of MCI and AD was performed according to NIA-AA criteria (Albert et al., 2011; G. M. McKhann et al., 2011). Controls were recruited as subjects without neurological or neuropsychiatric diseases. The controls provided from Sevilla were part of a cohort of healthy older subjects whose negative amyloid status had been confirmed by Aβ-PET scan and had normal cognitive performance according to the MMSE score. Epidemiological data including age, gender, and time of symptom onset were recorded using a structured interview conducted during the initial patient visit. Information regarding the levels of generic lipids– including TC, LDL-C, HDL-C, and TG– in serum was also provided for each participant.

For AD and MCI patients the exclusion criteria were: (1) diagnosis of dementia other than AD or any somatic, psychiatric, or neurological disorder that might cause cognitive impairment, and (2) suffering from thyroid and vitamin B12 deficiency.

Progression time from MCI to AD dementia was defined as the time between the baseline visit and the date of diagnosis of AD. Progressive cognitive deterioration to AD was defined as: (1) losing more than 3 points between first and last MMSE, (2) having dementia at follow-up, or (3) getting a score of less than 24 on the last MMSE (Caroli et al., 2015).

Due to the unavailability of some samples (CSF or plasma) from the same patient, we had slightly different study populations for each part of the study. For lipidomics, the determination of FA composition, and the quantification of protein oxidative damage markers in CSF we included 210 subjects: 91 AD, 93 MCI, and 26 controls. For the study of FA composition and markers of oxidative damage to proteins in plasma we included

286 samples: 104 AD, 89 MCI and 94 controls. Finally, for plasma lipidomics we included 213 samples: 104 AD, 89 MCI, and 20 controls.

4.1.1. Cognitive evaluation

The cognitive state of the study population was assessed using MMSE (Folstein et al., 1975) at the baseline. For MCI patients, this test was applied in each annual visit until the end of follow-up. The MMSE is a screening questionnaire for the detection of cognitive impairment. It contains 30 questions, and each question is scored with points, with a maximum possible score of 30 points (for more details, please see section 1.5.2.)

4.1.2. Sample collection

Fasting blood and CSF samples were collected between 8:00 and 10:00 a.m. to avoid variations related to circadian rhythm. CSF samples were collected by lumbar puncture at levels L4/L5. The first 20 drops of CSF were discarded, then CSF was collected in polypropylene tubes. The samples were centrifuged at 2000 g for 10 min at 4°C to exclude cells or other insoluble material. The blood samples were collected in EDTA containing tubes. The plasma was separated by centrifugation of blood sample at 1500 rpm for 20 min. The buffy coat was separated for DNA extraction and subsequent APOE genotyping. All samples were aliquoted and immediately stored at − 80°C until use. CSF was subjected to measurement of AD core biomarkers, FA composition, oxidative protein damage and lipidome determination. Plasma was subjected to determination of FA composition, oxidative protein damage, and lipidome.

4.2. AD Biomarkers measurement

The levels of CSF Aβ42, Ttau, and Ptau were determined by the ELISA method using INNOTEST® β-AMYLOID (1-42) (Ref: 81583), INNOTEST® hTAU Ag (Ref: 81572), and INNOTEST® PHOSPHO-TAU (181P) (Ref: 81574) Kits, respectively (Fujirebio Europe, Ghent, Belgium). We used our own cut-off points that were previously calculated based on another study population (different from this sample). Thus, we considered Aβ42

values ≤ 600 pg/ml, Ttau > 425 pg/ml and Ptau > 65 pg/ml as positive/abnormal (Ortega et al., 2019).

4.2.1. Test principle

These three ELISA tests are solid-phase enzyme immunoassays in which a monoclonal antibody (21F12 (IgG2a) for Aβ42, AT120 (IgG1) for Ttau, and HT7 (IgG1) for Ptau) is coated on the wells. The CSF sample is added and if the protein of interest is present at a higher concentration than the Kit detection limit, it is captured by the coated antibody. Afterward, a biotinylated antibody (3D6 (IgG2b) for Aβ42, BT2 and HT7 (IgG1) for Ttau, and AT270 (IgG1) for Ptau) is added and the resulting antigen-antibody sandwich is then detected by a peroxidase-labeled streptavidin (***Figure 13***). Following the addition of enzyme substrate, samples will develop a color. The color intensity is a measure for the amount of searched protein in the sample.

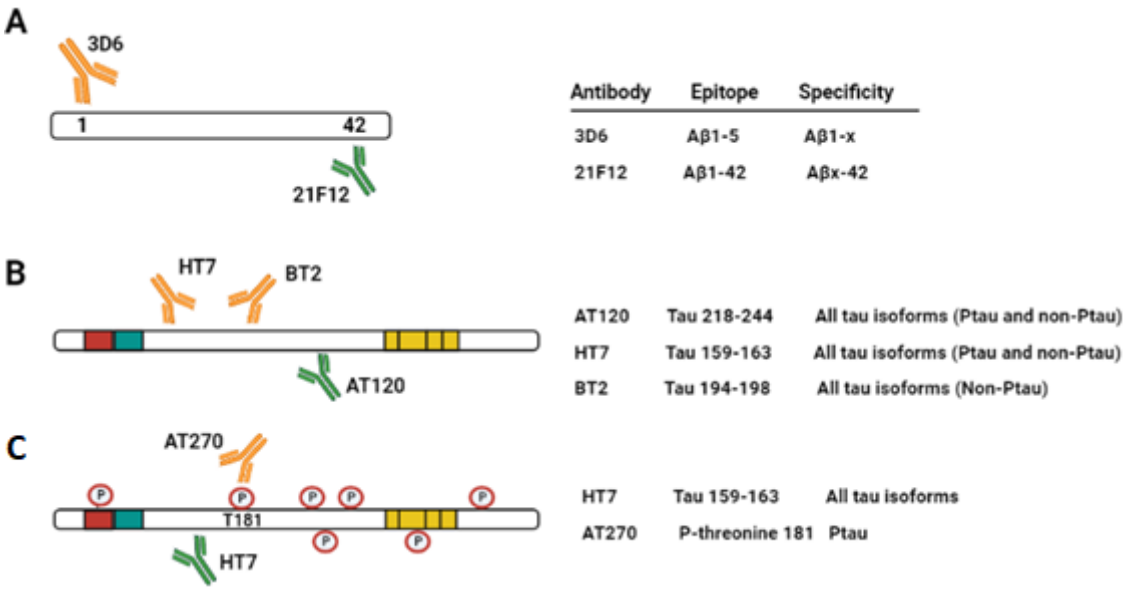

Figure 13. Antibodies used in INNOTEST ELISA for the measurement of amyloid beta 1-42 (Aβ42), total tau (Ttau) and phosphorylated tau (Ptau) proteins. Coated antibody is colored green and detection antibody is colored orange. (A) Using antibodies against N-terminal and C-terminal Aβ42 avoids cross-reaction with Aβ40, Aβ38 or truncated Aβ species. (B) For the measurement of Ttau, antibodies react with tau independent of phosphorylation state, and are against epitopes outside the alternatively spliced exons. Thus, all forms of tau are detected. (C) This ELISA is based on the combination of an antibody that recognizes all tau isoforms irrespective of phosphorylation state and an antibody specific to phosphorylation of threonine 181. Created with BioRender.com.

4.2.2. Test procedure

All material and samples, except the wash solution, were brought to room temperature 60 min before the experiment. The wash solution was warmed to 30–40°C before use. All samples and controls were vortexed before testing.

For Aβ42 and Ttau measurement: first, 75 µl of conjugate working solution 1 (100 µl conjugate 1 + 10 ml conjugate diluent 1) was added to each well of the antibody-coated plate. Then, 25 µl of calibrators, run validation controls and CSF samples were added to duplicate wells of the antibody-coated plate following their vortex for three seconds. Subsequently, the plate was covered with an adhesive sealer and incubated (60 min for Aβ42 and overnight in the case of Ttau) at room temperature (25 ± 2°C). The wells were washed (60 ml wash solution 25X + 1440 ml H2O) for 5 min. Afterwards, 100 µl of conjugate working solution 2 (120 µl conjugate 2 + 12 ml conjugate diluent 2) was added to each well. The plate was covered and incubated for 30 min at room temperature, followed by washing for five min. Then, 100 µl of substrate working solution (120 µl substrate + 12 µl substrate buffer) was added to each well and the plate was incubated for 30 min at room temperature in the dark. The reaction was stopped by adding 50 µl of stop solution to each well and absorbance was read at 450 nm.

For Ptau measurement: first, 25 µl of conjugate working solution 1 (40 µl conjugate 1 + 4 ml conjugate diluent 1) was added to each well of the antibody-coated plate. Then, 75 µl of calibrators, run validation controls and CSF samples were added to duplicate wells of the antibody-coated plate following their vortex for 3 seconds. Subsequently, the plate was covered with an adhesive sealer and incubated overnight at 2–8°C. The wells were washed (60 ml wash solution 25X + 1440 ml H2O) for 5 min. Afterwards, 100 µl of conjugate working solution 2 (120 µl conjugate 2 + 12 ml conjugate diluent 2) was added to each well. The plate was covered and incubated for 60 min at room temperature. The plate was washed for 5 min. Then, 100 µl of substrate working solution (120 µl substrate + 12 µl substrate buffer) was added to each well and the plate was incubated for 30 min at room temperature in the dark. The reaction was stopped by adding 50 µl of stop solution to each well and absorbance was read at 450 nm.

4.3. APOE genotyping

4.3.1. Test principle

The genotyping of APOE was performed using TaqMan® SNP (single nucleotide polymorphism) genotyping technology. It utilizes the 5' nuclease activity of Taq polymerase to generate a fluorescent signal that can be quantified during PCR. For the detection of each SNP, two TaqMan® probes are used that differ in sequence only at the SNP site, i.e. one probe complementary to the wild-type allele and the other one to the variant allele. The technique utilizes fluorescence resonance energy transfer (FRET) technology that is based on the energy transfer from a donor molecule to an acceptor molecule in a distance-dependent manner. In TaqMan® assays, the two probes (the wild-type and variant allele probes) are covalently linked to a reporter dye (FAM™ or VIC™ dyes) at 5' end and a quencher dye (NFQ™) at 3' end. Each assay also contains forward and reverse primers. During the PCR, the forward and reverse primers anneal to complementary sequences along the denatured DNA strands. The probe is hybridized specifically to the targeted SNP site between the forward and reverse primer sites. During PCR extension, if the completely matched probe is hybridized to the gene, the Taq polymerase will be able to cleave the probe and complete polymerization and consequently the characteristic fluorescence of the reporter dye will increase. Otherwise, the DNA polymerase will not be able to continue polymerization, since a probe containing a mismatched base will not be recognized by the enzyme (***Figure 14***). Therefore, at the end of the PCR reaction, the ratio of the fluorescent signals from the two reporter dyes will be indicative of the genotype of the sample (De La Vega et al., 2005).

4.3.2. DNA Extraction

DNA was extracted from the buffy coat cells automatically using the Maxwell RSC Buffy coat DNA Kit[2] (Ref: AS1540, Promega Biotech Ibérica SL, Madrid, Spain) on Maxwell RSC instrument and according to the manufacturer's instructions. Briefly, 50–250 µl of the

[2] The Maxwell® RSC Buffy Coat DNA Kit purifies samples using a silica-based paramagnetic particle. This particle provides a mobile solid phase that optimizes sample capture.

buffy coat was transferred to the first well of each cartridge and tip-mixed into the lysis buffer in the well. One plunger was placed into the 8th well of the cartridge. Then, 200 µl elution buffer was added to the bottom of the elution tube in the cartridge. The lysed samples and reagents were run on the Maxwell RSC instrument and the extraction was performed automatically. The quality of the extracted DNA was evaluated by calculating 260/280 nm absorption ratio using the Nanodrop 2000 (Thermo Fisher Scientific, Waltham, MA, USA).

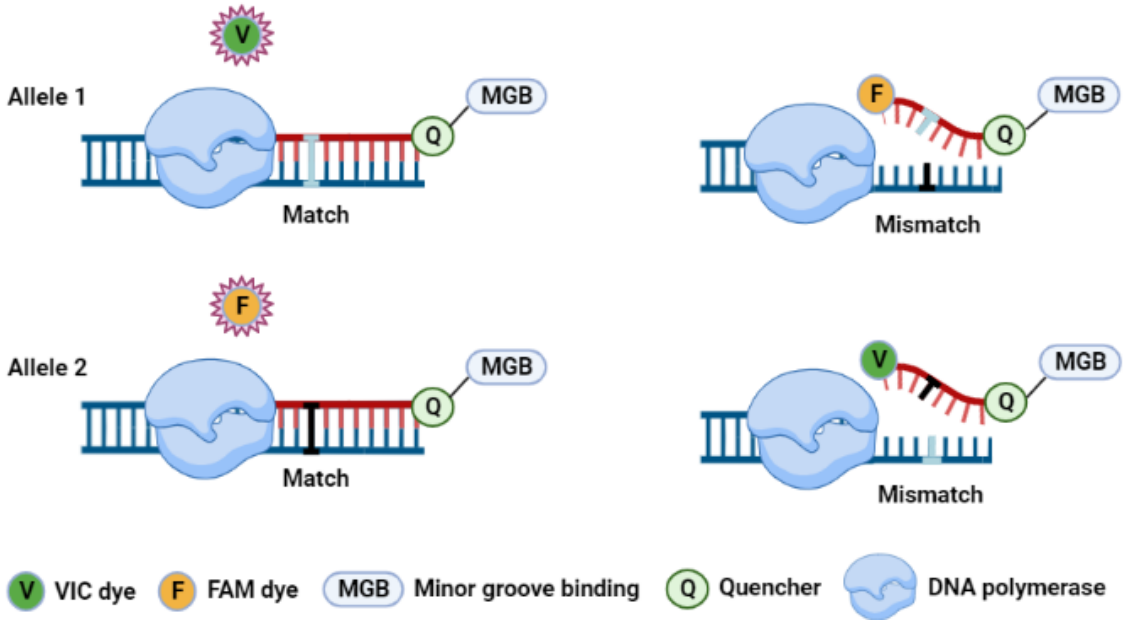

Figure 14. Allelic discrimination by TaqMan SNP genotyping. The selective hybridization of matching probe and template DNA generates an allele-specific fluorescent signal. Created with BioRender.com.

4.3.3. TaqMan® SNP genotyping

APOE genotyping of the study population was performed using two TaqMan® predesigned assays: Assay ID: C_3038793_20 (for SNP rs429358) and Assay ID: C_904973_10 (for SNP rs7412) (Thermo Fisher Scientific, Waltham, MA, USA). Each assay, in addition to the forward and reverse primers, contained 2 probes that were different in only one nucleic acid (C/T).

Genotyping was performed according to the TaqMan® SNP genotyping assay user guide (Publication Num. MAN0009593, revision B.0). Briefly, all samples were diluted to approximately 5 ng/µl. Two reaction mixes containing 2.5 µl 2X TaqMan® master mix (Ref: 4371355) and 0.25 µl 20X SNP rs429358 or SNP rs7412 were prepared and added to each well of the reaction plate (2.75 µl to each well). The sealed plate was centrifuged for 1 min at 1000 g. Then, 2.25 µl of the sample or controls were added to the wells. Nuclease-free water was used as a negative control. The plate was sealed and centrifuged for 1 min at 1000 g and then was placed into the QuantStudio 7 Flex (Life Technologies, Carlsbad, CA, USA) for real-time PCR.

4.3.4. Real-time PCR

PCR was performed using the QuantStudio 7 Flex Real-Time PCR System. A pre-PCR plate read was applied for elimination of pre-amplification background fluorescence, ensuring accurate results. The program was run in standard mode. The real-time PCR conditions were as indicated in ***Table 3***. Finally, the genotype of the samples was determined based on the fluorescence dye detected after DNA amplification (***Table 4***).

Table 3. Thermocycling conditions of the real-time PCR used for APOE genotyping.

	Thermal cycling conditions		
Step	Temperature	Length	Cycles
Polymerase activation	95°C	10 min	HOLD
Denaturation	95°C	15 sec	40
Annealing/extension	60°C	1 min	

4.4. Determination of fatty acid composition and markers of oxidative protein damage

We analyzed the samples by gas chromatography with flame ionization detector (GC-FID) to study FAs. The markers of oxidative protein damage in CSF and plasma were detected by gas chromatography coupled to mass spectrometer (GC-MS) in a targeted manner.

Table 4. the relationship between fluorescence signal and APOE genotype.

APOE genotype	rs429358	rs7412
APOE 2/2	T (FAM)	T (FAM)
APOE 3/3	T (FAM)	C (VIC)
APOE 4/4	C (VIC)	C (VIC)
APOE 2/3	T (FAM)	T/C (VIC & FAM)
APOE 2/4	C/T (VIC & FAM)	C/T (VIC & FAM)
APOE 3/4	C/T (VIC & FAM)	C (VIC)

rs429358 seq: GCTGGGCGCGGACATGGAGGACGTG[C/T]GCGGCCGCCTGGTGCAGTACCGCGG
rs7412 seq: CCGCGATGCCGATGACCTGCAGAAG[C/T]GCCTGGCAGTGTACCAGGCCGGGGC
T: Thymine; C: Cytosine

4.4.1. Principle of GC-FID

The chromatographic separation of the sample analytes is based on the affinity of the compounds for the stationary phase (column) and mobile phase. The mobile phase in a GC is a carrier gas, typically helium because of its low molecular weight and chemical inertness. The high temperature in the injection port vaporizes the sample which can then be carried out with helium and pass through the column. Separation is accomplished using a column coated with a stationary phase. The stationary phase is often derivatives of polydimethylsiloxane, with 5–10% of the groups functionalized to tune the separation. The time that an analyte spends in the column is defined as retention time (RT) which depends on the interaction of the analyte with the column. FID is a good general detector that detects the amount of carbon in a sample. After the column, analytes are burned in a hot, hydrogen-air flame and carbon ions are produced by combustion. The total amount of ions is directly proportional to the amount of carbon in the sample. Finally, the current from the ions is measured by electrodes (*Gas Chromatography (GC) with Flame-Ionization Detection | Analytical Chemistry | JoVE*, n.d.).

4.4.2. Principle of GC-MS

The chromatographic part has been explained in the previous section. Here, ionization and detection are performed by a MS. MS have three main parts: an ion source which converts the sample compound into ions (e.g., by bombarding with a high energy beam of electrons), a mass analyzer, which sorts the ions and separates them according to

their mass and charge, and a detector, which detects and measures the ions. Each of these three tasks may be accomplished in different ways in different MS models (Züllig et al., 2020).

4.4.3. Separation of protein and lipid fractions

The samples were processed in glass tubes pre-cleaned with chloroform and acetone (2X each). The same aliquot of plasma or CSF was used for both experiments. The initial protein concentration needed for these experiments is about 0.5 mg; therefore, we performed the experiments with 10 µl of plasma and 800 µl of CSF samples. The volume of plasma samples was adjusted to 500 µl by adding homogenizing buffer (for recipe, please see section 4.4.5.).

The samples were delipidated by adding methanol/chloroform[3] (2:1, v/v), mixing, and subsequent centrifugation for 15 min at 4400 rpm and at 4°C. The chloroform fraction was transferred to a new glass tube. The delipidation step was repeated three times and the tube containing chloroform was subjected to an FA composition experiment (section 4.4.4b.), while the methanol-containing tube was further processed for quantification of protein oxidative stress markers as follows.

4.4.4a. Quantification of oxidative protein damage markers by GC-MS

The following markers of oxidative protein damage were evaluated: Glutamic semialdehyde [GSA], Aminoadipic semialdehyde [AASA], N^{ε}-carboxyethyl-lysine [CEL], N^{ε}-carboxymethyl-lysine [CML], and malondialdehyde-lysine [MDAL]. Among these markers, GSA and AASA are produced after direct oxidative stress damage to proteins, while CEL, CML and MDAL are protein oxidative damage markers originated from glycoxidation or lipoxidation (for more details, please see section 1.10.1.3.).

[3] For the data regarding company and reference number of the chemical products, please refer to the **Supplementary Table 1**.

4.4.4a.1. Sample processing

The tubes containing methanol were subjected to protein precipitation by adding 1 mL trichloroacetic acid (TCA) 20% and subsequent centrifugation for 15 min at 4400 rpm and at 4°C. The supernatant was decanted and the tubes were placed face down on absorbent paper for 1-2 min. A droplet of 1-hexanol (as an anti-foaming agent) was added and the proteins were reduced by the addition of 1 mL 500 mM sodium borohydride (NaBH4) in a 0.2 M borate buffer (pH 9.2) overnight at room temperature. Subsequently, the reduced proteins were precipitated by adding 1 ml TCA 20% and subsequent centrifugation for 15 min at 4400 rpm and at 4°C. The supernatant decanted and deuterated internal standard mixture (***Table 5***) was added to each tube. Then, the proteins were hydrolyzed to amino acids using 1 ml hydrochloric acid (HCl) 6N during 30 min at 155°C (Tembloc Selecta, Barcelona, Spain) and subsequently dried in a speed vacuum centrifuge (SPD121P Speed Vac Savant, Barcelona, Spain) for at least 4 hours. Thereafter, 1 mL HCl generating solution was added to each tube, the tubes were vortex mixed and incubated for 30 min at 65°C and subsequently dried using an N2 evaporator (N-evap model 113 Organomation Association, Berlin, MA, USA) for 20 min. The Methyl ester N,O-trifluoroacetyl derivatives of the amino acids were prepared by incubating the dried samples with 1 mL trifluoroacetic anhydride for 1 h at room temperature. Subsequently, this solvent was evaporated under N2 stream and the precipitated amino acids were dissolved in dichloromethane (CH2Cl2) and transferred to the injection vials (Agilent technologies, Barcelona, Spain) (Pamplona et al., 2005).

Table 5. List of standards and their concentration that were used for quantification of oxidative stress protein damage markers in CSF and plasma.

Name	Concentration	Reference
[$^2H_8$]Lysine	120 nmol	D2555, CDN Isotopes
[$^2H_5$]HAVA	504 pmol	Previously produced in FPM* group
[$^2H_4$]HACA	105 pmol	Previously produced in FPM group
[$^2H_4$]CML	973 pmol	Previously produced in FPM group
[$^2H_4$]CEL	432 pmol	Previously produced in FPM group
[$^2H_8$]MDAL	62 pmol	Previously produced in FPM group

* Metabolic pathophysiology

4.4.4a.2. Preparation of standards

The following isotopically labeled standards were added to each sample: [$^2H_8$]lysine (d8-Lys); [$^2H_4$]CML (d4-CML), [$^2H_4$]CEL (d4-CEL), and [$^2H_8$]MDAL (d8-MDAL), and [$^2H_5$]5-HAVA[4] (for GSA quantification) and [2H4]6-HACA[5] (for AASA quantification) just before hydrolyzing with HCl. ***Table 5*** shows the final concentration of each deuterated standard added to the samples. The presence of deuterated standards in the samples serves to identify the corresponding amino acids in the sample. Deuterated amino acids have the same RT, but a higher mass/z value (***Table 6***).

Table 6. The m/z and RT of deuterated and non-deuterated amino acids.

Standard	Chemical name	m/z	RT (min)
Lysine	Lysine	180	25
[$^2H_8$]Lysine	L-Lysine-3,3,4,4,5,5,6,6-d8 HCl	187	
HAVA	5-hydroxy-2-aminovaleric acid	280	10
[$^2H_5$]HAVA	[$^2H_5$]-5-hydroxy-2-aminovaleric acid	285	
HACA	6-hydroxy-2-aminocaproic acid	294	14
[$^2H_4$]HACA	[$^2H_4$]-6-hydroxy-2-aminocaproic acid	298	
CEL	Nε-(carboxyethyl)lysine	379	35
[$^2H_4$]CEL	[$^2H_4$]Nε-(carboxyethyl)lysine	383	
CML	Nε-(carboxymethyl)lysine	392	35
[$^2H_2$]CML	[$^2H_2$]Nε-(carboxymethyl)lysine	393	
MDAL	Nε-(malondialdehyde)lysine	474	35
[$^2H_8$]MDAL	[$^2H_8$]Nε-(malondialdehyde)lysine	482	

m/z: mass-to-charge; RT: retention time

[4] HAVA (5-hydoxy-2-aminovaleric acid) is the reduced form of GSA. The latter is highly unstable and is reduced to HAVA, therefore, GSA can be measured by the quantification of HAVA.
[5] HACA (6-hydroxy-2-aminocaproic acid) is the reduced form of AASA. The latter is highly unstable and is reduced to HACA, therefore, AASA can be measured by the quantification of HACA.

4.4.4a.3. Standard curve of undeuterated standards

The various concentrations of standards, as shown in ***Table 7***, were prepared in triplicate. The fixed volumes of deuterated internal standards were also added to each concentration to facilitate the detection of undeuterated standards. These standards were processed and then injected into the GC-MS as samples. The under peak area for each concentration was used for preparing the standard curve for that marker.

Table 7. Concentration and the volume of deuterated and undeuterated standards used for preparation of standard curve.

Standard	Conc. (pmol/µl)	ST0 (µl)	ST1 (µl)	ST2 (µl)	ST3 (µl)	ST4 (µl)	ST5 (µl)	ST6 (µl)
d8-Lys	12000	10	10	10	10	10	10	10
d5-HAVA	72	7	7	7	7	7	7	7
d4-HACA	17.5	6	6	6	6	6	6	6
d2-CML	162.23	6	6	6	6	6	6	6
d4-CEL	144	3	3	3	3	3	3	3
d8-MDAL	20.69	3	3	3	3	3	3	3
Lys	13600	0	10	15	20	25	50	75
HAVA	90	0	2	4	8	10	15	20
HACA	12	0	5	10	15	20	30	40
CML	40	0	2	4	8	10	12	16
CEL	68.74	0	2	4	8	10	12	16
MDAL	9.93	0	2	3	4	5	7	10
Carrier	-	10	10	10	10	10	10	10
Total volume	-	45	68	85	107	125	171	222

4.4.4a.4. GC-MS analysis

GC-MS analyses were performed on a Hewlett-Packard model 6890 GC equipped with a 30-m HP-5MS capillary column (30 m x 0.25-mm x 0.25 µm) coupled to a Hewlett-Packard model 5973A mass selective detector (Agilent Technologies, Barcelona, Spain). The temperature of the injection port was held at 270°C. The temperature program was set as follows: 5 min at 110°C, then 2°C/min at 150°C, then 5°C/min at 240°C, then 25°C/min at 300°C, and is finally maintained at 300°C for 5 min. Flow rate was 0.2 ml/min. Analytes were detected by selected ion-monitoring GC-MS.

4.4.4a.5. Calculation of analyte content

Quantification was performed using standard curves constructed from mixtures of deuterated and non-deuterated standards for each marker (***Table 7***). Finally, the amount of each marker was expressed as micromoles of that marker per moles of lysine.

4.4.4b. Determination of fatty acid composition by GC-FID

4.4.4b.1. Sample processing

The tubes containing chloroform were subjected to FA composition determination. The chloroform was evaporated by the N2 evaporator (N-evap model 113 Organomation Association, Berlin, MA, USA) for 20 min. Then, the lipids were esterified by adding 2 mL methanolic HCl (HCl in methanol) 5% (v/v), and subsequent incubation for 90 min at 75°C (Tembloc Selecta, Barcelona, Spain). The resulting fatty acid methyl esters (FAMEs) were extracted by adding 1 mL saturated NaCl (36 g NaCl/100 mL deionized H2O) and 2 mL pentane to each sample (this order should not be inverted). The mixture was mixed on a vortex and then centrifuged at 4°C and 4400 rpm for 5-15 min. The pentane fraction (top) containing FAMEs was transferred to another clean glass tube and evaporated under N2 gas. Finally, the precipitation was dissolved in an appropriate[6] volume of carbon disulfide (CS2) (Sigma-Aldrich) of which 2 µl was used for GC analysis.

4.4.4b.2. GC analysis

The analysis was performed on a GC System model 7890A with a series injector 7683B and a FID equipped with a DB-23 capillary column (30 m x 0.25 mm x 0.25 µm) (Agilent Technologies, Barcelona, Spain). The injections were performed in splitless mode. The injection port is maintained at 220°C and the detector at 250°C. The flow rate of helium (99.99%) carrier gas was maintained at a constant rate of 2 ml/min. The column temperature was held at 100°C for 1min, then increased by 10°C/min to 200°C for 10 min, and increased by 5°C/min to 240°C for 7min, and was finally maintained at 240°C for 10 min.

[6] This volume depends on the initial volume of the sample and type of the sample.

4.4.4b.3. Fatty acid standards

We used a series of standard FAMEs and their combinations to determine the RT of the same FAMEs in the samples. ***Table 8*** shows the list of all FAMEs that were measured in plasma and CSF and the reference number corresponding to their standard.

Table 8. All FAMEs measured in plasma and CSF. The FA names is indicated instead of FAME (i.e. myristic acid instead of myristic acid methyl ester).

Common name	IUPAC name	Formula	Reference
Myristic acid*	Tetradecanoic acid	C14:0	M3378[#]
Palmitic acid*	Hexadecanoic scid	C16:0	76159[#]
Palmitoleic acid	cis-9-Hexadecenoic acid	C16:1 (n-7)	76176[#]
Stearic acid	Octadecanoic Acid	C18:0	85769[#]
Oleic acid	cis-9-Octadecenoic acid	C18:1 (n-9)	31111[#]
Vaccenic acid	cis-11-Octadecenoic acid	C18:1 (n-7)	CRM46904[#]
Linoleic acid	cis-9,12-Octadecadienoic acid	C18:2 (n-6)	62280[#]
α-Linolenic acid	cis-9, 12, 15-Octadecatrienoic acid	C18:3 (n-3)	L6031[#]
Stearidonic acid[P]	cis-6,9,12,15-octadecatetraenoic acid	C18:4 (n-3)	10005000[η]
Arachidic acid	Eicosanoic acid	C20:0	10941[#]
Eicosenoic acid	cis-11-Eicosenoic acid	C20:1 (n-9)	17263[#]
Eicosadienoic acid	cis-9,12-Eicosadienoic acid	C20:2 (n-6)	20-2021-2[δ]
Eicosatrienoic acid[P]	cis-11,14,17-Eicosatrienoic acid	C20:3 (n-3)	E6001[#]
Dihomo-γ-linolenic acid	cis-8,11,14-Eicosatrienoic acid	C20:3 (n-6)	10006580[η]
Arachidonic acid	cis- 5,8,11,14-Eicosatetraenoic acid	C20:4 (n-6)	90014[η]
Eicosapentaenoic acid[C]	cis-5,8,11,14,17-Eicosapentaenoic acid	C20:5 (n-3)	CRM47571[#]
Behenic acid	Docosanoic acid	C22:0	11940[#]
Erucic acid	cis-13-Docosenoic acid	C22:1 (n-9)	20568[#]
Adrenic acid	cis-7,10,13,16-Docosatetraenoic acid	C22:4 (n-6)	D3534[#]
Lignoceric acid	Tetracosanoic acid	C24:0	L6766[#]
Docosapentaenoic acid	cis-7,10,13,16,19-Docosapentaenoic acid	C22:5 (n-3)	17269[#]
Docosahexaenoic acid	cis-4,7,10,13,16,19-Docosahexaenoate	C22:6 (n-3)	D2659[#]
Nervonic acid[C]	cis-15-Tetracosenoic acid	C24:1 (n-9)	20-2401-9[δ]

[C]: Measured only in CSF; [P]: Measured only in plasma; IUPAC: International Union of Pure and Applied Chemistry; #: Sigma-Aldrich, St Louis, MO, USA; η: Cayman Chemicals, ANN Arbor, MI, USA; δ: Larodan AB, Solna, Sweden

4.4.4b.4. Data analysis

Identification of FAMEs (FAs) was performed by comparison with authentic standards (***Table 8***). Results were expressed as the percentage of measured FAME to all measured FAMEs (defined as 100%). The FA profile detected, identified and quantified represents

more than 95% of the total chromatogram. In addition, the following FA indexes were calculated:

- Saturated fatty acids (SFA)
    - SFA = Σ %mol saturated fatty acids
- Unsaturated fatty acids (UFA)
    - UFA = Σ %mol unsaturated fatty acids
- Monounsaturated fatty acids (MUFA)
    - UFA = Σ %mol monounsaturated fatty acids
- Polyunsaturated fatty acids (PUFA)
    - PUFA = Σ %mol polyunsaturated fatty acids
- Polyunsaturated fatty acids from n-3 series (PUFA n-3)
    - PUFA n-3 = Σ %mol polyunsaturated fatty acids n-3
- Polyunsaturated fatty acids from n-6 series (PUFA n-6)
    - PUFA n-6 = Σ %mol polyunsaturated fatty acids n-6
- Average chain length (ACL) =
    - ACL = [(Σ %mol total C_{14} x 14) + (Σ %mol total C_{16} x 16) + (Σ %mol total C_{18} x 18) + (Σ %mol total C_{20} x 20) + (Σ %mol total C_{22} x 22)+ (Σ %mol total C_{24} x 24)]/100]
- Double bond index (DBI)
    - DBI= [(1 x Σmol% monoenoic) + (2 x Σmol% dienoic) + (3 x Σmol% trienoic) + (4 x Σmol% tetraenoic) + (5 x Σmol% pentaenoic) + (6 x Σmol% hexaenoic)]
- Peroxidability index
    - Peroxidability index= [(0.025 x Σmol% monoenoic) + (1 x Σmol% dienoic) + (2 x Σmol% trienoic) + (4 x Σmol% tetraenoic) + (6 x Σmol% pentaenoic) + (8 x Σmol% hexaenoic)]
- Anti-inflammatory index (AI)
    - AI = [[(20:3n-6) + (20:5n-3) + (22:6n-3)]/ (20:4n-6)] × 100
- Estimation of delta-5 fatty acid desaturase (Δ5 Fads1) activity = C20:4 (n-6)/C20:3 (n-6)
- Estimation of Δ6 Fads2 activity = C18:4 (n-3)/C18:3 (n-3)

- Estimation of Δ8 Fads2 activity = C20:3 (n-6)/C20:2 (n-6)
- Estimation of Δ9 desaturase (stearoyl-CoA desaturase-1) activity = C16:1 (n-7)/C16:0
- Estimation of Δ9 desaturase activity = C18:1 (n-9)/C18:0
- Estimation of enzymatic activity of n-6 pathway = C22:5 (n-6)/C18:2 (n-6)
- Estimation of enzymatic activity of n-3 pathway = C22:6 (n-3)/C18:3 (n-3)
- Estimation of elongase 3 activity = C20:1 (n-9)/C18:1 (n-9)
- Estimation of elongase 5 activity = C20:2 (n-6)/C18:2 (n-6)
- Estimation of elongase 6 activity = C18:0/C16:0
- Estimation of elongase 1, 3, and 7 activities = C20:0/C18:0
- Estimation of elongase 1, 3, and 7 activities = C22:0/C20:0
- Estimation of elongase 2 and 5 activities = C22:4 (n-6)/C20:4 (n-6)
- Estimation of elongase 2 and 5 activities = C22:5 (n-3)/C20:5 (n-3)

4.4.5. Reagents:

Homogenizing buffer: To prepare 250 ml homogenizing buffer, 180 mM potassium chloride, 5 mM MOPs ((3-(N-morpholino)propanesulfonic acid), 2 mM EDTA, 1 mM DTPAC (Diethylenetriaminepentaacetic acid) was dissolved in 250 ml (final volume) MilliQ water and stored at 4°C. At the time of use, 1 µl BHT (Butylated hydroxytoluene) 1 µM was added to each ml of the solution.

HCl 6 N: 125 ml HCl (37%) was slowly added to 125 ml MilliQ water.

Methanolic HCl solution: To prepare 20 ml solution, 18.7 ml methanol was added to an appropriate Erlenmeyer flask, then, acetyl chloride was added dropwise by use of a Pasteur pipette fitted with a rubber bulb at the top[7].

Borate solution: 0.47 gr sodium borhydride (NaBH4) was added to 25 ml sodium tetraborate (Na2B4O7) (0.2 M pH 9.2) tampon solution. This solution is effervescent;

[7] Caution should be taken at the time of preparation because this solution is highly exothermic.

therefore, it should be prepared just before use. If tampon solution contained crystals, it should be warmed up previously in a microwave for some seconds.

Na2B4O7 (o.2 M pH 9.2) tampon solution: 19.07 g sodium tetraborate (borax) was dissolved gradually in 100 ml hot deionized water. The volume was adjusted to 250 ml and the pH to 9.2.

4.5. Untargeted Lipidomics

To study lipids, we analyzed CSF and plasma samples of patients with AD, MCI, and control subjects by means of untargeted high performance liquid chromatography coupled to mass spectrometry (HPLC-MS/MS) technique. This method was suitable for detecting the majority of classes of lipids. The statistically significant lipids were subsequently identified using the tandem mass spectrometry (MS/MS) method.

4.5.1. HPLC-MS/MS principle

The principle of HPLC-MS is as set out in section 4.4.2., except for the chromatographic part in which the mobile phase is a liquid and, therefore, the sample is not vaporized after injection.

MS/MS is a technique where two or more mass analyzers are coupled together to increase their abilities to analyze the chemical structure of molecules. The sample is ionized and the first spectrometer (MS1) separates these ions by their m/z ratio. Ions of a specific m/z ratio originated from MS1 are selected and then made to split into smaller fragment ions. The second mass spectrometer (MS2) separates these smaller fragments by their m/z ratio and detects them. The fragmentation step enables identifying and separating ions that have very similar m/z ratios in regular mass spectrometers (***Figure 15***).

4.5.2. Preparation of lipid standards

Lipid standards consisting of isotopically labeled lipids (***Table 9***) were used for external standardization (i.e., lipid family assignment) and internal standardization (i.e., for adjustment of inter- and intra-assay variances). Stock solutions were prepared by

dissolving lipid standards in methyl tert-butyl ether (MTBE) at a concentration of 1 mg/ml, and working solutions were diluted to 2.5 µg/mL in MTBE.

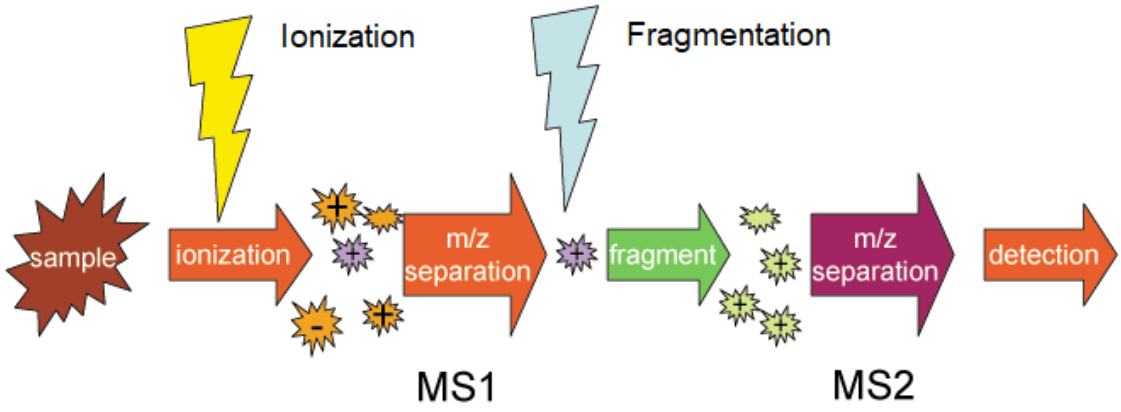

Figure 15. Schematic of tandem mass spectrometry. Adapted from https://en.wikipedia.org/wiki/Tandem_mass_spectrometry. Under the creative commons CC BY-SA license.

Table 9. Class representative internal standards added to the samples in lipidome study.

Lipid name	Reference
1,3(d5)-dihexadecanoyl-glycerol	110537*
1,3(d5)-dihexadecanoyl-2-octadecanoyl-glycerol	110543*
1-hexadecanoyl(d31)-2-(9Z-octadecenoyl)-sn-glycero-3-phosphate	110920*
1-hexadecanoyl(d31)-2-(9Z-octadecenoyl)-sn-glycero-3-phosphocholine	110918*
1-hexadecanoyl(d31)-2-(9Z-octadecenoyl)-sn-glycero-3-phosphoethanolamine	110921*
1-hexadecanoyl-2-(9Z-octadecenoyl)-sn-glycero-3-phospho-(1'-rac-glycerol-1',1',2',3',3'-d5)	110899*
1-hexadecanoyl(d31)-2-(9Z-octadecenoyl)-sn-glycero-3-phospho-myo-inositol	110923*
1-hexadecanoyl(d31)-2-(9Z-octadecenoyl)-sn-glycero-3-[phospho-L-serine]	110922*
26:0-d4 Lysophosphocholine	860389*
18:1 Chol (D7) ester	111015*
cholest-5-en-3ß-ol (d7)	LM-4100*
D-erythro-sphingosine-d7	860657*
D-erythro-sphingosine-d7-1-phosphate	860659*
N-palmitoyl-d31-D-erythro-sphingosine	868516*
N-palmitoyl-d31-D-erythro-sphingosylphosphorylcholine	868584*
Octadecanoic acid-2,2-d2	19905-58-9#

*: Avanti Polar Lipids, Alabaster, AL, USA; #: Sigma-Aldrich, St Louis, Mo, USA

4.5.3. Lipid Extraction

Lipidomics analysis was based on a previously validated method published by Pizarro et al., (Pizarro et al., 2013). Briefly, plasma and CSF samples were defrosted on ice and vortex mixed. In order to precipitate the protein fraction, 10 µl of the samples was mixed with 5 µl of deionized water and 20 µl of ice-cold methanol. The samples were vigorously shaken by vortex for 2 min. Subsequently, 250 µl standard mixture in MTBE was added and the samples were sonicated in a water bath (ATU Ultrasonidos, Valencia, Spain). In this process, ultrasound waves at a frequency of 40kHz and a power of 100W were applied for 30 min at 10°C. Then, 25 µl deionized water was added to the mixture, and organic phase was separated by centrifugation (1400 g) at 10°C for 10 min. Finally, 160 µl of the supernatant (containing lipids) was transferred to injection vials (Agilent Technologies, Barcelona, Spain). Furthermore, 20 µl of each processed sample was pooled and then aliquoted to be used as quality control.

4.5.4. Equipment

The analysis was performed through liquid chromatography coupled to a hybrid mass spectrometer with electrospray ionization and a quadrupole time of flight type (LC-ESI-QTOF-MS/MS). The equipment for the liquid chromatography phase was an ultra-high performance liquid chromatograph (UHPLC) model 1290 coupled to ESI-Q-TOF MS/MS model 6520 both from Agilent Technologies (Barcelona, Spain).

4.5.5. Analysis conditions

Lipid extracts were analyzed following the method published by Castro-Perez et al. (Castro-Perez et al., 2010). Sample compartment of the UHPLC was refrigerated at 4°C and for each sample, 10 µl of lipid extract was injected into a 1.8 µm particle 100 × 2.1mm id Waters Acquity HSS T3 column (Waters, Mildord, MA) heated to 55°C. The flow rate was 400 µl/min with solvent A composed of 10 mM ammonium acetate in acetonitrile-water (40:60, v/v) and solvent B composed of 10 mM ammonium acetate in acetonitrile-isopropanol (10:90, v/v).

The gradient started at 40% of mobile phase B and reached 100% B in 10 minutes and held for 2 min. Finally, the system was switched back to 60% of mobile phase B and was equilibrated for 3 min. Duplicate runs of the samples were performed to collect positive and negative electrospray ionized lipid species in TOF mode, operated in full-scan mode at 100 to 3000 m/z in an extended dynamic range (2 GHz), using N2 as nebulizer gas (5L/min, 350°C). The capillary voltage was set at 3500 V with a scan rate of 1 scan/s. Continuous infusion using a double spray with masses 121.050873, 922.009798 (positive ion mode) and 119.036320, 966.000725 (negative ion mode) was used for in-run calibration of the mass spectrometer.

4.5.6. Data analysis

MassHunter Data Analysis Software (Agilent Technologies, Barcelona, Spain) was used to collect the results and MassHunter Qualitative Analysis Software (Agilent Technologies, Barcelona, Spain) to obtain the molecular features of the samples, representing different, co-migrating ionic species of a given molecular entity using the molecular feature extractor algorithm (Agilent Technologies, Barcelona, Spain) (Jové et al., 2013). Briefly, the molecular feature extractor algorithm uses the accuracy of the mass measurements to group related ions (basing on charge-state envelope, isotopic distribution and/or the presence of different adducts and dimers/trimers) assigning multiple species (ions) to a single compound referred to as a feature. Finally, MassHunter Mass Profiler Professional Software (Agilent Technologies, Barcelona, Spain) was used to perform a non-targeted lipidomic analysis over the extracted features. Only those features with a minimum abundance of 5000 counts and 2 ions as a minimum were selected. After that, the molecular characteristics in the samples were aligned using a RT window of 0.1% ± 0.25 minutes and 20.0 ppm ± 2.0 mDa. Finally, to avoid background noise, only common features (found in at least 50% of the samples of the same condition) were taken into account to correct for individual bias. The features defined by exact mass and RT were searched for their identification in the human metabolome database website: https://hmdb.ca. The adduct types selected for search are listed in ***Table 10***. Molecular weight tolerance was adjusted to 30 ppm. The RT of the obtained identities were compared to the retention time of the authentic standards that

were added to the samples. Finally, the identities were confirmed by MS/MS through checking the MS/MS spectrums using LipidBlast software (Kind et al., 2013) and LipidMatch (an R-based tool for lipid identification) (Koelmel et al., 2017).

Table 10. Adduct types that were selected for search in HMDB.

Adduct type	
Positive mode	**Negative mode**
M+H	M-H
M+H-H2o	M+Hac-H
M+NH4-H2o	
M+NH4	
M+Na	
M+K	

4.6. Statistical analysis

All statistical analyses were performed using IBM SPSS version 25 (SPSS Inc., Chicago, IL, United States).

4.6.1. Demographic data

One-way ANOVA (or non-parametric Kruskal-Wallis) and Chi-square (or Fisher's exact) tests were used for the analysis of quantitative and qualitative variables between three diagnostic groups, respectively. Student's t (or the Mann Whitney U) and Chi-square (or Fisher's exact) tests were used for the analysis of quantitative and qualitative variables between progressive and non-progressive MCI groups. The quantitative variables were presented as means (± standard deviation, SD) or medians (25th;75th percentiles), and the qualitative variables were presented as percentages (number).

4.6.2. Experimental data analysis

For lipidomics, as the samples were injected in positive and negative ionization mode, we had four databases (plasma in positive ionization mode, plasma in negative mode, CSF in positive mode, and CSF in negative ionization mode) that were analyzed

separately. We did not mix the data corresponding to positive and negative ionizations for each biological fluid due to an overfitting problem.

The data regarding generic plasma lipid profile (TC, LDL-C, HDL-C, and TG), FA composition and oxidative stress damage markers were analyzed together. The cross-sectional association of experimental variables with quantitative outcomes (Aβ42, Ttau, Ptau, and time to progression) was assessed using Spearman's correlation. The data were adjusted for age, sex, APOE ε4 allele, MMSE, and appropriate AD core biomarkers. The cross-sectional association of the experimental variables with categorical outcomes (diagnosis, Aβ42 status, Ttau status, Ptau status, progression/no progression, and time to progression) was studied using logistic regression models. For these analyses, the values corresponding to each independent variable were dichotomized by their median and the high value (> median) of each variable was compared to its low value (≤ median) because when we have a high number of predictors, logistic regression analyses fit categorical predictors better. The logistic regression expresses the probability of an event occurring (pathologic levels of Aβ42, Ttau, and Ptau, and progression) versus the probability that it does not occur (non-pathologic levels of Aβ42, Ttau, and Ptau, and no progression) as a function of independent variables. The logistic model expresses the odds (relative risk) as an exponential function of the independent variables:

$$OR = \frac{p}{1-p} = e^{\beta 0+\beta 1X1+\beta 2X2\cdots \beta nXn}$$

In this equation p is the probability of an event occurring and Xi (i = 1, 2, 3, …, n) are independent variables (lipids). βi are regression coefficients that are going to be estimated in the analysis. An OR > 1 means that high levels of the variable increase the probability of the event compared to its low levels, while an OR < 1 means that high levels of the variable reduces the probability of the event compared to its low levels. Therefore, the presence of a dichotomous factor compared to its absence multiplies the odds by the $e^{\beta i}$ value. As a result, the significant influence of a factor will be measured in terms of the variation produced in the odds. For each model, a receiver operating curve (ROC) was provided to evaluate its quality. A model with AUC ≥ 70 was considered as valid. In addition, to see whether logistic regression models fitted to our data well, a Hosmer-Lemeshow test was performed for each model. In fact, this statistical test,

evaluates the goodness of fit of the regression model, that is, the degree to which the predicted probability fits the reality. The Hosmer-Lemeshow statistic indicates a poor fit if its significance value is less than 0.05. When analyzing variables associated with progression, the AUC of the regression model including lipids were compared to the same model without lipids with the Hanley-McNeil test (Hanley & McNeil, 1983) to see whether lipids have a significant effect in discriminating progressive from non-progressive patients. Values of z above the cutoff are taken as evidence that the "true" ROC areas are different.

To minimize the negative effects of overfitting when working with many predictor variables, two criteria were applied:

1) Selection of variables was performed based on step-by-step forward selection with conditional criteria. In detail, it begins with a model that contains no variable (null model). It then starts adding the most significant variables one after the other as long as they improve the predictive power of the model with respect to the variables already included. The process stops when there are no more significant variables for incorporation. The selection of variables by steps also allows detecting multicollinearity. It means that if two independent variables are highly related, only one of them will enter the model (if it has a significant impact). Detection of multicollinearity increases the precision of estimated coefficients and power of the statistical analysis, however, we will lose some variables that may be highly related to the dependent variables in the model (e.g., from the same metabolic pathway). To overcome this problem, after running each regression analysis we eliminated the variables that had been inputteded into the model, and the analysis was run again to let other influential lipids, if they exist, enter the model. In this way, we had several regression models for each comparison. This process was continued until the AUC of the model reached < 70.
2) The level of significance for the input of variables was adjusted to 1% ($\alpha = 0.01$) since a more relaxed level (5%) could increase the overall probability of finding results just by the mere fact of carrying out many analyses on different variables obtained in our sample. Exceptionally, for the database related to CSF samples

injected in negative ionization mode the significance level was adjusted to 0.05 because we had only 27 lipid variables in this database and, therefore, the risk of overfitting was low.

The association of variables with the rate of progression from MCI to AD was studied using the Cox hazard model. This analysis allows us to model survival (time to progression) as a function of time and a factor or set of independent factors. It allows the estimation of the relative risks related to the risk of progression from MCI to AD due to having certain levels of certain biological variables. The low levels of the biological variables are considered as reference in this model. Both aforementioned criteria for minimizing the negative effects of overfitting were also applied on these models.

Finally, all models were adjusted for age, sex, APOE ε4 allele, MMSE, and, if applicable, appropriate AD core CSF biomarkers (Aβ42, Ttau and Ptau), including these parameters as predictors. Plasma FA composition and oxidative protein damage analyses were only adjusted for age, sex, and presence of APOE ε4 allele because CSF biomarkers had not been measured for control samples originating from Sevilla.

RESULTS

5. Results

5.1. Determination of fatty acid composition and markers of oxidative protein damage in CSF

5.1.1. Study population

For this study, we included 210 participants that were divided into three diagnostic groups: 91 (43.3%) AD, 93 (44.3%) MCI, and 26 (12.4%) controls (CTL). There was no significant difference between groups for sex ($p = 0.44$), while age differed significantly between them ($p < 0.001$). As expected, there was a significant difference in MMSE, APOE ε4 allele frequency, and AD core biomarkers between diagnostic groups. Control subjects had a better cognitive state (median MMSE score of 30) compared to MCI and AD patients (median MMSE score of 27 and 23, respectively). They had significantly higher levels of Aβ42 (1029 pg/ml) compared to MCI (595 pg/ml) and AD (493 pg/ml) patients. On the other hand, Ttau and Ptau levels in CSF were higher in AD patients (494 and 81 pg/ml, respectively) compared to MCI (334 and 63 pg/ml) and CTL (247 and 45 pg/ml) groups. Regarding APOE ε4 allele, prevalence was higher among AD patients (51.6%), while it was 40.2% and 7.7% for MCI and CTL, respectively (***Table 11***).

The patients with MCI were followed-up for a mean of 58 months to evaluate their progression to AD. Our results showed that 48 patients (52.7%) progressed to AD, while 44 patients (47.3%) remained cognitively stable. There was not a significant difference in age, sex, and MMSE between progressive and non-progressive patients. The progressive MCI patients had significantly lower levels of Aβ42 (478 pg/ml) and higher levels of Ttau (447 pg/ml) and Ptau (76 pg/ml) in CSF compared to non-progressive patients (798, 265, and 54 pg/ml, respectively). The prevalence of APOE ε4 allele was also higher in progressive MCI patients (63%) versus non-progressive MCI patients (19.5%) (***Table 12***).

Table 11. Characteristics of the study population used to determine fatty acid composition and markers of oxidative protein damage in CSF.

	Total (N = 210)	AD (N = 91)	MCI (N = 93)	CTL (N = 26)	*p*
Age	74 [70;78]	76 [72;80]	73 [69; 77]	66 [60;74]	< 0.001
Sex (f)	54.3% (114)	59.3% (54)	51.1% (47)	50% (13)	0.437
MMSE	25 [23;28]	23 [22;25]	27 [25;28]	30 [28;30]	< 0.001
Aβ42*	551 [420;729]	493 [395;583]	595 [435;864]	1029 [634;1331]	< 0.001
Ttau*	400 [248;601]	494 [357;705]	334 [229;542]	247 [139;313]	< 0.001
Ptau*	67.35 [48;92]	81 [54; 98]	63 [44;87]	45 [30;63]	< 0.001
APOE ε4	43.4% (86)	51.6% (47)	40.2% (37)	7.7% (2)	0.003

f: female; * values are pg/ml; *P*-values were calculated by comparing diagnostic groups using one-way ANOVA (or non-parametric Kruskal-Wallis test) for quantitative variables and Chi-square test for qualitative variables.

Table 12. Characteristics of progressive and non-progressive MCI patients.

	Total (N = 92)	Progressive (N = 48)	Non-progressive (N = 44)	*p*
Age	72 (6.0)	73 (6.0)	72 (5.4)	0.328
Sex (f)	50% (46)	52.1% (25)	47.7% (21)	0.673
MMSE	27 [25;28]	26 [24;28]	27 [26;29]	0.063
Aβ42*	589[432;864]	478 [374;619]	798 [582;928]	< 0.001
Ttau*	333 [227;534]	447 [259;709]	265 [198;353]	< 0.001
Ptau*	64 [43;86]	76 [49;107]	54 [40;66]	0.001
APOE ε4	40.2% (37)	63% (29)	19.5% (8)	< 0.001

f: female;*: values are pg/ml; *P*-values were calculated by comparing groups using student's t-test (or Mann Whitney U test) for quantitative variables and Pearson's Chi-square test for qualitative variables.

5.1.2. Association of CSF fatty acids and oxidative protein damage markers with diagnosis of MCI and AD

Twenty-two FAs, 24 FA-related indexes and five oxidative protein damage markers in CSF were evaluated. The association of these variables with diagnosis (AD, MCI, and CTL) was evaluated by a multinomial regression analysis. When the control group was set as the reference category, none of the variables was associated with the diagnosis of AD or MCI versus control (**Supplementary Table 2**). However, selecting the MCI group as a reference, a model including age and anti-inflammatory index (AI) was able to separate AD from MCI patients with an AUC = 0.704 (99% CI 0.602 - 0.806, $p < 0.001$). In this model higher ages increased the probability of AD diagnosis (OR 1.144, 99% CI 1.046 – 1.251, *p*

< 0.001) versus MCI, while higher levels of AI reduced this probability (OR 0.350, 99% CI 0.132 – 0.924, p = 0.005) (***Table 13***). The Hosmer-Lemeshow test for goodness of fit yielded a p = 0.105. Markers of oxidative protein damage were not associated with diagnosis.

Table 13. Variables associated with diagnosis (AD vs MCI). MCI was set as the reference category.

Name	*p*	OR	99% CI for OR	AUC
Age	< 0.001	1.144	1.046 – 1.251	0.704, 99% CI
AI	0.005	0.350	0.132 – 0.924	0.602-0.806, p < 0.001

AI: anti-inflammatory index

5.1.3. Association of CSF fatty acids and oxidative protein damage markers with Aβ42 status in CSF

In this analysis, we searched for variables that significantly increase or decrease the probability of having pathological levels of Aβ42 in CSF (≤ 600 pg/ml). Our results showed that with the presence of age, sex, APOE ε4 allele, MMSE, Ptau, and Ttau as covariables, none of the under-study variables was associated with Aβ42 status.

5.1.4. Association of CSF fatty acids and oxidative protein damage markers with Ptau status in CSF

The association of the variables with tau pathology was evaluated by dividing the study population into two groups based on the measures of Ptau in CSF. Subjects who had Ptau > 65 pg/mL were considered positive, while those with Ptau ≤ 65 pg/mL were considered negative for tau pathology. Our results showed that with the presence of age, sex, APOE ε4 allele, MMSE, Aβ42, and Ttau as covariables, none of the under-study variables was associated with Ptau status.

5.1.5. Association of CSF fatty acids and oxidative protein damage markers with Ttau status in CSF

The association of the variables with Ttau pathology (neurodegeneration) was evaluated by dividing the study population into two groups based on the measures of Ttau in CSF. Subjects who had Ttau > 425 pg/mL were considered positive, while those with Ttau ≤ 425 pg/mL were considered negative for Ttau. Our results showed that with the presence of age, sex, APOE ε4 allele, MMSE, Aβ42, and Ptau as covariables, none of under-study variables was associated with Ttau status.

5.1.6. Association of CSF fatty acids and oxidative protein damage markers with progression from MCI to AD

The association of lipids with progression was evaluated by comparing the profile of variables of patients who progressed (N =49) vs patients who did not progress (N = 43) to AD after a mean follow-up of 58 (±12.5) months. To adjust the data for possible confounding variables, age, sex, APOE ε4 allele, and levels of Aβ42, Ttau, and Ptau in CSF were inputted to the analysis as covariates. The CSF levels of none of the oxidative protein damage markers were associated with progression. Our statistical analysis showed that DHA was associated with MCI to AD progression. In this model, the presence of the APOE ε4 allele increased the risk of progression, while higher scores for MMSE and higher levels of DHA in CSF were associated with a reduced risk of progression. The AUC of the model was 0.782 (95% CI 0.655 – 0.909, $p < 0.001$) (***Table 14***). To evaluate the effect of DHA in the model, we calculated the AUC of the model consisting of APOE ε4 allele and MMSE without DHA. The model only with APOE ε4 allele and MMSE had an AUC = 0.766 (95% CI 0.634 – 0.898, $p < 0.001$) that was not significantly different from the model that included DHA after comparison of AUCs by means of the Hanley-McNeil test ($z=0.351$, $|z|<1.96$).

5.1.7. Association of CSF fatty acids and oxidative protein damage markers with rate of progression and modeling rate of progression

The association of lipids with the rate of progression (progression as a continuous dependent variable) was evaluated by the Cox hazard model. This regression model relates time to progression with the event of progression in the presence of influential variables. In this analysis age, sex, APOE ε4 allele, and levels of amyloid, Ttau, and Ptau in CSF were inputted to the analysis as covariates. We did not detect any association between studied variables and the rate of progression.

Table 14. CSF fatty acids associated with progression from MCI to AD.

Name	*p*	OR	95% CI for OR	AUC
APOE ε4	< 0.001	32.837	5.550 – 194.300	0.782, 95% CI 0.655 – 0.909, $p < 0.001$
MMSE	0.016	0.692	0.514 – 0.932	
DHA (C22:6 (n-3))	0.021	0.135	0.025 – 0.736	

5.2. Determination of fatty acid composition and markers of oxidative protein damage in plasma

5.2.1. Study population

For this study, we included 286 participants that were divided into three diagnostic groups: 103 (36%) AD, 89 (31.1%) MCI, and 94 (32.9%) CTL. There was no significant difference between groups for sex ($p = 0.53$), while age differed significantly between them ($p < 0.001$). As expected, there was a significant difference in MMSE and APOE ε4 allele frequency between groups. CTL had a higher MMSE score (29.5) and lower APOE ε4 allele prevalence (5.9%) compared to MCI (27 and 42.7%, respectively) and AD (23 and 53.4%, respectively) groups. The external control samples lacked measures for AD CSF biomarkers (***Table 15***).

Table 15. Characteristics of the study population used to determine fatty acid composition and markers of oxidative protein damage in plasma.

	Total (N = 286)	AD (N =103)	MCI (N = 89)	CTL (N = 94)	*p*
Age	72 [68;77]	76 [72;80]	73 [69;77]	68 [61.75;73.75]	< 0.001
Sex (f)	153 (53.5%)	61 (59.2%)	45 (50.1%)	47 (50%)	0.348
MMSE	27 (24;29)	23 (22; 25)	27 (25;28)	29.5 (28;30)	< 0.001
Aβ42*	551 [420;718]	493 [395; 583]	604 [435; 872]	1016 [620; 1347]	< 0.001
Ttau*	408 [253;618]	494 [357;705]	332 [222; 542]	248 [139;337]	< 0.001
Ptau*	68 [48;92]	81 [54;98]	63 [42;87]	45 [30;63.17]	< 0.001
APOE ε4	38.4% (110)	53.4% (55)	42.7% (38)	5.9% (17)	< 0.001

f: female; *: values are pg/ml ; *P*-values were calculated by comparing diagnostic groups using one-way ANOVA (or non-parametric Kruskal-Wallis test) for quantitative variables and Chi-square test for qualitative variables.

5.2.2. Association of plasma fatty acids and oxidative protein damage markers with diagnosis of MCI and AD

We totally evaluated the composition of 22 FAs, 24 FA-related variables, four analytical variables (TC, LDL-C, HDL-C, and TG) and five oxidative protein damage markers. The association of these variables with the diagnosis (AD, MCI, and CTL) was evaluated by a multinominal regression analysis. We found that oleic acid (OA, C18:1 (n-9)) and vaccenic acid (VA, C18:1 (n-7)) were associated with the diagnosis. Our results showed that higher levels of VA increased the probability of being AD vs CTL (OR 5.382, 99% CI 1.623 – 17.851, $p < 0.001$) and also the probability of being AD vs MCI (OR 3.166, 99% CI 1.075 – 9.326, $p = 0.006$). On the other hand, the higher amounts of OA decreased the probability of being MCI vs CTL (OR 0.219, 99% CI 0.070 – 0.682), and AD vs CTL (OR 0.306, 99% CI 0.089 – 0.989 $p = 0.013$) (***Table 16***). The goodness of fit of the model was confirmed by -2Log likelihood ($p < 0.0001$). This statistic compares our model with the null model (without variables) and a $p < 0.05$ indicates that the variables have explanatory capacity. In addition, the goodness of fit of the model to the data was also confirmed by Pearson's Chi-square ($p = 0.597$) and deviance ($p = 0.999$) statistics that in both cases the higher *p*-values indicate that we have a good model. Plasma levels of oxidative protein damage markers were not associated with diagnosis.

Table 16. Plasma fatty acids associated with diagnosis of MCI and AD.

	Name	*p*	OR	99% CI for OR
AD vs CTL	Age	< 0.001	1.398	1.230 – 1.589
	APOE ε4	< 0.001	8.816	2.451 – 31.710
	OA(C18:1 (n-9))	0.013	0.306	0.089 – 0.989
	VA (C18:1 (n-7))	< 0.001	5.382	1.623 – 17.851
AD vs MCI	Age	< 0.001	1.194	1.073 – 1.328
	VA (C18:1 (n-7))	0.006	3.166	1.075 – 9.326
MCI vs CTL	Age	< 0.001	1.171	1.047 – 1.310
	APOE ε4	0.001	4.837	1.477 – 15.842
	OA (C18:1 (n-9))	0.001	0.219	0.070 – 0.682

5.2.3. Association of plasma fatty acids and oxidative protein damage markers with progression from MCI to AD

The association of lipids with progression was evaluated by comparing the profile of variables of patients who progressed (N = 47) vs patients who did not progress (N = 42) to AD after a mean follow-up of 58 (± 12.5) months (***Table 12***). To adjust the data for possible confounding variables, age, sex, and APOE ε4 allele, were inputted to the analysis as covariates. The data were not adjusted for AD biomarkers because control samples originating from Sevilla lacked this information. Our statistical analysis showed that higher levels of OA in plasma were associated with a reduced risk of progression to AD (OR 0.178, 95% CI 0.038 – 0.828). The AUC of the model was 0.816 (95% CI 0.700 – 0.932, $p < 0.001$) (***Table 17***). The Hosmer-Lemeshow test yielded a $p = 0.563$ indicating that the model was well fitted to the data. The model only with APOE ε4 allele had an AUC = 0.729 ($p < 0.001$, 95% CI 0.586 – 0.871) that was not significantly different from the AUC of the model consisting of APOE ε4 and OA (AUC = 0.816) ($z=1.337$, $|z|<1.96$).

Table 17. Plasma fatty acids associated with progression from MCI to AD.

Name	*p*	OR	95% CI for OR	AUC
APOE ε4	< 0.001	14.183	3.238 – 62.126	0.816, 95% CI
OA (C18:1 (n-9))	0.016	0.178	0.038 – 0.828	0.700 – 0.932, $p < 0.001$

5.2.4. Association of plasma fatty acids and oxidative protein damage markers with rate of MCI to AD progression and modeling rate of progression

The association of lipids with the rate of progression (progression as a continuous dependent variable) was evaluated by the Cox hazard analysis. This regression analysis relates time to progression with the event of progression in the presence of influential variables. Age, sex, and APOE ε4 allele were inputted to the analysis as covariates. Our result showed that higher levels of DHA in plasma were associated with a more rapid rate of progression (***Table 18***).

Finally, we compared the rate of progression predicted by the Cox hazard model with the rate of progression calculated by Kaplan-Meier analysis based on the clinical data. Our analysis demonstrated that the Cox model detected the variables associated with the rate of progression, however, these variables (APOE ε4 allele and DHA) could not predict this rate completely because the real rate of progression in the study population was faster. The rate of progression based on the Cox model was estimated at about 36% at 24 months (compared to the real rate of 50%) and 61% at 48 months (compared to the real rate of 70%) after MCI diagnosis (***Figure 16***).

Table 18. Plasma fatty acids associated with rate of progression from MCI to AD.

Name	*p*	OR	95% CI for OR	AUC
APOE ε4	< 0.001	8.008	3.092 – 20.744	0.766, 95% CI
DHA (C22:6 (n-3))	0.01	3.045	1.305 – 7.107	0.634 – 0.898, $p < 0.001$

5.3. CSF Lipidomics

5.3.1. Study population

The study population was the same as the population used for the determination of FA composition and markers of oxidative protein damage in CSF (***Table 11*** and ***Table 12***).

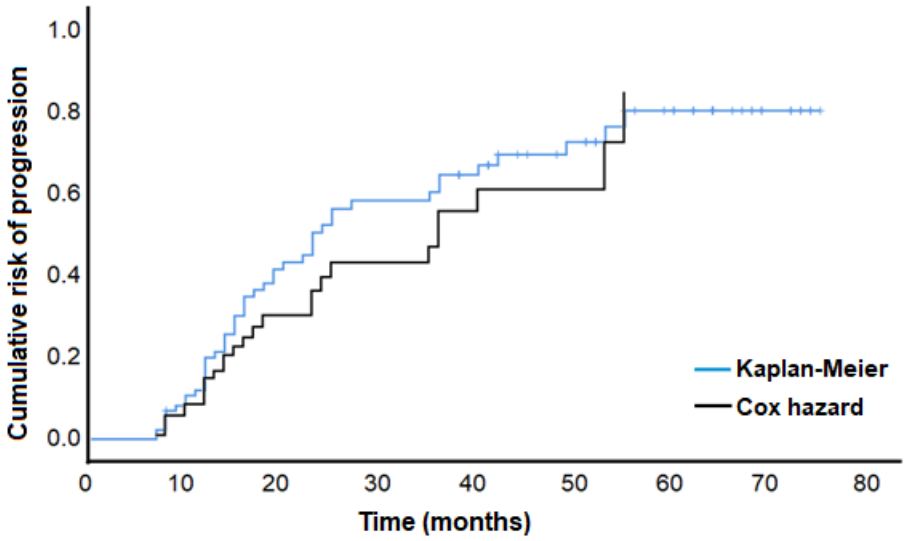

Figure 16. Comparison of the rate of progression predicted by the Cox hazard model (consisting of APOE ε4 and docosahexaenoic acid as influential variables (black line)) with the real rate of progression of the MCI population calculated by Kaplan-Meier analysis (blue line).

5.3.2. CSF lipids associated with diagnosis of MCI and AD

The CSF samples were analyzed in positive and negative ionization mode. After baseline correction, peak picking and alignment and further corrections, including quality control assessment, filtering, and correction of the signal, a total of 201 features remained for evaluation of which 174 molecules were detected in positive and 27 in negative ionization mode.

Partial least squares-discriminant analysis (PLS-DA) detected no lipid profile, neither among CSF lipids detected in positive ionization mode (***Figure 17*** A) nor those detected in negative ionization mode (**Supplementary Figure 1**), specific to each diagnostic group. The ANOVA analysis of the features detected in positive ionization mode identified 10 lipids that had significantly different levels between diagnostic groups, but after applying false discovery rate (FDR) correction, no lipid remained significant between groups (**Supplementary Table 3**). The heat map illustrated with these 10 FDR uncorrected significant lipids showed no clear separation between diagnostic groups (***Figure 17*** B). Multivariate regression analysis found no lipid associated with diagnosis either. From 27 lipid features detected in negative ionization mode, two features associated significantly with diagnosis, but they did not remain significant after FDR correction (**Supplementary Table 4**).

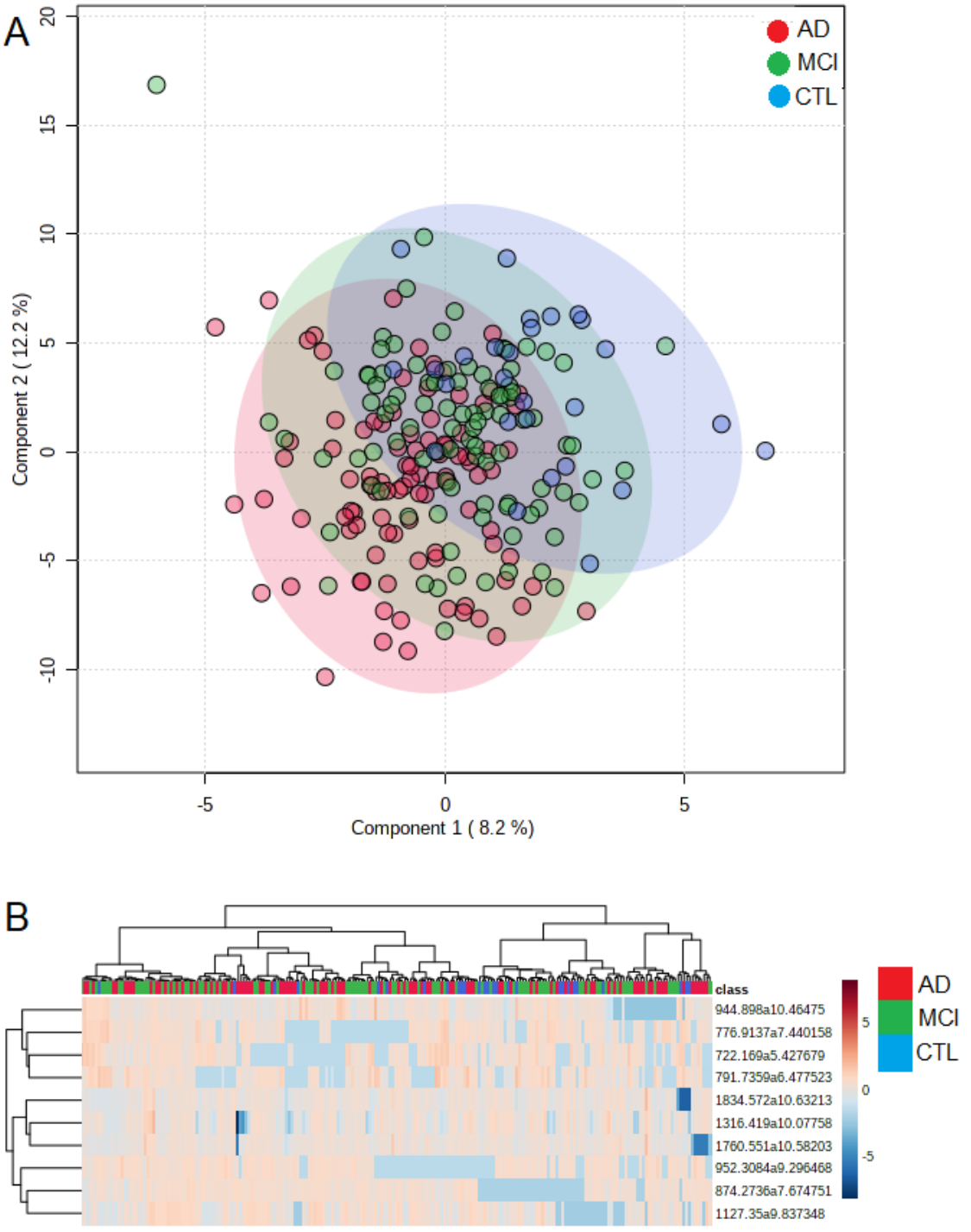

Figure 17. CSF lipidomic profile of AD, MCI and control (CTL) subjects detected in positive ionization mode. (A) Partial least squares-discriminant analysis for the diagnostic groups. (B) Heat map representation of 10 lipids with significantly different (not FDR adjusted) levels between diagnostic groups.

5.3.3. CSF lipids associated with Aβ42 status in CSF

To evaluate which lipids might be associated with amyloid pathology, we divided the study population into two groups based on the measure of Aβ42 in CSF. Subjects who had Aβ42 ≤ 600 pg/mL were considered positive for amyloid pathology and subjects with amyloid > 600 pg/mL were considered negative.

We performed a logistic regression analysis and introduced age, sex, APOE ε4 allele, MMSE, and Ptau and Ttau levels in CSF as covariates. Our analysis detected a model consisting of age, APOE ε4 allele, MMSE and five lipids, including hexacosanoic acid (C26:0), a ceramide (Cer(d38:4)), a phosphatidylethanolamine (PE(40:0)), and two unknown lipids (mass 746.7401, RT 7.47 and mass 1464.461, RT 10.27), as the best model to express the probability of a patient having pathologic levels of Aβ42 in CSF. In this model, higher levels of C26:0 and Cer(d38:4) in CSF decreased the probability of Aβ42 positivity (OR 0.159, 99% CI 0.049 – 0.521, $p < 0.001$ and OR 0.302, 99% CI 0.096 – 0.946, $p = 0.007$, respectively) compared to their low levels, while higher levels of two unknown lipids and PE(40:0) increased this risk compared to their low levels in CSF (OR 6.729, 99% CI 1.973 – 22.956, $p < 0.001$; OR 5.146, 99% CI 1.419 – 18.665, $p = 0.001$; and OR 3.696, 99% CI 1.063 – 12.850, $p = 0.007$, respectively). The AUC of the model was 0.902 (99% CI 0.846 – 0.957, $p < 0.001$). The Hosmer-Lemeshow test yielded a $p = 0.361$, meaning the model is perfectly adjusted to the data. The Spearman's correlation analysis showed that C26:0 had a significant positive correlation ($r = 0.241$, $p = 0.001$) and the unknown lipid with mass 1464.461 had a significant negative correlation with amyloid measures in CSF ($r = 0.228$, $p = 0.002$) (**Table 24**). We eliminated these significantly associated lipids to assess whether other CSF lipids are associated with amyloid pathology. We found eight other lipids associated with Aβ42 status that are listed in ***Table 19***.

In negative ionization mode, a model consisting of age, APOE ε4, MMSE, an ether-linked phosphocholine (PC(O-36:3)/PC(P-36:2)), and two unknown lipids (mass 1090.247, RT 7.75 and mass 1257.203, RT 11.23) was generated. This model had an AUC = 0.830 (95% CI 0.7730 – 0.886, $p < 0.001$) in discriminating the Aβ42 positive from Aβ42 negative patients. Based on this model, high levels of two unknown lipids in CSF increased the

probability of a patient having pathologic levels of Aβ42 in CSF (OR 2.420, 95% CI 1.113 – 5.259, *p* = 0.026 and OR 2.303, 95% CI 1.117 – 4.749, *p* = 0.024), compared to their low levels. On the other hand, high levels of PC(O-36:3)/PC(P-36:2) in CSF reduced this risk (OR 0.450, 95% CI 0.208 – 0.974, *p* = 0.043) (***Table 19***). The Hosmer-Lemeshow test yieldel a *P* = 0.384, confirming that the model was perfectly adjusted to the data. After eliminating these significant lipids, no other lipid was associated with Aβ42 status.

5.3.4. CSF lipids associated with Ptau status in CSF

The association of CSF lipids with tau pathology was evaluated by comparing the CSF lipid profile of patients who were negative for Ptau (≤ 65 pg/mL) with patients who were positive for this biomarker (> 65 pg/mL). This analysis was adjusted for age, sex, APOE ε4 allele, MMSE, and Aβ42 and Ttau levels in CSF. Our results showed that a model consisting of Ttau and three unknown lipids (mass 776.9137, RT 7.44; mass 1334.428, RT 8.58; and mass 500.4377, RT 4.43) was the best model to express the probability of a patient having pathologic levels of Ptau in CSF. This model had a high discriminating power (AUC = 0.982, 99% CI 0.958 – 1.000, *p* < 0.001) and the Hosmer-Lemeshow test indicated that the model was well fitted to the data (*p* = 0.076). Based on this model, higher levels of two unknown lipids (mass 1334.428, RT 8.58; and CLP16, mass 500.4377, RT 4.43) reduced the risk of having pathologic levels of Ptau in CSF, compared to their low levels in CSF. Instead, higher levels of the unknown lipid with mass 776.9137 and RT 7.44 in CSF were associated with increased risk of tau pathology, compared to its low levels (***Table 20***). Spearman's correlation analysis detected a significant negative correlation between the lipids with mass 1334.428 and mass 776.9137 with Ptau levels in CSF (*r* = -0.193, *p* = 0.008 and *r* = 0.158, *p* = 0.029, respectively) (**Table 24**). After eliminating these associated lipids, two other associated lipids with tau pathology were detected (***Table 20***).

In negative ionization mode, a sphingomyelin (SM(30:1)) was associated with tau pathology. In detail, high levels of SM(30:1) increased the risk of Ptau positivity compared to its low levels (OR 5.349, 95% CI 1.472 – 19.442, *p* = 0.011) (***Table 20***). The model had an AUC = 0.965 (99% CI 0.942 – 0.989, *p* < 0.001). The Hosmer-Lemeshow analysis indicated that the model was well fitted to the data (*p* = 0.464).

Table 19. CSF lipids associated with Aβ42 status in CSF.

Name	Mass	RT	IM	*p*	OR	99% CI for OR	AUC
Age				0.001	1.134	1.027 – 1.253	0.902, 99%
APOE ε4				< 0.001	17.002	4.763 – 60.693	CI 0.846 –
MMSE				0.002	0.779	0.636 – 0.956	0.957, *p* <
C26:0	396.3861	3.92	+	< 0.001	0.159	0.049 – 0.521	0.001
Unknown	746.7401	7.47	+	< 0.001	6.729	1.973 – 22.956	
Cer(d38:4)	587.5138	7.85	+	0.007	0.302	0.096 – 0.946	
PE(40:0)	803.6014	8.03	+	0.007	3.696	1.063 – 12.850	
Unknown	1464.461	10.27	+	0.001	5.146	1.419 – 18.665	
Age			+	0.001	1.111	1.022 – 1.207	0.840, 99%
APOE ε4			+	< 0.001	10.579	3.668 – 30.516	CI 0.767 –
MMSE			+	0.005	0.837	0.710 – 0.986	0.914, *p* <
Unknown	1612.504	10.43	+	0.001	3.347	1.277 – 8.771	0.001
Unknown	776.9137	7.44	+	0.010	2.626	1.003 – 6.877	
Age				0.002	1.107	1.017 – 1.024	0.841, 99%
APOE ε4				0.000	10.700	3.764 – 30.415	CI 0.765 –
MMSE				0.002	0.819	0.693 – 0.969	0.917, *p* <
Unknown	339.3383	3.92	+	0.007	0.366	0.140 – 0.957	0.001
Unknown	757.2425	8.75	+	0.003	3.033	1.156 – 7.956	
Age				0.001	1.122	1.023 – 1.231	0.875, 99%
APOE ε4				0.000	14.927	4.466 – 49.887	CI 0.813 –
MMSE				0.001	0.796	0.664 – 0.954	0.937, *p* <
Unknown	364.3928	3.01	+	0.001	4.054	1.394 – 11.788	0.001
Unknown	854.2311	6.68	+	0.000	0.187	0.059 – 0.586	
Unknown	784.3074	7.13	+	0.007	3.097	1.045 – 9.177	
Unknown	874.2736	7.67	+	0.007	3.131	1.044 – 9.388	
Age				0.001	1.120	1.050 – 1.193	0.830, 95%
APOE ε4				0.000	11.556	5.144 – 25.958	CI 0.773 –
MMSE				0.017	0.865	0.768 – 0.974	0.886, *p* <
Unknown	1090.247	7.75	−	0.026	2.420	1.113 – 5.259	0.001
PC(O-36:3)/PC(P-36:2)	751.5893	9.16	−	0.043	0.450	0.208 – 0.974	
Unknown	1257.203	11.23	−	0.024	2.303	1.117 – 4.749	

RT: retention time (min); IM: ionization mode

Table 20. CSF lipids associated with Ptau status in CSF.

Name	Mass	RT	IM	*p*	OR	99% CI for OR	AUC
Ttau				< 0.001	1.042	1.019 – 1.065	0.982, 99% CI 0.958 – 1.000, $p < 0.001$
Unknown	1334.428	8.58	+	0.005	0.078	0.008 – 0.809	
Unknown	500.4377	4.43	+	0.007	0.029	0.001 – 0.835	
Unknown	776.9137	7.44	+	0.003	36.069	1.658 – 784.822	
Ttau				< 0.001	1.030	1.016 – 1.045	0.974, 99% CI 0.947 – 1.000, $p < 0.001$
Unknown	452.4514	5.65	+	0.010	7.127	1.006 – 50.499	
Unknown	1482.468	8.93	+	0.005	0.127	0.019 – 0.834	
Ttau				< 0.001	1.026	1.017 – 1.035	0.965, 95% CI 0.942 – 0.989, $p < 0.001$
SM(30:1)	692.5416	8.73	–	0.011	5.349	1.472 – 19.442	

RT: retention time (min); IM: ionization mode

5.3.5. CSF lipids associated with Ttau status in CSF

The association of CSF lipids with Ttau, as a marker of neurodegeneration, was evaluated by comparing the CSF lipid profile of patients who were negative for Ttau (≤ 425 pg/mL) with patient who were positive for this biomarker (> 425 pg/mL). This analysis was adjusted for age, sex, APOE ε4 allele, MMSE, and Aβ42 and Ptau levels in CSF. In positive ionization mode, no lipid exceeded the input criteria into the model (AUC > 0.7 and $p \leq 0.01$).

In negative mode, a model consisting of Ptau and an unknown lipid (mass 636.5484, RT 8.21) with an AUC = 0.955 (95% CI 0.925 – 0.985) was generated. In this model, high levels of the unknown lipid increased the risk of Ttau positivity in CSF (OR 2.121, 95% CI 1.01 – 4.455, $p = 0.047$) (***Table 21***). The Hosmer-Lemeshow test yielded a $p = 0.055$ for this model.

Table 21. CSF lipids associated with Ttau status in CSF.

Name	Mass	RT	IM	*p*	OR	95% CI for OR	AUC
Ptau				< 0.001	1.065	1.046 – 1.084	0.955, 95% CI 0.925 – 0.985, $p < 0.001$
Unknown	636.5484	8.21	–	0.047	2.121	1.010 – 4.455	

RT: retention time (min); IM: ionization mode

5.3.6. CSF lipids associated with progression from MCI to AD

The association of lipids with progression was assessed by comparing the lipid profile from patients who had progressed to AD (N = 48) with that of patients who remained cognitively stable (N = 44) after a median follow-up of 58 (±12.5) months.

In positive ionization mode, we found no lipid associated with progression after the adjustment of the data for all covariables. In negative ionization mode, a model consisting of APOE ε4 allele, MMSE, Aβ42, Ttau, a cholesteryl ester (CE(11D3:1)), and an unknown lipid (mass 528.4519, RT 8.59) was able to predict the probability of a MCI patient progressing to AD with an AUC of 0.88 ($p < 0.001$, 95% CI (0.790 – 0.970). In this model, harboring APOE ε4 allele (OR 4.45, 95% CI 1.096 – 18.73, $p = 0.037$), higher levels of Ttau (OR 1.004, 95% CI 1.001 – 1.008, $p = 0.007$) and CE(11D3:1) (OR 9.288, 95% CI 1.670 – 51.647, $p = 0.011$) in CSF were associated with higher risk of progression, while MMSE (OR 0.629, 95% CI 0.460 – 0.859, $p = 0.004$) and higher levels of Aβ42 and the unknown lipid (OR 0.219, 95% CI 0.048 – 0.989) in CSF were associated with reduced risk of progression to AD (***Table 22***). The Hosmer-Lemeshow test yielded a $p = 0.357$ which indicates that the model was well fitted to the data. To see the effect of lipids in this model, we calculated the AUC of the model consisting of APOE ε4 allele, MMSE, Aβ42, and Ttau without lipids. Our results showed that the AUC of the model without influential lipids was 0.862 ($p < 0.001$, 95% CI 0.762 – 0.962) that was not significantly different from the model with lipids ($z = 0.425$, $|z| < 1.96$).

Table 22. CSF lipids associated with progression from MCI to AD.

Name	Mass	RT	IM	*p*	OR	95% CI for OR	AUC
APOE ε4				0.037	4.450	1.096 – 18.073	0.88, 95% CI
MMSE				0.004	0.629	0.460 – 0.859	0.790 –
Aβ42				0.010	0.996	0.993 – 0.999	0.970,
Ttau				0.007	1.004	1.001 – 1.008	$p < 0.001$
Unknown	528.4519	8.59	–	0.048	0.219	0.048 – 0.989	
CE(11D3:1)	688.5836	9.17	–	0.011	9.288	1.670 – 51.647	

RT: retention time (min); IM: ionization mode

5.3.7. CSF lipids associated with rate of MCI to AD progression and modeling rate of progression based on the associated CSF lipids

The association of lipids with rate of progression (progression as a continuous dependent variable) was evaluated by the Cox hazard model. This regression model relates time to progression with the event of progression in the presence of influential variables. Our results showed that in positive ionization mode, Aβ42, Ttau and an ether-linked triglyceride (TG(O-52:2)) were associated with rate of progression. In this model, higher Aβ42 levels increased time to progression (OR 0.997, 99% CI 0.995 – 0.999, $p <$ 0.001), while Ttau and higher amounts of TG(O-52:2) decreased this time (OR 1.002, 99% CI 1.001-1.003, $p < 0.001$ and OR 2.7, 99% CI 1.138 - 6.403, $p = 0.003$, respectively) (***Table 23***). To see whether this model can predict time to progression, we compared the rate of progression estimated based on the Cox hazard model (***Figure 18*** A, black line) with the real progression rate of progressive MCI patients calculated by Kaplan-Meier analysis (***Figure 18*** A, blue line). As illustrated, the Cox model is able to predict the growing progression rate in MCI patients, which indicates that the model has detected the lipids that affect the rate of progression; however, it generally underestimates it. Based on the Cox model, about 36% and 59% of progressive MCI patients would progress to AD within first two and four years from MCI diagnosis, while the real progression rate based on clinical data was more rapid (approximately 52% and 70%, respectively).

In negative ionization mode, our analysis generated a model consisting of APOE ε4 allele, Aβ42, Ttau, a ceramide (Cer(d36:2)), two phosphatidic acids (PA(42:5) and PA(46:7)), and two unknown lipids (mass 1265.302, RT 8.29 and mass 1257.203, RT 11.23) as factors that affected time to progression. In this model, harboring APOE ε4 allele (OR 2.812, 95% CI 1.25 – 6.329, P = 0.012), Ttau (OR 1.002, 95% CI 1.001 – 1.003, $p = 0.005$), high levels of the unknown lipid with mass 1265.302 (OR 2.449, 95% CI 1.226 – 4.892, $p = 0.011$), PA(42:5) (OR 2.227, 95% CI 1.119 – 4.430, $p = 0.023$), and PA(46:7) (OR 2.542, 95% CI 1.184 – 5.455, $p = 0.017$) decreased time to progression, while higher levels of Aβ42 (OR 0.997, 95% CI 0.995 – 0.999, p= 0.001), high levels of Cer(d36:2) (OR 0.173, 95% CI 0.066 – 0.449, $p < 0.001$), and the unknown lipid with mass 1257.203 (OR 0.442, 95% CI 0.231 – 0.845, $p = 0.014$) increased time to progression compared to their low levels in CSF (***Table 23***).

Table 23. CSF lipids associated with rate of progression from MCI to AD.

Name	Mass	RT	IM	*p*	OR	99% CI for OR
Aβ42				< 0.001	0.997	0.995 – 0.999
Ttau				< 0.001	1.002	1.001 – 1.003
TG(O-52:2)	861.8141	10.4	+	0.003	2.700	1.138 – 6.403
APOE ε4				0.012	2.812	1.250 – 6.329
Aβ42				0.001	0.997	0.995 – 0.999
Ttau				0.005	1.002	1.001 – 1.003
Cer(d36:2)	609.5135	8.21	−	< 0.001	0.173	0.066 – 0.449
Unknown	1265.302	8.29	−	0.011	2.449	1.226 – 4.892
PA(42:5)	760.5294	8.73	−	0.023	2.227	1.119 – 4.430
PA(46:7)	830.605	9.17	−	0.017	2.542	1.184 – 5.455
Unknown	1257.203	11.23	−	0.014	0.442	0.231 – 0.845

RT: retention time (min); IM: ionization mode

The comparison of the Cox hazard model, based on influential variables in the model, with the real progression rate of the progressive MCI patients calculated by Kaplan-Meier analysis demonstrated that our analysis detected the variables that affect the rate of progression but it underestimates the speed of progression (***Figure 18*** B). In detail, the rate of progression predicted by the Cox model was estimated at approximately 34% and 59% within first two and four years from MCI diagnosis, respectively, while the real progression rate was calculated at about 52% and 70% within these times, respectively. To assess which lipids in CSF, independently of the ionization mode, affect time to progression, we conducted our analysis only with the lipids that had been associated with the progression rate in both ionization modes. We also included the controlling variables in our analysis. Our results demonstrated that in the presence of the aforementioned lipids, the most influential lipid was TG(O-52:2) because exactly the same model as the first model in ***Table 23*** was generated (***Figure 18*** A).

5.3.8. Correlation of CSF lipids with AD core biomarkers and time to progression from MCI to AD

The rank correlation of associated CSF lipids with AD core biomarkers and time to progression was assessed by a Spearman's correlation analysis. Correlations of lipids with time to progression were adjusted for age, sex, APOE ε4 allele, MMSE, and AD core

biomarkers. Correlations of lipids with measures of AD core biomarkers in CSF were adjusted for age, sex, APOE ε4, MMSE, and appropriate CSF biomarkers (**Table 24**).

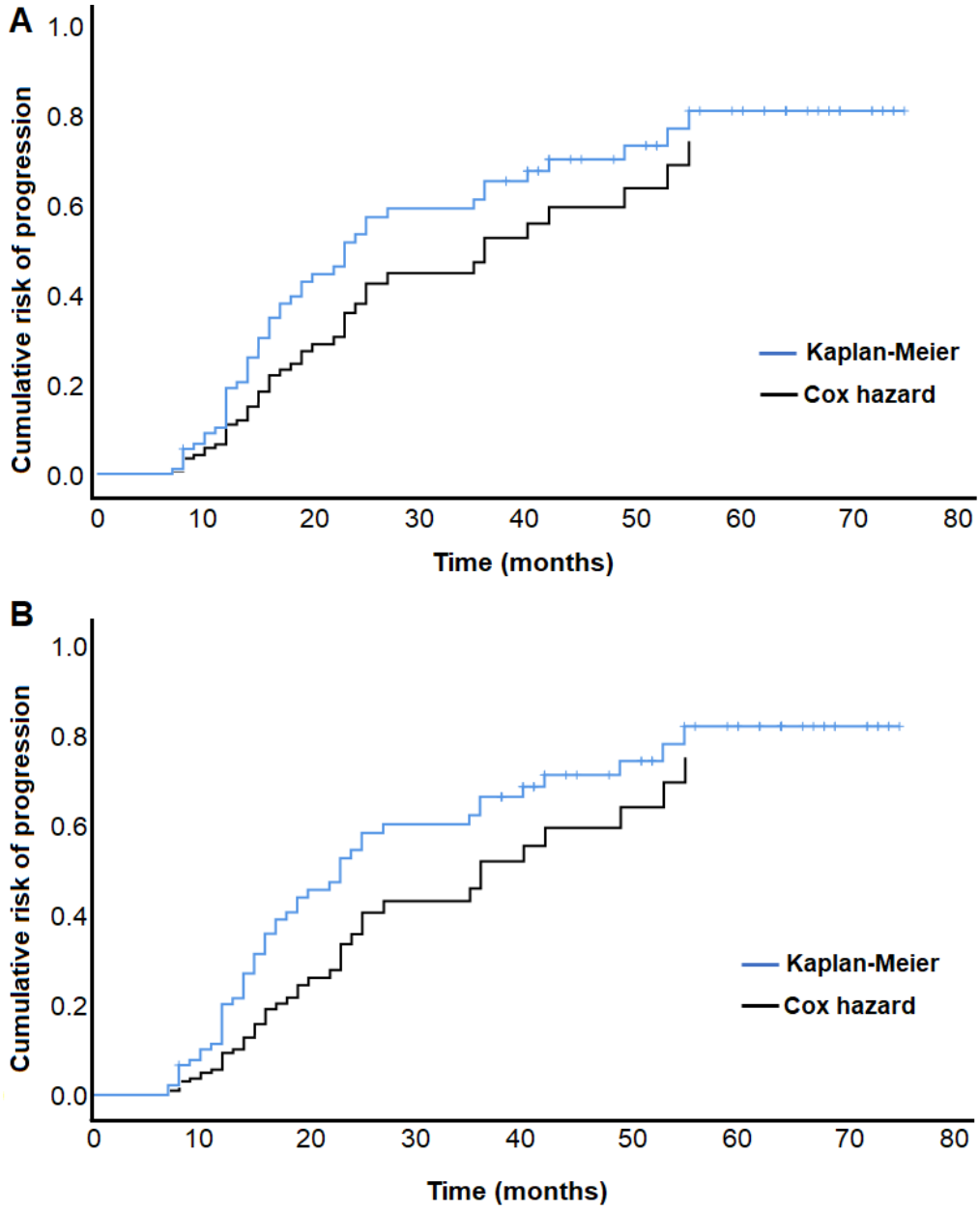

Figure 18. Comparison of the rate of progression predicted by the Cox hazard model (including CSF lipids) with the real rate of progression of MCI population. Rate of progression predicted by the Cox hazard model (black line) compared to the rate of progression based on the clinical data that were calculated by Kaplan-Meier (blue line). (A) Lipids were detected in positive ionization mode. (B) Lipids were detected in negative ionization mode.

Table 24. Correlation of associated CSF lipids with the measures of AD core biomarkers in CSF and time to progression from MCI to AD.

Lipid name	Mass	Aβ42	Ptau	Ttau	Time to progression
C26:0	396.3861	0.241 ($p < 0.001$)			
Unknown	1464.461	−0.228 ($P = 0.002$)			
Unknown	1612.504	−0.290 ($p < 0.001$)	-0.165 ($p = 0.023$)		
Unknown	339.3383	0.175 ($P = 0.016$)			
Unknown	757.2425	−0.277 ($p < 0.001$)			
Unknown	784.3074	−0.200 ($p = 0.005$)			
Unknown	874.2736	−0.231 ($p < 0.001$)			
Unknown	1334.428	−0.270 ($p < 0.001$)	−0.193 ($p = 0.008$)	0.165 ($p = 0.023$)	0.398 ($p = 0.013$)
Unknown	1482.468		−0.178 ($p = 0.014$)	0.151 ($p = 0.037$)	
TG(O-52:2)	861.8141	0.157 ($P = 0.03$)			

5.4. Plasma Lipidomics

5.4.1. Study population

For this study, we included 213 participants that were divided into three diagnostic groups: 104 (49.1%) AD, 89 (41.5%) MCI, and 20 (9.4%) CTL. There was no significant difference between groups for sex ($p = 0.53$), while age differed significantly between them ($p < 0.001$). As expected, there was a significant difference in MMSE, APOE ε4 allele frequency, and AD core biomarkers between diagnostic groups (***Table 25***). The MCI population was the same as the study of FA and oxidative protein damage markers (***Table 12***), but reduced to 89 patients because three patients did not have a blood sample. Of these patients, 47 (52.8%) progressed to AD, while 42 patients (47.2%) remained cognitively stable after a mean follow-up of 58 months.

Table 25. Characteristics of the study population used for plasma lipidomics.

	Total (N = 213)	AD (N =104)	MCI (N = 89)	CTL (N = 20)	*p*
Age	74 [70;78]	76 [72;80]	73 [69;78]	68 [62;74]	< 0.001
Sex (f)	54.5% (116)	58.6% (61)	50.6% (45)	50% (10)	0.530
MMSE	25 [23;27]	23.5 [22;25]	27 [25;28]	29.5 [28;30]	< 0.001
Aβ42*	550 [419;711]	494 [395;583]	589 [435;864]	1016 [620;1347]	< 0.001
Ttau*	408 [252; 618]	489 [354;700]	329 [220;543]	248 [139;337]	< 0.001
Ptau*	67.8 [48;92]	81 [55;98]	62.7 [42;86]	45 [30;63]	< 0.001
APOE ε4	44.6% (95)	52.9% (55)	42.7% (38)	10% (2)	0.002

f: female; *values are pg/ml; *P*-values were calculated by comparing diagnostic groups using one-way ANOVA (or non-parametric Kruskal-Wallis test) for quantitative variables and Chi-square test for qualitative variables.

5.4.2. Plasma lipids associated with diagnosis of MCI and AD

The plasma samples were injected in positive and negative ionization mode. After baseline correction, peak picking and alignment and further corrections, including quality control assessment, filtering, and correction of signal, a total of 1026 features remained for analysis of which 607 molecules were detected in positive and 419 in negative ionization mode.

The PLS-DA detected no lipid profile, neither among plasma lipids detected in positive ionization mode (***Figure 19*** A) nor those detected in negative ionization mode (**Supplementary Figure 2**), specific to each diagnostic group. The ANOVA analysis detected 31 and 33 lipids in positive and negative ionization mode, respectively, that were associated with diagnosis, but after applying FDR correction, no lipid remained significant between groups (**Supplementary Table 5 and 6**). The heat map illustrated with the top 25 FDR uncorrected significant lipids showed no clear separation between diagnostic groups (***Figure 19*** B and **Supplementary Figure 2**). Furthermore, the multivariate regression analysis had a convergence problem, probably because of the small number of samples in the CTL group. However, when we conducted a logistic regression only between AD and MCI patients, we found some lipids that were associated with diagnosis. In positive ionization mode, we found MMSE, Ttau levels in CSF, and eight lipids, including a PC (PC(38:5)), a PC(P) (PC(P-44:5), a hexosylceramide (HexCer(d18:1/12:0), a TG (TG(56:3), and four unknown lipids as factors associated with diagnosis. Among these lipids, high levels of PC(38:5) (OR 4.794, 99% CI 1.055 – 21.789,

p = 0.008), HexCer(d18:1/12:0) (OR 20.239, 99% CI 3.503 - 116.93, *p* < 0.001), PC(P-44:5) (OR 28.582, 99% CI 4.954 - 164.917, *p* < 0.001), and the unknown lipid with mass 727.221 in plasma increased the probability of AD diagnosis compared to their low levels in plasma. Instead, high levels of TG(56:3) and three unknown lipids (mass 194.2805 (OR 0.095, 99% CI 0.017 - 0.522, *p* < 0.001), mass 192.1746 (OR 0.063, 99% CI 0.011 - 0.356, *p* < 0.001), and mass 429.3348 (OR 0.115, 99% CI 0.028 - 0.481, *p* < 0.001)) in plasma reduced the probability of AD diagnosis vs MCI compared to their low levels. This model had an AUC = 0.927 (99% CI 0.878 – 0.975, *p* < 0.001) and the Hosmer-Lemeshow test indicated that the model was well fitted to the data (*p* = 0.056). After eliminating these significantly associated lipids, other associated lipids with the diagnosis were detected (***Table 26***).

In negative ionization mode, a model consisting of MMSE, Aβ42, an ether-linked PC (PC(O-32:1)/PC(P-32:0)), a PC (PC(34:1)), a ceramide (Cer(d18:1/22:0)), and seven unknown lipids (mass 586.492, 821.1918, 851.9697, 729.5663, 1156.334, 1616.381, and 382.372) was the best model to express the probability of a patient having AD diagnosis vs MCI. Among these lipids, high levels of PC(O-32:1)/PC(P-32:0) (OR 5.836, 99% CI 1.185 - 28.754, *p* = 0.004), PC(34:1) (OR 11.301, 99% CI 1.802 - 70.868, *p* = 0.001), Cer(d18:1/22:0) (OR 6.751, 99% CI 1.310 - 34.798, *p* = 0.003), and four unknown lipids (mass 586.492 (OR 12.733, 99% CI 2.450 - 66.191, *p* < 0.001) , mass 1156.334 (OR 6.524, 99% CI 1.563 - 27.239, *p* = 0.001), mass 1616.381 (OR 9.011, 99% CI 1.821 - 44.596, *p* < 0.001), and 382.372 (OR 4.465, 99% CI 0.993 - 20.070, *p* = 0.01)) in plasma increased the risk of AD diagnosis vs MCI compared to their low levels, while, high levels of mass 821.1918 (OR 0.043, 99% CI 0.006 - 0.312, *p* < 0.001), mass 851.9697 (OR 0.060, 99% CI 0.011 - 0.347, *p* < 0.001) , and mass 729.5663 (OR 0.022, 99% CI 0.003 - 0.186, *p* < 0.001) reduced this risk. This model discriminated AD from MCI patients with an AUC = 0.942 (99% CI 0.901 – 0.983, *p* < 0.001) (***Table 26***). The Hosmer-Lemeshow test indicated that the model was well fitted to the data (*p* = 0.769).

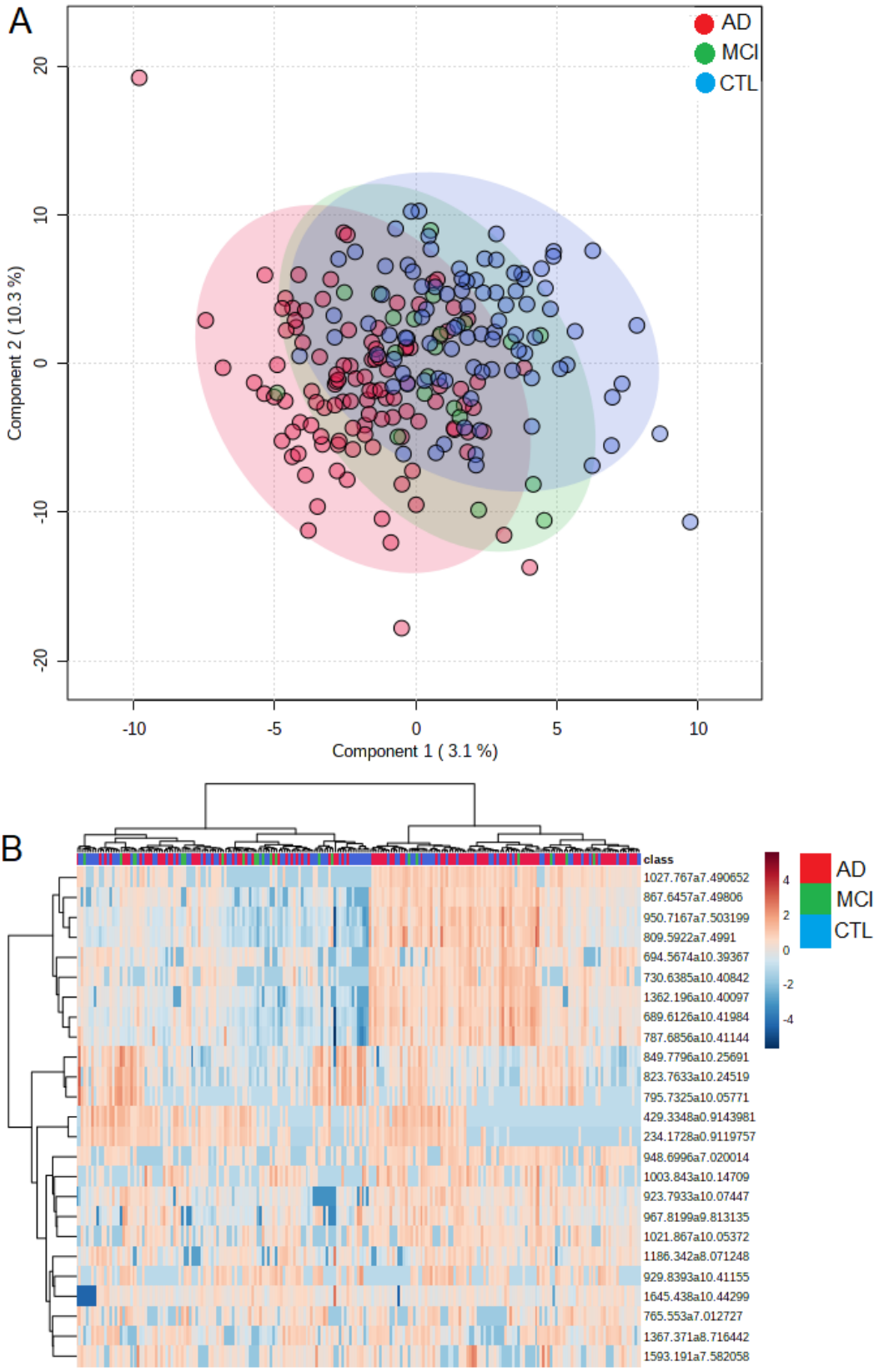

Figure 19. Plasma lipidomic profile of patients with AD, MCI, and control subjects detected in positive ionization mode. (A) Partial least squares-discriminant analysis for the diagnostic groups. (B) The heat map representation of the top 25 lipids with significantly different (not FDR adjusted) levels between three diagnostic groups.

Table 26. Plasma lipids associated with diagnosis (AD vs MCI). MCI was set as the reference category.

Name	Mass	RT	*p*	IM	OR	99% CI for OR	AUC
MMSE			< 0.001		0.412	0.277 - 0.612	0.927,
Ttau			0.004		1.003	1.001 - 1.006	99% CI
PC(38:5)	807.5754	7.01	0.008	+	4.794	1.055 - 21.789	(0.878 -
Unknown	727.221	8.36	0.005	+	4.332	1.136 - 16.522	0.975),
HexCer(d18:1/12:0)	642.5185	8.36	< 0.001	+	20.24	3.503 - 116.93	*p* <
PC(P-44:5)	875.6767	8.42	< 0.001	+	28.58	4.954 - 164.92	0.001
Unknown	194.2805	10.69	< 0.001	+	0.095	0.017 - 0.522	
Unknown	192.1746	10.74	< 0.001	+	0.063	0.011 - 0.356	
nknown	429.3348	0.91	< 0.001	+	0.115	0.028 - 0.481	
TG(56:3)	929.8393	10.41	0.002	+	0.202	0.052 - 0.781	
Age			0.001		1.129	1.031- 1.237	0.835,
MMSE			< 0.001		0.64	0.521 - 0.787	99% CI
PC(2OH-46:6)	948.6996	7.02	0.002	+	3.273	1.209 - 8.860	0.762 -
Unknown	146.5434	8.72	0.008	+	2.8	1.03 - 7.614	0.908,
Unknown	234.1728	0.92	0.004	+	0.327	0.119 - 0.897	*p* < 0.001
Age			< 0.001		1.143	1.039 - 1.257	0.827.
MMSE			< 0.001		0.574	0.452 - 0.727	99% CI
PC(40:7)	831.5754	6.9	0.003	+	3.385	1.177 - 9.735	0.751 -
Unknown	833.2103	7.62	0.005	+	3.051	1.087 - 8.565	0.903,
CE(15D5)	774.7006	10.52	< 0.001	+	0.198	0.064 - 0.614	*p* < 0.001
MMSE			< 0.001		0.575	0.440 - 0.752	0.918,
Aβ42			0.004		0.997	0.995 - 1.000	99% CI
Unknown	466.3116	0.91	0.003	−	0.220	0.058 - 0.833	0.864 -
C20:1 (n-7)	310.2865	4.74	< 0.001		5.627	1.619 - 19.562	0.973,
Unknown	567.7004	7.36	< 0.001	−	0.140	0.036 - 0.538	*p* < 0.001
Unknown	1090.25	7.78	0.002	−	0.172	0.040 - 0.750	
PE(36:1)	745.5606	7.86	0.001	−	0.186	0.048 - 0.726	
Unknown	766.5294	8.70	0.006	−	3.937	1.076 - 14.404	
Unknown	1674.449	9.75	0.003	−	5.029	1.216 - 20.796	
Age			0.005		1.117	1.009 - 1.235	0.895,
MMSE			< 0.001		0.625	0.491 - 0.795	99% CI
Aβ42			0.019		0.998	0.996 - 1.000	0.835 -
Unknown	362.2429	3.16	< 0.001	−	6.488	1.840- 22.884	0.956,
Unknown	337.3336	5.53	0.005	−	3.871	1.123 - 13.342	*p* < 0.001
PS(40:4)	899.5815	7.08	0.005	−	0.277	0.086 - 0.893	
Unknown	795.9053	7.36	< 0.001	−	0.090	0.022 - 0.336	
Unknown	671.739	7.37	0.005	−	3.510	1.104 - 11.157	
MMSE			< 0.001		0.490	0.345 - 0.695	

Name	Mass	RT	*p*	IM	OR	99% CI for OR	AUC
Aβ42			< 0.001		0.995	0.992 - 0.998	0.942, 99% CI 0.901 - 0.983, *p* < 0.001
Unknown	586.492	3.84	< 0.001	–	12.73	2.450 - 66.191	
Unknown	821.1918	6.05	< 0.001	–	0.043	0.006 - 0.312	
Unknown	851.9697	7.35	< 0.001	–	0.060	0.011 - 0.347	
PC(O-32:1)/PC(P-32:0)	777.5732	7.76	0.004	–	5.836	1.185 - 28.754	
PC(34:1)	805.6179	7.89	0.001	–	11.30	1.802 - 70.868	
Unknown	729.5663	8.12	< 0.001	–	0.022	0.003 - 0.186	
Cer(d18:1/22:0)	621.6035	8.72	0.003	–	6.751	1.310 - 34.798	
Unknown	1156.334	8.73	0.001	–	6.524	1.563 - 27.239	
Unknown	1616.381	9.70	< 0.001	–	9.011	1.821 - 44.596	
Unknown	382.372	6.99	0.010	–	4.465	0.993 - 20.070	

RT: retention time (min); IM: ionization mode

5.4.3. Plasma lipids associated with Aβ42 status in CSF

To evaluate which lipids could be associated with amyloid pathology, we divided the study population into two groups based on the measure of Aβ42 in CSF. Subjects who had Aβ42 ≤ 600 pg/mL were considered positive for amyloid pathology and those with Aβ42 > 600 pg/mL were considered negative.

We performed a logistic regression analysis and introduced age, sex and APOE ε4 allele, Ptau, Ttau, and MMSE as covariates. Our result showed that four lipids, consisting of two SMs (SM(36:0) and SM(40:1)), a diglyceride (DG(44:3)), and an unknown lipid (mass 1338.195, RT 10.46), age and APOE ε4 allele were the variables that best expressed the probability of a patient being amyloid positive. The AUC of the model was 0.882 (p < 0.001, 99% CI 0.820-0.943). Based on this model, higher levels of SM(36:0) (OR 4.96, 99% CI 1.717 – 14.327, p < 0.001) and DG(44:3)) (OR 5.873, 99% CI 1.848 – 18.664, p < 0.001) compared to their low levels increased the risk of being amyloid positive, while higher levels of SM(40:1) and the unknown lipid (mass 1338.195, RT 10.46) decreased this risk (***Table 27***). The Hosmer-Lemeshow test yielded a p = 0.998, that means the model was perfectly adjusted to the data. At the next step, to see whether other lipids are associated with amyloid pathology, we eliminated the aforementioned associated lipids from the list of variables and re-analyzed the data. Other lipids associated with amyloid pathology are listed in ***Table 27***.

In negative ionization mode, the logistic regression analysis detected the APOE ε4 allele, age, a PC (PC(36:2)/PC(P-36:2)/PC(O-36:2)), a PA (PA(48:2)), and an unknown lipid (mass 2192.572, RT 10.24) as factors that were best associated with amyloid positive status. In this model, the high levels of PC(36:2)/PC(P-36:2)/PC(O-36:2), and the unknown lipid (mass 2192.572) increased the risk of being amyloid positive, while PA(48:2) reduced this risk. The AUC of the model was 0.853 (99% CI, 0.784 – 0.921: $p < 0.001$). The Hosmer-Lemeshow test yielded a $P = 0.902$, indicating that the model was perfectly adjusted to the data. Among these lipids, PC(36:2)/PC(P-36:2)/PC(O-36:2) had a significant negative correlation with Aβ42 measures in CSF ($r = -0.226$, $p = 0.002$). After eliminating these significant lipids, other lipids were associated with amyloid pathology (***Table 27***).

5.4.4. Plasma lipids associated with Ptau status in CSF

To evaluate which lipids could be associated with tau pathology, we divided the study population into two groups based on the measure of Ptau in CSF. Subjects who had Ptau > 65 pg/mL were considered positive and subjects with Ptau ≤ 65 pg/mL were considered negative for tau pathology. Our results showed that the lipids most associated with the Ptau status in plasma were a TG(O) (TG(O-60:10)) and an unknown lipid (mass 1397.072, RT 6.99). Ttau was also inputted to this model because there was a high correlation between Ttau and Ptau measures in CSF ($r = 0.89$, $p < 0.001$). In this model the unknown lipid increased the probability of a patient having pathologic levels of Ptau (OR 5.3, 99% CI 1.01 – 27.798), while TG(O-60:10) reduced this risk (OR 0.127, 99% CI 0.018 – 0.903, $p = 0.007$). This model had an AUC of 0.980 (99% CI 0.957 – 1.000, $p < 0.001$). The Hosmer-Lemeshow yielded a $p = 0.144$. After eliminating the significant lipids, other significantly associated lipids to Ptau status were detected (***Table 28***). In negative ionization mode, no plasma lipid was associated with the Ptau status.

Table 27. Plasma lipids associated with Aβ42 status in CSF.

Name	Mass	RT	IM	*p*	OR	99% CI for OR	AUC
Age				< 0.001	1.158	1.060 – 1.265	0.882,
APOE ε4				< 0.001	23.171	6.579 – 81.606	99% CI
SM(36:0)	770.5816	6.57	+	< 0.001	4.960	1.717 – 14.327	0.820 –
SM(40:1)	786.6604	8.42	+	0.006	0.295	0.094 – 0.922	0.943, *p*
DG(44:3)	730.6385	10.41	+	< 0.001	5.873	1.848 – 18.664	< 0.001)
Unknown	1338.195	10.46	+	0.009	0.289	0.084 – 0.990	
APOE ε4				< 0.001	34.929	8.543 – 142.81	0.892,
Age				< 0.001	1.161	1.057 – 1.274	99% CI
Unknown	1493.132	7.40	+	0.001	4.498	1.403 – 14.424	0.834 -
Unknown	1186.342	8.07	+	0.001	3.837	1.310 - 11.233	0.950, *p*
SM(42:2)	800.6758	8.66	+	< 0.001	0.184	0.057 – 0.599	< 0.001)
Unknown	1709.463	10.1	+	< 0.001	0.176	0.053 – 0.577	
Unknown	674.6725	10.68	+	< 0.001	4.892	1.591 – 15.041	
APOE ε4				< 0.001	16.306	5.163 – 51.498	0.854,
Age				< 0.001	1.142	1.050 – 1.242	99% CI
TG(56:2)	931.8369	10.07	+	0.005	0.350	0.134 – 0.915	0.785 –
PS(42:3)	851.595	7.96	+	0.003	0.302	0.106 – 0.860	0.924, *p*
Unknown	1482.414	8.88	+	< 0.001	4.604	– 13.27	< 0.001)
APOE ε4				< 0.001	19.144	5.784 – 63.361	0.848,
Age				< 0.001	1.151	1.056 – 1.254	99% CI
TG(55:1)	922.6617	7.95	+	0.007	2.800	1.042 – 7.528	0.780 –
PC(P-42:4)/PC(O-42:5)	849.6643	8.35	+	0.001	3.373	1.282 – 8.876	0.916, *p* < 0.001
Unknown	1719.455	10.53	+	< 0.001	4.152	1.478 – 11.669	
APOE ε4				< 0.001	14.673	4.648 – 46.319	0.853,
Age				< 0.001	1.143	1.049 – 1.245	99% CI
PC(P-36:2)/PC(O-36:3)	829.619	7.89	−	0.002	3.312	1.242 – 8.834	0.784 – 0.921, *p*
Unknown	2192.572	10.24	−	0.001	3.592	1.304 – 9.894	< 0.001
PA(48:2)	868.7177	10.27	−	0.003	0.313	0.115 – 0.848	
Age				0.001	1.110	1.021 – 1.208	0.822,
APOE ε4				< 0.001	13.705	4.445 – 42.259	99% CI
MMSE				0.004	0.836	0.711 – 0.982	0.746 –
TG(O-55:6)	878.768	10.41	−	0.007	2.854	1.048 – 7.770	0.910, *p* <0.001
Age				0.002	1.108	1.019 – 1.204	0.841,
APOE ε4				< 0.001	14.702	4.778 – 45.239	99% CI
MMSE				0.004	0.832	0.704 – 0.983	0.764 –
Unknown	829.7762	8.26	−	0.004	3.071	1.132 – 8.331	0.918, *p*
Unknown	1265.304	8.32	−	0.001	3.684	1.320 – 10.281	<0.001

RT: retention time (min); IM: ionization mode

Table 28. Plasma lipids associated with Ptau status in CSF.

Name	Mass	RT	IM	*p*	OR	99% CI for OR	AUC
Ttau				< 0.001	1.030	1.016 – 1.044	0.980, 99% CI
Unknown	1397.072	6.99	+	0.010	5.300	1.01 – 27.798	0.957 – 1.000,
TG(O-60:10)	978.7357	7.05	+	0.007	0.127	0.018 – 0.903	$p < 0.001$
Ttau				< 0.001	1.027	1.015 – 1.027	0.977, 99%
TG(O-64:7)	984.8828	10.26	+	0.010	5.332	0.995 – 1.674	CI 0.952 – 1.000, $p <$ 0.001

RT: retention time (min); IM: ionization mode

5.4.5. Plasma lipids associated with Ttau status in CSF

The association of lipids with Ttau levels (neurodegeneration) was assessed by comparison of lipid profile between subjects who had Ttau > 425 pg/mL and those with Ttau ≤ 425 pg/mL. Our result showed that in positive ionization mode, an unknown lipid (mass 902.8486 and RT 7.31) and, as we expected, Ptau were associated with the Ttau levels in CSF. In this model, with an AUC = 0.959 (99% CI 0.921 – 0.997, $p < 0.001$), higher levels of the unknown lipid in plasma increased the risk that a patient has to be positive for Ttau (OR 2.712, 99% CI 1.017 – 7.230, $p = 0.009$) (***Table 29***). The Hosmer-Lemeshow yielded a $p = 0.059$. After eliminating this lipid, no other lipid entered to the model.

In negative ionization mode, a model containing Ptau, a fatty acid ester of hydroxy fatty acid (FAHFA(34:0)) and a PC(O) (PC(O-34:3)) was the best to express the probability of Ttau positivity for a patient. In this model, Ptau (OR 1.061, 99% CI 1.036 – 1.086, $p <$ 0.001) and high levels of FAHFA(34:0) (OR 3.106, 99% CI 1.122 – 8.600, $p = 0.004$), and PC(O-34:3) (OR 2.796, 99% CI 1.015 – 7.704) increased the risk that a patient has to have pathologic levels of Ttau. In addition, PC(O-34:3) had a significant positive correlation with the measures of Ttau in CSF ($r = 0.201$, $p = 0.005$). After eliminating these lipids, no other lipid was associated with the Ttau status (***Table 29***).

Table 29. Plasma lipids associated with Ttau status in CSF.

Name	Mass	RT	IM	*p*	OR	99% CI for OR	AUC
Ptau				< 0.001	1.066	1.041 – 1.092	0.959, 99% CI 0.921 – 0-997, *p* < 0.001
Unknown	902.8486	7.31	+	0.009	2.712	1.017 – 7.230	
Ptau				< 0.001	1.061	1.036 – 1.086	0.954, 99% CI 0.916 – 0.992, *p* < 0.001
FAHFA(34:0)	538.4952	3.65	−	0.004	3.106	1.122 – 8.600	
PC(O-34:3)	801.5872	7.39	−	0.009	2.613	1.015 – 7.704	

RT: retention time (min); IM: ionization mode

5.4.6. Plasma Lipids associated with progression from MCI to AD

The association of lipids with the progression was evaluated by comparing the lipid profile of patients who progressed (N = 47) vs patients who did not progress (N = 42) to AD after a mean follow-up of 58 (±12.5) months. We detected that, in positive ionization mode, a model consisting of APOE ε4 allele, two TGs (TG(64:1) and TG(46:0)), a TG(O) (TG(O-62:7)), and a PE (PE(P-36:4)) was the best in expressing the probability of progression from MCI to AD. In this model, harboring APOE ε4 allele, and high levels of TG(64:1) and TG(46:0) increased the risk of progression to AD (OR 98.654, 99% CI 1.989 – 4893.883, $p = 0.002$ and OR 64.863, 99% CI 2.050 – 2052.216, $p = 0.002$, respectively), while high levels of PE(P-36:4) (OR 0.005, 99% CI 0.000044-0.491, $p = 0.003$) and TG(O-62:7) (OR 0.013, 99% CI 0.000315 – 0.502, $p = 0.002$) yielded a protective effect compared to their low levels (***Table 30***). The AUC of the model was 0.972 ($p < 0.001$, 99% CI 0.936-1.000) and the Hosmer-Lemeshow test yielded a $p = 0.957$. The correlation analysis revealed that TG(O-62:7) had a high positive correlation with time to progression ($r = 0.444$, $p = 0.004$) (***Table 30***). In addition, to assess the effect of these lipids in discriminating progressive from non-progressive patients, we calculated the AUC of the model without these significantly associated lipids. Our results showed that the AUC of the model only with APOE ε4 allele was 0.729 ($p < 0.001$, 99% CI 0.586 – 0.871). The result of the Hanley and McNeil test indicated that the difference between two AUCs was statistically significant ($z = 4.595$, $|z| > 2.575$, $p < 0.01$). After eliminating the significant lipids, no other lipid was inputted to the model.

In negative ionization mode, the best model for the expression of the probability of disease progression was a model consisting of Aβ42, Ttau and four lipids including a phosphatidylserine (PS(40:4)), an epoxyeicosatrienoic acid (11,12-EET), a TG (TG(53:4)), and an unknown lipid (mass 651.7253, RT 7.35). Among these lipids, high levels of PS(40:4) (OR 13.418, 99% CI 1.352 – 133.195, p = 0.004) and 11,12-EET (OR 50.985, 99% CI 2.160 – 1399.431, p = 0.001) increased the risk of progression compared to their low levels, while high levels of the unknown lipid (mass 651.7253) and TG(53:4) reduced this risk (OR 0.056, 99% CI 0.005 – 0.616, p = 0.002 and OR 0.03, 99% CI 0.001 – 0.73, p = 0.005, respectively). The model had an AUC = 0.960 (p < 0.001, 99% CI 0.913 – 1.000). The Hosmer-Lemeshow test yielded a p = 0.568. Furthermore, this model with only control variables (Aβ42 and Ttau) had an AUC = 0.827 (p < 0.001, 99% CI 0.710 - 0.944) that was significantly different from the model with lipids (z = 2.933, |z|> 2.575, p < 0.01). After eliminating the lipids from the first model, another model was generated (***Table 30***).

Table 30. Plasma lipids associated with progression from MCI to AD.

Name	Mass	RT	IM	*p*	OR	99% CI for OR	AUC
APOE ε4				< 0.001	789.3	7.857 – 79290.07	0.972, 99% CI 0.936 – 1.000, *p* < 0.001
PE(P-36:4)	723.5188	7.25	+	0.003	0.005	0.000044 – 0.491	
TG(64:1)	974.7156	7.4	+	0.002	98.654	1.989 – 4893.883	
TG(46:0)	795.6105	7.87	+	0.002	64.863	2.050 – 2052.216	
TG(O-62:7)	973.8682	10.27	+	0.002	0.013	0.000315 – 0.502	
Aβ42				< 0.001	0.992	0.986 – 0.998	0.960, 99% CI 0.913 – 1.000, *p* < 0.001
Ttau				0.010	1.005	1.001 – 1.009	
11,12-EET	380.2599	4.61	−	0.001	54.985	2.160 – 1399.431	
PS(40:4)	899.5815	7.08	−	0.004	13.418	1.352 – 133.195	
Unknown	651.7253	7.35	−	0.002	0.056	0.005 – 0.616	
TG(53:4)	928.7665	10.1	−	0.005	0.030	0.001 – 0.730	
APOE ε4				0.010	5.809	1.055 – 35.059	0.896, 99% CI 0.811 – 0.980, *p* < 0.001
Aβ42				0.003	0.995	0.991 – 0.999	
PC(44:10)	927.6163	7.64	−	0.007	5.979	1.088 – 32.867	
CL(49:2)	1120.717	9.06	−	0.001	10.847	1.712 – 68.740	

RT: retention time (min); IM: ionization mode

5.4.7. Plasma lipids associated with rate of MCI to AD progression and modeling rate of progression by use of associated plasma lipids

The association of lipids with rate of progression (progression as a continuous dependent variable) was evaluated by the Cox hazard model. This regression model relates time to progression with the event of progression in the presence of influential variables.

In positive ionization mode, our analysis detected the APOE ε4 allele, two TGs (TG(60:5) and TG(48:1)), a TG(O) (TG(O-62:7)), a PC (PC(44:5)/PC(O-42:3)/PC(P-42:2)/PC(42:6)), and three unknown lipids (mass 2294, mass 1734.557, and mass 1760.574), as variables associated with time to progression. Our results showed that patients with APOE ε4 allele and high levels of PC(44:5)/PC(O-42:3)/PC(P-42:2)/PC(42:6) (OR 9.884, 99% CI 3.081 – 31.706, $p < 0.001$) and the lipid with mass 1734.557 (OR 34.806, 99% CI 4.879 – 248.299, $p < 0.001$) had a shorter time to progression, while patients with high levels of TG(60:5) (OR 0.164, 99% CI 0.056 – 0.479, $p < 0.001$) , TG(48:1) (OR 0.153, 99% CI 0.056 – 0.419, $p < 0.001$), TG(O-62:7) (OR 0.029,99% CI 0.007 – 0.131 , $p < 0.001$) and the two unknown lipids with mass 2294.667 and 1760.574 (OR 0.342, 99% CI 0.135 – 0.870, $p = 0.003$ and OR 0.148, 99% CI 0.034 – 0.644, $p = 0.001$, respectively) had a longer time to progression compared to patients with lower levels of these lipids (***Table 31***). To evaluate the extent to which these variables affect rate of progression, we compared the Cox hazard model with the real rate of progression calculated by Kaplan-Meier analysis. As shown in ***Figure 20*** A, the Cox model has detected the lipids that affect time to progression, but these influential lipids cannot predict this time totally. In other words, the hazard of MCI to AD progression based on the Cox model rises progressively, but in fact the real hazard of progression rises much faster, so that at 2 years almost 50% of progressive MCI patients progressed to AD and at four years approximately 70% of them, while these percentages were estimated at about 23% and 49% in the Cox model (***Figure 20*** A).

In negative ionization mode, our analysis detected Aβ42, Ttau, a PS (PS(40:4)), a PC (PC(36:2)), and five unknown lipids (mass 302.26, mass 446.0925, mass 662.7532, mass 1460.338, and mass 1038.717) as influential factors on time to progression. In this

model, Ttau levels in CSF, and high levels of PS(40:4) (OR 14.214, 99% CI, 4.166 – 48.502, p < 0.001), the unknown lipid with mass 302.26 (OR 5.766, 99% CI 2.069 – 16.065, p < 0.001), and the unknown lipid with mass 1038.717 (OR3.668, 99% CI 1.419 – 9.477, p < 0.001) in plasma were associated with a more rapid rate of progression compared to patients with low levels of these lipids, while levels of Aβ42 in CSF and high levels of PC(36:2) (OR 0.287, 99% CI 0.097 – 0.853, p = 0.003), and the three unknown lipids (mass 446.0925 (OR 0.239, 99% CI 0.087 – 0.655, p < 0.001), mass 662.7532 (OR 0.295,99% CI 0.101 – 0.862, p = 0.003), and mass 1460.338 (OR 0.097, 99% CI 0.031 – 0.309, p < 0.001)) in plasma were associated with a slower rate of progression (***Table 31***). The comparison of rate of progression predicted by the Cox hazard model with the real rate of progression calculated by Kaplan-Meier showed that the Cox model detected the variables that affect time to progression, but these lipids cannot determine the rate of progression completely. In other words, the Cox model underestimates the speed of progression compared to the real clinical data. Based on the Cox model, about 20% and 57% of patients would progress to AD within two and four years after MCI diagnosis, compared to the real rate of progression that was about 50% and 70% within these times (***Figure 20*** B).

Finally, to detect the most influential lipids on rate of progression in plasma, independently of the ionization mode, we conducted another Cox analysis. The analysis was carried out only with variables that had been associated with rate of progression, in both positive and negative ionization mode, and controlling variables. Our analysis detected TG(O-62:7) and the unknown lipid with mass 1038.717 as the most influential lipids on rate of progression in plasma samples (***Table 31***). Higher levels of TG(O-62:7) were associated with a slower rate of progression (OR 0.307, 99% CI 0.135 – 0.696, p < 0.001), while higher levels of the unknown lipid were associated with a more rapid rate of progression (OR 2.461, 99% CI 1.107 – 5.471, p = 0.004). This model had a better predictive accuracy because based on this model about 41% (compared to 50% based on clinical data) and 65% (compared to 70% based on clinical data) of progressive MCI patients would progress to AD within first two and four years of the MCI diagnosis, respectively (***Figure 20*** C).

Table 31. Plasma lipids associated with rate of progression from MCI to AD.

Name	Mass	RT	IM	*p*	OR	99% CI for OR
APOE ε4				< 0.001	12.383	4.137 – 37.065
Unknown	2294.667	7.03	+	0.003	0.342	0.135 – 0.870
PC(44:5)/PC(O-42:3)/PC(P-42:2)/PC(42:6)	891.6419	7.38	+	< 0.001	9.884	3.081 – 31.706
TG(60:5)	1045.868	9.99	+	< 0.001	0.164	0.056 – 0.479
TG(48:1)	821.7482	10.07	+	< 0.001	0.153	0.056 – 0.419
Unknown	1734.557	10.26	+	< 0.001	34.806	4.879 – 248.30
Unknown	1760.574	10.27	+	0.001	0.148	0.034 – 0.644
TG(O-62:7)	973.8682	10.26	+	< 0.001	0.029	0.007 – 0.131
Aβ42				< 0.001	0.996	0.994 – 0.998
Ttau				< 0.001	1.005	1.003 – 1.008
Unknown	302.26	4.62	−	< 0.001	5.766	2.069 – 16.06
PS(40:4)	899.5815	7.08	−	< 0.001	14.214	4.166 – 48.50
PC(36:2)	831.5991	7.32	−	0.003	0.287	0.097 – 0.853
Unknown	446.0925	7.60	−	< 0.001	0.239	0.087 – 0.655
Unknown	662.7532	7.84	−	0.003	0.295	0.101 – 0.862
Unknown	1460.338	8.88	−	< 0.001	0.097	0.031 – 0.309
Unknown	1038.717	9.06	−	< 0.001	3.668	1.419 – 9.477
APOE ε4				< 0.001	4.841	2.030 – 11.54
TG(O-62:7)	973.8682	10.27	+	< 0.001	0.307	0.135 – 0.696
Unknown	1038.717	9.06	−	0.004	2.461	1.107 – 5.471

RT: retention time (min); IM: ionization mode

5.4.8. Correlation of plasma lipids with AD core biomarkers and time to progression from MCI to AD

The rank correlation of associated plasma lipids with AD core biomarkers and time to progression was assessed by Spearman's correlation (***Table 32***). Correlations of lipids with progression time were adjusted for age, sex, APOE ε4 allele, MMSE, and AD core biomarkers. Correlations of lipids with measures of AD core biomarkers in CSF were adjusted for age, sex, APOE ε4, MMSE, and appropriate CSF biomarkers.

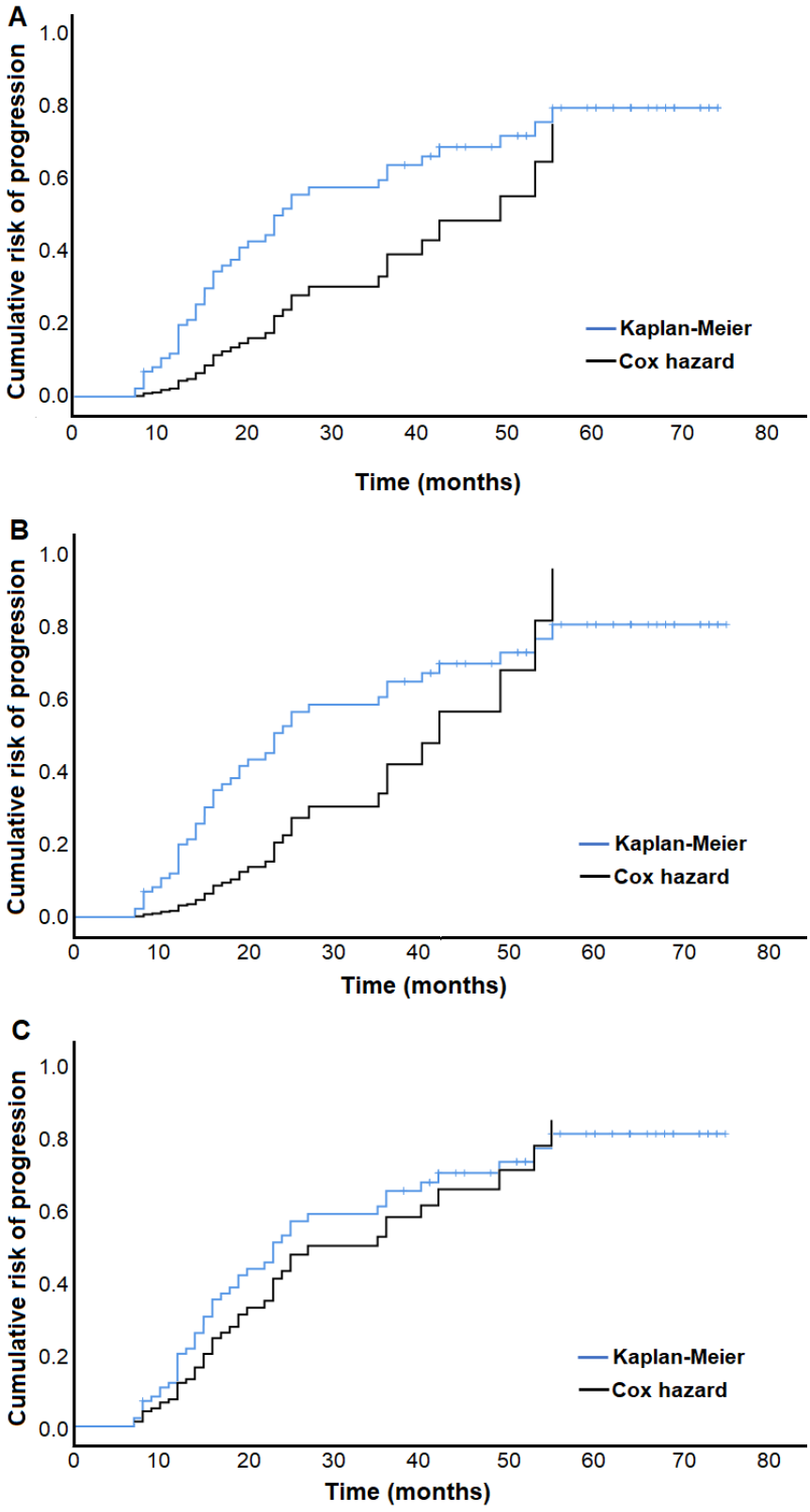

Figure 20. Comparison of the rate of progression predicted by the Cox hazard model (including plasma lipids) with the real rate of progression of MCI population. Rate of progression predicted by the Cox hazard model (black line) was compared to the rate of progression based on the clinical data that were calculated by Kaplan-Meier (blue line). (A) Lipids were detected in positive ionization mode. (B) Lipids were detected in negative ionization mode. (C) Lipids were detected in positive and negative ionization mode.

Table 32. Correlation of the associated plasma lipids with the measures of AD core biomarkers in CSF and time to progression.

Lipid name	Mass	Aβ42	Ptau	Ttau	Time to progression
TG(56:3)	929.8393				0.319 (p = 0.045)
Unknown	234.1728		0.165 (p = 0.023)	−0.181 (p = 0.013)	
Unknown	1186.342	−0.165 (p = 0.023)			
SM(41:0)	800.6758	0.178 (p = 0.014)			
Unknown	1709.463	0.153 (p = 0.035)	−0.171 (p = 0.018)		
TG(56:2)	931.8369	0.154 (p = 0.035)			
Unknown	1482.414	−0.188 (p = 0.01)			
PC(P-42:4)/PC(O-42:5)	849.6643	−0.158 (p = 0.03)			
TG(O-60:10)	978.7357				0.327 (p = 0.039)
TG(O-62:7)	973.8682				0.444 (p = 0.004)
PC(44:5)/PC(O-42:3)/PC(P-42:2)/PC(42:6)	891.6419			−0.149 (p = 0.041)	
Unknown	586.492			0.157 (p = 0.03)	
PC(36:2)/PC(P-36:2)/PC(O-36:3)	829.619	−0.226 (p = 0.002)			
PA(48:2)	868.7177				0.363 (p = 0.021)
TG(O-55:6)	878.768	−0.214 (p = 0.003)			
FAHFA(34:0)	538.4952		−0.146 (p = 0.043)	0.201 (p = 0.005)	
Unknown	662.7532	−0.156 (p = 0.031)			

DISCUSSION

6. Discussion

6.1. Fatty acid composition and markers of oxidative protein damage in CSF

6.1.1. Association of CSF fatty acids with diagnosis of MCI and AD

Investigating FA alterations in CSF of patients in the AD continuum is a less studied area. Searching the literature, we found only two research papers in which the CSF FA profile had been studied in the context of AD. Fonteh et al. quantified FA concentration in the supernatant fluid and nanoparticle fractions of CSF from 29 probable AD, 40 MCI, and 70 control subjects using CG-MS. AD patients were diagnosed based on NIA-AA criteria (G. M. McKhann et al., 2011), and MCI and controls based on the criteria of Peterson (Petersen et al., 1999). In the mentioned study, there was a significant difference regarding CSF levels of Aβ42 and Ttau (the only two markers that had been quantified) between diagnostic groups, and the percentage of APOE ε4 carriers was higher in the AD cohort than in the two other groups. These investigators separated supernatant and nanoparticle fraction by centrifugation of CSF at 3,000 g for 3 min, then 17,000 g for 15 min, and finally, 200,000 g for 60 min. The nanoparticle fraction was separated after the third centrifugation. They found significantly higher levels of C15:1, C19:1, C20:2 (n-6), C20:3 (n-3), C22:4 (n-6) and C22:5 (n-3) in AD patients compared to controls in nanoparticle fraction. Comparing MCI patients with the control group, they found higher levels of C15:0, C17:0, and C16:1 in MCI patients in nanoparticle fraction. The nanoparticle fraction levels of C19:1 and C22:4 (n-6) were higher in AD subjects compared to MCI patients. In supernatant fraction, they observed a higher concentration of DHA (C22:6 (n-3)) in control subjects compared to AD patients and higher levels of Linolenic acid (LNA, C18:3 (n-3)) in controls compared to MCI patients. Concerning unesterified FAs, they found that stearic acid (SA, C18:0) was higher in AD patients and C20:2 (n-6) was higher in MCI patients than in control subjects. SA and palmitic acid (C16:0) were higher, but C11:0, C16:1 and DHA were lower in AD patients than in MCI subjects. Control subjects had higher levels of C10:0, C15:0 and DHA than AD patients and higher levels of C17:0 and SA compared to the MCI group. In addition, they found higher levels of C20:2 (n-6) in MCI compared to control subjects (Fonteh et

al., 2014). Odd-chain FAs have a very low concentration in the human body. Therefore, the association between levels of these FAs and the diagnosis of AD may not be a reproducible result. Supporting this notion, in another study, the same investigators compared the FA composition of CSF fractions between 36 controls (cognitively healthy with normal Aβ42/T-tau), 34 preclinical AD (cognitively healthy with pathological Aβ42/T-tau) and 25 probable AD patients (G. M. McKhann et al., 2011). They did not report the measurement of odd-chain FAs in this more recent study that may indicate the lack of reproducibility of the results regarding odd-chain fatty acids between the latest and their previous report. In their recent report, these investigators quantified PUFA composition by GC-MS. They found no significant difference regarding the concentration of PUFA n-3, n-6, or total PUFA in nanoparticle fraction between study groups. After adjusting to the nanoparticle count, PUFA levels were significantly higher, but PUFA n-6 levels were lower in control and preclinical AD subjects compared to AD. In the supernatant fractions, only the levels of DHA were significantly higher in asymptomatic subjects than in AD patients. Unesterified DHA was reported higher in control subjects compared to the other clinical groups (Fonteh et al., 2020).

Although the two studies by Fonteh et al. reveal dysregulations regarding several FAs between diagnostic groups, we did not detect these alterations between our diagnostic groups. In CSF we found that AI (Dihomo-γ-linoleic acid (DGLA, 20:3 (n-6)) + eicosapentaenoic acid (EPA) + DHA/AA) was associated with AD diagnosis in a manner that higher AI in CSF reduced the risk of AD diagnosis vs MCI. Although we did not find a direct association between FAs with anti-inflammatory (DGLA, EPA, and DHA) or pro-inflammatory (AA) properties and diagnosis, probably because of their small effect individually, their summative impact on AI revealed the presence of this association. We should mention that there are some fundamental differences between our study and the studies by Fonteh et al. that make it difficult to compare our results with theirs. First, they fractionated CSF while we quantified FAs in the whole CSF sample. Second, they quantified a relatively different composition of FAs compared to us. Third, in spite of the fact that APOE plays a pivotal role in lipid homeostasis of the brain and that APOE genotypes affect FA metabolism, Fonteh et al. did not consider the effect of APOE ε4

allele in their study. Fourth, their study populations were smaller than ours and their samples were not quantified for Ptau levels, a specific biomarker of AD.

Since CSF is believed to reflect brain alterations, we then searched for studies on FA profile in the AD brain. In a study by Pamplona et al., the FA composition of the frontal cortex was compared between 8 AD (Braak and Braak stage V-VI, fully developed AD) and 5 age-matched controls. They observed significantly lower levels of C14:0, C16:1 (n-7), SA, OA, LNA, 20:2 (n-6), 20:3 (n-6), 22:4 (n-6), and MUFA in the AD brain compared to controls, while the levels of palmitic acid (PA, C16:0), C22:5 (n-3), C24:0, C22:1 (n-9), PUFA n-3, and DBI were higher in the AD brain compared to controls (Pamplona et al., 2005). In another study, Cunnane et al. analyzed the FA composition of 12 control, 12 MCI, and 12 AD subjects in mid-frontal, superior temporal and angular gyrus cortical regions by GC-FID. AD participants were diagnosed based on criteria defined by the National Institute of Neurological and Communicative Disorders and Stroke and the Alzheimer Disease and Related Disorders Association (NINCDS-ADRDA) (G. McKhann et al., 1984) and the diagnosis of MCI was made using the criteria described by Bennett et al. (D. A. Bennett et al., 2005). The authors neither specified the stage of AD neuropathological changes, nor indicated the post-mortem verification of these alterations. They found lower levels of esterified DHA in mid-frontal and superior temporal cortices from AD compared to control and MCI brains, but did not detect alterations regarding DHA levels in angular gyrus or between MCI and control subjects in any of the studied cortices (Cunnane et al., 2012). Using a non-targeted metabolomic approach, Snowden et al. found significant differences regarding levels of six UFAs (linoleic acid (LA, C18:2 (n-6)), LNA, DHA, EPA, OA, and AA) in the mid-frontal and inferior temporal gyri (AD vulnerable zones), but not in the cerebellum (AD resistance region) between 14 AD, 14 preclinical AD and 14 control subjects. The diagnosis of AD was made based on NINCDS-ADRDA criteria (G. McKhann et al., 1984), but the authors did not mention whether AD brains had been confirmed for neuropathological changes of AD. The AD group showed higher DHA tissue levels in the mid-frontal and inferior temporal regions relative to control subjects, and the increment followed the AD > preclinical AD > control pattern. On the other hand, the levels of another five PUFAs were reduced in these two brain regions of AD compared to control subjects (Snowden et al., 2017). In

another study, Sánchez-Campillo et al., analyzed the FA composition of the hippocampus from 11 control brains and 11 severe AD (global deterioration scale[8] 6, GDS6) using GC-FID. The authors specified neither the pre-mortem diagnostic criteria of AD individuals nor verification of AD neuropathological alterations post-mortem. They found no significant difference in FA composition between groups (Sánchez-Campillo et al., 2020).

The small number of studies and their heterogeneous results makes it difficult to create an idea in respect of FA alterations in the AD brain. However, it seems that alterations are region-specific and cannot be extrapolated to all brain areas. Therefore, one possibility concerning the lack of association between CSF FA profile and diagnosis or AD biomarkers in our results is that CSF may not be an accurate mirror reflecting the alteration that takes place only in some regions of the brain. In other words, as CSF is in contact with the whole brain, the released quantity of FA alterations in some regions of the brain in CSF may be so diluted that their detection with the method we used is challenged. In addition, we adjusted our data for APOE ε4 in order to detect lipids associated with diagnosis independently of this factor. The possible association of these confounding factors was not considered in the majority of previous studies and this may have caused the differences between our results and previous reports. Our result concerning the association of AI with diagnosis did not include control subjects in the association. Having a small control group was one of the limitations of our study that may have caused this lack of association. Achieving CSF of control subjects is one of the problems we face when using CSF as a sample for investigation.

Our result agrees with the existing evidence that inflammation is a key process in AD pathogenesis and progression. A recent study by Cullen et al. revealed an increase in CSF and plasma inflammation markers along the AD continuum (Cullen et al., 2021). Omega-3 and -6 FAs play an important role in inflammation since they are precursors of anti-inflammatory and pro-inflammatory mediators, respectively. Disruption in the

[8] Global deterioration scale is a staging system for cognitive functions for the assessment of primary degenerative dementia. It has seven stages: 1: no cognitive decline; 2: very mild cognitive decline or age associated impairment; 3: MCI, 4: moderate cognitive decline (mild dementia); 5: moderately severe cognitive decline (moderate dementia): 6: severe cognitive decline (moderately severe dementia); 7: very severe cognitive decline (severe dementia) (Reisberg et al., 1982).

equilibrium of anti-inflammatory and pro-inflammatory pathways can promote a proinflammatory environment in the central nervous system leading to neuroinflammation and cognitive decline (Kinney et al., 2018; Lopez-Rodriguez et al., 2021). DHA and EPA play a key role in resolving inflammation through conversion into resolvins and protectins. The importance of DHA and EPA is supported by studies that indicate that supplementation showed a correlative relationship with immunoregulation in AD (Freund-Levi et al., 2014). Similarly, blood mononuclear cells from AD patients treated with EPA have shown reduced IL-1β/IL-10 and IL-6/IL-10 ratios (Serini et al., 2012). Importantly, DHA has been shown to be able to prevent dendritic spine loss by activated microglia, one of the processes that mediate synaptic dysfunction and memory impairment (Chang et al., 2015). On the other hand, AA plays a crucial role in neuroinflammation through its conversion into various eicosanoids by cyclooxygenases, prostaglandin synthases, and lipoxygenases, whose activities have been associated with AD (Czapski et al., 2016; Figueiredo-Pereira et al., 2015). Finally, our result indicates an imbalance regarding (n-3) to (n-6) fatty acids that may reflect the involvement of inflammatory processes in the progression of AD.

6.1.2. Association of CSF fatty acids with AD CSF biomarkers

The association between CSF FAs and AD biomarkers is only investigated in one study by Fonteh et al., (Fonteh et al., 2020). They searched for correlations between levels of FAs in different fractions of CSF and measures of Aβ42 and Ttau in each diagnostic group (control, asymptomatic AD, and AD) separately. They did not find any correlation between levels of FAs and CSF Aβ42 in the supernatant fraction. Regarding the association of FAs in nanoparticle fraction and unesterified FAs with Aβ42, their results were not consistent in all diagnostic groups. For example, they found a negative correlation between levels of DHA and PUFA n-3 and CSF Aβ42 in the asymptomatic group, whereas this association was not seen in AD and control groups. They also found a positive correlation regarding AA/(EPA + DHA) ratio and CSF Aβ42 in the asymptomatic group, while the direction of this association was the opposite in the AD group and it was not observed in the control group. The most consistent correlations that were reported for all diagnostic groups were positive correlations between AA and DHA and

Ttau measures (Fonteh et al., 2020). In respect of the brain studies, Snowden et al., reported negative correlations between Braak and CERAD[9] scores and the abundance of EPA, LA, LNA, AA, and OA in mid-frontal and inferior temporal gyri. They also detected a significant positive correlation between Braak scores and the abundance of DHA and a negative correlation between CERAD scores and DHA abundance in the mid-frontal region.

We did not find any association, neither linear nor exponential, between levels of FAs in CSF and AD CSF biomarkers. Our study provides important differences from the study by Fonteh et al. that may have caused the discrepancies between our results and theirs. Apart from the differences that have been mentioned in the previous section (6.1.1.), Fonteh et al. analyzed the correlation of FAs with AD biomarkers for each diagnostic group, while we searched for these correlations in the whole sample, regardless of the diagnosis. In the case of the study by Snowden et al., there are fundamental differences concerning the type of sample (brain vs CSF) and measure of pathology (Braak and CERAD vs AD CSF biomarkers) that have probably led to different results. Finally, we should mention that to find a specific relationship between each pathology and FA dysregulation, apart from controlling for demographic data (i.e., age, sex, and APOE allele), we adjusted our results to all other pathological hallmark measures (e.g., Ttau and Ptau for amyloid pathology). Therefore, the lack of association between levels of FAs in CSF and AD CSF biomarkers may indicate that alteration in CSF FAs levels, if they exist, may be interconnected between pathological hallmarks of AD.

6.1.3. Association of CSF fatty acids with MCI to AD progression

Among FAs, long-chain omega-3 FAs have been observed to have positive effects on cognition (Martí & Fortique, 2019). DHA, in particular, has been widely studied because of its abundance in the brain and its importance in the brain development (Brenna & Carlson, 2014). The effect of DHA on cognition in AD has been under investigation. Epidemiological and observational studies have linked DHA consumption with a lower

[9] The Consortium to Establish a Registry for Alzheimer's Disease (CERAD) method is a staging system for Aβ pathology based on the semiquantitative assessment of neuritic plaques (0: None; A: Sparse; B: Moderate; C: Frequent) (Mirra et al., 1991).

risk of AD (Lopez et al., 2011; M. C. Morris et al., 2003). Although interventional trials with DHA supplements (alone or in combination with other nutrients) in patients already suffering AD have yielded conflicting results (Arellanes et al., 2020; Lin et al., 2022; Sagrario et al., 2019), evidence points to the possible positive effects of DHA supplementation in patients with very mild AD (Canhada et al., 2018) and MCI, by slowing the progression of cognitive decline and hippocampal atrophy (Bai et al., 2021; L. K. Lee et al., 2013; Y. P. Zhang et al., 2017). Further, higher blood levels of DHA have been seen to ameliorate the positive effects of vitamin B on cognitive (Oulhaj et al., 2016) in the MCI population. Moreover, animal studies have demonstrated that DHA is implicated in learning and memory and ameliorates cognitive functions (Arsenault et al., 2011; Cao et al., 2009). DHA deprivation during development has been seen to decrease synapsins and glutamate receptor subunits in the hippocampus of young animals with concomitant impairment of LTP. Animal and cellular studies have revealed that DHA may improve neurite growth, synaptogenesis, synapsin, and glutamate receptor expression, and glutamatergic synaptic function supporting the hippocampus-related positive effects on cognitive function (Cao et al., 2009). Synaptic dysfunction (loss of function and density) is the pathological aspect of AD that is most correlated with cognitive decline and progression. DHA has been shown to prevent synaptic loss mediated by microglia activation in organotypic hippocampal slice cultures (Chang et al., 2015). In addition, synaptic dysfunction may occur as a result of Aβ accumulation and disruption of synaptic transmission. DHA has been reported to lower Aβ production by membrane remodeling and affecting APP processing enzymes and other proteins involved in this process (Green et al., 2007; Sahlin et al., 2007). Furthermore, DHA has been demonstrated to facilitates the translocation and docking of serine-threonine Akt, a downstream effector of the phosphoinositide 3-kinases survival pathway, at the neuronal membrane and its subsequent phosphorylation that leads to the activation of neurotrophic and anti-apoptotic signaling pathways (Oster & Pillot, 2010). In our study, we found that higher levels of DHA in CSF were associated with a reduced risk of progression. This result is in line with the previous observational studies and interventional trials performed in MCI patients. However, our study is the first report that links DHA levels in CSF with the risk of progression. Considering the results of animal and cellular studies, the association of high levels of DHA in CSF with a reduced risk of

progression may be related to its positive effects on the modulation of neuroinflammation, reduction of Aβ production and accumulation, and promoting signaling pathways leading to neuronal survival at synapses.

6.1.4. Association of CSF oxidative protein damage markers with diagnosis, AD biomarkers and progression

Oxidative stress is a documented phenomenon in AD and has generated considerable observational and experimental literature. At tissue level, oxidative damage markers have been studied in various brain regions. The majority of studies have evaluated the markers that directly measure lipoxidation levels, such as MDA or 4-HNE, but there are also studies in which oxidative damage to proteins is measured in AD brain tissue. Oxidative damage to proteins is assessed either by the quantification of protein carbonyls or by measuring ALEs and AGEs that are modified amino acids produced as a consequence of lipid peroxidation and glycoxidation, respectively. To have a general idea concerning the extent of oxidative stress in the AD brain, here we report some of the previously published studies. Tayler et al. evaluated MDA levels by thiobarbituric acid reactive substance assay in frontal, temporal and parietal cortices from 35 AD and 31 age- and gender-matched control subjects. AD diagnoses were made based on CERAD criteria (J. C. Morris et al., 1989). Their results showed no significant difference in MDA concentration between AD and control brains in any of the examined regions of cortex (Tayler et al., 2010). In another study using the same method, James et al. measured the MDA levels in frontal, temporal and cerebellum regions of 15 clinically and histopathologically confirmed cases of moderate or severe AD and age-matched controls. They found no significant differences regarding MDA levels in cerebellum between the two groups, while the levels of MDA were significantly higher in both frontal and temporal lobes in AD compared to control subjects. Butterfield et al. assessed the protein-bound levels of HNE in the hippocampus and inferior parietal lobule from 6 MCI (Braak stage III-V) and 6 control (Braak stage I-II) brains immunochemically. The MCI patients met the criteria of Petersen (Petersen, 2003). They found significantly higher levels of protein-bound HNE in both examined brain regions of MCI than in control brains (Butterfield, Reed, et al., 2006). In another study,

Butterfield et al. in the same study population, using an immunochemical (adducts of 2,4-dinitrophenylhydrazine) and redox proteomics approach, compared the levels of total protein carbonyls and oxidatively modified proteins, respectively, in the hippocampus of MCI and control subjects. They reported higher levels of total protein carbonyls in the hippocampus of MCI than age and gender-matched controls. In addition, they found that four enzymes (enolase 1, glutamine synthetase, pyruvate kinase M2, and peptidyl-prolyl cis/trans isomerase) were more oxidized in the MCI brain (Butterfield, Poon, et al., 2006). In another study by Bradley et al., levels of 4-HNE and acrolein, another marker of lipoxidation, and protein carbonyls were measured in the hippocampus, temporal lobe, and cerebellum of 10 preclinical AD and 10 age-matched controls. Preclinical AD subjects had neuropathological alterations of AD (moderate or frequent neuritic plaque scores according to the CERAD with Braak scores of III–VI) and were cognitively normal at death. Free 4-HNE and acrolein were measured using GC-MS and protein-bound HNE and acrolein and protein carbonyl levels were quantified using dot-blot immunohistochemistry. They observed higher levels of free acrolein in the the hippocampus and lower levels of this marker in the cerebellum of preclinical AD than in the control group. None of the examined brain regions showed a significant difference concerning free HNE between preclinical AD and controls. In contrast, levels of protein-bound HNE were significantly increased in the hippocampus and significantly decreased in the cerebellum of the test group compared to the control group. There were no significant differences in levels of protein-bound HNE in the temporal region of preclinical AD subjects compared to control subjects. Regarding protein-bound acrolein, none of the brain regions examined showed a significant difference between preclinical and control subjects. Additionally, protein carbonyls were not significantly different between the test and the control groups. These investigators also reported a significant positive correlation between the levels of protein-bound HNE and Braak staging scores in the hippocampus (Bradley et al., 2010). Schuessel et al. conducted a study to quantify the levels of MDA and HNE in the frontal, parietal, and temporal cortices and cerebellum of 11 AD and 10 age- and gender-matched controls. The AD patients had been diagnosed based on NINCDS-ADRDA criteria and neuropathological alterations of AD were confirmed using CERAD criteria. They assessed the levels of MDA and 4-HNE by a colorimetric method after the reaction of these aldehydes with 1-methyl-2-phenyl-

indole. They found no significant difference regarding levels of MDA and 4-HNE in any of the examined brain regions (Schuessel et al., 2004). Using an immunohistochemical approach, Dei et al. quantified MDA and CML in the cytoplasm of neurons and astrocytes of the the hippocampus from 20 AD and 21 age-matched control subjects. The AD brains were categorized as Braak and Braak stage V-VI. They found no significant differences regarding neuronal MDA and CML between AD and control subjects. In glial cells, no significant differences were seen in reactivity for MDA between normal brains and AD, but, CML reactivity was higher in AD compared to control brains, although this difference was not statistically significant (Dei et al., 2002). Pamplona et al. quantified levels of GSA, AASA (markers of direct oxidative modification of amino acids) and CEL, CML, and MDAL in brain cortex (the region was not specified) of 8 AD and 5 age-matched control subjects. The AD brains were staged as Braak stage V-VI and CERAD stage C. They quantified these markers using GC-MS and observed significantly higher levels of all examined protein oxidation markers in the AD compared to control subject brains (Pamplona et al., 2005). As it can be seen, the previously published articles regarding oxidative stress in the AD brain show very diverse and somewhat contradictory results.

In CSF, differential expression of markers of lipid peroxidation, such as 4-HNE and isoprostane, have been reported in AD. Lovell et al. measured levels of free 4-HNE, using HPLC, and protein-bound 4-HNE, via dot-blot immunoassay, in the ventricular fluid of 19 probable AD patients and 13 control subjects (older than the AD group). AD patients were diagnosed based on NINCDS-ADRDA criteria (G. McKhann et al., 1984). They found that AD patients had higher levels of free 4-HNE in ventricular fluid compared to control subjects, but the levels of protein-bound 4-HNE were not significantly different between groups (Lovell et al., 1997). In another study by Selley et al., higher levels of 4-HNE were detected in the CSF of eight mild-to-moderate AD patients (MMSE 11-24) compared to six healthy controls. 4-HNE was measured using GC-MS (Selley et al., 2002). Praticò et al. measured the levels of isoprostane in CSF of 14 probable or possible AD patients diagnosed based on NINCDS-ADRDA criteria and 10 age- and sex-matched control subjects. The CSF isoprostane levels were evaluated using GC-MS. They reported elevated levels of isoprostane in patients with AD compared to control subjects. They also reported a negative correlation between CSF levels of isoprostane and MMSE scores

and Aβ42 levels and a positive correlation between levels of isoprostane in CSF and tau. These investigators also claimed higher CSF isoprostane in subjects with two copies of APOE ε4 allele, compared to one or no ε4 alleles (Praticò et al., 2000). The same investigators published another study in which they measured isoprostane levels in CSF of 28 probable AD, 17 MCI, and 18 control subjects by GC-MS analysis. The AD patients were diagnosed based on NINCDS-ADRDA criteria and MCI patients based on clinical judgment. They found higher levels of CSF isoprostane in a disease-dependent manner. In contrast to their previous report, these investigators found no difference in isoprostane levels between patients homozygous for APOE ε4 allele and those with 1 or no ε4 allele. In addition, they did not report any correlation between CSF levels of isoprostane and measures of CSF AD biomarkers, as they did in their previous report (Praticò et al., 2002). In another study, Montine et al. quantified CSF isoprostane levels by GC-MS in 19 probable AD, 8 non-AD demented, and 10 control subjects. The AD patients were diagnosed based on NINCDS-ADRDA criteria and non-AD dementia was diagnosed based on clinical judgment. They found higher levels of isoprostane in AD patients compared to the two other groups (Montine et al., 2001). In a recent work, the CSF levels of isoprostane were measured in a cohort of 113 participants, including 25 control, 40 AD, 16 MCI, and 32 non-AD dementia subjects using ELISA. In contrast to the two latter studies, isoprostane levels only yielded a significant difference between AD and control groups (Jensen et al., 2021). Therefore, in spite of some inconsistencies, the results of previous studies indicate an increase in lipid peroxidation in AD that was evidenced by higher lipid peroxidation markers in CSF of AD patients compared to the control subjects.

Regarding quantification of oxidative damage to proteins in CSF there are also some previously published data. Ahmed et al. measured concentrations of CML, CEL, pentosidine and some other protein modification products in CSF of 18 AD and 18 dementia free control subjects. Pentosidine was detected by HPLC and CML and CEL were quantified by LC-MS. The AD patients were diagnosed based on NINCDS-ADRDA criteria (G. McKhann et al., 1984) and their APOE genotype was not assessed. These investigators reported increased concentrations of CML in AD patients compared to control subjects (Ahmed et al., 2005). In another study, Bär et al. quantified levels of

pentosidine and CML in serum and CSF of 15 probable AD (8 mild and 7 moderate to severe), 20 vascular dementia, and 31 control subjects (14 age-matched and 17 controls <35 years). They found higher levels of CML in CSF of AD patients compared to controls (Bär et al., 2003). Monacelli et al. evaluated the levels of pentosidine and CML in CSF of 25 patients, including AD (N = 4, MMSE 10-20) and other neurological disorders (6 multiple sclerosis, 7 polyneuropathies, 3 vascular, and 5 others). Pentosidine was measured by HPLC and CML using ELISA. In contrast to the two previous studies, they observed a significant decrease in the concentration of pentosidine in AD subjects and no change in CML concentration between AD and other neurological disorders (Monacelli et al., 2014). The limited number of studies that measured oxidative protein damage and their inconsistent results makes it difficult to draw a clear picture regarding these alterations in AD CSF.

In our study, we did not find any association between oxidative protein damage markers in CSF and diagnosis, AD biomarkers, and progression. Although the result of the previous studies shows differences regarding the markers of oxidative stress in CSF between AD and healthy condition, they are limited in number and their results are somewhat contradictory. In addition, they have some major limitations that hinder their comprehensive interpretation. First, they use a small study population. Second, they employ different analytical methods for the quantification of oxidative stress markers. Third, there are limitations regarding the study design (e.g., inclusion of younger controls). Fourth, most of the studies do not specify the stage of deterioration in AD patients. We believe that our study has several strengths regarding previous studies. First, we included a larger study population than previous studies (N = 210). Second, we quantified oxidative stress markers using targeted GC-MS that is more precise and reliable than colorimetric or immunologic methods used in some previous studies. Third, we adjusted our data regarding confounding variables such as age, gender, and APOE4 status, while some of the aforementioned studies had not taken these interactions into account. Especially, the APOE genotype had not been determined in the majority of previous studies and, therefore, its possible effect had not been controlled.

Searching for oxidative stress markers in CSF originates from the fact that CSF is in equilibrium with the fluids of the brain extracellular space and, therefore, may reflect

the extent of oxidative stress present in the AD brain. However, as mentioned earlier, brain studies also show considerable heterogeneity of results. Surprisingly, a recent meta-analysis revealed very small changes related to the markers of oxidative damage to proteins and lipids that were detected only in some regions of the brain and no significant alterations regarding oxidative DNA damage level in any brain region. This analysis also suggests no change in antioxidant enzyme system levels in the AD brain. In the aforementioned meta-analysis, among MDA, 4-HNE, and acrolein (markers of lipid peroxidation), only MDA levels showed a significant increase in frontal and temporal lobes and hippocampus in AD subjects. Oxidative damage to proteins was detected in the occipital lobe and hippocampus, however, the authors insisted on the possible presence of publication bias due to the limited number of studies (Zabel et al., 2018).

Therefore, it seems that the global accumulation of oxidative damage in the AD brain is less substantial than has generally been reported and the redox balance is well-regulated in the brain. Therefore, the lack of association we found between CSF markers of oxidative protein damage and diagnosis, AD biomarkers and progression may suggest that oxidative protein damage in the brain is not of such an extent to be reflected in the CSF.

6.2. Fatty acid composition and markers of oxidative protein damage in plasma

6.2.1. Association of plasma fatty acids with diagnosis of MCI and AD

Plasma FAs are present in unesterified (free FAs) or esterified form in the structure of GLs, PLs, SPs and cholesterol esters (CE). Our results showed that higher levels of VA in plasma were associated with increased risk of AD vs controls (OR 5.382, 99% CI 1.623 – 17.851, $p < 0.001$) and AD vs MCI diagnosis (OR 3.166, 99% CI 1.075 – 9.326, $p = 0.006$). We also detected that compared to controls, higher plasma levels of OA were associated with a reduced risk of MCI (OR 0.219, 99% CI 0.070 – 0.682, $p = 0.001$) and AD diagnosis (OR 0.306 99% CI 0.089 – 1.048, $p = 0.013$).

Dysregulation regarding plasma levels of FAs in AD have been reported in previous studies (Reviewed by Hosseini et al., 2020). However, there are some differences

between previous studies, in terms of number of participants, stage of AD, measuring absolute quantity of FAs or percentage-to-total FAs, profile of FAs measured and the applied assay method, among others, that obscure our understanding regarding FA dysregulations in AD.

Concerning VA dysregulation, our finding is in agreement with the previous reports. Iuliano et al., assessed the plasma FA profile of 30 controls, 30 probable AD (MMSE 21 ± 4) and 14 aMCI (MMSE 27 ± 2) using GC-FID. AD and MCI patients were diagnosed based on NINCDS-ADRDA and Petersen criteria, respectively. In accordance with our results, they reported significantly higher levels of VA in plasma from AD and aMCI patients than controls. They also detected that compared to controls, aMCI and AD patients had higher levels of C20:0 and C22:1 (n-9). In addition, the plasma levels of LA were significantly lower in the AD vs the control group (Iuliano et al., 2013).

Lower abundance of OA in AD/MCI patients has also been reported previously. For example, using the GC-MS method, Cui et al. determined the levels of 15 serum FAs in 33 control subjects and 31 AD patients that were diagnosed based on NINCDS-ADRDA criteria. Although the authors mentioned that the functional and cognitive state of patients had been evaluated using MMSE and CDR scaling, no data were reported in this regard to clarify the cognitive state of AD patients and stage of the disease. They detected that in the AD patients, three saturated fatty acids (C14:0, C16:0, C18:0)) and six unsaturated fatty acids (C16:1 (n-9), OA, LA, γ-C18:3 (n-6), C20:2 (n-6), and DHA) had lower levels compared to controls, whereas the serum level of LNA was significantly higher in the AD patients (Cui et al., 2015). Another study using GC-MS, after assessment of free FAs in serum, reported a mostly similar result indicating lower levels of C14:0, C16:0, OA, LA, and DHA in 46 AD patients than in 39 control subjects (D. C. Wang et al., 2012). No data regarding disease stage were provided in this latter study either. In another investigation conducted by Cunnane et al., the FA profile was analyzed in pre-mortem plasma from 10 control, 7 MCI, and 9 AD patients. AD was diagnosed based on NINCDS-ADRDA criteria and MCI based on an internally validated protocol (D. A. Bennett et al., 2005) before death. The authors did not clarify either the pre-mortem cognitive state of participants or their post-mortem disease stage. They detected significantly

lower plasma levels of OA, LA and PUFA n-6 in AD and MCI patients compared to controls (Cunnane et al., 2012).

However, other studies did not detect dysregulations in respect of VA and OA in the context of AD. For example, Sánchez-Campillo et al. evaluated the serum FA composition from 38 control subjects, 48 GDS4 AD patients (MMSE 18.7 ± 0.7), and 47 GDS6 AD patients (MMSE 8.3 ± 0.8) using GC-FID. They did not detect a significant difference regarding either OA or VA between AD and control groups. Instead, they observed a significant increase in levels of C17:0, C20:2 (n-6), n-6/n-3 PUFA and a significant reduction in levels of SA, C22:0, C23:0, PUFA n-3, and long chain PUFA n-3 in AD patients, especially moderate-severe, compared to controls (Sánchez-Campillo et al., 2020). Another example is a community-based study of 935 older participants conducted by Cherubini et al. who evaluated the association between plasma FA composition and increased risk of dementia and cognitive impairment. They divided the study population into three groups: 725 cognitively normal, 153 cognitively impaired, and 57 dementia subjects. VA was not measured in this study, but plasma levels of OA were assessed. They did not find any significant difference in plasma FA profile between cognitively normal and impaired participants. However, participants with dementia had significantly lower UFA n-3, particularly LA compared to the cognitively normal group (Cherubini et al., 2007).

Coherent with our results, those of a recent meta-analysis showed dysregulation of both VA and OA in AD/MCI patients. In this meta-analysis, Hosseini et al. analyzed the results of 19 studies in which plasma, red blood cells, serum, and CSF FA profile had been investigated between MCI/AD patients and controls. They reported higher levels of VA and lower levels of DHA in MCI vs controls. Comparing AD vs controls, plasma/serum levels of DHA, C14:0, LA, C16:1 (n-7), SA, OA, and PUFA n-3 were downregulated, but C20:3 (n-9) had a higher plasma/serum abundance (Hosseini et al., 2020). It is worth mentioning that C20:3 (n-9) is produced by elongation and desaturation of OA only in the case of deficiency of n-6 and n-3 FAs (Ichi et al., 2014). Therefore, an increase in C20:3 (n-9) may be an indicator of deficiency in essential FAs in AD.

Therefore, although our results differ from those of previous reports in which other FAs than OA and VA were detected as dysregulated, many of the previous studies confirm

the direction of dysregulation we found for OA and VA. We think that our results compared to previous reports are robust and reliable because we included a large study population (N =286, 103 AD, 89 MCI, and 94 CTL). We adjusted our data for possible confounding factors, i.e., age, sex, and APOE ε4 status, and we were more demanding regarding the statistical analysis of the data. Furthermore, we had an MCI group, while many studies had only compared AD patients with control subjects.

OA is one of the most abundant FAs in the human body and has been demonstrated to be associated with better cognition. For instance, in a study conducted by Sakurai et al. using 154 community-dwelling elderly individuals, the consumption of MUFAs, particularly oleic acid, was significantly associated with better cognitive status (Sakurai et al., 2021). Although some *in vitro* results pointed to the deleterious effects of OA on AD pathology (Y. Liu et al., 2004), there is a substantial body of data that evidences the protective effects of OA on AD. For example, OA has been shown to exert inhibitory activity on serine protease prolyl endopeptidase, the enzyme that had higher levels in the AD brain and has been related to amyloidgenesis (Park et al., 2006). In another study, a significant decrease in MUFAs, including OA, was reported in the frontal cortex and hippocampus of the AD brain (Prasad et al., 1998). In addition, Amtul et al. detected reduced secreted Aβ levels in cells transfected with APP and supplemented with OA. They demonstrated that OA supplementation of transgenic mice exhibited an increase in Aβ40/Aβ42 ratio, reduced levels of BACE- and reduced presenilin levels along with reduced amyloid plaques in the brain. The reduction in BACE activity was accompanied by increased levels of a non-amyloidogenic soluble form of APP (sAPPα). Furthermore, this diet resulted in an augmentation of IDE and insulin-like growth factor-II (Amtul et al., 2011). OA dysregulation has also been evidenced by demonstrating that stearoyl-CoA desaturase activity, implicating in MUFA synthesis, was dysregulated in the AD brain (Astarita et al., 2011). Interestingly, adult hippocampal neurogenesis, that is diminished in aging, and especially in AD, has been linked to OA accessibility by neuronal stem cells. In a study by Kandel et al., OA was demonstrated to be a ligand for the transcription factor NR2E1 (nuclear receptor subfamily 2 group E member 1) that is responsible for the regulation of neural stem and progenitor cell self-renewal and proliferation (Kandel et al., 2020). Apart from possible effects of OA on AD pathology and neurogenesis, there

is also evidence that OA present in olive oil is responsible for the decrease in blood pressure attributed to this oil. OA can regulate blood pressure by affecting the structure of the cell membrane and, consequently, the regulation of adrenergic signaling receptors that are key elements in the central and peripheral control of blood pressure (Terés et al., 2008). OA consists more than 70% of FAs in olive oil. Several studies have confirmed the effectiveness of the Mediterranean diet, with olive oil as one of its main components, in preventing hypertension and dementia (Berr et al., 2009; Martinez-Lapiscina et al., 2013; Valls-Pedret et al., 2015; Van Den Brink et al., 2019). Hypertension is one of the important risk factors of AD. Therefore, the association of higher plasma OA with a reduced risk of AD and MCI vs controls we found in our study population could be related to the possible effect of this FA on reducing Aβ production, promoting neurogenesis, and reducing hypertension.

VA is a trans FA (TFA). TFAs occur in small amounts in nature but they are widely produced by the food industry. Several reports associate higher consumption of TFA with an increased risk of AD. For instance, in an observational prospective study of aged people (N =815), Morris et al. found a positive association between the development of AD (N =131, 3.9 years' follow-up) and intake of TFAs (M. C. Morris et al., 2003). In another study, Honda et al. prospectively followed 1,628 Japanese community residents aged ≥ 60 without dementia for a median of 10 years. They reported a significant association between higher serum levels of TFA (elaidic acid, C18:1 (n-9) trans) and a greater risk of developing all-cause dementia and AD (Honda et al., 2019).

In addition, previous literature has linked TFA consumption with an increased risk of cardiovascular diseases (Mozaffarian et al., 2006). Cardiovascular diseases are among the risk factors for the development of AD. Therefore, VA, by incrementing cardiovascular pathologies, may indirectly contribute to a reduction in cerebral perfusion leading to brain dysfunction, cognitive impairment and, in combination with other factors, to the neuropathology of AD. In a double-blind, randomized controlled trial conducted by Gebauer et al., the consumption of VA was associated with increased plasma LDL-C (Gebauer et al., 2015). Previous studies have shown that cholesterol increases the risk of AD (Solomon et al., 2009) and cholesterol-lowering drugs have been associated with reduced AD risk in some, although not all, studies (Haag et al., 2009). It

has also been shown that at cellular levels, membrane cholesterol concentration affects Aβ processing (Di Paolo & Kim, 2011). Therefore, taking into account that VA can increase plasma cholesterol, it may indirectly contribute to amyloid pathology in the AD brain. However, considering that BBB prevents the transfer of cholesterol and it is synthesized de novo in the brain, the impact of plasma cholesterol on brain cholesterol pool and the effect that may have on AD pathology is not clear. Taken together, our results regarding the detrimental and beneficial effects of VA and OA, respectively, on AD development open a therapeutic window to nutritional interventions to protect against AD.

Finally, in our study, the AD-related FA profile in CSF and plasma point to different pathological aspects implicated in AD pathogenesis. While CSF results highlight the effect of inflammation on AD pathogenesis and progression, our results in plasma indicate the importance of healthy nutrition in AD. The difference in the results between CSF and plasma studies suggests that there may be somewhat dissimilar pathways conducting AD development at central and peripheral levels. Therefore, further studies are needed to shed light on how systemic and central FA dysregulations take part in AD development.

6.2.2. Association of plasma fatty acids with progression and rate of progression from MCI to AD

Annually, about 10% of MCI patients progress to AD (Farias et al., 2009). Identification of factors contributing to MCI to AD progression is pivotal for clinical prognosis and risk stratification. Interestingly, we found that higher plasma levels of OA were also associated with a reduced risk of progression (OR 0.178, 95% CI 0.038 – 0.828, $p = 0.016$). This result further emphasizes the protective effect of OA against cognitive deterioration in AD found previously in other cohort studies (Sakurai et al., 2021). The precise molecular pathways involved in progression from MCI to AD are not completely clear, however, any pathological condition affecting synaptic transmission could be a key player in driving MCI to AD progression. As mentioned in the introduction, both Aβ and tau soluble species have been shown to be toxic for synaptic terminals. In particular, the toxic effects of soluble oligomers of Aβ on synapses is widely documented. For example,

it has been shown that Aβ species may affect normal synaptic functions by inhibiting LTP or facilitating LTD of excitatory synapses and, as a result, contribute to the cognitive dysfunction in AD (Z. X. Wang et al., 2016). In addition, the formation of pore-like structures and the disturbance of intracellular homeostasis might be another mechanism whereby Aβ species cause synaptic failure (Crews & Masliah, 2010).

Inflammation may be another possible player in progression. Pro-inflammatory responses have been shown to have direct excitotoxic effects on synapses and indirectly affect other pathways, such as BBB permeability, leading to synaptic failure and cognitive decline. In addition, synaptic pruning activity of microglia is highly important in maintaining a healthy synaptic environment and its dysregulation would negatively affect synaptic transmission and cognition.

Impaired hippocampal neurogenesis could be another player in AD progression. Adult hippocampal neurogenesis has been proposed to play a major role in the formation of hippocampal-dependent memory (Boldrini et al., 2018). The replacement of unfunctional neurons by newly-generated neurons would be a strategy for maintaining normal hippocampal cognitive activities. Studies using transgenic AD mice have demonstrated that impairment in hippocampal neurogenesis precedes cognitive decline, suggesting that the former might have a causal role in cognitive decline (Li Puma et al., 2021). In human brain studies, MCI patients have shown a significantly reduced number of newly formed neuroblasts compared to cognitively normal subjects (Tobin et al., 2019). These data suggest that impairment in adult hippocampal neurogenesis may be a driver of MCI to AD progression.

Midlife hypertension is recognized as a strong risk factor for the development of AD (Joas et al., 2012). In addition, the results of animal studies have demonstrated that hypertension accelerates the pathogenesis of AD (Shih et al., 2018). Several mechanisms have been proposed regarding how hypertension would lead to reduced cognitive abilities and progression to AD. Hypertension compromises the function of cerebral microcirculation by reducing microvascular density and neurovascular functionality, disruption of BBB, genesis of cerebral microhemorrhages, lacunar infarcts and white matter damage (Ungvari et al., 2021). Furthermore, hypertension has been shown to impair synaptic plasticity, reduce synaptic density, and promote the dysregulation of

genes involved in synaptic function in mouse hippocampus. Therefore, these hypertension-induced neuronal alterations may impair the establishment of memories in the hippocampus and contribute to the pathogenesis and progression of AD (Tucsek et al., 2017).

Taken together, the protective effect of OA against MCI to AD progression indicates that OA could be involved in some of the processes affecting synaptic function. In fact, as detailed in the previous section (6.2.1.), OA has been shown to modulate APP processing enzymes (Amtul et al., 2011), increase hippocampal neurogenesis (Kandel et al., 2020), and reduce blood pressure (Terés et al., 2008), and have anti-inflammatory effects (Medeiros-De-Moraes et al., 2018; Santamarina et al., 2021). Herein, for the first time, we show an association between plasma OA content and the progression of AD. Further studies are required to elucidate exact mechanistic implications of OA on pathological pathways leading to AD progression.

We should mention that our result in plasma was not a replicate of the result we obtained in the CSF study. While the result of the CSF study suggests that DHA has a protective effect on progression from MCI to AD (OR 0.135, 95% CI 0.025 – 0.736, p = 0.021), at the systemic level, OA was detected as a protecting factor in this regard. Therefore, again, our results highlight the existence of somewhat different pathways implicated in AD development and progression at the levels of central and peripheral systems.

The clinical evolution of MCI and AD patients is heterogeneous. Recognizing disease heterogeneity and understanding the biological variables involved is important for advancing diagnostic procedures, improving the estimation of progression and the development of treatment strategies. Although the clinical, biochemical and genetic factors that influence the risk of developing AD and those that modulate the progression of MCI to AD are widely studied, little is known about the factors that affect and help to predict the rate of progression.

Previous research suggests that genetic (e.g., APOE or some point mutations in PSEN1 gene), comorbidities and clinical signs (e.g., level of education level, diabetes mellitus, chronic inflammation or presence of psychotic and motor signs), and CSF biomarkers

(e.g., very high Ttau and Ptau and very low Aβ42 levels) may affect the rate of progression. However, a lack of replicability and even contradictory results by independent studies did not support the possible influence of these conditions on the rate of progression (Schmidt et al., 2011). However, the extent of neuronal injury (abnormal CSF Ttau, Ptau, and hippocampal volume) may be a predictor of time to progression from MCI to AD (Pelkmans et al., 2022; Van Rossum, Visser, et al., 2012; Van Rossum, Vos, et al., 2012).

Given the involvement of lipids in the development of AD and MCI to AD progression, we hypothesized that lipids may also play a role in determining time to progression. To the best of our knowledge, our study is the first to have searched for the effect of plasma FAs on rate of progression from MCI to AD. Based on our results, higher levels of plasma DHA were associated with the faster rate of progression (OR 3.045, 95% CI 1.305 – 7.107, $p = 0.01$). In spite of positive neurocognitive effects of DHA proposed by AD and non-AD animal models (Arsenault et al., 2011; Cao et al., 2009), the results of human studies are less consistent. In relation to DHA and risk of AD development, Schaefer et al. found that higher serum phosphatidylcholine DHA levels were associated with a 47% reduction in the risk of dementia over 9 years of follow-up (Schaefer et al., 2006), but in another prospective observational study, dietary DHA intake was not associated with relative risk of AD (Devore et al., 2009).

Concerning the risk of cognitive decline in patients already suffering from AD, the results are also inconsistent. In a prospective cohort of 129 AD patients receiving AChEIs conducted by Chu et al., lower baseline serum DHA was associated with a greater risk of cognitive decline (OR = 1.131, 95% CI: 1.020, 1.254; p = 0.020) during two years of follow-up. However, these investigators did not find an association between DHA and rate of cognitive changes (Chu et al., 2022). In another study, 234 mild AD patients received DHA supplementation for 18 months. The authors reported no effect of DHA supplementation either on composite measures of cognition or on change in volume of hippocampus, whole brain, or ventricles compared to the placebo group (N = 164) (Quinn et al., 2010). In the latter study, the APOE ε4 non-carrier subgroup who received DHA had performed significantly better in some cognitive tests compared to non-carriers of the placebo group, but the cognitive benefit was not evident for APOE ε4

carriers. Comparing the CSF levels of DHA at baseline and at the 18-month follow-up in a small subsample of this DHA trial, these investigators observed that DHA-treated APOE ε4 carriers had less increase in CSF DHA compared to DHA-treated non-carriers (Quinn et al., 2010). This finding indicates that DHA concentration in plasma and CSF is affected by APOE isoforms. A recent investigation has demonstrated that APOE ε4 isoform disrupts BBB function in the hippocampus and medial temporal lobe, compared to the other APOE isoforms (ε2/ε3) (Montagne et al., 2020). A large percentage of our progressive MCI patients were APOE ε4 carriers (63%) and, therefore, we hypothesize that APOE ε4 isoform may have affected their brain accessibility to DHA and their plasma DHA concentration and consequently their rate of cognitive decline. That is, the association we found between higher plasma levels of DHA and more rapid rate of cognitive decline may indirectly indicate a disruption in the transport of DHA from plasma to CSF. In agreement with our hypothesis, Coughlan et al. reported an inverse association between serum DHA levels and spatial navigation performance in APOE ε4 carriers (Coughlan et al., 2021). However, we did not compare the association of DHA with time to progression between carriers and non-carriers of the APOE ε4 allele.

In addition to the influence of APOE ε4 genotype, the existence of deficiency in DHA transporters across the BBB is another possibility that may have led to this result. A major facilitator superfamily domain containing 2A (MFSD2A) is a transporter of DHA in the form of lysophosphatidylcholine (lysoPC) across the BBB (Nguyen et al., 2014). A recent study demonstrated progressive lower blood levels of this transporter in mild and severe AD patients compared to controls (Sánchez-Campillo et al., 2020). Therefore, it is possible that more rapid progressive MCI patients have lower levels of the transporters that in turn limits DHA access to the brain (CSF) but increases DHA levels in the blood. However, it cannot be ruled out that an increase in plasma DHA levels could be an adaptive response to increasing lipoxidation at peripheral and central systems to maintain homeostasis and membrane integrity of neurons. Nevertheless, this adaptation strategy would lead to potentially dangerous consequences for the cells because DHA is highly susceptible to oxidation (Naudí et al., 2015). However, we believe that our preliminary result should be put to the test by larger cohorts of MCI patients.

6.2.3. Association of plasma oxidative protein damage markers with AD diagnosis and progression from MCI to AD

In our study markers of oxidative protein damage in plasma were not associated with diagnosis, AD biomarkers, progression or time to progression. Searching the literature, we found many studies in which plasma/serum markers of oxidative damage have been investigated in AD. Therefore, we limited the comparison of our results with studies in which plasma markers of oxidative protein damage (oxidative modification of lysine and other amino acids) had been evaluated. In the previous studies, a variety of techniques have been used to evaluate oxidative damage to proteins, including ELISA, chemiluminescence, turbidimetry, chromatography, and chromatography-MS. For instance, in a study by Bär et al., levels of pentosidine and CML in serum of 15 probable AD (8 mild AD and 7 moderate to severe AD), 20 vascular dementia, and 31 control subjects (younger than other groups) were compared. AD patients were diagnosed based on NINCDA-ADRDA criteria (G. McKhann et al., 1984). Petosidine was measured using reversed phase-HPLC and CML using ELISA. They found a significant lower levels of CML in serum of AD patients compared to control subjects, but levels of pentosidine were not significantly different between groups (Bär et al., 2003). Sharma et al. analyzed the levels of CML and CEL in 40 AD patients (age 73 ± 5 years) and 34 control subjects (age 68 ± 8 years) by the UPLC-MS/MS method. They also searched for plasma protein carbonylation and 3-NT using ELISA and MDA using reversed phase-HPLC coupled with fluorescence detection. In their article, these investigators did not specify the criteria used for diagnosing AD patients. They only mentioned that AD patients with MMSE > 12 and < 25 had been selected for the analysis. Furthermore, although they claimed that controls were age-matched, no statistical results accompanied this claim. In contrast to the results reported by Bär et al., they found significantly higher levels of CML in AD relative to controls, and plasma levels of CEL were not significantly different between male subjects of the two groups, whereas it was lower in AD females than in female control subjects. Concerning protein carbonylation, they found higher levels in male AD subjects compared to control subjects, while no significant difference was observed among female control subjects. The levels of plasma MDA and 3-NT were also reported to be affected by sex (Sharma et al., 2020). In a study conducted by Haddad et al., the

serum levels of CML and pentosidine were measured for 38 AD, 14 MCI and 13 control subjects by ELISA. The AD patients were diagnosed based on NINCDA-ADRDA criteria (G. McKhann et al., 1984). MCI patients were selected based on cognitive test scores and Pertersen criteria (Petersen et al., 1999). They found no significant differences in serum levels of either CML or pentosidine between groups (Haddad et al., 2019). One of the main limitations of the study by Haddad et al. was that in spite of significant differences regarding age between AD, MCI and control groups, their data seemed not to be adjusted for age. In a study by Greilberger et al., the plasma levels of carbonyl proteins were measured for 16 AD, 6 MCI (both 67.6 ± 5.2 years), and 15 controls (60.8 ± 4.7 years) using the chemiluminescence technique after derivatization with dinitrophenylhydrazine. The redox state of serum albumin was also evaluated using HPLC. The AD and MCI patients were diagnosed based on the same criteria used by Haddad et al. (G. McKhann et al., 1984; Petersen et al., 1999). They found significantly higher carbonyl proteins and albumin disulphide in AD/MCI compared to controls (Greilberger et al., 2008). The latter study also had some limitations. In addition to the small sample size, the control group was apparently younger than the AD/MCI group. In spite of the emphasis by the authors that controls were age-matched, they do not present any statistical data to justify this claim and no evidence of age-adjustment is found in their report. Moreover, they did not report the levels of oxidative protein stress comparing the three diagnostic groups. This may indicate a lack of significance regarding these markers when the groups were separated into AD, MCI, and control. In a slightly larger cohort, Bermejo et al. assessed plasma protein oxidation levels in 45 AD, 34 MCI, and 28 controls. The MCI and AD patients were diagnosed based on the same criteria as the two previously mentioned studies. The plasma protein carbonyl levels were evaluated using measurement of optical density after derivatization with dinitrophenylhydrazine. They found significantly lower levels of protein carbonyls in plasma of controls compared to AD and MCI patients, while no significant difference was observed between these two latter groups. The authors concluded that oxidative protein damage may not be implicated in the progression of AD (Bermejo et al., 2008).

The diversities regarding measured marker, technique, and characteristics of the cohort subjects in the previous studies determine a diversity in the results that makes it difficult

to draw any conclusion regarding the degree of oxidative protein damage that may exist in plasma of patients with MCI and AD. In fact, the majority of the previously published studies were conducted using a small number of participants, used imprecise and less reliable techniques for the quantification of oxidative protein damage, such as ELISA or colorimetric methods, and did not consider the effect of confounding factors, such as age in the studies by Bär et al., Haddad et al., and Greilberger et. al. Furthermore, the AD diagnosis in the majority of the previous studies was based on the criteria published in 1984 that do not include the use of biomarkers in diagnosis.

As a result, we decided to see whether there is any meta-analysis concerning evaluation of oxidative protein damage in the blood of MCI and AD patients. Interestingly, and in accordance with our results, in a meta-analysis published in 2013 by Schrag et al., although MDA –as a direct marker of lipid peroxidation – was significantly increased in AD, no significant evidence of a change in plasma/serum protein oxidation levels was observed between AD (N = 334) and control subjects (N = 329). Regarding MCI subjects, at that time, the authors only found two studies that considered serum protein carbonylation in MCI and both had reported increased levels of carbonylation. However, the results of only two studies do not permit a reliable conclusion. Schrag et al. reported that only oxidation of LDL was increased in AD patients, likely indicating the pro-oxidative environment in the lipid fraction rather than a pattern of protein-targeted oxidation. In addition, their analysis revealed no evidence of alteration in enzymatic antioxidant capacity in the blood of AD patients (Schrag et al., 2013). In a more recent meta-analysis conducted by Nantachai et al., the oxidative stress in peripheral blood of exclusively MCI patients was meta-analyzed. In agreement with our results and the study by Schrag et al., they detected no significant difference regarding protein oxidation between MCI (N = 335) and control subjects (N = 248) (Nantachai et al., 2021). Therefore, the results of these two meta-analyses are in accordance with our results concerning the lack of alteration in plasma oxidative protein damage markers in AD and MCI compared to control subjects. We believe that having a large study population (n = 286), the use of targeted GC/MS that is a robust and precise method, and controlling for possible confounding factors, makes the results of our study more reliable than previous reports. In addition, the findings of these two meta-analyses also validate our results

regarding a lack of association between plasma oxidative protein damage and the development and progression of AD. Finally, our data suggest that plasma do not show alterations regarding protein oxidation in MCI/AD, that is in accordance with our CSF results and the previous data from brain tissue, as discussed earlier.

6.3. CSF Lipidomics

6.3.1. CSF lipids associated with diagnosis of MCI and AD

Altered metabolism of lipids in AD has been studied using different biological samples including post-mortem brain tissue and CSF. Concerning brain tissue studies, the majority have quantified some pre-defined classes of lipids. For instance, in a study conducted by Culter et al., levels of sphingomyelins (SM), ceramides, and cholesterol from the middle frontal gyrus and cerebellum of seven neuropathologically-confirmed AD patients and seven age-matched neurologically normal controls were compared. Total lipids from brain tissues and isolated membranes were injected directly into an electrospray tandem MS (ESI-MS/MS). They found significant increases in the levels of ceramide 24:0, galactosylceramide and free cholesterol in the middle frontal gyrus, but not in the cerebellum of AD patients compared to controls. In addition, they reported that the levels of SM were significantly decreased in the middle frontal gyrus, but not in the cerebellum of AD patients compared to control subjects (Cutler et al., 2004). In another study, He et al. evaluated the levels of SM, ceramide, sphingosine 1-phosphate (S1P), and sphingosine in frontal gray matter from nine neuropathologically-confirmed AD and six age-matched control samples using HPLC. They separated the soluble (cytosolic) fraction from membrane fraction (pelleted after ultracentrifugation). They found a significant reduction of SMs in membrane fraction and a significant increase of ceramides and sphingosine in the cytosolic fraction of AD samples compared to the controls. In the cytosolic fraction, S1P content showed a more significant reduction in AD samples than controls (He et al., 2010). Han et al., assessed the sulfatide, galactocerebroside, ceramide, PC, and SM content in cerebrum (frontal, parietal and temporal) and cerebellum gray and white matter in 22 brain samples from subjects at different stages of AD dementia using ESI-MS. Their study population was composed of

subjects who had a clinical dementia rating[10] (CDR) score of 0, 0.5, 1, 2, or 3 at the time of death and AD patients that had neuropathological confirmation of the disease. Surprisingly, the authors did not mention the number of patients in each group. They observed significantly lower levels of sulfatide in all regions of both gray and white matter in AD patients than in controls. Regarding ceramide, temporal and cerebellum white matter from AD patients had significantly higher levels of ceramide compared to controls, while in the gray matter the differences were not significant. They also reported no significant alteration in galactoscerebroside, PC and SM levels between the two groups (Han et al., 2002). In another study, the latter group of investigators, using the same analytical method, reported a significant reduction in phosphatidylethanolamine plasmalogen (PE(P)) content of white and gray matter in AD brain samples (CDR 0.5, 1, 2, and 3, N = 6 in each) compared to controls (N = 6). The reduction of PE(P) content in gray matter was correlated with disease severity (Han et al., 2001). Using a non-targeted lipidomic approach, Wood et al. evaluated the frontal cortex gray and white matter lipidome of 28 controls (Braak stage 0-4), 19 MCIs (Braak stage 4), and 34 subjects with dementia (Braak stage 6). All demented patients had been clinically diagnosed with dementia (G. McKhann et al., 1984) and neuropathological characterizations. The authors did not mention the diagnostic criteria for MCI subjects. In addition, they did not specify the types of dementia in the demented group. They found a reduction in levels of PE(P) in the gray matter of the demented group compared to control subjects. This difference was not significant in white matter between the two groups. A significantly greater reduction in levels of polyunsaturated PE in the gray matter of MCI and demented subjects than in control subjects was also observed. The gray matter of MCI and demented subjects also showed dysregulations regarding neutral lipid, showing increased MG and DG compared to control subjects. They found no significant alterations regarding either other PLs, ceramides and SM or TGs between groups (Wood et al., 2015). Varma et al. used a targeted metabolomic approach to quantify metabolic alterations of AD brain using a cohort consisting of 15 AD, 14 control, and 15 asymptomatic AD subjects. The neuropathological alterations of AD were

[10] The Clinical Dementia Rating is a numeric scale used to quantify the severity of symptoms of dementia. It has four scales: CDR 0: no dementia; CDR 0.5: questionable dementia, CDR 1: MCI; CDR2: moderate cognitive impairment; CDR 3: severe cognitive impairment (Hughes et al., 1982).

confirmed based on CERAD and Braak criteria. They quantified metabolite alterations in inferior temporal and middle frontal gyri and cerebellum of the participants. The targeted metabolomics was performed using a commercial Kit that allows for the quantification of amino acids, acylcarnitines, SMs, PCs, hexoses, and biogenic amines. The lipids were analyzed by flow injection analysis tandem mass spectrometry (FIA-MS/MS). They found that lipid dysregulation profile in inferior temporal gyrus had greater discriminating power between AD and controls compared to middle frontal gyrus. They observed dysregulation regarding both PCs and SMs between the two groups. These two lipid classes were also associated with disease severity comparing all three diagnostic groups. Globally, SMs had higher levels in AD and PCs were higher in control brains (Varma et al., 2018).

Reviewing previous lipidomic studies of the AD brain illustrates an inconsistent picture of overall changes in lipid metabolism. These inconsistencies may be related to the method used to quantify lipids, the brain region selected for analysis and the differences concerning the cohorts of subjects. However, the previous findings support the idea that lipid dysregulation is indeed present in the context of AD.

Regarding CSF lipidome, although the number of studies is highly limited, the picture is relatively the same and there are reports with inconsistent results. Most of the studies look for alterations in a specific class or species of lipids in CSF. For example, in a study that was restricted to evaluating ceramides using DG kinase and subsequent chromatographic separation, Satoi et al. measured the CSF levels of ceramides for 16 AD, 14 amyotrophic lateral sclerosis (ALS), and 14 control subjects. The AD patients were diagnosed based on the diagnostic and statistical manual of mental disorders, 4th edition (DSM-IV) and graded by CDR. They found significantly higher levels of ceramides in CSF of AD compared to controls, but this difference was not significant between either AD and ALS or control and ALS groups (Satoi et al., 2005). Targeting only PLs, Kosicek et al. analyzed CSF from 7 control subjects (age 55 ± 4) and 9 probable AD patients (age 71 ± 3) using nano-HPLC-MS. AD patients were diagnosed based on NINCDS-ADRDA and DSM-IV criteria. They found no significant differences in CSF levels of PE, PC, and phosphatidylinositol (PI) between AD and controls, but AD patients had significantly higher levels of SMs (SM(16:0), (16:1), and (22:0)) compared to controls. However, the

authors did not mention whether their results had been adjusted for age (Kosicek et al., 2010). Using the same analytical method, the latter group of investigators examined SM levels in CSF from 7 moderate AD (MMSE 10-20), 7 mild AD (MMSE 21-23), 5 prodromal AD (MMSE 24-29), and 16 control subjects (MMSE 30). AD patients were categorized as probable based on NINCDS-ADRDA criteria. Prodromal AD was diagnosed according to the Dubois criteria (Dubois et al., 2007). In contrast to their previous results, they did not observe a statistically significant difference in CSF levels of SM between individuals with mild and moderate AD compared to cognitively normal individuals. Only the prodromal AD subjects showed significantly higher levels of SM compared to control subjects. Individual SM species that were significantly different between these two groups included SM(14:0), (16:0), (16:1), (20:0), (22:0), (22:1), (24:0), (24:1), (24:2) (Kosicek et al., 2012). In another study conducted by Mulder et al., levels of PC, lysoPC, and lysoPC/PC ratio were assessed using ESI-MS/MS for 19 probable AD patients (NINCDS-ADRDA criteria) and 19 individuals with subjective memory complaints. No difference regarding CSF PC and lysoPC were observed between AD patients and control subjects. However, they found that the lysoPC/PC ratio was significantly decreased in the AD group compared to the controls (Mulder et al., 2003).

Regarding CSF untargeted lipidomics, the approach we used in our study, we found two previous reports. The first report was published by Wood et al. The cohort characteristics are set out in the previous paragraph. They found no alteration in post-mortem CSF of demented patients compared to controls except for decreased levels of DHA in MCI and demented patients over control subjects (Wood et al., 2015). In a study conducted by Byeon et al., the CSF lipidome profile of 17 AD, 15 MCI, and 18 control subjects were analyzed using LC-MS/MS. The control group was younger than the other two groups and mainly consisted of women (65%). Diagnostic criteria for the subjects with AD (CDR1, mild AD) and MCI followed the NIA-AA criteria. For the AD group, they only included subjects with Aβ42/Aβ40 ratio <0.1 and increased Ptau level. The statistical analysis was performed based on the differences in lipid fold change between groups. A differential expression was considered if fold change > 1.5 or < 0.67 and $P < 0.05$. No FDR correction or other restricting criteria were applied to the analyzed data. In addition, these investigators did not mention any adjustment regarding age and sex

for their data. They found reduced levels of several PL species, including PC, PE (some with ether bond), and PI and also decreased levels of some monohexosyceramide, SM, and CE species in AD patients compared to controls. They reported that CSF levels of some TG and DG species were increased in AD compared to control subjects. Some of these species showed the same direction of changes in the MCI group, but to a lower extent (Byeon et al., 2021).

In CSF we found no lipid associated with the diagnosis. The majority of the previous studies used a targeted lipidomic approach while we analyzed the CSF samples in an untargeted manner. This difference makes the comparison of our results with theirs somewhat inaccurate. Our study, in spite of considerable differences, is consistent with the result found by Wood et al. who reported no lipid associated with diagnosis between dementia, MCI and controls after an untargeted lipidomic evaluation. Compared to the previous CSF studies, we had a larger study population (N = 210) thus increasing the robustness of our results. In addition, to reduce the probability of false positive results, we applied some statistical filters (step-by-step forward selection with conditional criteria and adjustment of significance level to 1%) that were not considered in previous untargeted studies, such as the study by Wood et al. Our result regarding the lack of association between CSF lipids and diagnosis may also be related to the small size of the control group, as discussed earlier, and/or our restrictive statistical analysis. We adjusted our data for age, sex, and APOE status. In addition, considering that our objective was to detect lipids associated with diagnosis that act independently of known pathological events (amyloid and tau pathologies) of AD, we included CSF levels of Aβ42, Ttau, and Ptau as covariates in our statistical analysis. Therefore, it is possible that lipid dysregulation reflected in CSF may be mainly related to the pathological hallmarks of AD.

6.3.2. CSF lipids associated with AD biomarkers

Searching for an association of lipids with pathological hallmarks of AD is of special importance. The existing literature has shown that lipid dysregulation is a key player in AD, however, it is not well understood which lipid species are linked to each pathological alteration. Unraveling lipid dyshomeostasis related to each AD pathological aspect not

only increases our understanding of the role of lipids in AD pathology, but may also have important implications in the development of diagnostic biomarkers and drug discovery. Notably, only a small number of studies have searched for the association between lipids and pathological alterations of AD. Regarding lipid alterations in brain tissue, some studies have looked for the association between lipids and CERAD or Braak scores. For example, Varma et al. found, generally, a significant positive correlation between brain SM concentration and CERAD and Braak scores, while brain PC concentration was negatively correlated with both of these pathological scales (Varma et al., 2018).

In CSF, Mielke et al., found a positive association between SM species and measures of CSF Aβ42, Ttau, Ptau and also a positive association between 18-carbon acyl chain length ceramide species and Ttau measures in cognitively normal individuals aged 36-69 years at increased risk of AD due to a parental family history (Mielke et al., 2014). Koal et al. compared the metabolome differences between 50 subjects with pathological levels of CSF Aβ42, Ttau and Ptau and 50 subjects with normal CSF levels of these biomarkers. They found that CSF levels of two SMs (SM(d18:1/18:0) and SM(d18:1/18:1)), five PCs (PC(32:0), PC(34:1), PC(36:1), PC(38:4), and PC(38:6)) and one acylcarnitine were significantly higher in samples with AD pathology compared to control samples (Koal et al., 2015). In another research study, Teitsdottir et al. analyzed the CSF lipids using UPLC-MS. They included 13 participants with subjective memory impairment, 23 MCI, 20 AD, three Lewy body dementia, and one Parkinson's disease subjects. They compared the CSF lipidome of the participants who had pathologic levels of Aβ42 and Ttau (N = 34, 20 AD, 10 MCI, three subjective memory impairment and one Lewy body dementia subjects) with those that had a non-AD profile (13 MCI, 10 subjective memory impairment, two Lewy body dementia, and one Parkinson's disease subjects). T-tau/Aβ42 ratio >0.52 was defined as a CSF AD profile signature. From eight features associated with the CSF biomarker profile they confirmed the identity of C18 ceramide. The CSF levels of this lipid were higher in patients with a CSF AD profile compared to patients with a CSF non-AD profile. Pearson correlation analysis revealed that CSF content of C18 was positively correlated with Ttau measure and Ttau/Aβ42 ratio and negatively with CSF Aβ42 (Teitsdottir et al., 2021).

In contrast to our study, in these two latter studies, the pathological alterations of AD are considered as a whole and the association of lipids with each AD biomarker was not assessed separately. In addition, the study by Mielke et al. (Mielke et al., 2014) measured only SMs and ceramides and their study population was younger and free of dementia. Furthermore, they did not take into account the possible presence of shared pathological pathways between each AD pathological hallmark. Therefore, in an attempt to find lipid alterations related to each AD biomarker, in addition to controlling for other possible confounding variables, such as age, sex, and APOE ε4 status, we adjusted our data for CSF biomarkers other than the one that had been used as a dependent variable. Therefore, this is the first report regarding the specific association of CSF lipids with each AD pathological hallmark (CSF Aβ42 as a marker of amyloid pathology, Ptau as a marker of tau pathology, and Ttau as a marker of neurodegeneration).

Consistent with the previous literature that highlights the direct and indirect implication of lipids in APP processing, Aβ aggregation and clearance (reviewed by Grimm et al., 2017), we found more lipid species associated with Aβ42 status than Ttau and Ptau statuses. Among 16 lipid species that were associated with amyloid pathology we identified four species: hexacosanoic acid (C26:0), Cer(d38:4), PE(40:0), and PC-O(36:3)/PC-P(36:2)). C26:0 is a saturated very long chain fatty acid (VLCFA). Based on our results, subjects with higher CSF levels of this FA have reduced risk of pathologic levels of Aβ42 in CSF. In line with our finding, Iuliano et al. found lower levels of C26:0 in plasma of AD and aMCI patients compared to controls (Iuliano et al., 2013). However, these data are not in line with some other studies. For example, an *in vitro* experiment showed that C26:0 increased APP processing and Aβ42 generation (J. J. Liu et al., 2019). There is no previous report concerning the effect of C26:0 on production/clearance of Aβ42 *in vivo*. A brain tissue analysis showed higher levels of VLCFAs at Braak stage V-VI compared to stage I-II and higher levels of brain cortical C26:0 in stage V-VI compared to stage I-II, III-IV. In addition, higher levels of VLCFA were more related to NFT than plaque pathology (Kou et al., 2011). In accordance with the latter study, in a study by Zarrouk et al., plasma and red blood cell levels of C26:0 were reported significantly higher in 64 demented patients compared to 128 control subjects (Zarrouk et al., 2015).

VLCFAs, including C26:0, are metabolized in peroxisomes. Peroxisomes are subcellular organelles that play a key role in the β-oxidation of VLCFAs, the biosynthesis of PUFAs and plasmalogens, i.e., ether phospholipids, and metabolism and scavenging of ROS. We also found higher CSF levels of PC(O-36:3)/PC(P-36:2) as a protective factor for amyloid pathology. In agreement with this result, a decrease in plasmalogen levels has been observed in post-mortem brain samples from AD patients (Ginsberg et al., 1995; Lizard et al., 2012). Therefore, dysregulation regarding C26:0 and PC(P) may indicate the implication of peroxisome dysfunction in amyloid pathology. Although peroxisomal dysfunction has been previously reported in AD (Jo et al., 2020; Kou et al., 2011; Lizard et al., 2012), a direct effect of peroxisome dysfunction on amyloid pathology has not been studied.

Peroxisome proliferator-activated receptor-alpha (PPARα) regulates the expression of genes involved in peroxisomal and mitochondrial FA β-oxidation and is a major regulator of energy homeostasis. Some PPARα ligands have been shown to reduce amyloid plaque pathology in transgenic animal models of AD. Further, the ADAM10 gene has been demonstrated to be a PPARα target (Sáez-Orellana et al., 2020). Therefore, it is possible that PPARα mediates both APP processing and peroxisomal lipid homeostasis and, therefore, its dysregulation in AD (De La Monte & Wands, 2006; Heun et al., 2012) affects both processes. On the other hand, peroxisomal lipid dysregulation possibly affects membrane composition because both plasmalogens and PUFA, which are major components of brain membranes, are produced in peroxisomes. As a consequence, peroxisomal abnormalities may affect APP processing and Aβ42 production through affecting membrane fluidity. In addition, peroxisomal dysfunction may also lead to altered APP processing by increased oxidative stress. An increase in ROS could be involved in the production of Aβ by disruption of membrane integrity and altering functionality of the membrane proteins, including APP processing enzymes (Muche et al., 2017).

Another lipid species associated with amyloid pathology was Cer(d38:4). Ceramides are structural constituents of biological membranes, and are also involved, as bioactive molecules, in a variety of biological events, including cell differentiation, redox metabolism, cytokine release, inflammation, growth arrest, and cell proliferation.

Increased levels in the brain of some ceramide species have been reported in the AD brain (Cutler et al., 2004; He et al., 2010), while other reports found no significant difference in ceramide levels between AD and controls (Wood et al., 2015). In CSF, Satoi et al. found higher levels of ceramides in AD patients compared to controls (Satoi et al., 2005). There is no previous report concerning the association between CSF ceramide levels and amyloid pathology.

We found that higher levels of Cer(d38:4) decreased the risk of Aβ42 positivity. Some *in vitro* experiments link amyloid pathology to ceramide homeostasis. The β- and γ-secretases, APP processing enzymes in the amyloidogenic pathway, are stabilized and have an increased half-life in ceramide enriched membranes that leads to increased Aβ production (Puglielli et al., 2003; Takasugi et al., 2015). Furthermore, extracellular ceramide transfer protein has been found in amyloid plaques (Mencarelli et al., 2012). A recent *in vitro* study has shown that ceramide transfer protein can bind to APP, modify Aβ aggregation, and reduce Aβ neurotoxicity (Crivelli et al., 2021). In turn, Aβ can stimulate ceramide production by activating the sphingomyelinase which converts SM into ceramide (J. T. Lee et al., 2004; Malaplate-Armand et al., 2006). Although the results of *in vitro* experiments seem to be opposite to our result, this discrepancy may be related to the difference between ceramide species used for these experiments and the one we found in our study. It has been demonstrated that specific ceramide species have distinct cellular functions (Wattenberg, 2018). In the study conducted by Puglielli et al., exogenous Cer(d18:1/6:0) was used and Takasuagi et al. used two synthetic ceramide analogues (dl-threo-1-phenyl-2-decanoylamino-3-morpholino-1-propanol (PDMP) and (1S,2R-d-erythro-2-N-myristoylamino)-1-phenyl-1-propanol (DMAPP) for their experiments. In addition, the cellular localization of ceramides has also been shown to affect their biological activity. For example, it has been shown that mitochondrial ceramide, but not ceramide in other compartments, induces cellular apoptosis (Birbes et al., 2001). Therefore, the positive association we found between levels of Cer(d38:4) and Aβ42 in CSF, may indicate that not all of the ceramide species have a negative impact on AD pathology and they should not be considered as a solid pool with negative or positive effects on AD pathological pathways.

The mechanistic pathways whereby ceramides could affect Aβ pathology are not well understood. The existing evidence indicates that ceramides may directly interact with APP processing enzymes and regulate their activity (Puglielli et al., 2003; Takasugi et al., 2015). In addition, they can modulate physical properties of biological membranes and, as a consequence, indirectly affect the activity of membrane-embedded enzymes (Trajkovic et al., 2008). Furthermore, as second messenger molecules, they can affect other processes implicated in amyloid pathology, such as inflammation and oxidative stress (Gaggini et al., 2022). Herein, for the first time, we detected an association between CSF levels of a certain ceramide and Aβ42. Our result, in line with the previous *in vitro* findings, links ceramide homeostasis with amyloid pathology.

CSF measures of Ptau and Ttau are considered biomarkers of two distinct pathological aspects of AD. While Ptau is a specific biomarker of AD and is measured using antibodies against the phosphorylated tau protein, antibodies used for the measurement of Ttau in CSF are against epitopes outside the alternatively spliced exons and recognize all tau isoforms independently of phosphorylation state. Ttau is considered a biomarker of neurodegeneration and its increase is also reported in other neurodegenerative diseases, such as Creutzfeldt-Jakob disease, stroke, frontotemporal dementia, and vascular dementia (Jack et al., 2018). Our analysis detected a lipid that was specifically associated with Ttau status. However, the identity of this lipid remained unknown. Regarding Ptau, we found six lipid species that were specifically associated with CSF Ptau status of which, we only were able to identify one species. We observed that higher CSF levels of SM(30:1) increased the risk of Ptau positivity in our study population. In agreement with our result, Varma et al., reported a positive correlation between brain levels of several SM species and disease severity determined by Braak scores (Varma et al., 2018). Therefore, our data and the study by Varma et al. indicate a possible link between disturbance in SM homeostasis and phosphorylation of tau protein.

How SMs could affect phosphorylation of tau or vis versa is not clear. SM is the most abundant SP in the brain and is highly enriched in myelin sheaths. Myelin sheaths produced by oligodendrocytes cover axonal projections, where large quantities of tau are localized. This proximity may also suggest some bidirectional impact between SMs and tau protein. In addition, in oligodendrocytes, proteins and messenger RNAs

necessary for myelination should be translocated to their target site at the tips of very long processes via cytoskeleton translocation machinery. Therefore, tau as a cytoskeleton associated protein and a regulator of motor proteins could play a key role in myelination. In fact, myelin formation requires tau in oligodendrocyte processes and process tips during the lifetime of neurons. Hyperphosphorylation of tau disrupts tau sorting into these projections and interfere with the sorting mechanism that underlies myelin formation (Lopresti, 2018). Although Ptau is more abundant in neurons, AD animal studies have shown that Ptau is also abundant in oligodendrocytes (Soto-Faguás et al., 2021). Interestingly, a recent finding suggests that oligodendrocytes may have role in the seeding and spreading of Ptau (Ferrer et al., 2019). It is also shown that some tau phosphorylation kinases affect myelination. For example, cyclin-dependent kinase 5 (CDK5) positively affects myelination, whereas glycogen synthase kinase 3β (GSK3β) signaling pathways are known to be detrimental. Recent evidence points to the possible role of SPs in the phosphorylation of tau protein. Using a humanized yeast, Randez-Gil et al. showed that genetic and pharmacological inhibition of SP biosynthesis increased the hyperphosphorylation of tau, while the opposite effect was observed by increasing SPs synthesis. They demonstrated that Sit4, the yeast ortholog of human protein phosphatase 2, is a downstream effector of SP signaling in mediating the tau phosphorylation state (Randez-Gil et al., 2020).

Altogether, our data and findings by other labs suggest a relationship between the phosphorylation of tau and the disturbance of SM biosynthesis. Additional studies are required to understand the functional consequences of tau phosphorylation on myelination and SM biogenesis and vice versa.

6.3.3. CSF lipids associated with progression and rate of progression from MCI to AD

Some previous studies included an MCI group to search for lipids that could discriminate these patients from AD or control subjects. However, looking for CSF lipids that affect the progression from MCI to AD by comparing the lipid profile of progressive versus non-progressive MCI patients has not been carried out previously. Our analysis related two lipid species with MCI to AD progression: a CE and an unidentified lipid feature. We

found that higher CSF levels of CE(11D3:1) were associated with an increased risk of progression. These two lipids slightly increased the predictive value of the statistical model from 0.86 to 0.88, indicating that lipids can have an additive value to the predictive power of known markers (markers of pathology, APOE ε4 allele, and baseline cognition) that affect the progression from MCI to AD.

In the adult brain, astrocytes are the key producers of cholesterol necessary for the maintenance of neuronal plasticity and glial performance. Cholesterol is transported from astrocytes to neurons by APOE lipoproteins. Excess cholesterol is esterified to CEs for storage in lipid droplets (LDs) and this reservoir can be used as a source of cholesterol for future needs. Excessively high cholesterol levels are toxic for the cells and in this condition esterification of cholesterol and reserving them in LDs could be a strategy for protecting the cells from detrimental effects of abnormal levels of cholesterol (Feringa & van der Kant, 2021).

Cholesterol has long been associated with an increased risk of AD (Reviewed by Feringa & van der Kant, 2021). In addition, APOE, the major genetic risk factor for LOAD, acts as a CE transporter in the brain. The accumulation of CEs has been reported in the AD brain (Cutler et al., 2004; C. C. Liu et al., 2013) and in AD transgenic mice (Chan et al., 2012; Tajima et al., 2013; Yang et al., 2014). Some previous lipidomic studies have linked plasma and CSF levels of CE species with the diagnosis of MCI and AD (Proitsi et al., 2015). These associations have also been confirmed after demonstrating that CE is a modulator of amyloid and tau pathologies. For example, studies have demonstrated that CE regulates APP processing and increases the production of Aβ (Huttunen et al., 2009; van der Kant, Goldstein, et al., 2019). Recently, it has been shown that CE is also implicated in Ptau regulation through proteasome upregulation and degradation of Ptau (van der Kant, Langness, et al., 2019). These findings highlight cholesterol and its metabolites as central players in AD pathogenesis upstream of amyloid and tau pathologies. The effect of CE on amyloid and tau pathologies also links this molecule to neuronal injury, the pathological aspect of AD that most correlates with clinical progression and cognitive decline, because oligomeric species of both amyloid and tau proteins are toxic for synapses and are implicated in synaptic damage. Therefore, by regulating amyloid and tau pathologies, intracellular levels of cholesterol, in the form of

CEs, could play an important role in neurodegeneration. In addition, LDs (the storage site for CE) have been shown to be active signaling organelles that regulate processes such as proteasome activity, inflammation, and oxidative stress, all as possible drivers of neuronal injury and cell death (Farmer et al., 2020).

On the other hand, cholesterol, as a main component of cellular membranes, could have a direct effect on synaptic function. It has been shown that this molecule plays fundamental roles in synaptic plasticity and function in the brain. Both presynaptic and postsynaptic membranes are enriched in cholesterol which suggests a direct implication of cholesterol in synaptic transmission. Cholesterol has been shown to be essential for presynaptic vesicle fusion by facilitating membrane curvature and interaction with synaptic vesicle proteins. At postsynaptic membranes, cholesterol and its metabolites are involved in regulating the number of postsynaptic receptors and facilitating LTP in hippocampus (Reviewed by Martín et al., 2014; Petrov et al., 2016). Cholesterol has been recognized as a negative modulator of spontaneous presynaptic glutamate release. In the postsynapse membranes, physiological levels of cholesterol have been shown to be important for keeping the normal probability of opening of NMDA receptors and for maintaining these receptors localized in synapses. In the presynapse membranes, cholesterol has been shown to take part in the propagation of axonal action potentials (Korinek et al., 2020). In another study, 27-hydroxycholesterol, an oxidized form of cholesterol, has been shown to impair neuronal morphology and reduce hippocampal spine density and the levels of the postsynaptic protein PSD95 (Merino-Serrais et al., 2019). Taken together, these data highlight the fundamental role of cholesterol in synaptic function. Therefore, dysregulation in brain cholesterol homeostasis would affect cognitive abilities as evidenced recently (Martinez et al., 2022) and CSF levels of intracellular cholesterol (CE) could be a potential biomarker of progression from MCI to AD.

Interestingly, in a recent study, statin therapy for dyslipidemia was associated with a reduced risk of progression from MCI to dementia (Cheng et al., 2020). Peripheral cholesterol dysregulation has also been shown to affect the cognitive performance of elderly adults (Stough et al., 2019). However, considering that BBB prevents the transfer of cholesterol and it is synthesized de novo in the brain, the impact of plasma cholesterol

on the brain cholesterol pool and the effect that it could have on neurodegeneration is unclear. The systemic pool of cholesterol, if it affects neurodegeneration, would possibly act by activating other pathways, such as chronic inflammation or by increasing the risk of other cardiovascular conditions, such as hypertension that in turn negatively affect AD progression and cognition.

The increased levels of CE in CSF that were associated, in our study, with an increased risk of progression may have been caused by dysregulation in several pathways. APOE is the major transporter of cholesterol from astrocytes to neurons. It has been shown that ε4 allele is less efficient than ε3 in transporting brain cholesterol. In addition, ε4 astrocytes form more LD than ε3 astrocytes (Farmer et al., 2019). In spite of the documented effect of APOE genotype on cholesterol homeostasis in the brain, the higher frequency of ε4 allele in our progressive MCI patients may not be the only reason for increased CE in this population because we had adjusted our data for the effect of APOE genotype. Another possibility could be that transport of cholesterol from brain to periphery is more disrupted in progressive patients than non-progressive MCIs. Excess cholesterol is converted into oxysterols by cholesterol hydroxylase enzymes. Oxysterols can diffuse from BBB and metabolize in the liver. Increased levels of oxysterols have been reported in MCI patients (Q. Liu et al., 2016). In addition, dysregulation regarding cholesterol hydroxylase enzymes has been associated with increased risk of AD (M. Li et al., 2013) and a more rapid course of cognitive decline in later life (Lai et al., 2014). Another reason for which progressive patients had a higher amounts of CEs could be that they may have suffered more neuronal injury and neurodegeneration. Dying neurons generate high levels of cholesterol-rich debris that could be swallowed by glial cells and lead to increased intracellular cholesterol in the form of CE in these cells (Feringa & van der Kant, 2021). Whether an increase in CEs is a cause or consequence of neurodegeneration, our data, for the first time, links higher levels of CEs in CSF with an increased risk of progression from MCI to AD.

As mentioned earlier, little is known about whether lipids could affect the course of cognitive decline in MCI patients who progress to AD. In this regard, CSF would be an interesting and reliable source for examination because it is in contact with the extracellular space of the brain cells. Our study is the first to search for the association

of CSF lipids with time to progression from MCI to AD. Our data showed that higher CSF levels of an ether-linked triglyceride (TG(O-52:2)) and two PAs (PA(42:5) and (PA(46:7)) were associated with a shorter time to progression, while higher CSF levels of Cer(d36:2) were associated with a longer time to progression.

TG(O) are lipid species that have been found exclusively in LDs. Structurally, they are TGs in that the sn-1 position of the glycerol backbone is attached by an ether, instead of ester, bond. The presence of the ether bonds makes these lipids more susceptible to oxidative stress than TG with ester bonds. TG(O)s account for approximately 20% of TGs in the LDs. However, the exact role of TG(O) lipids in cell biology is not clear. One of the possible functions of TG(O) in LDs could be the protection of FAs attached to other TGs in LDs from oxidative stress. This function has been demonstrated for their phospholipid counterparts (ether phospholipids or plasmalogens) whose presence in the membrane protects other lipids against oxidation (Brites et al., 2004). Our data regarding increased CSF TG(O-52:2) and a more rapid course of progression and the result regarding the association of higher levels of CSF CE and increased risk of progression suggests that LDs are implicated, as a cause or consequence, in pathophysiological processes of neurodegeneration. In fact, LDs are not simply a depot of lipid storage but are dynamic and functionally active organelles involved in a variety of cellular functions including energy and redox homeostasis, inflammation, protection from ER stress, and the regulation of autophagy.

In the brain, LDs have been found both in neurons and in glial cells. In the AD brain it seems that the accumulation of LDs is more pronounced in glia. In fact, Alois Alzheimer described “adipose saccules” in glial cells of an AD patient over a century ago (Stelzmann et al., 1995). Now, it is documented that oxidative stress increases the number of LDs in glial cells, especially in astrocytes. Oxidized lipids produced in neurons are transported in a process mediated by APOE to surrounding astrocytes for their detoxification and storage in LDs. Previous studies have found elevated lipoxidation markers in AD and MCI brain (Zabel et al., 2018). Therefore, the formation of LDs in AD could be a strategy for delaying neurotoxicity. Interestingly, as the APOE ε4 allele is less efficient at lipid transport and clearance, harboring this allele has been linked to accelerated neurodegeneration (L. Liu et al., 2017). Therefore, the positive association we found

between CSF levels of CE and progression and the negative association between TG(O) levels in CSF and time to progression suggest that lipoxidation could be a driving force behind neurodegeneration, and the protecting mechanisms for reducing this neurotoxicity, such as LD formation, could affect time to progression. In spite of the efficiency of glia in sequestering peroxidated lipids, they have a limited capacity to do so. Glial cells eventually fail to resist the harmful consequences of peroxidated lipid storage which finally leads to a subsequent neuronal death (Moulton et al., 2021).

Another possibility is that LD formation (increase in TG(O)) is not a cause, but rather a consequence of neuronal damage. As mentioned in the previous section, microglia also can accumulate LDs by phagocytosis of lipid-rich debris generated after neurodegeneration. Interestingly, LD-containing microglia have reduced phagocytic capacity suggesting a possible feedback system where excessive LD accumulation in these cells impedes rates of phagocytosis. Therefore, although the formation of LD begins with a good intention, excessive LD accumulation in microglia consequently exacerbates neuronal loss (Ralhan et al., 2021). However, both conditions may simultaneously increase LDs in AD. Nevertheless, our data, for the first time, link the brain intracellular neutral lipids that are sequestered in LDs to cognitive impairment and the clinical evolution of MCI patients. Therefore, measurement of these lipids may have a prognostic value in these patients.

In addition to TG(O-52:2), we identified three other lipids associated with rate of progression: PA(42:5), PA(46:7), and Cer(d36:2). LDs have been identified as a source of lipid mediators and both PAs and ceramides are important signaling molecules. However, we do not know whether or not these lipids originated from LDs. PA is a peculiar lipid because most of the PLs are synthesized from this molecule. On the other hand, PA can be released from PLs by hydrolysis activity of phospholipase D (PLD) enzymes and act as a signaling molecule. As a signaling lipid, PA regulates a great number of intracellular signaling pathways and cellular functions (Tanguy et al., 2019). PLDs have been suggested to contribute to the development of AD pathology (Paolo & Kim, 2012). Astrocyte PLD1 and its lipid product, PA, have been shown to regulate dendritic branching and synapse formation in neurons (Y. B. Zhu et al., 2016). Interestingly, Oliviera et al. showed that PLD2 knockout ameliorated AD-related synaptic

dysfunction and cognitive deficits in a model of AD (Oliveira et al., 2010). Therefore, these data, in line with our result, suggest that PA homeostasis may affect synaptic dysfunction and cognitive impairment in AD.

PA can also be produced by phosphorylation of DG. Recent evidence suggests that the DG-PA signaling pathway may be implicated in dysregulation regarding protein phosphorylation, including tau protein, in AD (Ferrer et al., 2021). In fact, PA can target many protein kinases, among which some have been strongly linked to both amyloid and tau pathology, such as mTOR kinase (Mueed et al., 2019).

Ceramide dysregulation, as discussed earlier, has been reported in the AD brain. Evidence also links ceramides to the cognitive performance of MCI patients. For example, in a cohort consisting of 25 controls, 17 aMCI, and 21 early probable AD subjects, higher levels of some plasma ceramide species (Cer(d22:0) and Cer(d24:0)) predicted cognitive decline and hippocampal volume loss one year later (Mielke et al., 2010). Our data revealed that ceramides are associated with amyloid pathology. In addition, cellular studies suggest that ceramides may modulate APP processing (Puglielli et al., 2003; Takasugi et al., 2015). Therefore, ceramides, by modulating Aβ production, could affect the synaptic toxicity mediated by Aβ soluble species. Furthermore, as second messenger molecules, they can affect other processes implicated in synaptic failure, such as inflammation and oxidative stress (Gaggini et al., 2022). However, the exact nature and role of PA and ceramide imbalance in pathophysiological processes underlying cognitive impairment remains to be fully defined.

6.4. Plasma lipidomics

6.4.1. Plasma lipids associated with diagnosis of MCI and AD

Searching for the association between blood lipids and the diagnosis of AD has been a hot topic during the last decade. Both the general blood lipid profile (i.e., TC, HDL-C, LDL-C, and TG) and a more detailed lipid profile examined using lipidomics have been under investigation. The scope of investigation in this field is so wide that to date several review articles and meta-analyses have been published in this regard. Therefore, in

order to examine the state of the art regarding the dysregulation of lipids in AD, we will discuss the results of these meta-analyses.

The dysregulation regarding plasma/serum TC, HDL-C, LDL-C, and TG levels in AD and the association between these lipid markers and risk of incident AD or prevalence of AD have been meta-analyzed mainly by Anstey et al. (Anstey et al., 2017), Wu et al. (Wu et al., 2019), Zhou et al. (Zhou et al., 2020), Tang et al. (Tang et al., 2020), Saiz Vazquez et al. (Sáiz-Vazquez et al., 2020), and Zhu et al. (Y. Zhu et al., 2022). The results of these studies showed that AD cases generally had higher levels of TC, and LDL-C compared to controls, while no association was found between levels of HDL-C and TG and diagnosis of AD. In addition, TC (Anstey et al., 2017; Y. Zhu et al., 2022) and TG (Y. Zhu et al., 2022) have been shown to increase the risk of AD dementia. In the present study, we did not find any association between plasma levels of these markers and diagnosis of AD. Our results are in accordance with some previous reports in which no association was found between blood levels of TC, HDL-C, LDL-C, and TG and diagnosis of AD (Proitsi et al., 2017). Possibly this lack of association is because we adjusted our data for some confounding variables such as APOE genotype that affect peripheral lipid metabolism and transport, while the majority of the previous studies did not take this effect into consideration. In addition, we analyzed the effect of these lipids on diagnosis together with many other lipids and in order to reduce the probability of FDR we applied some filters that may have affected our results. Therefore, by applying a more restrictive statistical analysis some possible weak relations may disappear.

Previous lipidomic investigations (chromatography-MS) evaluating circulating lipids in AD reported dysregulation regarding PLs (Y. Liu et al., 2021; Proitsi et al., 2017; Toledo et al., 2017; Wong et al., 2017), SPs (Y. Liu et al., 2021; Savica et al., 2016; Varma et al., 2018; Wong et al., 2017), cholesterol species (Y. Liu et al., 2021; Popp et al., 2013; Proitsi et al., 2017), and glycerolipids (Y. Liu et al., 2021; Proitsi et al., 2017; Wood et al., 2015) in AD patients. There are some discrepancies regarding the lipid species that may have a more important role in AD development or may have been more affected during AD development. Differences in the specific lipids identified in the previous studies may be due to the dissimilarities in cohort characteristics, disease severity, or the absence or presence of controlling for different confounders in the data analysis between studies.

However, these findings suggest that deregulation in the biosynthesis and turnover of lipids could participate in AD development.

In the present study, we did not find any lipid species associated with the diagnosis of AD and MCI vs control. In agreement with this lack of association between lipids and differential diagnosis, Toledo et al. found no association between dysregulation in serum lipid species and diagnosis of MCI and AD vs control. These investigators only after substratification of the diagnostic groups (Control, MCI, and AD) based on CSF biomarkers, were able to detect lipid dysregulations in participants with CSF pathology (Toledo et al., 2017). However, the lack of association between diagnostic groups may have been caused by the small size of the control group and our restrictive data analysis that may have led to a lack of convergence in our statistical models. In fact, when we analyzed only the data regarding AD (N = 104) and MCI (N = 89) groups, we found several lipid species that were associated with the differential diagnosis between these two populations. Among the identified lipids, the majority were ester- and ether-linked PLs (PC(38:5), PC(P-44:5), PC(2OH-46:6); PC(40:7), PC(O-32:1)/PC(P-32:0), PC(34:1), PE(36:1), and PS(40:4)). Consistently, all PC species increased the risk of AD vs MCI diagnosis, whereas PE and PS species decreased this risk. We also detected two ceramide species (HexCer(d18:1/12:0) and Cer(d18:1/22:0)) that both increased the risk of AD vs MCI, and two neutral lipids (TG(56:3) and CE(15D5)) both reducing the risk of AD vs MCI. These results indicate the possible role of PLs, SMs and neutral lipids in pathophysiological processes of the dementia stage of AD.

6.4.2. Plasma lipids associated with AD biomarkers

The majority of prior blood lipid studies have not linked signals in the blood to those in the brain and have relied mainly on discriminating between AD/MCI and control samples. Among the studies that have searched for these links, some have evaluated the blood lipid profile with brain pathology and some have assessed the relation between peripheral lipid dysregulation and CSF AD biomarker, as we did. For example, using plasma samples from 21 cognitively normal subjects with normal aging pathology, 18 pathology-confirmed AD (mean CDR 2 and MMSE 14), and 26 subjects with Lewy body dementia, Savica et al. searched for SPs and FAs specifically associated with AD

pathology. They found no association between plasma lipids and the Braak NFT stage. However, they showed that plasma levels of sphingosine were significantly higher in low-likelihood AD pathology (NIA Reagan criteria (Wisniewski & Silverman, 1997)) compared to all other groups (no likelihood, intermediate, and high likelihood) (Savica et al., 2016). In another study, Varma et al., using a targeted quantitative metabolomics approach (Biocrates AbsoluteIDQ-p150 kit), evaluated the serum levels of several PC and SM species in 109 cognitively normal, 186 MCI, and 100 AD participants. They explored associations between lipid concentrations and CSF measures of Aβ42, Ttau, and Ptau and adjusted their data for age and gender. They found significant positive associations between serum levels of SM(16:0), SM(18:1), SM(16:1), SM(OH-14:1), SM(OH-22:1), PC(38:4), PC(O-43:0) and measures of both Ttau and Ptau. Ptau was additionally associated with SM(26:1) and SM(OH-24:1). In addition, they observed a negative association between SM(16:0) and SM(OH-14:1) and Aβ42 (Varma et al., 2018). Toledo et al., evaluated the association of serum lipids with the CSF Aβ42 as a categorical outcome and also with the Ttau/Aβ42 ratio as a quantitative outcome in a cohort consisting 97 controls, 185 MCI, and 96 probable AD patients. They used the same quantitative targeted metabolomics approach used by Varma et al. and adjusted their data for age and gender (and APOE status only for Aβ42 model). They found that PC(O-36:2), PC(O-40:3), PC(O-42:4), PC(O-44:4), SM(OH-14:1), and SM(16:0) were positively associated with CSF Aβ42 positivity and Cer(18:0), PC(O-36:2), SM(16:0) and SM(20:2) were positively associated with the Ttau/Aβ42 ratio (Toledo et al., 2017). One of the limitations of the aforementioned studies is that they used a targeted platform that does not enable discovering the association between all classes of lipids with AD pathology. For example, in the study by Savica et al., only SMs were evaluated and the Kit used by Varma et al. and Toledo et al. only includes measurement of some PCs and SPs species. In any case, these results indicate that there are some specific lipid species, such as ether lipids, in the circulation that are associated with the measure of brain pathology.

One of the unique aspects of our data, as explained in this discussion chapter, was that we searched for specific associations of lipids with each AD CSF biomarker. Our objective was to see whether there were lipids associated with CSF Aβ42 status independent of the lipids that may affect Ttau and Ptau status and independent of the effect of APOE

alleles. We found 21 lipid species that were associated with CSF Aβ42 status from which we identified 11 species: three SM species (SM(36:0), SM(40:1), SM(42:2); four PL species (PS(42:3), PC(P-42:4)/PC(O-42:5), PC(P-36:2)/PC(O-36:3), PA(48:2)); and four GL species (DG(44:3), TG(56:2), TG(55:1), and TG(O-55:6)). The association of SM and PL species has been related to CSF Aβ42 levels in the previous reports (Toledo et al., 2017; Varma et al., 2018). These associations all point to problems with PL and SP metabolism and possibly a loss of membrane function and early neurodegeneration. Our findings regarding the association between PL dysregulation and CSF Aβ42 levels is in line with our CSF data. Interestingly, in CSF PC(P-36:2)/PC-(O-36:3) was also associated with CSF Aβ42 levels. Ether-linked PC metabolites are highly abundant in plasma membranes and serve as a source for signaling molecules and may also have a role in protecting other membrane lipids against lipoxidation. They are highly abundant in immune cells and may be part of the link between inflammation and AD. In addition, ether-containing lipids and SMs may be located in membrane lipid rafts, supporting the hypothesis that lipid rafts can directly regulate APP processing, Aβ42 production, and facilitate its aggregation (Paolo & Kim, 2012). Dysregulation of ether-linked PCs may also indicate the implication of peroxisome dysfunction in amyloid pathology. Although peroxisomal dysfunction has been previously reported in AD (Jo et al., 2020; Kou et al., 2011; Lizard et al., 2012), its direct link with amyloid pathology is unknown.

For the first time, we have shown that triglycerides may also be involved in Aβ pathology. As mentioned earlier, LDs are highly dynamic organelles involved in energy metabolism, cell signaling, and redox homeostasis. Therefore, our data indicate that not only lipids in the membrane but also intracellular lipids have an important role in Aβ pathology. This is an interesting issue because regarding Aβ pathology, the existing literature has given greater importance to membrane lipids, while our findings, in addition to membrane lipids, point to intracellular neutral lipids as possible mediators of Aβ pathology.

Like our CSF data, we found more lipid species associated with amyloid pathology than Ttau and Ptau. There was a high correlation between measures of Ttau and Ptau. Interestingly, in spite of these high correlation, we found some lipids that were associated with each pathology after adjustment of the data. Our analysis detected two

ether-linked TGs (TG(O-60:10) and TG(O-64:7)) associated with the Ptau levels in CSF. These data suggest that TGs may affect tau pathology independently of amyloid pathology and neurodegeneration (Ttau pathology). Our result is in agreement with the role of LDs as regulators of proteasome activity that subsequently affects Ptau degradation (van der Kant, Langness, et al., 2019). In addition, considering the role of LDs in redox homeostasis, dysregulation regarding ether-linked TGs may indicate the implication of lipoxidation in Ptau pathology.

We also found three plasma lipids associated with Ttau levels in CSF, one of unknown identity, a fatty acid ester of hydroxy fatty acid (FAHFA(34:0)), and PC(O-34:3). FAHFAs are lipids consisting of an FA coupled to a hydroxy FA by an ester bond. It is assumed that the levels of FAHFAs in serum and adipose tissue are mainly derived from the endogenous synthesis in adipocytes. FAHFAs are mainly esterified to TGs and CEs. Therefore, again these data highlight the important role of LDs in AD pathological processes even at systemic level. We found no previous data regarding the detection of FAHFA lipids in CSF. Therefore, the association of FAHFA with Ttau pathology suggests that peripheral lipid dysregulation could affect brain pathology. In addition, as adipocytes are a source of FAHFAs in the body, our data regarding the dysregulation of these lipids in AD highlights the importance of systemic metabolic failure in AD pathology. Previous research has shown that FAHFAs have an anti-diabetic and anti-inflammatory effect. However, as theoretically any combination of an FA and hydroxyl FA is possible, there are probably bioactive species with negative effects on target receptors (Riecan et al., 2022).

Although we discussed the role of ether-linked PLs as signaling molecules and participation in redox homeostasis of the membrane, we do not know how an increase in plasma PC(O-34:3) could participate in the neurodegeneration of the brain. Possibly these molecules, by modulation of inflammation and oxidative stress, play an indirect role in this process or perhaps this dysregulation is an adaptive response against other pathological alterations in AD.

6.4.3. Plasma Lipids associated with progression and rate of progression from MCI to AD

Identification of lipid dysregulation related to MCI to AD progression requires studies with a long follow-up time. As a result, the majority of the previous studies have limited their research to cross-sectional analyses. However, some limited studies have evaluated this issue. For examples, Toledo et al. searched for the association of lipids with progression in 356 MCI subjects. They followed up the patients for a median of three years and adjusted the data for age, gender, APOE ε4 presence and level of education. They found that serum levels of some ether-linked PCs (PC(O-36:2), PC(O-40:3), PC(O-42:4) and PC(O-44:4)) and SMs (SM(OH-14:1), SM(16:0) and SM(20:2) were positively associated with an increased risk of progression. In the study by Varma et al., higher serum levels of SM(18:1) and PC(38:4) were associated with an increased risk of MCI (N = 366) to AD progression. These patients were followed up for a mean of 2.97 (± 2.33 years) years. In addition, in this study higher serum levels of SM(16:0), SM(18:1), SM(16:1), SM(OH-14:1), and PC(O-34:2) were associated with a greater risk of conversion to incident AD in cognitively normal older adults, and higher plasma levels of PC(38:4) reduced this risk (in contrast to its effect on MCI to AD progression). The targeted quantitative platform (Biocrates AbsoluteIDQ-p150 kit) used by these two studies does not enable assessing dysregulation regarding all classes of lipids, such as all PLs or neutral lipids. In another study, Huynh et al. measured 569 lipids from 32 classes and subclasses in a study population of 1345 older individuals. They found that plasma levels of 71 lipid species were associated with the risk of AD development. These included individual species from the ether lipids, sphingolipids, PE and TG classes. These investigators adjusted their data for age, sex, BMI, APOE ε4 presence, TC, HDL-C, TGs, omega-3 supplementation and statin use (K. Huynh et al., 2020).

In our plasma study, we found ten lipid species associated with the risk of progression from MCI to AD. An epoxyeicosatrienoic acid (EETs), a PE(P) (PE(P-36:4)), two PLs (PS(53:4) and PC(44:10)), four TGs (TG(64:1), TG(46:0), TG-O(62:7), and TG(53:4), and a cardiolipin (CL(49:2)). In fact, our best model for discriminating progressive MCI from non-progressive MCI subjects included neutral lipids (TG(64:1), TG(46:0), TG(O-62:7)) and a PE(P) in addition to the presence of APOE ε4 allele (AUC = 0.972). Importantly, the

model without the presence of lipids had a significantly reduced discriminating power (AUC = 0.729) indicating that these lipids may have a prognostic value in the detection of progressive MCI patients. We should mention that despite of very good predictive power of the Cox models, in all cases they underestimated the progression rate, compared to Kaplan-Meier analysis. This underestimation, rather than the lower predictive power of each model, may be partly due to the bias in the clinical diagnosis of AD due to access by the neurologist to core CSF AD biomarkers. It means that the neurologist may have diagnosed AD ahead of time when an MCI patient had CSF biomarker alterations compatible with AD pathology even in the absence of cognitive deficits that may have caused dependency on a caregiver for undertaking daily life activities.

Our plasma result is in agreement with our CSF finding in which a neutral lipid (CE(11D3:1)) was also associated with an increased risk of progression. As the possible mechanisms whereby dyshomeostasis in neutral lipids in the brain may affect AD pathology has been explained in the previous sections, here we discuss the possible roles of this dysregulation at systemic level.

LDs are reservoirs of neutral lipids in the cells. At systemic level they are mainly produced in adipose tissue, but all cells can produce LDs. In the periphery, LDs not only serve as lipid storage and supply but also affect physiological processes, such as inflammation and insulin signaling. For example, LDs in various immune cell types contain a large amount of AA, which can serve as a precursor for eicosanoid synthesis (Farmer et al., 2020). Interestingly our data also associated an eicosanoid to increased risk of progression, highlighting the possible role of systemic inflammation as a driving force of AD progression in the periphery. Additionally, genome-wide association studies have identified many immune response genes related to an increased risk of AD (Bellenguez et al., 2020). Furthermore, LDs have been linked to peripheral metabolic dysfunction such as insulin resistance and obesity that are among risk factors for LOAD. Therefore, peripheral neutral lipid dyshomeostasis may play a role in MCI to AD progression by increasing inflammation and provoking general metabolic dysfunction that has been proven to affect BBB integrity and lead to increased AD pathology and

synaptic damage and reduced cognition (Kinney et al., 2018; Maiuolo et al., 2021; Sankowski et al., 2015).

Dysregulation regarding PLs and plasmalogen PLs at systemic level and the risk of MCI to AD progression was also reported previously (Toledo et al., 2017; Varma et al., 2018). Our finding regarding higher levels of PE(P-36:4) and a reduced risk of progression is in line with the previous data that reported reduced levels of ethanolamine plasmalogens in the brain, CSF and plasma of AD patients (Su et al., 2019). In addition, the circulating levels of these plasmalogens have been related to the cognitive performance of AD patients (Wood et al., 2010). Considering that PLs and plasmalogens are building blocks of cellular membranes and provide an optimal environment for interaction, trafficking and functions of proteins, dysregulation of these lipids may reasonably have detrimental effects on synapses and the clinical progression of AD. In line with this notion, previous studies have shown that plasmalogens are a major lipid component in synapse membranes and synaptic vesicles and they may have a role in membrane fusion and fission processes. Moreover, plasmalogens tend to carry PUFAs, that in turn may regulate the SNARE proteins, which mediate synaptic vesicle exocytosis and membrane fusion (Lauwers et al., 2016). The reduction of PE(P)s in the AD brain has been shown to change the biophysical properties of the phospholipid-bilayer and correlate with the impairments of synaptic transmission and neurotransmitter release and severity of AD cognitive impairment (S. A. L. Bennett et al., 2013; Dorninger et al., 2019). Although a reduction in PE(P)s has been reported previously in plasma of AD patients, we do not know, first, whether this dysregulation occurs at systemic level or it originates from the brain, and secondly, whether plasma PL and plasmalogen dyshomeostasis could modulate brain pathology and lead to cognitive decline. Interestingly, in a very recent study by Gu et al., intragastric administration of plasmalogens in an animal model of aging promoted synaptic plasticity and neurogenesis, and halted age-related microglia-mediated neuroinflammation. Additionally, treated animals had significantly better spatial learning and memory capacity compared to untreated aged control mice (Gu et al., 2022). Therefore, regarding the important role of PLs and plasmalogens as a source of lipid mediators, these data demonstrate that not only central but also systemic homeostasis of these lipids could participate in physiological processes underlying

synaptic function and cognitive performance. Therefore, the protective effect of PE(P-36:4) against clinical progression from MCI to AD may be related to the positive effects of this lipid on inflammation at both systemic and central levels.

CL, the other lipid whose higher plasma levels were associated with an increased risk of MCI to AD progression in our study, is a mitochondria-exclusive PL. CL is essential for mitochondria morphology, bioenergetics, dynamics, and signaling pathways. Alterations in brain CL are associated with impaired neuronal function and neurodegeneration. For example, various animal models of neurodegeneration showed a substantial reduction in CL content in the brain (Falabella et al., 2021). Concerning the role of CL dyshomeostasis on pathophysiological processes of AD the data are limited. A study using transgenic animal models of AD has shown reduced CL content in synaptic mitochondria suggesting a contribution of CL to the disease pathogenesis (Monteiro-Cardoso et al., 2015). Additionally, it has been shown that tau preferentially binds to CL-rich regions of the mitochondrial membrane and leads to mitochondrial swelling, cytochrome c release, and decreased membrane potential (Camilleri et al., 2020). Furthermore, extracellular CL released by damaged cells has been proposed as a potential intercellular signaling molecule that can increase microglial phagocytosis and may lead to reduced Aβ deposits in the brain. However, the association of higher levels of CL(49:2) in plasma with increased risk of progression is not in line with the reduction of CLs in the brain of AD animals. This discrepancy may be related to the type of tissue examined and we hypothesize that an increase of CL in plasma may be indicative of its reduction, as a result of neurodegeneration, in the brain. Supporting this hypothesis, in animal models of traumatic brain injury, a decreased amount of brain CL was accompanied by increased levels of CL in plasma (Falabella et al., 2021). Therefore, the association of increased levels of CL(49:2) and increased risk of MCI to AD progression may be indicative of a higher rate of neuronal death in progressive MCI patients and have a prognostic value regarding the measurement of neurodegeneration in the circulatory system. In addition, given the important role of CLs in nearly all aspects of mitochondrial functionality, our finding highlights the possible implication of mitochondrial dysfunction as another player in AD progression. Mitochondrial dysfunction, characterized by reduced ATP synthesis, enhanced ROS generation, Ca2+

dyshomeostasis, and defects in mitochondrial dynamics and transport, has long been proposed as a triggering factor for both amyloid and tau pathologies and has been extensively reported in the brain of AD patients (W. Wang et al., 2020). Aβ was found to impair mitochondrial function and the degree of cognitive impairment in AD animal models has also been linked to the extent of mitochondrial dysfunction and mitochondrial Aβ levels, especially at synapses. In fact, mitochondrial dysfunction could have a detrimental effect on the proper functionality of synapses because synaptic transmission is the most energy-demanding process in neurons and mitochondria are the major energy source supplying ATP. Besides energy production, mitochondria have a fundamental role in regulating calcium concentration during signal transduction, which is specifically important for excitable cells such as neurons. Moreover, an increase in ROS by dysfunctional mitochondria could also participate in neuronal injury and cognitive impairment (Reviewed by Cai & Tammineni, 2017). The association of increased CL concentration in plasma and an increased risk of progression may also indicate the possible role of other concomitant pathologies related to mitochondrial dysfunction at systemic level. For example, mitochondrial dysfunction has an active role in pathophysiological processes of metabolic syndrome that is highly prevalent in AD patients and has also been related to the increased risk of MCI to AD progression (Ng et al., 2016).

Our plasma analysis detected the same class of lipids associated with time to progression as those that were associated with progression, indicating the implication of the same pathological pathways. Importantly, comparing our plasma results with those of CSF revealed that in both cases ether-linked TGs are lipids that had the most impact on rate of progression. However, we should mention that the direction of the impact was inverse because based on our CSF result, increased levels of TG(O-52:2) were associated with shorter time to progression, while increased plasma levels of TG(O-62:7) were associated with longer time to progression. These apparent discrepancies may be related to the cellular origin of these lipids, as CSF TG(O-52:2) may possibly originate from the brain, but plasma TG(O-62:7) may have a systemic origin and be related to some dysregulation at systemic level. In addition, TGs act as a source of signaling molecules and although both are ether-linked TGs, the FAs released from them may

have a different effect on their target receptor. Taken together, our CSF and plasma data indicate the possible implication of intracellular neutral lipids, plasmalogens, and CLs in pathological processes underlying clinical progression and rate of progression from MCI to AD.

STRENGTHS AND LIMITATIONS

7. Strengths and limitations

7.1. Strengths

The strengths of our study include: first, the fact that we analyzed both plasma and CSF for the same cohort of patients. Second, we had a larger study population compared to the majority of CSF lipid studies, thus increasing the accuracy of our findings. Third, we evaluated the association of lipids with AD biomarkers to unravel their role in AD pathology. This issue has not been addressed in previously published CSF lipidomics studies. Fourth, we adjusted our data for various confounding factors, increasing the robustness of our results. Fifth, our MCI group had a long follow-up period that increases the accuracy of our results regarding progression or lack of progression. Sixth, for the first time we assessed the association of lipids with AD diagnosis and progression, independently of their possible role in known pathological hallmarks of the disease.

7.2. Limitations

The limitations of our study include: first, our control group in the lipidomic studies and CSF FA study was small. This may have limited our power to detect lipids associated with diagnosis. The small number of CSF control samples reflects the challenges of obtaining this biological fluid from subjects who do not have any neuropathological or psychiatric disorder. Second, in spite of controlling for some confounders, we did not account for the impact of all possible confounding factors, for example medication and body mass index, that may have an important effect on lipid homeostasis. Third, our MCI group was small and, as a result, our analyses resulted in excessively high or low ORs. However, our objective was to assess the direction of the effect rather than its extent. Fourth, we did not connect metabolic changes within a pathway and network context. Fifth and finally, we did not validate our result in an independent cohort.

PROSPECTIVE

8. Prospective

Lipid dysregulation is one of the fundamental aspects of AD pathogenesis. Importantly, many of the AD risk genes are related to lipid metabolism. However, a lack of analytical tools has postponed investigation into the effects of this class of molecules on pathological processes of AD and its progression. Lipidomics has given us an opportunity to precisely analyze lipid changes occurring in AD. These lipid alterations may help us to unravel the biochemical pathways that are affected or are causal in AD. In addition, lipidomics offers enormous potential for the identification of AD-related biomarkers in biological fluids, which can prove particularly helpful for the diagnosis of AD, the prognosis of MCI to AD progression, and its trajectory. In this regard, we recommend simultaneous analyses of both blood and CSF from the same cohort of patients given that AD is not only a brain disease, as AD patients also suffer from many systemic abnormalities. Therefore, analyzing both central and peripheral changes, simultaneously, could improve our understanding of this complex disease. Additionally, in future research, when searching for changes in AD-related lipid pathways, stratification of patients based on AD core biomarkers should be specifically taken into consideration as it will provide more clues on the role of lipids in AD pathology. The specific role of lipids in AD progression and its trajectory is an infra-studied area and we believe that with the breakthroughs in lipidomics and the use of large, well-defined cohorts of MCI patients we may be able to disentangle the role of lipids in AD progression.

CONCLUSIONS

9. Conclusions

1. In CSF, we found that AI decreased the risk of AD vs MCI. This result indicates the importance of inflammatory processes in AD development and progression. The association between higher levels of oleic acid and lower levels of vaccenic acid in plasma and a reduced risk of AD development opens a therapeutic window to nutritional interventions to protect against AD.

2. Neither in CSF nor in plasma were the levels of oxidative protein damage markers associated with AD development, pathology, or progression. Possibly, oxidative damage to proteins in AD is not to such a degree as to be reflected in biological fluids.

3. In CSF, the lipids most associated with amyloid pathology were hexacosanoic acid (C26:0), Cer(d38:4) and PE(40:0), suggesting the involvement of peroxisomal, ceramide metabolism and membrane lipid dyshomeostasis in amyloid pathology.

4. In plasma, the lipids most associated with amyloid pathology were from PL, SM, and TG classes. PLs and SM are present in membrane and have previously been related to amyloid pathology, but for the first time our data demonstrate that intracellular neutral lipids also have a role in amyloid pathology.

5. Our CSF data related SM30:1 to tau pathology, suggesting an association between oligodendrocytes, as the major producers of SM, and hyperphosphorylation of tau, whereas our plasma results pointed to the importance of neutral lipids, especially TGs, in tau pathology.

6. We detected that plasma levels of FAHFA(34:0) and PC(O-34:3) were associated with pathological levels of Ttau in CSF. This result suggests a role for systemic metabolic failure in development of neurodegeneration.

7. Both CSF and plasma results highlighted the involvement of intracellular neutral lipids in MCI to AD progression. In addition, the association of these lipids with progression was independent of their relation with the pathological hallmarks of AD and the possible effect of APOE ε4 allele.

8. Regarding lipids that affect time to progression, both our CSF and plasma data indicated that ether-linked TGs have predictive power regarding time to progression.
9. Our data indicated that not only membrane lipids, but also intracellular neutral lipids, are important drivers of AD pathology, progression, and affect time to progression at both central and systemic levels.
10. Finally, we conclude that systemic and central lipid dysregulations participate in AD pathology and progression by affecting somewhat different pathways.

REFERENCES

References

Ahmed, N., Ahmed, U., Thornalley, P. J., Hager, K., Fleischer, G., & Münch, G. (2005). Protein glycation, oxidation and nitration adduct residues and free adducts of cerebrospinal fluid in Alzheimer's disease and link to cognitive impairment. *Journal of Neurochemistry*, *92*(2), 255–263. https://doi.org/10.1111/J.1471-4159.2004.02864.X

Akbaraly, T. N., Singh-Manoux, A., Dugravot, A., Brunner, E. J., Kivimäki, M., & Sabia, S. (2019). Association of Midlife Diet With Subsequent Risk for Dementia. *JAMA*, *321*(10), 957. https://doi.org/10.1001/JAMA.2019.1432

Albert, M. S., DeKosky, S. T., Dickson, D., Dubois, B., Feldman, H. H., Fox, N. C., Gamst, A., Holtzman, D. M., Jagust, W. J., Petersen, R. C., Snyder, P. J., Carrillo, M. C., Thies, B., & Phelps, C. H. (2011). The diagnosis of mild cognitive impairment due to Alzheimer's disease: recommendations from the National Institute on Aging-Alzheimer's Association workgroups on diagnostic guidelines for Alzheimer's disease. *Alzheimer's & Dementia : The Journal of the Alzheimer's Association*, *7*(3), 270–279. https://doi.org/10.1016/J.JALZ.2011.03.008

Alquezar, C., Arya, S., & Kao, A. W. (2021). Tau Post-translational Modifications: Dynamic Transformers of Tau Function, Degradation, and Aggregation. *Frontiers in Neurology*, *11*, 1826. https://doi.org/10.3389/FNEUR.2020.595532/BIBTEX

Amtul, Z., Westaway, D., Cechetto, D. F., & Rozmahel, R. F. (2011). Oleic acid ameliorates amyloidosis in cellular and mouse models of Alzheimer's disease. *Brain Pathology (Zurich, Switzerland)*, *21*(3), 321–329. https://doi.org/10.1111/J.1750-3639.2010.00449.X

Anjum, I., Jaffery, S. S., Fayyaz, M., Samoo, Z., & Anjum, S. (2018). The Role of Vitamin D in Brain Health: A Mini Literature Review. *Cureus*, *10*(7). https://doi.org/10.7759/CUREUS.2960

Anstey, K. J., Ashby-Mitchell, K., & Peters, R. (2017). Updating the Evidence on the Association between Serum Cholesterol and Risk of Late-Life Dementia: Review and Meta-Analysis. *Journal of Alzheimer's Disease : JAD*, *56*(1), 215–228. https://doi.org/10.3233/JAD-160826

Arellanes, I. C., Choe, N., Solomon, V., He, X., Kavin, B., Martinez, A. E., Kono, N., Buennagel, D. P., Hazra, N., Kim, G., D'Orazio, L. M., McCleary, C., Sagare, A., Zlokovic, B. V., Hodis, H. N., Mack, W. J., Chui, H. C., Harrington, M. G., Braskie, M. N., … Yassine, H. N. (2020). Brain delivery of supplemental docosahexaenoic acid (DHA): A randomized placebo-controlled clinical trial. *EBioMedicine*, *59*. https://doi.org/10.1016/J.EBIOM.2020.102883

Armstrong, R. A., Richard, P., & Armstrong, A. (2019). Risk factors for Alzheimer's disease. *Folia Neuropathologica*, *57*(2), 87–105. https://doi.org/10.5114/fn.2019.85929

Arnsten, A. F. T., Datta, D., Del Tredici, K., & Braak, H. (2021). Hypothesis: Tau pathology is an initiating factor in sporadic Alzheimer's disease. *Alzheimer's & Dementia*, *17*(1), 115–124. https://doi.org/10.1002/ALZ.12192

Arsenault, D., Julien, C., Tremblay, C., & Calon, F. (2011). DHA Improves Cognition and Prevents Dysfunction of Entorhinal Cortex Neurons in 3xTg-AD Mice. *PLOS ONE*, *6*(2), e17397. https://doi.org/10.1371/JOURNAL.PONE.0017397

Astarita, G., Jung, K. M., Vasilevko, V., DiPatrizio, N. V., Martin, S. K., Cribbs, D. H., Head, E., Cotman, C. W., & Piomelli, D. (2011). Elevated Stearoyl-CoA Desaturase in Brains of Patients with Alzheimer's Disease. *PLoS ONE*, *6*(10). https://doi.org/10.1371/JOURNAL.PONE.0024777

Ayodele, T., Rogaeva, E., Kurup, J. T., Beecham, G., & Reitz, C. (2021). Early-Onset Alzheimer's Disease: What Is Missing in Research? *Current Neurology and Neuroscience Reports*, *21*(2). https://doi.org/10.1007/S11910-020-01090-Y

Bai, D., Fan, J., Li, M., Dong, C., Gao, Y., Fu, M., Huang, G., & Liu, H. (2021). Effects of Folic Acid Combined with DHA Supplementation on Cognitive Function and Amyloid-β-Related Biomarkers in Older Adults with Mild Cognitive Impairment by a Randomized, Double Blind, Placebo-Controlled Trial. *Journal of Alzheimer's Disease*, *81*(1), 155–167. https://doi.org/10.3233/JAD-200997

Bär, K. J., Franke, S., Wenda, B., Müller, S., Kientsch-Engel, R., Stein, G., & Sauer, H. (2003). Pentosidine and Nε-(carboxymethyl)-lysine in Alzheimer's disease and vascular dementia. *Neurobiology of Aging*, *24*(2), 333–338. https://doi.org/10.1016/S0197-4580(02)00086-6

Barthélemy, N. R., Li, Y., Joseph-Mathurin, N., Gordon, B. A., Hassenstab, J., Benzinger, T. L. S., Buckles, V., Fagan, A. M., Perrin, R. J., Goate, A. M., Morris, J. C., Karch, C. M., Xiong, C., Allegri, R., Mendez, P. C., Berman, S. B., Ikeuchi, T., Mori, H., Shimada, H., … Xu, X. (2020). A soluble phosphorylated tau signature links tau, amyloid and the evolution of stages of dominantly inherited Alzheimer's disease. *Nature Medicine*, *26*(3), 398–407. https://doi.org/10.1038/S41591-020-0781-Z

Barthelson, K., Newman, M., & Lardelli, M. (2020). Sorting Out the Role of the Sortilin-Related Receptor 1 in Alzheimer's Disease. *Journal of Alzheimer's Disease Reports*, *4*(1), 123. https://doi.org/10.3233/ADR-200177

Bellenguez, C., Grenier-Boley, B., & Lambert, J. C. (2020). Genetics of Alzheimer's disease: where we are, and where we are going. *Current Opinion in Neurobiology*, *61*, 40–48. https://doi.org/10.1016/J.CONB.2019.11.024

Bennett, D. A., Schneider, J. A., Bienias, J. L., Evans, D. A., & Wilson, R. S. (2005). Mild cognitive impairment is related to Alzheimer disease pathology and cerebral infarctions. *Neurology*, *64*(5), 834–841. https://doi.org/10.1212/01.WNL.0000152982.47274.9E

Bennett, S. A. L., Valenzuela, N., Xu, H., Franko, B., Fai, S., & Figeys, D. (2013). Using neurolipidomics to identify phospholipid mediators of synaptic (dys)function in Alzheimer's Disease. *Frontiers in Physiology*, *4*. https://doi.org/10.3389/FPHYS.2013.00168

Bergström, P., Agholme, L., Nazir, F. H., Satir, T. M., Toombs, J., Wellington, H., Strandberg, J., Bontell, T. O., Kvartsberg, H., Holmström, M., Boreström, C., Simonsson, S., Kunath, T., Lindahl, A., Blennow, K., Hanse, E., Portelius, E., Wray, S., & Zetterberg, H. (2016). Amyloid precursor protein expression and processing are differentially regulated during cortical neuron differentiation. *Scientific Reports*, *6*(1), 29200. https://doi.org/10.1038/srep29200

Bermejo, P., Martín-Aragón, S., Benedí, J., Susín, C., Felici, E., Gil, P., Ribera, J. M., & Villar, Á. M. (2008). Peripheral levels of glutathione and protein oxidation as markers in the development of Alzheimer's disease from Mild Cognitive Impairment. *Free Radical Research*, *42*(2), 162–170. https://doi.org/10.1080/10715760701861373

Berr, C., Portet, F., Carriere, I., Akbaraly, T. N., Feart, C., Gourlet, V., Combe, N., Barberger-Gateau, P., & Ritchie, K. (2009). Olive Oil and Cognition: Results from the Three-City Study. *Dementia and Geriatric Cognitive Disorders*, *28*(4), 357. https://doi.org/10.1159/000253483

Birbes, H., Bawab, S. El, Hannun, Y. A., & Obeid, L. M. (2001). Selective hydrolysis of a mitochondrial pool of sphingomyelin induces apoptosis. *FASEB Journal : Official Publication*

of the Federation of American Societies for Experimental Biology, *15*(14), 2669–2679. https://doi.org/10.1096/FJ.01-0539COM

Blennow, K., Brody, D. L., Kochanek, P. M., Levin, H., McKee, A., Ribbers, G. M., Yaffe, K., & Zetterberg, H. (2016). Traumatic brain injuries. *Nature Reviews. Disease Primers*, *2*. https://doi.org/10.1038/NRDP.2016.84

Blessed, G., Tomlinson, B. E., & Roth, M. (1968). The association between quantitative measures of dementia and of senile change in the cerebral grey matter of elderly subjects. *The British Journal of Psychiatry : The Journal of Mental Science*, *114*(512), 797–811. https://doi.org/10.1192/BJP.114.512.797

Boldrini, M., Fulmore, C. A., Tartt, A. N., Simeon, L. R., Pavlova, I., Poposka, V., Rosoklija, G. B., Stankov, A., Arango, V., Dwork, A. J., Hen, R., & Mann, J. J. (2018). Human Hippocampal Neurogenesis Persists throughout Aging. *Cell Stem Cell*, *22*(4), 589. https://doi.org/10.1016/J.STEM.2018.03.015

Braak, H., & Braak, E. (1995). Staging of Alzheimer's disease-related neurofibrillary changes. *Neurobiology of Aging*, *16*(3), 271–278. https://doi.org/10.1016/0197-4580(95)00021-6

Bradley, M. A., Markesbery, W. R., & Lovell, M. A. (2010). Increased levels of 4-hydroxynonenal and acrolein in the brain in preclinical Alzheimer's disease (PCAD). *Free Radical Biology & Medicine*, *48*(12), 1570. https://doi.org/10.1016/J.FREERADBIOMED.2010.02.016

Brenna, J. T., & Carlson, S. E. (2014). Docosahexaenoic acid and human brain development: evidence that a dietary supply is needed for optimal development. *Journal of Human Evolution*, *77*, 99–106. https://doi.org/10.1016/J.JHEVOL.2014.02.017

Briggs, R., Kennelly, S. P., & O'Neill, D. (2016). Drug treatments in Alzheimer's disease. *Clinical Medicine (London, England)*, *16*(3), 247–253. https://doi.org/10.7861/CLINMEDICINE.16-3-247

Brites, P., Waterham, H. R., & Wanders, R. J. A. (2004). Functions and biosynthesis of plasmalogens in health and disease. *Biochimica et Biophysica Acta (BBA) - Molecular and Cell Biology of Lipids*, *1636*(2–3), 219–231. https://doi.org/10.1016/J.BBALIP.2003.12.010

Browne, D., McGuinness, B., Woodside, J. V., & McKay, G. J. (2019). Vitamin E and Alzheimer's disease: what do we know so far? *Clinical Interventions in Aging*, *14*, 1303. https://doi.org/10.2147/CIA.S186760

Buckner, R. L., & DiNicola, L. M. (2019). The brain's default network: updated anatomy, physiology and evolving insights. *Nature Reviews Neuroscience 2019 20:10*, *20*(10), 593–608. https://doi.org/10.1038/s41583-019-0212-7

Budd Haeberlein, S., Aisen, P. S., Barkhof, F., Chalkias, S., Chen, T., Cohen, S., Dent, G., Hansson, O., Harrison, K., von Hehn, C., Iwatsubo, T., Mallinckrodt, C., Mummery, C. J., Muralidharan, K. K., Nestorov, I., Nisenbaum, L., Rajagovindan, R., Skordos, L., Tian, Y., … Sandrock, A. (2022). Two Randomized Phase 3 Studies of Aducanumab in Early Alzheimer's Disease. *Journal of Prevention of Alzheimer's Disease*, *9*(2), 197–210. https://doi.org/10.14283/JPAD.2022.30/TABLES/3

Butterfield, D. A., & Halliwell, B. (2019). Oxidative stress, dysfunctional glucose metabolism and Alzheimer disease. *Nature Reviews Neuroscience*, *20*(3), 148–160. https://doi.org/10.1038/s41583-019-0132-6

Butterfield, D. A., Poon, H. F., St. Clair, D., Keller, J. N., Pierce, W. M., Klein, J. B., & Markesbery, W. R. (2006). Redox proteomics identification of oxidatively modified hippocampal

proteins in mild cognitive impairment: Insights into the development of Alzheimer's disease. *Neurobiology of Disease*, *22*(2), 223–232. https://doi.org/10.1016/J.NBD.2005.11.002

Butterfield, D. A., Reed, T., Perluigi, M., De Marco, C., Coccia, R., Cini, C., & Sultana, R. (2006). Elevated protein-bound levels of the lipid peroxidation product, 4-hydroxy-2-nonenal, in brain from persons with mild cognitive impairment. *Neuroscience Letters*, *397*(3), 170–173. https://doi.org/10.1016/J.NEULET.2005.12.017

Byeon, S. K., Madugundu, A. K., Jain, A. P., Bhat, F. A., Jung, J. H., Renuse, S., Darrow, J., Bakker, A., Albert, M., Moghekar, A., & Pandey, A. (2021). Cerebrospinal fluid lipidomics for biomarkers of Alzheimer's disease. *Molecular Omics*, *17*(3), 454–463. https://doi.org/10.1039/D0MO00186D

Byrn, M. A., & Sheean, P. M. (2019). Serum 25(OH)D and Cognition: A Narrative Review of Current Evidence. *Nutrients*, *11*(4). https://doi.org/10.3390/NU11040729

Cai, Q., & Tammineni, P. (2017). Mitochondrial Aspects of Synaptic Dysfunction in Alzheimer's Disease. *Journal of Alzheimer's Disease*, *57*(4), 1087–1103. https://doi.org/10.3233/JAD-160726

Camilleri, A., Ghio, S., Caruana, M., Weckbecker, D., Schmidt, F., Kamp, F., Leonov, A., Ryazanov, S., Griesinger, C., Giese, A., Cauchi, R. J., & Vassallo, N. (2020). Tau-induced mitochondrial membrane perturbation is dependent upon cardiolipin. *Biochimica et Biophysica Acta. Biomembranes*, *1862*(2). https://doi.org/10.1016/J.BBAMEM.2019.183064

Canhada, S., Castro, K., Perry, I. S., & Luft, V. C. (2018). Omega-3 fatty acids' supplementation in Alzheimer's disease: A systematic review. In *Nutritional Neuroscience* (Vol. 21, Issue 8, pp. 529–538). Taylor and Francis Ltd. https://doi.org/10.1080/1028415X.2017.1321813

Cao, D., Kevala, K., Kim, J., Moon, H. S., Jun, S. B., Lovinger, D., & Kim, H. Y. (2009). Docosahexaenoic acid promotes hippocampal neuronal development and synaptic function. *Journal of Neurochemistry*, *111*(2), 510. https://doi.org/10.1111/J.1471-4159.2009.06335.X

Castro-Perez, J. M., Kamphorst, J., Degroot, J., Lafeber, F., Goshawk, J., Yu, K., Shockcor, J. P., Vreeken, R. J., & Hankemeier, T. (2010). Comprehensive LC-MS E lipidomic analysis using a shotgun approach and its application to biomarker detection and identification in osteoarthritis patients. *Journal of Proteome Research*, *9*(5), 2377–2389. https://doi.org/10.1021/PR901094J

Ceccom, J., Loukh, N., Lauwers-Cances, V., Touriol, C., Nicaise, Y., Gentil, C., Uro-Coste, E., Pitson, S., Maurage, C. A., Duyckaerts, C., Cuvillier, O., & Delisle, M. B. (2014). Reduced sphingosine kinase-1 and enhanced sphingosine 1-phosphate lyase expression demonstrate deregulated sphingosine 1-phosphate signaling in Alzheimer's disease. *Acta Neuropathologica Communications*, *2*(1). https://doi.org/10.1186/2051-5960-2-12

Cenini, G., & Voos, W. (2019). Mitochondria as potential targets in Alzheimer disease therapy: An update. *Frontiers in Pharmacology*, *10*(JULY), 902. https://doi.org/10.3389/FPHAR.2019.00902/BIBTEX

Chai, B., Gao, F., Wu, R., Dong, T., Gu, C., Lin, Q., & Zhang, Y. (2019). Vitamin D deficiency as a risk factor for dementia and Alzheimer's disease: an updated meta-analysis. *BMC Neurology*, *19*(1). https://doi.org/10.1186/S12883-019-1500-6

Chan, R. B., Oliveira, T. G., Cortes, E. P., Honig, L. S., Duff, K. E., Small, S. A., Wenk, M. R., Shui,

G., & Di Paolo, G. (2012). Comparative Lipidomic Analysis of Mouse and Human Brain with Alzheimer Disease. *The Journal of Biological Chemistry*, *287*(4), 2678. https://doi.org/10.1074/JBC.M111.274142

Chang, P. K. Y., Khatchadourian, A., McKinney, A. A., & Maysinger, D. (2015). Docosahexaenoic acid (DHA): A modulator of microglia activity and dendritic spine morphology. *Journal of Neuroinflammation*, *12*(1), 1–15. https://doi.org/10.1186/S12974-015-0244-5/FIGURES/7

Cheignon, C., Tomas, M., Bonnefont-Rousselot, D., Faller, P., Hureau, C., & Collin, F. (2018). Oxidative stress and the amyloid beta peptide in Alzheimer's disease. *Redox Biology*, *14*, 450. https://doi.org/10.1016/J.REDOX.2017.10.014

Chen, M. K., Mecca, A. P., Naganawa, M., Finnema, S. J., Toyonaga, T., Lin, S. F., Najafzadeh, S., Ropchan, J., Lu, Y., McDonald, J. W., Michalak, H. R., Nabulsi, N. B., Arnsten, A. F. T., Huang, Y., Carson, R. E., & Van Dyck, C. H. (2018). Assessing Synaptic Density in Alzheimer Disease With Synaptic Vesicle Glycoprotein 2A Positron Emission Tomographic Imaging. *JAMA Neurology*, *75*(10), 1215. https://doi.org/10.1001/JAMANEUROL.2018.1836

Cheng, Y. W., Chiu, M. J., Chen, Y. F., Cheng, T. W., Lai, Y. M., & Chen, T. F. (2020). The contribution of vascular risk factors in neurodegenerative disorders: from mild cognitive impairment to Alzheimer's disease. *Alzheimer's Research & Therapy*, *12*(1). https://doi.org/10.1186/S13195-020-00658-7

Cherubini, A., Andres-Lacueva, C., Martin, A., Lauretani, F., Di Iorio, A., Bartali, B., Corsi, A., Bandinelli, S., Mattson, M. P., & Ferrucci, L. (2007). Low Plasma N-3 Fatty Acids and Dementia in Older Persons: The InCHIANTI Study. *The Journals of Gerontology: Series A*, *62*(10), 1120–1126. https://doi.org/10.1093/GERONA/62.10.1120

Chew, H., Solomon, V. A., & Fonteh, A. N. (2020). Involvement of Lipids in Alzheimer's Disease Pathology and Potential Therapies. *Frontiers in Physiology*, *11*, 598. https://doi.org/10.3389/FPHYS.2020.00598/BIBTEX

Chu, C.-S., Hung, C.-F., Ponnusamy, V. K., Chen, K.-C., & Chen, N.-C. (2022). Higher Serum DHA and Slower Cognitive Decline in Patients with Alzheimer's Disease: Two-Year Follow-Up. *Nutrients*, *14*(6), 1159. https://doi.org/10.3390/NU14061159

Citri, A., & Malenka, R. C. (2007). Synaptic Plasticity: Multiple Forms, Functions, and Mechanisms. *Neuropsychopharmacology 2008 33:1*, *33*(1), 18–41. https://doi.org/10.1038/sj.npp.1301559

Colom-Cadena, M., Spires-Jones, T., Zetterberg, H., Blennow, K., Caggiano, A., Dekosky, S. T., Fillit, H., Harrison, J. E., Schneider, L. S., Scheltens, P., De Haan, W., Grundman, M., Van Dyck, C. H., Izzo, N. J., & Catalano, S. M. (2020). The clinical promise of biomarkers of synapse damage or loss in Alzheimer's disease. *Alzheimer's Research & Therapy*, *12*(1). https://doi.org/10.1186/S13195-020-00588-4

Connor, D. J., & Sabbagh, M. N. (2008). Administration and Scoring Variance on the ADAS-Cog. *Journal of Alzheimer's Disease : JAD*, *15*(3), 461. https://doi.org/10.3233/JAD-2008-15312

Coughlan, G., Larsen, R., Kim, M., White, D., Gillings, R., Irvine, M., Scholey, A., Cohen, N., Legido-Quigley, C., Hornberger, M., & Minihane, A.-M. (2021). APOE ε4 alters associations between docosahexaenoic acid and preclinical markers of Alzheimer's disease. *Brain Communications*, *3*(2). https://doi.org/10.1093/BRAINCOMMS/FCAB085

Crews, L., & Masliah, E. (2010). Molecular mechanisms of neurodegeneration in Alzheimer's disease. *Human Molecular Genetics*, *19*(R1), R12–R20.

https://doi.org/10.1093/HMG/DDQ160

Crivelli, S. M., Luo, Q., Stevens, J. A. A., Giovagnoni, C., van Kruining, D., Bode, G., den Hoedt, S., Hobo, B., Scheithauer, A. L., Walter, J., Mulder, M. T., Exley, C., Mold, M., Mielke, M. M., De Vries, H. E., Wouters, K., van den Hove, D. L. A., Berkes, D., Ledesma, M. D., … Martinez-Martinez, P. (2021). CERTL reduces C16 ceramide, amyloid-β levels, and inflammation in a model of Alzheimer's disease. *Alzheimer's Research & Therapy*, *13*(1). https://doi.org/10.1186/S13195-021-00780-0

Cui, Y., Chen, X., Liu, L., Xie, W., Wu, Y., Wu, Q., & Wang, D. (2015). Gas chromatography–mass spectrometry analysis of the free fatty acids in serum obtained from patients with Alzheimer's disease1. *Bio-Medical Materials and Engineering*, *26*(s1), S2165–S2177. https://doi.org/10.3233/BME-151522

Cullen, N. C., Mälarstig, A. nders, Stomrud, E., Hansson, O., & Mattsson-Carlgren, N. (2021). Accelerated inflammatory aging in Alzheimer's disease and its relation to amyloid, tau, and cognition. *Scientific Reports 2021 11:1*, *11*(1), 1–9. https://doi.org/10.1038/s41598-021-81705-7

Cunnane, S. C., Schneider, J. A., Tangney, C., Tremblay-Mercier, J., Fortier, M., Bennett, D. A., & Morris, M. C. (2012). Plasma and Brain Fatty Acid Profiles in Mild Cognitive Impairment and Alzheimer's Disease. *Journal of Alzheimer's Disease : JAD*, *29*(3), 691. https://doi.org/10.3233/JAD-2012-110629

Cutler, R. G., Kelly, J., Storie, K., Pedersen, W. A., Tammara, A., Hatanpaa, K., Troncoso, J. C., & Mattson, M. P. (2004). Involvement of oxidative stress-induced abnormalities in ceramide and cholesterol metabolism in brain aging and Alzheimer's disease. *Proceedings of the National Academy of Sciences of the United States of America*, *101*(7), 2070–2075. https://doi.org/10.1073/PNAS.0305799101

Czapski, G. A., Czubowicz, K., Strosznajder, J. B., & Strosznajder, R. P. (2016). The Lipoxygenases: Their Regulation and Implication in Alzheimer's Disease. *Neurochemical Research*, *41*(1–2), 243–257. https://doi.org/10.1007/S11064-015-1776-X

Dabrowska, N., & Wiczkowski, A. (2017). Analytics of oxidative stress markers in the early diagnosis of oxygen DNA damage. *Advances in Clinical and Experimental Medicine : Official Organ Wroclaw Medical University*, *26*(1), 155–166. https://doi.org/10.17219/ACEM/43272

Dakterzada, F., López-Ortega, R., Arias, A., Riba-Llena, I., Ruiz-Julián, M., Huerto, R., Tahan, N., & Piñol-Ripoll, G. (2021). Assessment of the Concordance and Diagnostic Accuracy Between Elecsys and Lumipulse Fully Automated Platforms and Innotest. *Frontiers in Aging Neuroscience*, *13*. https://doi.org/10.3389/FNAGI.2021.604119

De La Monte, S. M., & Wands, J. R. (2006). Molecular indices of oxidative stress and mitochondrial dysfunction occur early and often progress with severity of Alzheimer's disease. *Journal of Alzheimer's Disease : JAD*, *9*(2), 167–181. https://doi.org/10.3233/JAD-2006-9209

De La Vega, F. M., Lazaruk, K. D., Rhodes, M. D., & Wenz, M. H. (2005). Assessment of two flexible and compatible SNP genotyping platforms: TaqMan® SNP Genotyping Assays and the SNPlex™ Genotyping System. *Mutation Research/Fundamental and Molecular Mechanisms of Mutagenesis*, *573*(1–2), 111–135. https://doi.org/10.1016/J.MRFMMM.2005.01.008

Dei, R., Takeda, A., Niwa, H., Li, M., Nakagomi, Y., Watanabe, M., Inagaki, T., Washimi, Y., Yasuda,

Y., Horie, K., Miyata, T., & Sobue, G. (2002). Lipid peroxidation and advanced glycation end products in the brain in normal aging and in Alzheimer's disease. *Acta Neuropathologica 2002 104:2*, *104*(2), 113–122. https://doi.org/10.1007/S00401-002-0523-Y

Demir, E. A., Tutuk, O., Dogan, H., & Tumer, C. (2019). Depression in Alzheimer's Disease: The Roles of Cholinergic and Serotonergic Systems. *Alzheimer's Disease*, 223–235. https://doi.org/10.15586/ALZHEIMERSDISEASE.2019.CH14

Devore, E. E., Grodstein, F., Van Rooij, F. J. A., Hofman, A., Rosner, B., Stampfer, M. J., Witteman, J. C. M., & Breteler, M. M. B. (2009). Dietary intake of fish and omega-3 fatty acids in relation to long-term dementia risk. *The American Journal of Clinical Nutrition*, *90*(1), 170. https://doi.org/10.3945/AJCN.2008.27037

Dhouafli, Z., Cuanalo-Contreras, K., Hayouni, E. A., Mays, C. E., Soto, C., & Moreno-Gonzalez, I. (2018). Inhibition of protein misfolding and aggregation by natural phenolic compounds. *Cellular and Molecular Life Sciences : CMLS*, *75*(19), 3521–3538. https://doi.org/10.1007/S00018-018-2872-2

Di Paolo, G., & Kim, T. W. (2011). Linking lipids to Alzheimer's disease: cholesterol and beyond. *Nature Reviews Neuroscience 2011 12:5*, *12*(5), 284–296. https://doi.org/10.1038/nrn3012

Ding, Y., Qiao, A., Wang, Z., Goodwin, J. S., Lee, E. S., Block, M. L., Allsbrook, M., McDonald, M. P., & Fan, G. H. (2008). Retinoic acid attenuates beta-amyloid deposition and rescues memory deficits in an Alzheimer's disease transgenic mouse model. *The Journal of Neuroscience : The Official Journal of the Society for Neuroscience*, *28*(45), 11622–11634. https://doi.org/10.1523/JNEUROSCI.3153-08.2008

Dinkins, M. B., Enasko, J., Hernandez, C., Wang, G., Kong, J., Helwa, I., Liu, Y., Terry, A. V., & Bieberich, E. (2016). Neutral Sphingomyelinase-2 Deficiency Ameliorates Alzheimer's Disease Pathology and Improves Cognition in the 5XFAD Mouse. *The Journal of Neuroscience : The Official Journal of the Society for Neuroscience*, *36*(33), 8653–8667. https://doi.org/10.1523/JNEUROSCI.1429-16.2016

Dorninger, F., König, T., Scholze, P., Berger, M. L., Zeitler, G., Wiesinger, C., Gundacker, A., Pollak, D. D., Huck, S., Just, W. W., Forss-Petter, S., Pifl, C., & Berger, J. (2019). Disturbed neurotransmitter homeostasis in ether lipid deficiency. *Human Molecular Genetics*, *28*(12), 2046–2061. https://doi.org/10.1093/HMG/DDZ040

Dubois, B., Feldman, H. H., Jacova, C., DeKosky, S. T., Barberger-Gateau, P., Cummings, J., Delacourte, A., Galasko, D., Gauthier, S., Jicha, G., Meguro, K., O'Brien, J., Pasquier, F., Robert, P., Rossor, M., Salloway, S., Stern, Y., Visser, P. J., & Scheltens, P. (2007). Research criteria for the diagnosis of Alzheimer's disease: revising the NINCDS-ADRDA criteria. *Lancet Neurology*, *6*(8), 734–746. https://doi.org/10.1016/S1474-4422(07)70178-3

Dunkelberger, J. R., & Song, W. C. (2009). Complement and its role in innate and adaptive immune responses. *Cell Research 2010 20:1*, *20*(1), 34–50. https://doi.org/10.1038/cr.2009.139

Edwards, G. A., Gamez, N., Escobedo, G., Calderon, O., & Moreno-Gonzalez, I. (2019). Modifiable risk factors for Alzheimer's disease. *Frontiers in Aging Neuroscience*, *11*(JUN), 146. https://doi.org/10.3389/FNAGI.2019.00146/BIBTEX

Epperly, T. D., Dunay, M. A., & Boice, J. L. (2017). Alzheimer Disease: Pharmacologic and Nonpharmacologic Therapies for Cognitive and Functional Symptoms. *American Family Physician*, *95*(12), 771–778. www.aafp.org/afp

Falabella, M., Vernon, H. J., Hanna, M. G., Claypool, S. M., & Pitceathly, R. D. S. (2021). Cardiolipin, Mitochondria, and Neurological Disease. *Trends in Endocrinology & Metabolism*, *32*(4), 224–237. https://doi.org/10.1016/J.TEM.2021.01.006

Farias, S. T., Mungas, D., Reed, B. R., Harvey, D., & DeCarli, C. (2009). Progression of mild cognitive impairment to dementia in clinic- vs community-based cohorts. *Archives of Neurology*, *66*(9), 1151–1157. https://doi.org/10.1001/ARCHNEUROL.2009.106

Farmer, B. C., Kluemper, J., & Johnson, L. A. (2019). Apolipoprotein E4 Alters Astrocyte Fatty Acid Metabolism and Lipid Droplet Formation. *Cells*, *8*(2), 182. https://doi.org/10.3390/CELLS8020182

Farmer, B. C., Walsh, A. E., Kluemper, J. C., & Johnson, L. A. (2020). Lipid Droplets in Neurodegenerative Disorders. *Frontiers in Neuroscience*, *14*. https://doi.org/10.3389/FNINS.2020.00742

Feringa, F. M., & van der Kant, R. (2021). Cholesterol and Alzheimer's Disease; From Risk Genes to Pathological Effects. *Frontiers in Aging Neuroscience*, *13*. https://doi.org/10.3389/FNAGI.2021.690372

Ferrer, I., Andrés-Benito, P., Ausín, K., Pamplona, R., del Rio, J. A., Fernández-Irigoyen, J., & Santamaría, E. (2021). Dysregulated protein phosphorylation: A determining condition in the continuum of brain aging and Alzheimer's disease. *Brain Pathology*, *31*(6), e12996. https://doi.org/10.1111/BPA.12996

Ferrer, I., García, M. A., Carmona, M., Andrés-Benito, P., Torrejón-Escribano, B., Garcia-Esparcia, P., & Del Rio, J. A. (2019). Involvement of oligodendrocytes in tau seeding and spreading in tauopathies. *Frontiers in Aging Neuroscience*, *11*(MAY), 112. https://doi.org/10.3389/FNAGI.2019.00112/BIBTEX

Figueiredo-Pereira, M. E., Rockwell, P., Schmidt-Glenewinkel, T., & Serrano, P. (2015). Neuroinflammation and J2 prostaglandins: linking impairment of the ubiquitin-proteasome pathway and mitochondria to neurodegeneration. *Frontiers in Molecular Neuroscience*, *7*(JAN), 1–20. https://doi.org/10.3389/FNMOL.2014.00104

Folstein, M. F., Folstein, S. E., & McHugh, P. R. (1975). "Mini-mental state": A practical method for grading the cognitive state of patients for the clinician. *Journal of Psychiatric Research*, *12*(3), 189–198. https://doi.org/10.1016/0022-3956(75)90026-6

Fonteh, A. N., Cipolla, M., Chiang, A. J., Edminster, S. P., Arakaki, X., & Harrington, M. G. (2020). Polyunsaturated Fatty Acid Composition of Cerebrospinal Fluid Fractions Shows Their Contribution to Cognitive Resilience of a Pre-symptomatic Alzheimer's Disease Cohort. *Frontiers in Physiology*, *11*. https://doi.org/10.3389/FPHYS.2020.00083/FULL

Fonteh, A. N., Cipolla, M., Chiang, J., Arakaki, X., & Harrington, M. G. (2014). Human Cerebrospinal Fluid Fatty Acid Levels Differ between Supernatant Fluid and Brain-Derived Nanoparticle Fractions, and Are Altered in Alzheimer's Disease. *PLoS ONE*, *9*(6). https://doi.org/10.1371/JOURNAL.PONE.0100519

Forner, S., Baglietto-Vargas, D., Martini, A. C., Trujillo-Estrada, L., & LaFerla, F. M. (2017). Synaptic Impairment in Alzheimer's Disease: A Dysregulated Symphony. *Trends in Neurosciences*, *40*(6), 347–357. https://doi.org/10.1016/J.TINS.2017.04.002

Freund-Levi, Y., Vedin, I., Hjorth, E., Basun, H., Faxén Irving, G., Schultzberg, M., Eriksdotter, M., Palmblad, J., Vessby, B., Wahlund, L. O., Cederholm, T., & Basu, S. (2014). Effects of supplementation with omega-3 fatty acids on oxidative stress and inflammation in patients

with Alzheimer's disease: the OmegAD study. *Journal of Alzheimer's Disease : JAD*, *42*(3), 823–831. https://doi.org/10.3233/JAD-132042

Frisoni, G. B., Boccardi, M., Barkhof, F., Blennow, K., Cappa, S., Chiotis, K., Démonet, J. F., Garibotto, V., Giannakopoulos, P., Gietl, A., Hansson, O., Herholz, K., Jack, C. R., Nobili, F., Nordberg, A., Snyder, H. M., Ten Kate, M., Varrone, A., Albanese, E., … Winblad, B. (2017). Strategic roadmap for an early diagnosis of Alzheimer's disease based on biomarkers. *The Lancet. Neurology*, *16*(8), 661–676. https://doi.org/10.1016/S1474-4422(17)30159-X

Gaggini, M., Ndreu, R., Michelucci, E., Rocchiccioli, S., & Vassalle, C. (2022). Ceramides as Mediators of Oxidative Stress and Inflammation in Cardiometabolic Disease. *International Journal of Molecular Sciences*, *23*(5). https://doi.org/10.3390/IJMS23052719

Gardener, S., Gu, Y., Rainey-Smith, S. R., Keogh, J. B., Clifton, P. M., Mathieson, S. L., Taddei, K., Mondal, A., Ward, V. K., Scarmeas, N., Barnes, M., Ellis, K. A., Head, R., Masters, C. L., Ames, D., Macaulay, S. L., Rowe, C. C., Szoeke, C., Martins, R. N., & AIBL Research Group. (2012). Adherence to a Mediterranean diet and Alzheimer's disease risk in an Australian population. *Translational Psychiatry*, *2*(10). https://doi.org/10.1038/TP.2012.91

Gas Chromatography (GC) with Flame-Ionization Detection | Analytical Chemistry | JoVE. (n.d.). Retrieved February 16, 2022, from https://www.jove.com/es/v/10187/gas-chromatography-gc-with-flame-ionization-detection

Gaugler, J., James, B., Johnson, T., Scholz, K., & Weuve, J. (2016). 2016 Alzheimer's disease facts and figures. *Alzheimer's and Dementia*, *12*(4), 459–509. https://doi.org/10.1016/J.JALZ.2016.03.001

Gebauer, S. K., Destaillats, F., Dionisi, F., Krauss, R. M., & Baer, D. J. (2015). Vaccenic acid and trans fatty acid isomers from partially hydrogenated oil both adversely affect LDL cholesterol: a double-blind, randomized controlled trial. *The American Journal of Clinical Nutrition*, *102*(6), 1339–1346. https://doi.org/10.3945/AJCN.115.116129

Ginsberg, L., Rafique, S., Xuereb, J. H., Rapoport, S. I., & Gershfeld, N. L. (1995). Disease and anatomic specificity of ethanolamine plasmalogen deficiency in Alzheimer's disease brain. *Brain Research*, *698*(1–2), 223–226. https://doi.org/10.1016/0006-8993(95)00931-F

Gomez, W., Morales, R., Maracaja-Coutinho, V., Parra, V., & Nassif, M. (2020). Down syndrome and Alzheimer's disease: common molecular traits beyond the amyloid precursor protein. *Aging (Albany NY)*, *12*(1), 1011. https://doi.org/10.18632/AGING.102677

Gosselet, F., Saint-Pol, J., & Fenart, L. (2014). Effects of oxysterols on the blood-brain barrier: implications for Alzheimer's disease. *Biochemical and Biophysical Research Communications*, *446*(3), 687–691. https://doi.org/10.1016/J.BBRC.2013.11.059

Green, K. N., Martinez-Coria, H., Khashwji, H., Hall, E. B., Yurko-Mauro, K. A., Ellis, L., & LaFerla, F. M. (2007). Dietary docosahexaenoic acid and docosapentaenoic acid ameliorate amyloid-beta and tau pathology via a mechanism involving presenilin 1 levels. *The Journal of Neuroscience : The Official Journal of the Society for Neuroscience*, *27*(16), 4385–4395. https://doi.org/10.1523/JNEUROSCI.0055-07.2007

Greilberger, J., Koidl, C., Greilberger, M., Lamprecht, M., Schroecksnadel, K., Leblhuber, F., Fuchs, D., & Oettl, K. (2008). Malondialdehyde, carbonyl proteins and albumin-disulphide as useful oxidative markers in mild cognitive impairment and Alzheimer's disease. *Free Radical Research*, *42*(7), 633–638. https://doi.org/10.1080/10715760802255764

Grimm, M. O. W., Mett, J., Grimm, H. S., & Hartmann, T. (2017). APP Function and Lipids: A

Bidirectional Link. *Frontiers in Molecular Neuroscience*, *10*(March), 1–18. https://doi.org/10.3389/fnmol.2017.00063

Gu, J., Chen, L., Sun, R., Wang, J. L., Wang, J., Lin, Y., Lei, S., Zhang, Y., Lv, D., Jiang, F., Deng, Y., Collman, J. P., & Fu, L. (2022). Plasmalogens Eliminate Aging-Associated Synaptic Defects and Microglia-Mediated Neuroinflammation in Mice. *Frontiers in Molecular Biosciences*, *9*, 159. https://doi.org/10.3389/FMOLB.2022.815320/BIBTEX

Guerreiro, R., & Hardy, J. (2014). Genetics of Alzheimer's disease. *Neurotherapeutics : The Journal of the American Society for Experimental NeuroTherapeutics*, *11*(4), 732–737. https://doi.org/10.1007/S13311-014-0295-9

Haag, M. D. M., Hofman, A., Koudstaal, P. J., Stricker, B. H. C., & Breteler, M. M. B. (2009). Statins are associated with a reduced risk of Alzheimer disease regardless of lipophilicity. The Rotterdam Study. *Journal of Neurology, Neurosurgery & Psychiatry*, *80*(1), 13–17. https://doi.org/10.1136/JNNP.2008.150433

Haddad, M., Perrotte, M., Landri, S., Lepage, A., Fülöp, T., & Ramassamy, C. (2019). Circulating and Extracellular Vesicles Levels of N-(1-Carboxymethyl)-L-Lysine (CML) Differentiate Early to Moderate Alzheimer's Disease. *Journal of Alzheimer's Disease : JAD*, *69*(3), 751–762. https://doi.org/10.3233/JAD-181272

Hamilton, L. K., Dufresne, M., Joppé, S. E., Petryszyn, S., Aumont, A., Calon, F., Barnabé-Heider, F., Furtos, A., Parent, M., Chaurand, P., & Fernandes, K. J. L. (2015). Aberrant Lipid Metabolism in the Forebrain Niche Suppresses Adult Neural Stem Cell Proliferation in an Animal Model of Alzheimer's Disease. *Cell Stem Cell*, *17*(4), 397–411. https://doi.org/10.1016/J.STEM.2015.08.001

Han, X., Holtzman, D. M., & McKeel, D. W. (2001). Plasmalogen deficiency in early Alzheimer's disease subjects and in animal models: molecular characterization using electrospray ionization mass spectrometry. *Journal of Neurochemistry*, *77*(4), 1168–1180. https://doi.org/10.1046/J.1471-4159.2001.00332.X

Han, X., Holtzman, D. M., McKeel, D. W., Kelley, J., & Morris, J. C. (2002). Substantial sulfatide deficiency and ceramide elevation in very early Alzheimer's disease: potential role in disease pathogenesis. *Journal of Neurochemistry*, *82*(4), 809–818. https://doi.org/10.1046/J.1471-4159.2002.00997.X

Hanley, J. A., & McNeil, B. J. (1983). A method of comparing the areas under receiver operating characteristic curves derived from the same cases. *Radiology*, *148*(3), 839–843. https://doi.org/10.1148/RADIOLOGY.148.3.6878708

Hannun, Y. A., & Obeid, L. M. (2017). Sphingolipids and their metabolism in physiology and disease. *Nature Reviews Molecular Cell Biology 2017 19:3*, *19*(3), 175–191. https://doi.org/10.1038/nrm.2017.107

He, X., Huang, Y., Li, B., Gong, C. X., & Schuchman, E. H. (2010). Deregulation of sphingolipid metabolism in Alzheimer's disease. *Neurobiology of Aging*, *31*(3), 398–408. https://doi.org/10.1016/J.NEUROBIOLAGING.2008.05.010

Heun, R., Kölsch, H., Ibrahim-Verbaas, C. A., Combarros, O., Aulchenko, Y. S., Breteler, M., Schuur, M., van Duijn, C. M., Hammond, N., Belbin, O., Cortina-Borja, M., Wilcock, G. K., Brown, K., Barber, R., Kehoe, P. G., Coto, E., Alvarez, V., Lehmann, M. G., Deloukas, P., … Lehmann, D. J. (2012). Interactions between PPAR-α and inflammation-related cytokine genes on the development of Alzheimer's disease, observed by the Epistasis Project. *International Journal of Molecular Epidemiology and Genetics*, *3*(1), 39.

/pmc/articles/PMC3316448/

Hill, E., Wall, M. J., Moffat, K. G., & Karikari, T. K. (2020). Understanding the Pathophysiological Actions of Tau Oligomers: A Critical Review of Current Electrophysiological Approaches. *Frontiers in Molecular Neuroscience*, *13*. https://doi.org/10.3389/FNMOL.2020.00155

Honda, T., Ohara, T., Shinohara, M., Hata, J., Toh, R., Yoshida, D., Shibata, M., Ishida, T., Hirakawa, Y., Irino, Y., Sakata, S., Uchida, K., Kitazono, T., Kanba, S., Hirata, K. I., & Ninomiya, T. (2019). Serum elaidic acid concentration and risk of dementia: The Hisayama Study. *Neurology*, *93*(22), E2053–E2064. https://doi.org/10.1212/WNL.0000000000008464

Hong, S., Ostaszewski, B. L., Yang, T., O'Malley, T. T., Jin, M., Yanagisawa, K., Li, S., Bartels, T., & Selkoe, D. J. (2014). Soluble Aβ oligomers are rapidly sequestered from brain ISF in vivo and bind GM1 ganglioside on cellular membranes. *Neuron*, *82*(2), 308–319. https://doi.org/10.1016/J.NEURON.2014.02.027

Hosseini, M., Poljak, A., Braidy, N., Crawford, J., & Sachdev, P. (2020). Blood fatty acids in Alzheimer's disease and mild cognitive impairment: A meta-analysis and systematic review. *Ageing Research Reviews*, *60*. https://doi.org/10.1016/J.ARR.2020.101043

Hughes, C. P., Berg, L., Danziger, W. L., Coben, L. A., & Martin, R. L. (1982). A New Clinical Scale for the Staging of Dementia. *The British Journal of Psychiatry*, *140*(6), 566–572. https://doi.org/10.1192/BJP.140.6.566

Hui, J. S., Wilson, R. S., Bennett, D. A., Bienias, J. L., Gilley, D. W., & Evans, D. A. (2003). Rate of cognitive decline and mortality in Alzheimer's disease. *Neurology*, *61*(10), 1356–1361. https://doi.org/10.1212/01.WNL.0000094327.68399.59

Hussain, G., Wang, J., Rasul, A., Anwar, H., Imran, A., Qasim, M., Zafar, S., Kamran, S. K. S., Razzaq, A., Aziz, N., Ahmad, W., Shabbir, A., Iqbal, J., Baig, S. M., & Sun, T. (2019). Role of cholesterol and sphingolipids in brain development and neurological diseases. *Lipids in Health and Disease*, *18*(1), 1–12. https://doi.org/10.1186/S12944-019-0965-Z/FIGURES/5

Huttunen, H. J., Puglielli, L., Ellis, B. C., MacKenzie Ingano, L. A., & Kovacs, D. M. (2009). Novel N-terminal Cleavage of APP Precludes Aβ Generation in ACAT-Defective AC29 Cells. *Journal of Molecular Neuroscience : MN*, *37*(1), 6. https://doi.org/10.1007/S12031-008-9088-0

Huynh, K., Lim, W. L. F., Giles, C., Jayawardana, K. S., Salim, A., Mellett, N. A., Smith, A. A. T., Olshansky, G., Drew, B. G., Chatterjee, P., Martins, I., Laws, S. M., Bush, A. I., Rowe, C. C., Villemagne, V. L., Ames, D., Masters, C. L., Arnold, M., Nho, K., … Meikle, P. J. (2020). Concordant peripheral lipidome signatures in two large clinical studies of Alzheimer's disease. *Nature Communications 2020 11:1*, *11*(1), 1–11. https://doi.org/10.1038/s41467-020-19473-7

Huynh, T.-P. V., Davis, A. A., Ulrich, J. D., & Holtzman, D. M. (2017). Apolipoprotein E and Alzheimer's disease: the influence of apolipoprotein E on amyloid-β and other amyloidogenic proteins. *Journal of Lipid Research*, *58*(5), 824–836. https://doi.org/10.1194/jlr.R075481

Ichi, I., Kono, N., Arita, Y., Haga, S., Arisawa, K., Yamano, M., Nagase, M., Fujiwara, Y., & Arai, H. (2014). Identification of genes and pathways involved in the synthesis of Mead acid (20:3n-9), an indicator of essential fatty acid deficiency. *Biochimica et Biophysica Acta*, *1841*(1), 204–213. https://doi.org/10.1016/J.BBALIP.2013.10.013

Increased 8,12-iso-iPF2α-VI in Alzheimer's disease: Correlation of a noninvasive index of lipid

peroxidation with disease severity - Praticò - 2000 - Annals of Neurology - Wiley Online Library. (n.d.). Retrieved June 20, 2022, from https://onlinelibrary.wiley.com/doi/abs/10.1002/1531-8249%28200011%2948%3A5%3C809%3A%3AAID-ANA19%3E3.0.CO%3B2-9?sid=nlm%3Apubmed

Iqbal, K., Liu, F., Gong, C.-X., & Grundke-Iqbal, I. (2010). Tau in Alzheimer Disease and Related Tauopathies. *Current Alzheimer Research*, *7*(8), 656. https://doi.org/10.2174/156720510793611592

Iuliano, L., Pacelli, A., Ciacciarelli, M., Zerbinati, C., Fagioli, S., Piras, F., Orfei, M. D., Bossù, P., Pazzelli, F., Serviddio, G., Caltagirone, C., & Spalletta, G. (2013). Plasma Fatty Acid Lipidomics in Amnestic Mild Cognitive Impairment and Alzheimer's Disease. *Journal of Alzheimer's Disease*, *36*(3), 545–553. https://doi.org/10.3233/JAD-122224

Jack, C. R., Bennett, D. A., Blennow, K., Carrillo, M. C., Dunn, B., Haeberlein, S. B., Holtzman, D. M., Jagust, W., Jessen, F., Karlawish, J., Liu, E., Molinuevo, J. L., Montine, T., Phelps, C., Rankin, K. P., Rowe, C. C., Scheltens, P., Siemers, E., Snyder, H. M., … Silverberg, N. (2018). NIA-AA Research Framework: Toward a biological definition of Alzheimer's disease. *Alzheimer's & Dementia : The Journal of the Alzheimer's Association*, *14*(4), 535–562. https://doi.org/10.1016/J.JALZ.2018.02.018

Jackson, J., Jambrina, E., Li, J., Marston, H., Menzies, F., Phillips, K., & Gilmour, G. (2019). Targeting the synapse in Alzheimer's disease. *Frontiers in Neuroscience*, *13*(JUL), 735. https://doi.org/10.3389/FNINS.2019.00735/BIBTEX

Jensen, C. S., Kellberg, A. O., Hasselbalch, S. G., & Simonsen, A. H. (2021). Cerebrospinal fluid levels of 8-isoprostane, a marker of oxidative stress, are elevated in patients with Alzheimer's disease compared to healthy subjects: Does the malfunction in the cell's powerhouse lead to Alzheimer's disease? *Alzheimer's & Dementia*, *17*(S5), e052071. https://doi.org/10.1002/ALZ.052071

Jo, D. S., Park, N. Y., & Cho, D. H. (2020). Peroxisome quality control and dysregulated lipid metabolism in neurodegenerative diseases. *Experimental & Molecular Medicine 2020 52:9*, *52*(9), 1486–1495. https://doi.org/10.1038/s12276-020-00503-9

Joas, E., Bäckman, K., Gustafson, D., Östling, S., Waern, M., Guo, X., & Skoog, I. (2012). Blood pressure trajectories from midlife to late life in relation to dementia in women followed for 37 years. *Hypertension (Dallas, Tex. : 1979)*, *59*(4), 796–801. https://doi.org/10.1161/HYPERTENSIONAHA.111.182204

Johnson, K. A., Fox, N. C., Sperling, R. A., & Klunk, W. E. (2012). Brain Imaging in Alzheimer Disease. *Cold Spring Harbor Perspectives in Medicine*, *2*(4). https://doi.org/10.1101/CSHPERSPECT.A006213

Jové, M., Ayala, V., Ramírez-Núñez, O., Naudí, A., Cabré, R., Spickett, C. M., Portero-Otín, M., & Pamplona, R. (2013). Specific lipidome signatures in central nervous system from methionine-restricted mice. *Journal of Proteome Research*, *12*(6), 2679–2689. https://doi.org/10.1021/PR400064A

Kandel, P., Semerci, F., Bajic, A., Baluya, D., Ma, L., Chen, K., Cao, A., Phongmekhin, T., Matinyan, N., Choi, W., Jiménez-Panizo, A., Chamakuri, S., Raji, I. O., Chang, L., Fuentes-Prior, P., MacKenzie, K. R., Benn, C. L., Estébanez-Perpiñá, E., Venken, K., … Duncan, D. (2020). Oleic acid triggers hippocampal neurogenesis by binding to TLX/NR2E1. *BioRxiv*, 2020.10.28.359810. https://doi.org/10.1101/2020.10.28.359810

Kao, Y. C., Ho, P. C., Tu, Y. K., Jou, I. M., & Tsai, K. J. (2020). Lipids and Alzheimer's Disease. *International Journal of Molecular Sciences*, *21*(4). https://doi.org/10.3390/IJMS21041505

Kehm, R., Baldensperger, T., Raupbach, J., & Höhn, A. (2021). Protein oxidation - Formation mechanisms, detection and relevance as biomarkers in human diseases. *Redox Biology*, *42*, 101901. https://doi.org/10.1016/J.REDOX.2021.101901

Kind, T., Liu, K. H., Lee, D. Y., Defelice, B., Meissen, J. K., & Fiehn, O. (2013). LipidBlast - in-silico tandem mass spectrometry database for lipid identification. *Nature Methods*, *10*(8), 755. https://doi.org/10.1038/NMETH.2551

Kinney, J. W., Bemiller, S. M., Murtishaw, A. S., Leisgang, A. M., Salazar, A. M., & Lamb, B. T. (2018). Inflammation as a central mechanism in Alzheimer's disease. *Alzheimer's & Dementia : Translational Research & Clinical Interventions*, *4*, 575. https://doi.org/10.1016/J.TRCI.2018.06.014

Kivipelto, M., Helkala, E. L., Laakso, M. P., Hänninen, T., Hallikainen, M., Alhainen, K., Soininen, H., Tuomilehto, J., & Nissien, A. (2001). Midlife vascular risk factors and Alzheimer's disease in later life: longitudinal, population based study. *BMJ : British Medical Journal*, *322*(7300), 1447. https://doi.org/10.1136/BMJ.322.7300.1447

Koal, T., Klavins, K., Seppi, D., Kemmler, G., & Humpel, C. (2015). Sphingomyelin SM(d18:1/18:0) is Significantly Enhanced in Cerebrospinal Fluid Samples Dichotomized by Pathological Amyloid-β42, Tau, and Phospho-Tau-181 Levels. *Journal of Alzheimer's Disease : JAD*, *44*(4), 1193. https://doi.org/10.3233/JAD-142319

Koelmel, J. P., Kroeger, N. M., Ulmer, C. Z., Bowden, J. A., Patterson, R. E., Cochran, J. A., Beecher, C. W. W., Garrett, T. J., & Yost, R. A. (2017). LipidMatch: an automated workflow for rule-based lipid identification using untargeted high-resolution tandem mass spectrometry data. *BMC Bioinformatics*, *18*(1). https://doi.org/10.1186/S12859-017-1744-3

Korinek, M., Gonzalez-Gonzalez, I. M., Smejkalova, T., Hajdukovic, D., Skrenkova, K., Krusek, J., Horak, M., & Vyklicky, L. (2020). Cholesterol modulates presynaptic and postsynaptic properties of excitatory synaptic transmission. *Scientific Reports 2020 10:1*, *10*(1), 1–18. https://doi.org/10.1038/s41598-020-69454-5

Kosicek, M., Kirsch, S., Bene, R., Trkanjec, Z., Titlic, M., Bindila, L., Peter-Katalinic, J., & Hecimovic, S. (2010). Nano-HPLC-MS analysis of phospholipids in cerebrospinal fluid of Alzheimer's disease patients-a pilot study. *Analytical and Bioanalytical Chemistry*, *398*(7–8), 2929–2937. https://doi.org/10.1007/S00216-010-4273-8

Kosicek, M., Zetterberg, H., Andreasen, N., Peter-Katalinic, J., & Hecimovic, S. (2012). Elevated cerebrospinal fluid sphingomyelin levels in prodromal Alzheimer's disease. *Neuroscience Letters*, *516*(2), 302–305. https://doi.org/10.1016/J.NEULET.2012.04.019

Koskas, P., Henry-Feugeas, M., Feugeas, J.-P., Ou, P., & Drunat, O. (2017). Factors of Rapid Cognitive Decline in Late Onset Alzheimer's Disease. *Current Aging Science*, *10*(2), 129–135. https://doi.org/10.2174/1874609810666170102143257

Kou, J., Kovacs, G. G., Höftberger, R., Kulik, W., Brodde, A., Forss-Petter, S., Hönigschnabl, S., Gleiss, A., Brügger, B., Wanders, R., Just, W., Budka, H., Jungwirth, S., Fischer, P., & Berger, J. (2011). Peroxisomal alterations in Alzheimer's disease. *Acta Neuropathologica*, *122*(3), 271. https://doi.org/10.1007/S00401-011-0836-9

Kumar, A., Singh, A., & Ekavali. (2015). A review on Alzheimer's disease pathophysiology and its management: An update. *Pharmacological Reports*, *67*(2), 195–203.

https://doi.org/10.1016/j.pharep.2014.09.004

Lacombe, R. J. S., Chouinard-Watkins, R., & Bazinet, R. P. (2018). Brain docosahexaenoic acid uptake and metabolism. *Molecular Aspects of Medicine*, *64*, 109–134. https://doi.org/10.1016/J.MAM.2017.12.004

Lai, C. L., Liou, L. M., Liu, C. K., Yang, Y. H., & Lin, R. T. (2014). Effects of metabolic syndrome, apolipoprotein E, and CYP46 on cognition among Taiwanese Chinese. *The Kaohsiung Journal of Medical Sciences*, *30*(7), 343–349. https://doi.org/10.1016/J.KJMS.2014.03.005

Lashley, T., Schott, J. M., Weston, P., Murray, C. E., Wellington, H., Keshavan, A., Foti, S. C., Foiani, M., Toombs, J., Rohrer, J. D., Heslegrave, A., & Zetterberg, H. (2018). Molecular biomarkers of Alzheimer's disease: progress and prospects. *Disease Models & Mechanisms*, *11*(5). https://doi.org/10.1242/DMM.031781

Lauwers, E., Goodchild, R., & Verstreken, P. (2016). Membrane Lipids in Presynaptic Function and Disease. *Neuron*, *90*(1), 11–25. https://doi.org/10.1016/J.NEURON.2016.02.033

Layé, S., Nadjar, A., Joffre, C., & Bazinet, R. P. (2018). Anti-Inflammatory Effects of Omega-3 Fatty Acids in the Brain: Physiological Mechanisms and Relevance to Pharmacology. *Pharmacological Reviews*, *70*(1), 12–38. https://doi.org/10.1124/PR.117.014092

Lee, J. T., Xu, J., Lee, J. M., Ku, G., Han, X., Yang, D. I., Chen, S., & Hsu, C. Y. (2004). Amyloid-beta peptide induces oligodendrocyte death by activating the neutral sphingomyelinase-ceramide pathway. *The Journal of Cell Biology*, *164*(1), 123–131. https://doi.org/10.1083/JCB.200307017

Lee, L. K., Shahar, S., Chin, A. V., & Yusoff, N. A. M. (2013). Docosahexaenoic acid-concentrated fish oil supplementation in subjects with mild cognitive impairment (MCI): a 12-month randomised, double-blind, placebo-controlled trial. *Psychopharmacology*, *225*(3), 605–612. https://doi.org/10.1007/S00213-012-2848-0

Lee, S. J. C., Nam, E., Lee, H. J., Savelieff, M. G., & Lim, M. H. (2017). Towards an understanding of amyloid-β oligomers: characterization, toxicity mechanisms, and inhibitors. *Chemical Society Reviews*, *46*(2), 310–323. https://doi.org/10.1039/C6CS00731G

Lewczuk, P., Matzen, A., Blennow, K., Parnetti, L., Molinuevo, J. L., Eusebi, P., Kornhuber, J., Morris, J. C., & Fagan, A. M. (2017). Cerebrospinal Fluid Aβ42/40 Corresponds Better than Aβ42 to Amyloid PET in Alzheimer's Disease. *Journal of Alzheimer's Disease : JAD*, *55*(2), 813–822. https://doi.org/10.3233/JAD-160722

Li, D., & Mielke, M. M. (2019). An Update on Blood-Based Markers of Alzheimer's Disease Using the SiMoA Platform. *Neurology and Therapy*, *8*(Suppl 2), 73. https://doi.org/10.1007/S40120-019-00164-5

Li, M., Wang, W., Li, Y., Wang, L., Shen, X., & Tang, Z. (2013). CYP46A1 intron-2T/C polymorphism and Alzheimer's disease: an updated meta-analysis of 16 studies including 3,960 cases and 3,828 controls. *Neuroscience Letters*, *549*, 18–23. https://doi.org/10.1016/J.NEULET.2013.06.011

Li Puma, D. D., Piacentini, R., & Grassi, C. (2021). Does Impairment of Adult Neurogenesis Contribute to Pathophysiology of Alzheimer's Disease? A Still Open Question. *Frontiers in Molecular Neuroscience*, *13*, 258. https://doi.org/10.3389/FNMOL.2020.578211/BIBTEX

Lin, P. Y., Cheng, C., Satyanarayanan, S. K., Chiu, L. T., Chien, Y. C., Chuu, C. P., Lan, T. H., & Su, K. P. (2022). Omega-3 fatty acids and blood-based biomarkers in Alzheimer's disease and mild cognitive impairment: A randomized placebo-controlled trial. *Brain, Behavior, and*

Immunity, *99*, 289–298. https://doi.org/10.1016/J.BBI.2021.10.014

Liu, C. C., Kanekiyo, T., Xu, H., & Bu, G. (2013). Apolipoprotein E and Alzheimer disease: risk, mechanisms, and therapy. *Nature Reviews. Neurology*, *9*(2), 106. https://doi.org/10.1038/NRNEUROL.2012.263

Liu, J. J., Zhang, W., Wang, S. S., Jia, Z. Q., Shi, Y. H., Yang, L., & Shi, R. L. (2019). Effects of chain length of saturated fatty acids on Aβ generation in SH-SY5Y cells. *Neuroscience Letters*, *698*, 169–172. https://doi.org/10.1016/J.NEULET.2019.01.024

Liu, L., MacKenzie, K. R., Putluri, N., Maletić-Savatić, M., & Bellen, H. J. (2017). The Glia-Neuron Lactate Shuttle and Elevated ROS Promote Lipid Synthesis in Neurons and Lipid Droplet Accumulation in Glia via APOE/D. *Cell Metabolism*, *26*(5), 719-737.e6. https://doi.org/10.1016/J.CMET.2017.08.024

Liu, Q., An, Y., Yu, H., Lu, Y., Feng, L., Wang, C., & Xiao, R. (2016). Relationship between oxysterols and mild cognitive impairment in the elderly: a case-control study. *Lipids in Health and Disease*, *15*(1), 1–6. https://doi.org/10.1186/S12944-016-0344-Y/FIGURES/1

Liu, Y., Thalamuthu, A., Mather, K. A., Crawford, J., Ulanova, M., Wong, M. W. K., Pickford, R., Sachdev, P. S., & Braidy, N. (2021). Plasma lipidome is dysregulated in Alzheimer's disease and is associated with disease risk genes. *Translational Psychiatry 2021 11:1*, *11*(1), 1–18. https://doi.org/10.1038/s41398-021-01362-2

Liu, Y., Yang, L., Conde-Knape, K., Beher, D., Shearman, M. S., & Shachter, N. S. (2004). Fatty acids increase presenilin-1 levels and γ-secretase activity in PSwt-1 cells. *Journal of Lipid Research*, *45*(12), 2368–2376. https://doi.org/10.1194/JLR.M400317-JLR200

Lizard, G., Rouaud, O., Demarquoy, J., Cherkaoui-Malki, M., & Iuliano, L. (2012). Potential roles of peroxisomes in Alzheimer's disease and in dementia of the Alzheimer's type. *Journal of Alzheimer's Disease : JAD*, *29*(2), 241–254. https://doi.org/10.3233/JAD-2011-111163

Lopez-Rodriguez, A. B., Hennessy, E., Murray, C. L., Nazmi, A., Delaney, H. J., Healy, D., Fagan, S. G., Rooney, M., Stewart, E., Lewis, A., de Barra, N., Scarry, P., Riggs-Miller, L., Boche, D., Cunningham, M. O., & Cunningham, C. (2021). Acute systemic inflammation exacerbates neuroinflammation in Alzheimer's disease: IL-1β drives amplified responses in primed astrocytes and neuronal network dysfunction. *Alzheimer's & Dementia*, *17*(10), 1735–1755. https://doi.org/10.1002/ALZ.12341

Lopez, L. B., Kritz-Silverstein, D., & Barrett-Connor, E. (2011). HIgh dietary and plasma levels of the omega-3 fatty acid docosahexaenoic acid are associated with decreased dementia risk: the rancho bernardo study. *The Journal of Nutrition, Health & Aging 2011 15:1*, *15*(1), 25–31. https://doi.org/10.1007/S12603-011-0009-5

Lopresti, P. (2018). Tau in Oligodendrocytes Takes Neurons in Sickness and in Health. *International Journal of Molecular Sciences*, *19*(8). https://doi.org/10.3390/IJMS19082408

Lovell, M. A., Ehmann, W. D., Mattson, M. P., & Markesbery, W. R. (1997). Elevated 4-hydroxynonenal in ventricular fluid in Alzheimer's disease. *Neurobiology of Aging*, *18*(5), 457–461. https://doi.org/10.1016/S0197-4580(97)00108-5

Mahley, R. W. (2016). Central Nervous System Lipoproteins: ApoE and Regulation of Cholesterol Metabolism. *Arteriosclerosis, Thrombosis, and Vascular Biology*, *36*(7), 1305. https://doi.org/10.1161/ATVBAHA.116.307023

Maiuolo, J., Gliozzi, M., Musolino, V., Carresi, C., Scarano, F., Nucera, S., Scicchitano, M., Bosco, F., Ruga, S., Zito, M. C., Macri, R., Bulotta, R., Muscoli, C., & Mollace, V. (2021). From

Metabolic Syndrome to Neurological Diseases: Role of Autophagy. *Frontiers in Cell and Developmental Biology*, *9*, 619. https://doi.org/10.3389/FCELL.2021.651021/BIBTEX

Malaplate-Armand, C., Florent-Béchard, S., Youssef, I., Koziel, V., Sponne, I., Kriem, B., Leininger-Muller, B., Olivier, J. L., Oster, T., & Pillot, T. (2006). Soluble oligomers of amyloid-beta peptide induce neuronal apoptosis by activating a cPLA2-dependent sphingomyelinase-ceramide pathway. *Neurobiology of Disease*, *23*(1), 178–189. https://doi.org/10.1016/J.NBD.2006.02.010

Martí, A., & Fortique, F. (2019). Omega-3 fatty acids and cognitive decline: a systematic review. *Nutricion Hospitalaria*, *36*(4), 939–949. https://doi.org/10.20960/NH.02496

Martin, L., Latypova, X., Wilson, C. M., Magnaudeix, A., Perrin, M. L., Yardin, C., & Terro, F. (2013). Tau protein kinases: Involvement in Alzheimer's disease. In *Ageing Research Reviews* (Vol. 12, Issue 1, pp. 289–309). Elsevier. https://doi.org/10.1016/j.arr.2012.06.003

Martín, M. G., Pfrieger, F., & Dotti, C. G. (2014). Cholesterol in brain disease: sometimes determinant and frequently implicated. *EMBO Reports*, *15*(10), 1036–1052. https://doi.org/10.15252/EMBR.201439225

Martinez-Lapiscina, E. H., Clavero, P., Toledo, E., San Julian, B., Sanchez-Tainta, A., Corella, D., Lamuela-Raventos, R. M., Martinez, J. A., & Martinez-Gonzalez, M. A. (2013). Virgin olive oil supplementation and long-term cognition: the PREDIMED-NAVARRA randomized, trial. *The Journal of Nutrition, Health & Aging*, *17*(6), 544–552. https://doi.org/10.1007/S12603-013-0027-6

Martinez, A. E., Weissberger, G., Kuklenyik, Z., He, X., Meuret, C., Parekh, T., Rees, J. C., Parks, B. A., Gardner, M. S., King, S. M., Collier, T. S., Harrington, M. G., Sweeney, M. D., Wang, X., Zlokovic, B. V., Joe, E., Nation, D. A., Schneider, L. S., Chui, H. C., … Yassine, H. N. (2022). The small HDL particle hypothesis of Alzheimer's disease. *Alzheimer's & Dementia*, *September 2021*, 1–14. https://doi.org/10.1002/ALZ.12649

McKhann, G., Drachman, D., Folstein, M., Katzman, R., Price, D., & Stadlan, E. M. (1984). Clinical diagnosis of Alzheimer's disease: report of the NINCDS-ADRDA Work Group under the auspices of Department of Health and Human Services Task Force on Alzheimer's Disease. *Neurology*, *34*(7), 939–944. https://doi.org/10.1212/WNL.34.7.939

McKhann, G. M., Knopman, D. S., Chertkow, H., Hyman, B. T., Jack, C. R., Kawas, C. H., Klunk, W. E., Koroshetz, W. J., Manly, J. J., Mayeux, R., Mohs, R. C., Morris, J. C., Rossor, M. N., Scheltens, P., Carrillo, M. C., Thies, B., Weintraub, S., & Phelps, C. H. (2011). The diagnosis of dementia due to Alzheimer's disease: Recommendations from the National Institute on Aging-Alzheimer's Association workgroups on diagnostic guidelines for Alzheimer's disease. In *Alzheimer's and Dementia*. https://doi.org/10.1016/j.jalz.2011.03.005

Medeiros-De-Moraes, I. M., Gonçalves-De-Albuquerque, C. F., Kurz, A. R. M., De Jesus Oliveira, F. M., Pereira de Abreu, V. H., Torres, R. C., Carvalho, V. F., Estato, V., Bozza, P. T., Sperandio, M., De Castro-Faria-Neto, H. C., & Silva, A. R. (2018). Omega-9 Oleic Acid, the Main Compound of Olive Oil, Mitigates Inflammation during Experimental Sepsis. *Oxidative Medicine and Cellular Longevity*, *2018*. https://doi.org/10.1155/2018/6053492

Melis, R. J. F., Haaksma, M. L., & Muniz-Terrera, G. (2019). Understanding and predicting the longitudinal course of dementia. *Current Opinion in Psychiatry*, *32*(2), 123. https://doi.org/10.1097/YCO.0000000000000482

Mencarelli, C., Bode, G. H., Losen, M., Kulharia, M., Molenaar, P. C., Veerhuis, R., Steinbusch, H. W. M., De Baets, M. H., Nicolaes, G. A. F., & Martinez-Martinez, P. (2012). Goodpasture

antigen-binding protein/ceramide transporter binds to human serum amyloid P-component and is present in brain amyloid plaques. *The Journal of Biological Chemistry*, *287*(18), 14897–14911. https://doi.org/10.1074/JBC.M111.299545

Merino-Serrais, P., Loera-Valencia, R., Rodriguez-Rodriguez, P., Parrado-Fernandez, C., Ismail, M. A., Maioli, S., Matute, E., Jimenez-Mateos, E. M., Björkhem, I., Defelipe, J., & Cedazo-Minguez, A. (2019). 27-Hydroxycholesterol Induces Aberrant Morphology and Synaptic Dysfunction in Hippocampal Neurons. *Cerebral Cortex*, *29*(1), 429–446. https://doi.org/10.1093/CERCOR/BHY274

Mielke, M. M., Haughey, N. J., Bandaru, V. V. R., Zetterberg, H., Blennow, K., Andreasson, U., Johnson, S. C., Gleason, C. E., Blazel, H. M., Puglielli, L., Sager, M. A., Asthana, S., & Carlsson, C. M. (2014). CSF sphingolipids, β-amyloid, and tau in adults at risk for Alzheimer's disease. *Neurobiology of Aging*, *35*(11), 2486. https://doi.org/10.1016/J.NEUROBIOLAGING.2014.05.019

Mielke, M. M., Haughey, N. J., Ratnam Bandaru, V. V., Schech, S., Carrick, R., Carlson, M. C., Mori, S., Miller, M. I., Ceritoglu, C., Brown, T., Albert, M., & Lyketsos, C. G. (2010). Plasma ceramides are altered in mild cognitive impairment and predict cognitive decline and hippocampal volume loss. *Alzheimer's & Dementia*, *6*(5), 378–385. https://doi.org/10.1016/J.JALZ.2010.03.014

Mirra, S. S., Heyman, A., McKeel, D., Sumi, S. M., Crain, B. J., Brownlee, L. M., Vogel, F. S., Hughes, J. P., van Belle, G., Berg, L., Ball, M. J., Bierer, L. M., Claasen, D., Hansen, L. R., Hart, M., Hedreen, J., Baltimore, B., Hen Derson, V., Hyman, B. T., … Terry, R. D. (1991). The Consortium to Establish a Registry for Alzheimer's Disease (CERAD). Part II. Standardization of the neuropathologic assessment of Alzheimer's disease. *Neurology*, *41*(4), 479–486. https://doi.org/10.1212/WNL.41.4.479

Misrani, A., Tabassum, S., & Yang, L. (2021). Mitochondrial Dysfunction and Oxidative Stress in Alzheimer's Disease. *Frontiers in Aging Neuroscience*, *13*. https://doi.org/10.3389/FNAGI.2021.617588

Monacelli, F., Borghi, R., Pacini, D., Serrati, C., Traverso, N., & Odetti, P. (2014). Pentosidine determination in CSF: A potential biomarker of Alzheimer's disease? *Clinical Chemistry and Laboratory Medicine*, *52*(1), 117–120. https://doi.org/10.1515/CCLM-2012-0829/MACHINEREADABLECITATION/RIS

Montagne, A., Nation, D. A., Sagare, A. P., Barisano, G., Sweeney, M. D., Chakhoyan, A., Pachicano, M., Joe, E., Nelson, A. R., D'orazio, L. M., Buennagel, D. P., Harrington, M. G., Benzinger, T. L. S., Fagan, A. M., Ringman, J. M., Schneider, L. S., Morris, J. C., Reiman, E. M., Caselli, R. J., … Sweeney, M. D. ✉. (2020). APOE4 leads to blood-brain barrier dysfunction predicting cognitive decline. *Nature*, *581*. https://doi.org/10.1038/s41586-020-2247-3

Monteiro-Cardoso, V. F., Oliveira, M. M., Melo, T., Domingues, M. R. M., Moreira, P. I., Ferreiro, E., Peixoto, F., & Videira, R. A. (2015). Cardiolipin profile changes are associated to the early synaptic mitochondrial dysfunction in Alzheimer's disease. *Journal of Alzheimer's Disease : JAD*, *43*(4), 1375–1392. https://doi.org/10.3233/JAD-141002

Montine, T. J., Kaye, J. A., Montine, K. S., McFarland, L., Morrow, J. D., & Quinn, J. F. (2001). Cerebrospinal Fluid Aβ42, Tau, and F2-Isoprostane Concentrations in Patients With Alzheimer Disease, Other Dementias, and in Age-Matched Controls. *Archives of Pathology & Laboratory Medicine*, *125*(4), 510–512. https://doi.org/10.5858/2001-125-0510-CFATAF

Morbelli, S., & Bauckneht, M. (2018). Amyloid PET Imaging: Standardization and Integration with

Other Alzheimer's Disease Biomarkers. *Methods in Molecular Biology (Clifton, N.J.)*, *1750*, 203–212. https://doi.org/10.1007/978-1-4939-7704-8_13

Moreno-Gonzalez, I., Estrada, L. D., Sanchez-Mejias, E., & Soto, C. (2013). *ARTICLE Smoking exacerbates amyloid pathology in a mouse model of Alzheimer's disease*. https://doi.org/10.1038/ncomms2494

Morris, J. C., Heyman, A., Mohs, R. C., Hughes, J. P., van Belle, G., Fillenbaum, G., Mellits, E. D., & Clark, C. (1989). The Consortium to Establish a Registry for Alzheimer's Disease (CERAD). Part I. Clinical and neuropsychological assesment of Alzheimer's disease. *Neurology*, *39*(9), 1159–1159. https://doi.org/10.1212/WNL.39.9.1159

Morris, M. C., Evans, D. A., Bienias, J. L., Tangney, C. C., Bennett, D. A., Aggarwal, N., Schneider, J., & Wilson, R. S. (2003). Dietary fats and the risk of incident Alzheimer disease. *Archives of Neurology*, *60*(2), 194–200. https://doi.org/10.1001/ARCHNEUR.60.2.194

Moulton, M. J., Barish, S., Ralhan, I., Chang, J., Goodman, L. D., Harland, J. G., Marcogliese, P. C., Johansson, J. O., Ioannou, M. S., & Bellen, H. J. (2021). Neuronal ROS-induced glial lipid droplet formation is altered by loss of Alzheimer's disease-associated genes. *Proceedings of the National Academy of Sciences of the United States of America*, *118*(52). https://doi.org/10.1073/PNAS.2112095118

Mozaffarian, D., Katan, M. B., Ascherio, A., Stampfer, M. J., & Willett, W. C. (2006). Trans fatty acids and cardiovascular disease. *The New England Journal of Medicine*, *354*(15), 1601–1613. https://doi.org/10.1056/NEJMRA054035

Muche, A., Arendt, T., & Schliebs, R. (2017). Oxidative stress affects processing of amyloid precursor protein in vascular endothelial cells. *PLoS ONE*, *12*(6). https://doi.org/10.1371/JOURNAL.PONE.0178127

Mueed, Z., Tandon, P., Maurya, S. K., Deval, R., Kamal, M. A., & Poddar, N. K. (2019). Tau and mTOR: The hotspots for multifarious diseases in Alzheimer's development. *Frontiers in Neuroscience*, *13*(JAN), 1017. https://doi.org/10.3389/FNINS.2018.01017/BIBTEX

Mulder, C., Wahlund, L.-O., Teerlink, T., Blomberg, M., Veerhuis, R., Van Kamp, G. J., Scheltens, P., & Scheffer, P. G. (2003). Decreased lysophosphatidylcholine=phosphatidylcholine ratio in cerebrospinal fluid in Alzheimer's disease. *J Neural Transm*, *110*, 949–955. https://doi.org/10.1007/s00702-003-0007-9

Murphy, M. P., & Levine, H. (2010). Alzheimer's Disease and the β-Amyloid Peptide. *Journal of Alzheimer's Disease : JAD*, *19*(1), 311. https://doi.org/10.3233/JAD-2010-1221

Nantachai, G., Vasupanrajit, A., Tunvirachaisakul, C., Solmi, M., & Maes, M. (2021). Oxidative stress and antioxidant defenses in mild cognitive impairment: a systematic review and meta-analysis. *MedRxiv*, 2021.11.22.21266698. https://doi.org/10.1101/2021.11.22.21266698

Nasreddine, Z. S., Phillips, N. A., Bédirian, V., Charbonneau, S., Whitehead, V., Collin, I., Cummings, J. L., & Chertkow, H. (2005). The Montreal Cognitive Assessment, MoCA: A Brief Screening Tool For Mild Cognitive Impairment. *Journal of the American Geriatrics Society*, *53*(4), 695–699. https://doi.org/10.1111/J.1532-5415.2005.53221.X

Naudí, A., Cabré, R., Jové, M., Ayala, V., Gonzalo, H., Portero-Otín, M., Ferrer, I., & Pamplona, R. (2015). Lipidomics of Human Brain Aging and Alzheimer's Disease Pathology. *International Review of Neurobiology*, *122*, 133–189. https://doi.org/10.1016/BS.IRN.2015.05.008

Ng, T. P., Feng, L., Nyunt, M. S. Z., Feng, L., Gao, Q., Lim, M. L., Collinson, S. L., Chong, M. S., Lim,

W. S., Lee, T. S., Yap, P., & Yap, K. B. (2016). Metabolic Syndrome and the Risk of Mild Cognitive Impairment and Progression to Dementia: Follow-up of the Singapore Longitudinal Ageing Study Cohort. *JAMA Neurology*, *73*(4), 456–463. https://doi.org/10.1001/JAMANEUROL.2015.4899

Nguyen, L. N., Ma, D., Shui, G., Wong, P., Cazenave-Gassiot, A., Zhang, X., Wenk, M. R., Goh, E. L. K., & Silver, D. L. (2014). Mfsd2a is a transporter for the essential omega-3 fatty acid docosahexaenoic acid. *Nature*, *509*(7501), 503–506. https://doi.org/10.1038/NATURE13241

Nichols, E., Steinmetz, J. D., Vollset, S. E., Fukutaki, K., Chalek, J., Abd-Allah, F., Abdoli, A., Abualhasan, A., Abu-Gharbieh, E., Akram, T. T., Al Hamad, H., Alahdab, F., Alanezi, F. M., Alipour, V., Almustanyir, S., Amu, H., Ansari, I., Arabloo, J., Ashraf, T., … Vos, T. (2022). Estimation of the global prevalence of dementia in 2019 and forecasted prevalence in 2050: an analysis for the Global Burden of Disease Study 2019. *The Lancet Public Health*, *7*(2), e105–e125. https://doi.org/10.1016/S2468-2667(21)00249-8/ATTACHMENT/60E03FD1-38B2-4B40-A91D-9AFDDA22B45E/MMC1.PDF

Nichols, E., Szoeke, C. E. I., Vollset, S. E., Abbasi, N., Abd-Allah, F., Abdela, J., Aichour, M. T. E., Akinyemi, R. O., Alahdab, F., Asgedom, S. W., Awasthi, A., Barker-Collo, S. L., Baune, B. T., Béjot, Y., Belachew, A. B., Bennett, D. A., Biadgo, B., Bijani, A., Bin Sayeed, M. S., … Murray, C. J. L. (2019). Global, regional, and national burden of Alzheimer's disease and other dementias, 1990-2016: a systematic analysis for the Global Burden of Disease Study 2016. *The Lancet. Neurology*, *18*(1), 88–106. https://doi.org/10.1016/S1474-4422(18)30403-4

Niki, E. (2014). Biomarkers of lipid peroxidation in clinical material. *Biochimica et Biophysica Acta (BBA) - General Subjects*, *1840*(2), 809–817. https://doi.org/10.1016/J.BBAGEN.2013.03.020

Nordberg, A., Hellström-Lindahl, E., Lee, M., Johnson, M., Mousavi, M., Hall, R., Perry, E., Bednar, I., & Court, J. (2002). Chronic nicotine treatment reduces beta-amyloidosis in the brain of a mouse model of Alzheimer's disease (APPsw). *Journal of Neurochemistry*, *81*(3), 655–658. https://doi.org/10.1046/J.1471-4159.2002.00874.X

O'Brien, R. J., & Wong, P. C. (2011). Amyloid precursor protein processing and Alzheimer's disease. *Annual Review of Neuroscience*, *34*, 185–204. https://doi.org/10.1146/annurev-neuro-061010-113613

Oliveira, T. G., Chan, R. B., Tian, H., Laredo, M., Shui, G., Staniszewski, A., Zhang, H., Wang, L., Kim, T. W., Duff, K. E., Wenk, M. R., Arancio, O., & Di Paolo, G. (2010). Phospholipase D2 Ablation Ameliorates Alzheimer's Disease-Linked Synaptic Dysfunction and Cognitive Deficits. *The Journal of Neuroscience*, *30*(49), 16419. https://doi.org/10.1523/JNEUROSCI.3317-10.2010

Ortega, R. L., Dakterzada, F., Arias, A., Blasco, E., Naudí, A., Garcia, F. P., & Piñol-Ripoll, G. (2019). Usefulness of CSF Biomarkers in Predicting the Progression of Amnesic and Nonamnesic Mild Cognitive Impairment to Alzheimer's Disease. *Current Aging Science*, *12*(1), 35–42. https://doi.org/10.2174/1874609812666190112095430

Ossenkoppele, R., Smith, R., Mattsson-Carlgren, N., Groot, C., Leuzy, A., Strandberg, O., Palmqvist, S., Olsson, T., Jögi, J., Stormrud, E., Cho, H., Ryu, Y. H., Choi, J. Y., Boxer, A. L., Gorno-Tempini, M. L., Miller, B. L., Soleimani-Meigooni, D., Iaccarino, L., La Joie, R., … Hansson, O. (2021). Accuracy of Tau Positron Emission Tomography as a Prognostic Marker in Preclinical and Prodromal Alzheimer Disease: A Head-to-Head Comparison Against Amyloid Positron Emission Tomography and Magnetic Resonance Imaging. *JAMA*

Neurology, *78*(8), 961–971. https://doi.org/10.1001/JAMANEUROL.2021.1858

Oster, T., & Pillot, T. (2010). Docosahexaenoic acid and synaptic protection in Alzheimer's disease mice. *Biochimica et Biophysica Acta (BBA) - Molecular and Cell Biology of Lipids*, *1801*(8), 791–798. https://doi.org/10.1016/J.BBALIP.2010.02.011

Oulhaj, A., Jernerén, F., Refsum, H., Smith, A. D., & De Jager, C. A. (2016). Omega-3 Fatty Acid Status Enhances the Prevention of Cognitive Decline by B Vitamins in Mild Cognitive Impairment. *Journal of Alzheimer's Disease*, *50*(2), 547–557. https://doi.org/10.3233/JAD-150777

Owen, J. B., Sultana, R., Aluise, C. D., Erickson, M. A., Price, T. O., Bu, G., Banks, W. A., & Butterfield, D. A. (2010). Oxidative modification to LDL receptor-related protein 1 in hippocampus from subjects with Alzheimer disease: implications for Aβ accumulation in AD brain. *Free Radical Biology & Medicine*, *49*(11), 1798–1803. https://doi.org/10.1016/J.FREERADBIOMED.2010.09.013

Pamplona, R., Dalfó, E., Ayala, V., Bellmunt, M. J., Prat, J., Ferrer, I., & Portero-Otín, M. (2005). Proteins in human brain cortex are modified by oxidation, glycoxidation, and lipoxidation. Effects of Alzheimer disease and identification of lipoxidation targets. *The Journal of Biological Chemistry*, *280*(22), 21522–21530. https://doi.org/10.1074/JBC.M502255200

Paolo, G. Di, & Kim, T. (2012). Linking Lipids to Alzheimer ' s Disease : Cholesterol and Beyond. *Aging*, *12*(5), 284–296. https://doi.org/10.1038/nrn3012.Linking

Park, Y. S., Jang, H. J., Lee, K. H., Hahn, T. R., & Paik, Y. S. (2006). Prolyl Endopeptidase Inhibitory Activity of Unsaturated Fatty Acids. *Journal of Agricultural and Food Chemistry*, *54*(4), 1238–1242. https://doi.org/10.1021/JF052521H

Pelkmans, W., Vromen, E. M., Dicks, E., Scheltens, P., Teunissen, C. E., Barkhof, F., van der Flier, W. M., Tijms, B. M., & Alzheimer's Disease Neuroimaging Initiative. (2022). Grey matter network markers identify individuals with prodromal Alzheimer's disease who will show rapid clinical decline. *Brain Communications*, *4*(2), fcac026. https://doi.org/10.1093/braincomms/fcac026

Perluigi, M., Sultana, R., Cenini, G., Di Domenico, F., Memo, M., Pierce, W. M., Coccia, R., & Butterfield, D. A. (2009). Redox proteomics identification of 4-hydroxynonenal-modified brain proteins in Alzheimer's disease: Role of lipid peroxidation in Alzheimer's disease pathogenesis. *Proteomics. Clinical Applications*, *3*(6), 682. https://doi.org/10.1002/PRCA.200800161

Petersen, R. C. (2003). Mild cognitive impairment clinical trials. *Nature Reviews Drug Discovery 2003 2:8*, *2*(8), 646–653. https://doi.org/10.1038/nrd1155

Petersen, R. C., Smith, G. E., Waring, S. C., Ivnik, R. J., Tangalos, E. G., & Kokmen, E. (1999). Mild Cognitive Impairment: Clinical Characterization and Outcome. *Archives of Neurology*, *56*(3), 303–308. https://doi.org/10.1001/ARCHNEUR.56.3.303

Petrov, A. M., Kasimov, M. R., & Zefirov, A. L. (2016). Brain Cholesterol Metabolism and Its Defects: Linkage to Neurodegenerative Diseases and Synaptic Dysfunction. *Acta Naturae*, *8*(1), 58. https://doi.org/10.32607/20758251-2016-8-1-58-73

Pihlaja, R., Takkinen, J., Eskola, O., Vasara, J., López-Picón, F. R., Haaparanta-Solin, M., & Rinne, J. O. (2015). Monoacylglycerol lipase inhibitor JZL184 reduces neuroinflammatory response in APdE9 mice and in adult mouse glial cells. *Journal of Neuroinflammation*, *12*(1). https://doi.org/10.1186/S12974-015-0305-9

Pizarro, C., Arenzana-Rámila, I., Pérez-Del-Notario, N., Pérez-Matute, P., & González-Sáiz, J. M. (2013). Plasma lipidomic profiling method based on ultrasound extraction and liquid chromatography mass spectrometry. *Analytical Chemistry*, *85*(24), 12085–12092. https://doi.org/10.1021/AC403181C

Popp, J., Meichsner, S., Kölsch, H., Lewczuk, P., Maier, W., Kornhuber, J., Jessen, F., & Lütjohann, D. (2013). Cerebral and extracerebral cholesterol metabolism and CSF markers of Alzheimer's disease. *Biochemical Pharmacology*, *86*(1), 37–42. https://doi.org/10.1016/J.BCP.2012.12.007

Prasad, M. R., Lovell, M. A., Yatin, M., Dhillon, H., & Markesbery, W. R. (1998). Regional Membrane Phospholipid Alterations in Alzheimer's Disease. *Neurochemical Research 1998 23:1*, *23*(1), 81–88. https://doi.org/10.1023/A:1022457605436

Praticò, D., Clark, C. M., Liun, F., Lee, V. Y. M., & Trojanowski, J. Q. (2002). Increase of brain oxidative stress in mild cognitive impairment: a possible predictor of Alzheimer disease. *Archives of Neurology*, *59*(6), 972–976. https://doi.org/10.1001/ARCHNEUR.59.6.972

Proitsi, P., Kim, M., Whiley, L., Pritchard, M., Leung, R., Soininen, H., Kloszewska, I., Mecocci, P., Tsolaki, M., Vellas, B., Sham, P., Lovestone, S., Powell, J. F., Dobson, R. J. B., & Legido-Quigley, C. (2015). Plasma lipidomics analysis finds long chain cholesteryl esters to be associated with Alzheimer's disease. *Translational Psychiatry*, *5*(1), e494. https://doi.org/10.1038/TP.2014.127

Proitsi, P., Kim, M., Whiley, L., Simmons, A., Sattlecker, M., Velayudhan, L., Lupton, M. K., Soininen, H., Kloszewska, I., Mecocci, P., Tsolaki, M., Vellas, B., Lovestone, S., Powell, J. F., Dobson, R. J. B., & Legido-Quigley, C. (2017). Association of blood lipids with Alzheimer's disease: A comprehensive lipidomics analysis. *Alzheimer's & Dementia : The Journal of the Alzheimer's Association*, *13*(2), 140–151. https://doi.org/10.1016/J.JALZ.2016.08.003

Puglielli, L., Ellis, B. C., Saunders, A. J., & Kovacs, D. M. (2003). Ceramide stabilizes beta-site amyloid precursor protein-cleaving enzyme 1 and promotes amyloid beta-peptide biogenesis. *The Journal of Biological Chemistry*, *278*(22), 19777–19783. https://doi.org/10.1074/JBC.M300466200

Quinn, J. F., Raman, R., Thomas, R. G., Yurko-Mauro, K., Nelson, E. B., Van Dyck, C., Galvin, J. E., Emond, J., Jack, C. R., Weiner, M., Shinto, L., & Aisen, P. S. (2010). Docosahexaenoic acid supplementation and cognitive decline in Alzheimer disease: A randomized trial. *JAMA - Journal of the American Medical Association*, *304*(17), 1903–1911. https://doi.org/10.1001/jama.2010.1510

Rahman, A., Jackson, H., Hristov, H., Isaacson, R. S., Saif, N., Shetty, T., Etingin, O., Henchcliffe, C., Brinton, R. D., & Mosconi, L. (2019). Sex and Gender Driven Modifiers of Alzheimer's: The Role for Estrogenic Control Across Age, Race, Medical, and Lifestyle Risks. *Frontiers in Aging Neuroscience*, *11*. https://doi.org/10.3389/FNAGI.2019.00315

Ralhan, I., Chang, C. L., Lippincott-Schwartz, J., & Ioannou, M. S. (2021). Lipid droplets in the nervous system. *The Journal of Cell Biology*, *220*(7). https://doi.org/10.1083/JCB.202102136

Randez-Gil, F., Bojunga, L., Estruch, F., Winderickx, J., Del Poeta, M., & Prieto, J. A. (2020). Sphingolipids and Inositol Phosphates Regulate the Tau Protein Phosphorylation Status in Humanized Yeast. *Frontiers in Cell and Developmental Biology*, *8*. https://doi.org/10.3389/FCELL.2020.592159

Reisberg, B., Ferris, S. H., De Leon, M. J., & Crook, T. (1982). The Global Deterioration Scale for

assessment of primary degenerative dementia. *The American Journal of Psychiatry*, *139*(9), 1136–1139. https://doi.org/10.1176/AJP.139.9.1136

Reiss, A. B., Arain, H. A., Stecker, M. M., Siegart, N. M., & Kasselman, L. J. (2018). Amyloid toxicity in Alzheimer's disease. *Reviews in the Neurosciences*, *29*(6), 613–627. https://doi.org/10.1515/REVNEURO-2017-0063/XML

Riecan, M., Paluchova, V., Lopes, M., Brejchova, K., & Kuda, O. (2022). Branched and linear fatty acid esters of hydroxy fatty acids (FAHFA) relevant to human health. *Pharmacology & Therapeutics*, *231*, 107972. https://doi.org/10.1016/J.PHARMTHERA.2021.107972

Rodríguez-Rivera, C., Garcia, M. M., Molina-Álvarez, M., González-Martín, C., & Goicoechea, C. (2021). Clusterin: Always protecting. Synthesis, function and potential issues. *Biomedicine & Pharmacotherapy*, *134*, 111174. https://doi.org/10.1016/J.BIOPHA.2020.111174

Sáez-Orellana, F., Octave, J. N., & Pierrot, N. (2020). Alzheimer's Disease, a Lipid Story: Involvement of Peroxisome Proliferator-Activated Receptor α. *Cells 2020, Vol. 9, Page 1215*, *9*(5), 1215. https://doi.org/10.3390/CELLS9051215

Sagrario, M., Palomo, M., Anaya Caravaca, B., Angeles Balsa Bretón, M., Castrillo, S. M., De La, A., Vicente, M., Arce, E. C., & Alves Pérez, M. T. (2019). Mild Cognitive Impairment with a High Risk of Progression to Alzheimer's Disease Dementia (MCI-HR-AD): Effect of Souvenaid ® Treatment on Cognition and 18F-FDG PET Scans. *Journal of Alzheimer's Disease Reports*, *3*(1), 95–102. https://doi.org/10.3233/ADR-190109

Sahlin, C., Pettersson, F. E., Nilsson, L. N. G., Lannfelt, L., & Johansson, A. S. (2007). Docosahexaenoic acid stimulates non-amyloidogenic APP processing resulting in reduced Aβ levels in cellular models of Alzheimer's disease. *European Journal of Neuroscience*, *26*(4), 882–889. https://doi.org/10.1111/J.1460-9568.2007.05719.X

Sáiz-Vazquez, O., Puente-Martínez, A., Ubillos-Landa, S., Pacheco-Bonrostro, J., & Santabárbara, J. (2020). Cholesterol and Alzheimer's Disease Risk: A Meta-Meta-Analysis. *Brain Sciences 2020, Vol. 10, Page 386*, *10*(6), 386. https://doi.org/10.3390/BRAINSCI10060386

Sakurai, K., Shen, C., Shiraishi, I., Inamura, N., & Hisatsune, T. (2021). Consumption of Oleic Acid on the Preservation of Cognitive Functions in Japanese Elderly Individuals. *Nutrients*, *13*(2), 1–10. https://doi.org/10.3390/NU13020284

Sánchez-Campillo, M., Ruiz-Pastor, M. J., Gázquez, A., Marín-Muñoz, J., Noguera-Perea, F., Ruiz-Alcaraz, A. J., Manzanares-Sánchez, S., Antúnez, C., & Larqué, E. (2020). Decreased Blood Level of MFSD2a as a Potential Biomarker of Alzheimer's Disease. *International Journal of Molecular Sciences*, *21*(1). https://doi.org/10.3390/IJMS21010070

Sankowski, R., Mader, S., & Valdés-Ferrer, S. I. (2015). Systemic Inflammation and the Brain: Novel Roles of Genetic, Molecular, and Environmental Cues as Drivers of Neurodegeneration. *Frontiers in Cellular Neuroscience*, *9*(FEB). https://doi.org/10.3389/FNCEL.2015.00028

Santamarina, A. B., Pisani, L. P., Baker, E. J., Marat, A. D., Valenzuela, C. A., Miles, E. A., & Calder, P. C. (2021). Anti-inflammatory effects of oleic acid and the anthocyanin keracyanin alone and in combination: effects on monocyte and macrophage responses and the NF-κB pathway. *Food & Function*, *12*(17), 7909–7922. https://doi.org/10.1039/D1FO01304A

Satoi, H., Tomimoto, H., Ohtani, R., Kitano, T., Kondo, T., Watanabe, M., Oka, N., Akiguchi, I., Furuya, S., Hirabayashi, Y., & Okazaki, T. (2005). Astroglial expression of ceramide in Alzheimer's disease brains: a role during neuronal apoptosis. *Neuroscience*, *130*(3), 657–

666. https://doi.org/10.1016/J.NEUROSCIENCE.2004.08.056

Savica, R., Murray, M. E., Persson, X. M., Kantarci, K., Parisi, J. E., Dickson, D. W., Petersen, R. C., Ferman, T. J., Boeve, B. F., & Mielke, M. M. (2016). Plasma sphingolipid changes with autopsy-confirmed Lewy body or Alzheimer's pathology. *Alzheimer's & Dementia : Diagnosis, Assessment & Disease Monitoring*, *3*, 43. https://doi.org/10.1016/J.DADM.2016.02.005

Schaefer, E. J., Bongard, V., Beiser, A. S., Lamon-Fava, S., Robins, S. J., Au, R., Tucker, K. L., Kyle, D. J., Wilson, P. W. F., & Wolf, P. A. (2006). Plasma phosphatidylcholine docosahexaenoic acid content and risk of dementia and Alzheimer disease: the Framingham Heart Study. *Archives of Neurology*, *63*(11), 1545–1550. https://doi.org/10.1001/ARCHNEUR.63.11.1545

Schmidt, C., Wolff, M., Weitz, M., Bartlau, T., Korth, C., & Zerr, I. (2011). Rapidly Progressive Alzheimer Disease. *Archives of Neurology*, *68*(9), 1124–1130. https://doi.org/10.1001/ARCHNEUROL.2011.189

Schrag, M., Mueller, C., Zabel, M., Crofton, A., Kirsch, W. M., Ghribi, O., Squitti, R., & Perry, G. (2013). Oxidative stress in blood in Alzheimer's disease and mild cognitive impairment: a meta-analysis. *Neurobiology of Disease*, *59*, 100–110. https://doi.org/10.1016/J.NBD.2013.07.005

Schuessel, K., Leutner, S., Cairns, N. J., Müller, W. E., & Eckert, A. (2004). Impact of gender on upregulation of antioxidant defence mechanisms in Alzheimer's disease brain. *Journal of Neural Transmission (Vienna, Austria : 1996)*, *111*(9), 1167–1182. https://doi.org/10.1007/S00702-004-0156-5

Selkoe, D. J., & Hardy, J. (2016). The amyloid hypothesis of Alzheimer's disease at 25 years. *EMBO Molecular Medicine*, *8*(6), 595–608. https://doi.org/10.15252/emmm.201606210

Selley, M. L., Close, D. R., & Stern, S. E. (2002). The effect of increased concentrations of homocysteine on the concentration of (E)-4-hydroxy-2-nonenal in the plasma and cerebrospinal fluid of patients with Alzheimer's disease. *Neurobiology of Aging*, *23*(3), 383–388. https://doi.org/10.1016/S0197-4580(01)00327-X

Sengupta, U., Nilson, A. N., & Kayed, R. (2016). The Role of Amyloid-β Oligomers in Toxicity, Propagation, and Immunotherapy. *EBioMedicine*, *6*, 42–49. https://doi.org/10.1016/J.EBIOM.2016.03.035

Serini, S., Bizzarro, A., Piccioni, E., Fasano, E., Rossi, C., Lauria, A., R.M. Cittadini, A., Masullo, C., & Calviello, G. (2012). EPA and DHA differentially affect in vitro inflammatory cytokine release by peripheral blood mononuclear cells from Alzheimer's patients. *Current Alzheimer Research*, *9*(8), 913–923. https://doi.org/10.2174/156720512803251147

Serrano-Pozo, A., Das, S., & Hyman, B. T. (2021). APOE and Alzheimer's disease: advances in genetics, pathophysiology, and therapeutic approaches. *The Lancet. Neurology*, *20*(1), 68–80. https://doi.org/10.1016/S1474-4422(20)30412-9

Sharma, A., Weber, D., Raupbach, J., Dakal, T. C., Fließbach, K., Ramirez, A., Grune, T., & Wüllner, U. (2020). Advanced glycation end products and protein carbonyl levels in plasma reveal sex-specific differences in Parkinson's and Alzheimer's disease. *Redox Biology*, *34*. https://doi.org/10.1016/J.REDOX.2020.101546

Shih, Y. H., Wu, S. Y., Yu, M., Huang, S. H., Lee, C. W., Jiang, M. J., Lin, P. Y., Yang, T. T., & Kuo, Y. M. (2018). Hypertension accelerates Alzheimer's disease-related pathologies in pigs and

3xTg mice. *Frontiers in Aging Neuroscience*, *10*(MAR), 73. https://doi.org/10.3389/FNAGI.2018.00073/BIBTEX

Silva, Y. P., Bernardi, A., & Frozza, R. L. (2020). The Role of Short-Chain Fatty Acids From Gut Microbiota in Gut-Brain Communication. *Frontiers in Endocrinology*, *11*, 25. https://doi.org/10.3389/FENDO.2020.00025/BIBTEX

Smailovic, U., & Jelic, V. (2019). Neurophysiological Markers of Alzheimer's Disease: Quantitative EEG Approach. *Neurology and Therapy 2019 8:2*, *8*(2), 37–55. https://doi.org/10.1007/S40120-019-00169-0

Snowden, S. G., Ebshiana, A. A., Hye, A., An, Y., Pletnikova, O., O'Brien, R., Troncoso, J., Legido-Quigley, C., & Thambisetty, M. (2017). Association between fatty acid metabolism in the brain and Alzheimer disease neuropathology and cognitive performance: A nontargeted metabolomic study. *PLoS Medicine*, *14*(3). https://doi.org/10.1371/JOURNAL.PMED.1002266

Solomon, A., Kivipelto, M., Wolozin, B., Zhou, J., & Whitmer, R. A. (2009). Midlife serum cholesterol and increased risk of Alzheimer's and vascular dementia three decades later. *Dementia and Geriatric Cognitive Disorders*, *28*(1), 75–80. https://doi.org/10.1159/000231980

Sommer, I., Griebler, U., Kien, C., Auer, S., Klerings, I., Hammer, R., Holzer, P., & Gartlehner, G. (2017). Vitamin D deficiency as a risk factor for dementia: a systematic review and meta-analysis. *BMC Geriatrics*, *17*(1), 1–13. https://doi.org/10.1186/S12877-016-0405-0

Soto-Faguás, C. M., Sanchez-Molina, P., & Saura, C. A. (2021). Loss of presenilin function enhances tau phosphorylation and aggregation in mice. *Acta Neuropathologica Communications*, *9*(1), 1–20. https://doi.org/10.1186/S40478-021-01259-7/FIGURES/10

Sperling, R. A., Aisen, P. S., Beckett, L. A., Bennett, D. A., Craft, S., Fagan, A. M., Iwatsubo, T., Jack, C. R., Kaye, J., Montine, T. J., Park, D. C., Reiman, E. M., Rowe, C. C., Siemers, E., Stern, Y., Yaffe, K., Carrillo, M. C., Thies, B., Morrison-Bogorad, M., … Phelps, C. H. (2011). Toward defining the preclinical stages of Alzheimer's disease: Recommendations from the National Institute on Aging-Alzheimer's Association workgroups on diagnostic guidelines for Alzheimer's disease. *Alzheimer's & Dementia : The Journal of the Alzheimer's Association*, *7*(3), 280. https://doi.org/10.1016/J.JALZ.2011.03.003

Stelzmann, R. A., Norman Schnitzlein, H., & Reed Murtagh, F. (1995). An English translation of Alzheimer's 1907 paper, "Uber eine eigenartige Erkankung der Hirnrinde." *Clinical Anatomy (New York, N.Y.)*, *8*(6), 429–431. https://doi.org/10.1002/CA.980080612

Stough, C., Pipingas, A., Camfield, D., Nolidin, K., Savage, K., Deleuil, S., & Scholey, A. (2019). Increases in total cholesterol and low density lipoprotein associated with decreased cognitive performance in healthy elderly adults. *Metabolic Brain Disease*, *34*(2), 477–484. https://doi.org/10.1007/S11011-018-0373-5

Su, X. Q., Wang, J., & Sinclair, A. J. (2019). Plasmalogens and Alzheimer's disease: A review. *Lipids in Health and Disease*, *18*(1), 1–10. https://doi.org/10.1186/S12944-019-1044-1/FIGURES/3

Sultan, A., Nesslany, F., Violet, M., Bégard, S., Loyens, A., Talahari, S., Mansuroglu, Z., Marzin, D., Sergeant, N., Humez, S., Colin, M., Bonnefoy, E., Buée, L., & Galas, M. C. (2011). Nuclear tau, a key player in neuronal DNA protection. *The Journal of Biological Chemistry*, *286*(6), 4566–4575. https://doi.org/10.1074/JBC.M110.199976

Tajima, Y., Ishikawa, M., Maekawa, K., Murayama, M., Senoo, Y., Nishimaki-Mogami, T., Nakanishi, H., Ikeda, K., Arita, M., Taguchi, R., Okuno, A., Mikawa, R., Niida, S., Takikawa, O., & Saito, Y. (2013). Lipidomic analysis of brain tissues and plasma in a mouse model expressing mutated human amyloid precursor protein/tau for Alzheimer's disease. *Lipids in Health and Disease*, *12*(1), 68. https://doi.org/10.1186/1476-511X-12-68

Takasugi, N., Sasaki, T., Shinohara, M., Iwatsubo, T., & Tomita, T. (2015). Synthetic ceramide analogues increase amyloid-β 42 production by modulating γ-secretase activity. *Biochemical and Biophysical Research Communications*, *457*(2), 194–199. https://doi.org/10.1016/J.BBRC.2014.12.087

Tan, M. S., Yu, J. T., & Tan, L. (2013). Bridging integrator 1 (BIN1): form, function, and Alzheimer's disease. *Trends in Molecular Medicine*, *19*(10), 594–603. https://doi.org/10.1016/J.MOLMED.2013.06.004

Tang, Q., Wang, F., Yang, J., Peng, H., Li, Y., Li, B., & Wang, S. (2020). Revealing a Novel Landscape of the Association Between Blood Lipid Levels and Alzheimer's Disease: A Meta-Analysis of a Case-Control Study. *Frontiers in Aging Neuroscience*, *11*, 370. https://doi.org/10.3389/FNAGI.2019.00370/BIBTEX

Tanguy, E., Wang, Q., Moine, H., & Vitale, N. (2019). Phosphatidic Acid: From Pleiotropic Functions to Neuronal Pathology. *Frontiers in Cellular Neuroscience*, *13*. https://doi.org/10.3389/FNCEL.2019.00002

Targa, A. D. S., Benítez, I. D., Dakterzada, F., Carnes, A., Pujol, M., Jorge, C., Minguez, O., Dalmases, M., Sánchez-De-La-Torre, M., Barbé, F., & Piñol-Ripoll, G. (2021). Sleep profile predicts the cognitive decline of mild-moderate Alzheimer's disease patients. *Sleep*, *44*(10). https://doi.org/10.1093/SLEEP/ZSAB117

Tayler, H., Fraser, T., Miners, J. S., Kehoe, P. G., & Love, S. (2010). Oxidative balance in Alzheimer's disease: relationship to APOE, Braak tangle stage, and the concentrations of soluble and insoluble amyloid-β. *Journal of Alzheimer's Disease : JAD*, *22*(4), 1363–1373. https://doi.org/10.3233/JAD-2010-101368

Taylor, M. K., Sullivan, D. K., Swerdlow, R. H., Vidoni, E. D., Morris, J. K., Mahnken, J. D., & Burns, J. M. (2017). A high-glycemic diet is associated with cerebral amyloid burden in cognitively normal older adults. *The American Journal of Clinical Nutrition*, *106*(6), 1463–1470. https://doi.org/10.3945/AJCN.117.162263

Tchalla, A. E., Clément, J. P., Saulnier, I., Beaumatin, B., Lachal, F., Gayot, C., Bosetti, A., Desormais, I., Perrochon, A., Preux, P. M., Couratier, P., & Dantoine, T. (2018). Predictors of Rapid Cognitive Decline in Patients with Mild-to-Moderate Alzheimer Disease: A Prospective Cohort Study with 12-Month Follow-Up Performed in Memory Clinics. *Dementia and Geriatric Cognitive Disorders*, *45*(1), 56–65. https://doi.org/10.1159/000487938

Tebar, F., Bohlander, S. K., & Sorkin, A. (1999). Clathrin Assembly Lymphoid Myeloid Leukemia (CALM) Protein: Localization in Endocytic-coated Pits, Interactions with Clathrin, and the Impact of Overexpression on Clathrin-mediated Traffic. *Molecular Biology of the Cell*, *10*(8), 2687. https://doi.org/10.1091/MBC.10.8.2687

Teitsdottir, U. D., Halldorsson, S., Rolfsson, O., Lund, S. H., Jonsdottir, M. K., Snaedal, J., & Petersen, P. H. (2021). Cerebrospinal Fluid C18 Ceramide Associates with Markers of Alzheimer's Disease and Inflammation at the Pre- and Early Stages of Dementia. *Journal of Alzheimer's Disease*, *81*(1), 231–244. https://doi.org/10.3233/JAD-200964

Terés, S., Barceló-Coblijn, G., Benet, M., Álvarez, R., Bressani, R., Halver, J. E., & Escribá, P. V. (2008). Oleic acid content is responsible for the reduction in blood pressure induced by olive oil. *Proceedings of the National Academy of Sciences of the United States of America*, *105*(37), 13811–13816. https://doi.org/10.1073/PNAS.0807500105

Tobin, M. K., Musaraca, K., Disouky, A., Shetti, A., Bheri, A., Honer, W. G., Kim, N., Dawe, R. J., Bennett, D. A., Arfanakis, K., & Lazarov, O. (2019). Human hippocampal neurogenesis persists in aged adults and Alzheimer's disease patients. *Cell Stem Cell*, *24*(6), 974. https://doi.org/10.1016/J.STEM.2019.05.003

Toledo, J. B., Arnold, M., Kastenmüller, G., Chang, R., Baillie, R. A., Han, X., Thambisetty, M., Tenenbaum, J. D., Suhre, K., Thompson, J. W., John-Williams, L. S., MahmoudianDehkordi, S., Rotroff, D. M., Jack, J. R., Motsinger-Reif, A., Risacher, S. L., Blach, C., Lucas, J. E., Massaro, T., … Kaddurah-Daouk, R. (2017). Metabolic network failures in Alzheimer's disease: A biochemical road map. *Alzheimer's and Dementia*, *13*(9), 965–984. https://doi.org/10.1016/j.jalz.2017.01.020

Tönnies, E., & Trushina, E. (2017). Oxidative Stress, Synaptic Dysfunction, and Alzheimer's Disease. *Journal of Alzheimer's Disease*, *57*(4), 1105–1121. https://doi.org/10.3233/JAD-161088

Topiwala, A., Allan, C. L., Valkanova, V., Zsoldos, E., Filippini, N., Sexton, C., Mahmood, A., Fooks, P., Singh-Manoux, A., Mackay, C. E., Kivimäki, M., & Ebmeier, K. P. (2017). Moderate alcohol consumption as risk factor for adverse brain outcomes and cognitive decline: longitudinal cohort study. *BMJ*, *357*(16), 1190–1192. https://doi.org/10.1136/BMJ.J2353

Trajkovic, K., Hsu, C., Chiantia, S., Rajendran, L., Wenzel, D., Wieland, F., Schwille, P., Brügger, B., & Simons, M. (2008). Ceramide triggers budding of exosome vesicles into multivesicular endosomes. *Science (New York, N.Y.)*, *319*(5867), 1244–1247. https://doi.org/10.1126/SCIENCE.1153124

Tucsek, Z., Noa Valcarcel-Ares, M., Tarantini, S., Yabluchanskiy, A., Fülöp, G., Gautam, T., Orock, A., Csiszar, A., Deak, F., & Ungvari, Z. (2017). Hypertension-induced synapse loss and impairment in synaptic plasticity in the mouse hippocampus mimics the aging phenotype: implications for the pathogenesis of vascular cognitive impairment. *GeroScience*, *39*(4), 385–406. https://doi.org/10.1007/S11357-017-9981-Y

Ungvari, Z., Toth, P., Tarantini, S., Prodan, C. I., Sorond, F., Merkely, B., & Csiszar, A. (2021). Hypertension-induced cognitive impairment: from pathophysiology to public health. *Nature Reviews. Nephrology*, *17*(10), 639–654. https://doi.org/10.1038/S41581-021-00430-6

Valls-Pedret, C., Sala-Vila, A., Serra-Mir, M., Corella, D., De La Torre, R., Martínez-González, M. Á., Martínez-Lapiscina, E. H., Fitó, M., Pérez-Heras, A., Salas-Salvadó, J., Estruch, R., & Ros, E. (2015). Mediterranean Diet and Age-Related Cognitive Decline: A Randomized Clinical Trial. *JAMA Internal Medicine*, *175*(7), 1094–1103. https://doi.org/10.1001/JAMAINTERNMED.2015.1668

Van Den Brink, A. C., Brouwer-Brolsma, E. M., Berendsen, A. A. M., & Van De Rest, O. (2019). The Mediterranean, Dietary Approaches to Stop Hypertension (DASH), and Mediterranean-DASH Intervention for Neurodegenerative Delay (MIND) Diets Are Associated with Less Cognitive Decline and a Lower Risk of Alzheimer's Disease—A Review. *Advances in Nutrition*, *10*(6), 1040. https://doi.org/10.1093/ADVANCES/NMZ054

van der Kant, R., Goldstein, L. S. B., & Ossenkoppele, R. (2019). Amyloid-β-independent regulators of tau pathology in Alzheimer disease. *Nature Reviews Neuroscience 2019 21:1*,

21(1), 21–35. https://doi.org/10.1038/s41583-019-0240-3

van der Kant, R., Langness, V. F., Herrera, C. M., Williams, D. A., Fong, L. K., Leestemaker, Y., Steenvoorden, E., Rynearson, K. D., Brouwers, J. F., Helms, J. B., Ovaa, H., Giera, M., Wagner, S. L., Bang, A. G., & Goldstein, L. S. B. (2019). Cholesterol Metabolism Is a Druggable Axis that Independently Regulates Tau and Amyloid-β in iPSC-Derived Alzheimer's Disease Neurons. *Cell Stem Cell*, *24*(3), 363-375.e9. https://doi.org/10.1016/J.STEM.2018.12.013

Van Rossum, I. A., Visser, P. J., Knol, D. L., Van Der Flier, W. M., Teunissen, C. E., Barkhof, F., Blankenstein, M. A., & Scheltens, P. (2012). Injury markers but not amyloid markers are associated with rapid progression from mild cognitive impairment to dementia in Alzheimer's disease. *Journal of Alzheimer's Disease : JAD*, *29*(2), 319–327. https://doi.org/10.3233/JAD-2011-111694

Van Rossum, I. A., Vos, S. J. B., Burns, L., Knol, D. L., Scheltens, P., Soininen, H., Wahlund, L. O., Hampel, H., Tsolaki, M., Minthon, L., L'Italien, G., Van Der Flier, W. M., Teunissen, C. E., Blennow, K., Barkhof, F., Rueckert, D., Wolz, R., Verhey, F., & Visser, P. J. (2012). Injury markers predict time to dementia in subjects with MCI and amyloid pathology. *Neurology*, *79*(17), 1809–1816. https://doi.org/10.1212/WNL.0b013e3182704056

Varma, V. R., Oommen, A. M., Varma, S., Casanova, R., An, Y., Andrews, R. M., O'Brien, R., Pletnikova, O., Troncoso, J. C., Toledo, J., Baillie, R., Arnold, M., Kastenmueller, G., Nho, K., Doraiswamy, P. M., Saykin, A. J., Kaddurah-Daouk, R., Legido-Quigley, C., & Thambisetty, M. (2018). Brain and blood metabolite signatures of pathology and progression in Alzheimer disease: A targeted metabolomics study. *PLoS Medicine*, *15*(1). https://doi.org/10.1371/JOURNAL.PMED.1002482

Vedin, I., Cederholm, T., Levi, Y. F., Basun, H., Garlind, A., Irving, G. F., Jönhagen, M. E., Vessby, B., Wahlund, L. O., & Palmblad, J. (2008). Effects of docosahexaenoic acid-rich n-3 fatty acid supplementation on cytokine release from blood mononuclear leukocytes: the OmegAD study. *The American Journal of Clinical Nutrition*, *87*(6), 1616–1622. https://doi.org/10.1093/AJCN/87.6.1616

Viña, J., Viña, V., & Lloret, A. (2010). Why Women Have More Alzheimer's Disease Than Men: Gender and Mitochondrial Toxicity of Amyloid-β Peptide. *Journal of Alzheimer's Disease*, *20*, 527–533. https://doi.org/10.3233/JAD-2010-100501

Violet, M., Delattre, L., Tardivel, M., Sultan, A., Chauderlier, A., Caillierez, R., Talahari, S., Nesslany, F., Lefebvre, B., Bonnefoy, E., Buée, L., & Galas, M. C. (2014). A major role for Tau in neuronal DNA and RNA protection in vivo under physiological and hyperthermic conditions. *Frontiers in Cellular Neuroscience*, *8*(MAR). https://doi.org/10.3389/FNCEL.2014.00084

Wang, D. C., Sun, C. H., Liu, L. Y., Sun, X. H., Jin, X. W., Song, W. L., Liu, X. Q., & Wan, X. L. (2012). Serum fatty acid profiles using GC-MS and multivariate statistical analysis: potential biomarkers of Alzheimer's disease. *Neurobiology of Aging*, *33*(6), 1057–1066. https://doi.org/10.1016/J.NEUROBIOLAGING.2010.09.013

Wang, D., Chen, F., Han, Z., Yin, Z., Ge, X., & Lei, P. (2021). Relationship Between Amyloid-β Deposition and Blood–Brain Barrier Dysfunction in Alzheimer's Disease. *Frontiers in Cellular Neuroscience*, *15*, 271. https://doi.org/10.3389/FNCEL.2021.695479/BIBTEX

Wang, W., Zhao, F., Ma, X., Perry, G., & Zhu, X. (2020). Mitochondria dysfunction in the pathogenesis of Alzheimer's disease: recent advances. *Molecular Neurodegeneration 2020 15:1*, *15*(1), 1–22. https://doi.org/10.1186/S13024-020-00376-6

Wang, Y., & Mandelkow, E. (2016). Tau in physiology and pathology. In *Nature Reviews Neuroscience* (Vol. 17, Issue 1, pp. 5–21). Nature Publishing Group. https://doi.org/10.1038/nrn.2015.1

Wang, Z. X., Tan, L., Liu, J., & Yu, J. T. (2016). The Essential Role of Soluble Aβ Oligomers in Alzheimer's Disease. *Molecular Neurobiology*, *53*(3), 1905–1924. https://doi.org/10.1007/S12035-015-9143-0

Wattenberg, B. W. (2018). The long and the short of ceramides. *Journal of Biological Chemistry*, *293*(25), 9922–9923. https://doi.org/10.1074/JBC.H118.003522

Willemse, E. A. J., Sieben, A., Somers, C., Vermeiren, Y., De Roeck, N., Timmers, M., Van Broeckhoven, C., De Vil, B., Cras, P., De Deyn, P. P., Martin, J. J., Teunissen, C. E., Engelborghs, S., & Bjerke, M. (2021). Neurogranin as biomarker in CSF is non-specific to Alzheimer's disease dementia. *Neurobiology of Aging*, *108*, 99–109. https://doi.org/10.1016/J.NEUROBIOLAGING.2021.08.002

Wisniewski, H. M., & Silverman, W. (1997). Diagnostic criteria for the neuropathological assessment of Alzheimer's disease: Current status and major issues. *Neurobiology of Aging*, *18*(4 SUPPL.). https://doi.org/10.1016/S0197-4580(97)00068-7

Wong, M. W., Braidy, N., Poljak, A., Pickford, R., Thambisetty, M., & Sachdev, P. S. (2017). Dysregulation of lipids in Alzheimer's disease and their role as potential biomarkers. *Alzheimer's & Dementia : The Journal of the Alzheimer's Association*, *13*(7), 810–827. https://doi.org/10.1016/J.JALZ.2017.01.008

Wood, P. L., Barnette, B. L., Kaye, J. A., Quinn, J. F., & Woltjer, R. L. (2015). Non-targeted lipidomics of CSF and frontal cortex grey and white matter in control, mild cognitive impairment, and Alzheimer's disease subjects. *Acta Neuropsychiatrica*, *27*(5), 270–278. https://doi.org/10.1017/NEU.2015.18

Wood, P. L., Mankidy, R., Ritchie, S., Heath, D., Wood, J. A., Flax, J., & Goodenowe, D. B. (2010). Circulating plasmalogen levels and Alzheimer Disease Assessment Scale–Cognitive scores in Alzheimer patients. *Journal of Psychiatry & Neuroscience : JPN*, *35*(1), 59. https://doi.org/10.1503/JPN.090059

Wu, Y., Wang, Z., Jia, X., Zhang, H., Zhang, H., Li, J., & Zhang, K. (2019). Prediction of Alzheimer's disease with serum lipid levels in Asian individuals: a meta-analysis. *Biomarkers : Biochemical Indicators of Exposure, Response, and Susceptibility to Chemicals*, *24*(4), 341–351. https://doi.org/10.1080/1354750X.2019.1571633

Xin, S. H., Tan, L., Cao, X., Yu, J. T., & Tan, L. (2018). Clearance of Amyloid Beta and Tau in Alzheimer's Disease: from Mechanisms to Therapy. *Neurotoxicity Research 2018 34:3*, *34*(3), 733–748. https://doi.org/10.1007/S12640-018-9895-1

Yang, D. S., Stavrides, P., Saito, M., Kumar, A., Rodriguez-Navarro, J. A., Pawlik, M., Huo, C., Walkley, S. U., Saito, M., Cuervo, A. M., & Nixon, R. A. (2014). Defective macroautophagic turnover of brain lipids in the TgCRND8Alzheimer mouse model: prevention by correcting lysosomal proteolyticdeficits. *Brain*, *137*(12), 3300. https://doi.org/10.1093/BRAIN/AWU278

Young, P. N. E., Estarellas, M., Coomans, E., Srikrishna, M., Beaumont, H., Maass, A., Venkataraman, A. V., Lissaman, R., Jiménez, D., Betts, M. J., McGlinchey, E., Berron, D., O'Connor, A., Fox, N. C., Pereira, J. B., Jagust, W., Carter, S. F., Paterson, R. W., & Schöll, M. (2020). Imaging biomarkers in neurodegeneration: Current and future practices. *Alzheimer's Research and Therapy*, *12*(1), 1–17. https://doi.org/10.1186/S13195-020-

00612-7/FIGURES/4

Zabel, M., Nackenoff, A., Kirsch, W. M., Harrison, F. E., Perry, G., & Schrag, M. (2018). Markers of oxidative damage to lipids, nucleic acids and proteins and antioxidant enzymes activities in Alzheimer's disease brain: A meta-analysis in human pathological specimens. *Free Radical Biology & Medicine*, *115*, 351–360. https://doi.org/10.1016/J.FREERADBIOMED.2017.12.016

Zarrouk, A., Riedinger, J. M., Ahmed, S. H., Hammami, S., Chaabane, W., Debbabi, M., Ben Ammou, S., Rouaud, O., Frih, M., Lizard, G., & Hammami, M. (2015). Fatty acid profiles in demented patients: identification of hexacosanoic acid (C26:0) as a blood lipid biomarker of dementia. *Journal of Alzheimer's Disease : JAD*, *44*(4), 1349–1359. https://doi.org/10.3233/JAD-142046

Zhang, J., & Chen, C. (2018). Alleviation of neuropathology by inhibition of monoacylglycerol lipase in APP transgenic mice lacking CB2 receptors. *Molecular Neurobiology*, *55*(6), 4802. https://doi.org/10.1007/S12035-017-0689-X

Zhang, Y. P., Miao, R., Li, Q., Wu, T., & Ma, F. (2017). Effects of DHA Supplementation on Hippocampal Volume and Cognitive Function in Older Adults with Mild Cognitive Impairment: A 12-Month Randomized, Double-Blind, Placebo-Controlled Trial. *Journal of Alzheimer's Disease*, *55*(2), 497–507. https://doi.org/10.3233/JAD-160439

Zhou, Z., Liang, Y., Zhang, X., Xu, J., Lin, J., Zhang, R., Kang, K., Liu, C., Zhao, C., & Zhao, M. (2020). Low-Density Lipoprotein Cholesterol and Alzheimer's Disease: A Systematic Review and Meta-Analysis. *Frontiers in Aging Neuroscience*, *12*. https://doi.org/10.3389/FNAGI.2020.00005

Zhu, Y. B., Gao, W., Zhang, Y., Jia, F., Zhang, H. L., Liu, Y. Z., Sun, X. F., Yin, Y., & Yin, D. M. (2016). Astrocyte-derived phosphatidic acid promotes dendritic branching. *Scientific Reports 2016 6:1*, *6*(1), 1–13. https://doi.org/10.1038/srep21096

Zhu, Y., Liu, X., Zhu, R., Zhao, J., & Wang, Q. (2022). Lipid levels and the risk of dementia: A dose–response meta-analysis of prospective cohort studies. *Annals of Clinical and Translational Neurology*, *9*(3), 296–311. https://doi.org/10.1002/ACN3.51516

Züllig, T., Trötzmüller, M., & Köfeler, H. C. (2020). Lipidomics from sample preparation to data analysis: a primer. *Analytical and Bioanalytical Chemistry*, *412*(10), 2191–2209. https://doi.org/10.1007/S00216-019-02241-Y/FIGURES/4

SUPPLEMENTARY MATERIALS

Supplementary materials

Supplementary Table 1. List of chemical products used in this study.

Name	Company	Reference
1-hexanol	Sigma-Aldrich	H13303
3-(N-morpholino)propanesulfonic acid	Sigma-Aldrich	M1254
Acetone	Honeywell	32201
Acetonitrile	Sigma-Aldrich	900667
Acetyl chloride	Sigma-Aldrich	990
Ammonium acetate	Sigma-Aldrich	73594
Butylated hydroxytoluene (BHT)	Sigma-Aldrich	W218405
Carbon disulfide	Sigma-Aldrich	270660
Chloroform	Honeywell-Riedel de Haën	34854
Dichloromethane	Sigma-Aldrich	650463
Diethylenetriaminepentaacetic acid	Sigma-Aldrich	32319
Ethylenediaminetetraacetic acid (EDTA)	Sigma-Aldrich	E9884
Hidrochloric acid	Chem-Lab	CL00.0360.1000
Isopropanol	Sigma-Aldrich	34863
Methanol	Honeywell-Riedel de Haën	34860
Methyl tert-butyl ether	Sigma-Aldrich	1.01995
Nuclease free water	Invitrogen	AM9930
Pentane	Honeywell-Riedel de Haën	34956
Potassium chloride	Honeywell-Fluka	31248
Sodium borhydride	Sigma-Aldrich	632287
Sodium chloride	Honeywell-Fluka	S9625
Sodium Hydroxide	Chem-Lab	CL00.1404.0250
Sodium tetraborate decahydrate	Sigma-Aldrich	S9640
Trichloroacetic acid	Sigma-Aldrich	T6399
Trifluoroacetic anhydre	Sigma-Aldrich	106232

Supplementary Table 2. Association of CSF FA, FA related indexes, and oxidative protein damage markers with diagnosis of MCI and AD versus control.

	AD (N = 83)	MCI (N = 92)	CTL (N = 23)	*p**
C14:0[$]	3.11 [2.6;3.7]	3.12 [2.6;3.6]	3.16 [2.5;3.6]	0.135
C16:0[$]	25.86 [24;30]	27.12 [24;31]	23.5 [22;29]	0.497
C16:1 (n-7)[$]	3.44 [2.6;4.1]	2.79 [2.4;3.9]	3.67 [2.6;4.1]	0.445
C18:0[$]	11.06 [9.9;12.7]	11.29 [10.2;13.1]	9.95 [9.2;11.9]	0.709
C18:1 (n-9)[$]	17.65 [14.2;20.1]	17.86 [15;19.7]	18.04 [15.6;19.7]	0.387
C18:1 (n-7)[$]	16.63 [14.1;18.7]	16.02 [14.4;17.8]	16.46 [15.5;17.9]	0.861
18:2 (n-6)[$]	5.71 [4.7;6.8]	5.49 [4.4;6.5]	6.07 [4.1;8.7]	0.832
18:3 (n-3)[$]	1.43 [0.6;2.1]	1.16 [0.6;2.3]	0.84 [0.6;1.9]	0.106
C20:0[$]	0.89 [0.8;1.1]	1.02 [0.8;1.1]	0.86 [0.7;1.2]	0.505
C20:1 (n-9)[$]	1.01 [40.9;1.2]	1.08 [0.8;1.1]	1 [0.7;1.2]	0.252
C20:2 (n-6)[$]	0.59 [0.5;0.7]	0.6 [0.5;0.7]	0.65 [0.5;0.7]	0.281
C20:3 (n-6)[$]	0.43 [0.4;0.5]	0.43 [0.3;0.5]	0.44 [0.4;0.6]	0.123
C20:4 (n-6)[$]	1.13 [1;1.3]	1.1 [0.9;1.2]	1.1 [1;1.3]	0.983
C20:5 (n-3)[$]	0.26 [0.2;0.3]	0.28 [0.2;0.3]	0.22 [0.2;0.3]	0.915
C22:0[$]	0.52 [0.4;0.6]	0.58 [0.5;0.6]	0.54 [0.5;0.6]	0.891
C22:1 (n-9)[$]	5.91 [2.8;8.6]	6.2 [3.3;8.6]	3.5 [2.4;9.3]	0.473
C22:4 (n-6)[$]	0.11 [0.09;0.14]	0.11 [0.09;0.13]	0.11 [0.09;0.14]	0.277
C22:5 (n-6)[$]	0.07 [0.05;0.08]	0.06 [0.05;0.08]	0.07 [0.06;0.08]	0.019
C24:0[$]	0.33 [0.28;0.41]	0.36 [0.33;0.43]	0.38 [0.3;0.43]	0.788
C22:5 (n-3)[$]	0.19 [0.1;0.3]	0.22 [0.2;0.3]	0.18 [0.1;0.3]	0.393
C22:6 (n-3)[$]	0.36 [0.3;0.4]	0.38 [0.3;0.4]	0.36 [0.3;0.4]	0.93
C24:1 (n-9)[$]	0.59 [0.5;0.79]	0.67 [0.55;0.81]	0.63 [0.53;0.78]	0.543
ACL	17.68 [17.5;17.9]	17.72 [17.5;17.9]	17.61 [17.5;17.9]	0.995
SFA	43.44 [39;48]	43.77 [40;49]	39.27 [36;45]	0.865
UFA	56.56 [52;61]	56.23 [51;60]	60.73 [55;64]	0.865
MUFA	45.15 [41;49]	44.61 [41;48]	49.14 [39;52]	0.759
PUFA	11.05 [10;12]	10.64 [9;12]	12.04 [9;14]	0.872
PUFA n-3	3.17 [2.2;4.1]	3.21 [2.4;4.5]	2.39 [2.1;4]	0.326
PUFA n-6	1.73 [17.5;17.9]	1.7 [17.5;17.9]	1.85 [17.5;17.9]	0.245
DBI	78.7 [72;84]	76.99 [71;83]	82.96 [81;86]	0.323
PI	26.08 [23;29]	26.49 [23;31]	28.36 [24;32]	0.734
C20:4/C20:3	2.69 [2.3;3.2]	2.39 [2.1;3.0]	2.85 [2.2;3.1]	0.789
C18:4/C18:3	0.68 [0.5;1.23]	0.81 [0.5;1.4]	0.71 [0.6;1.2]	0.174
C16:1/C16:0	0.13 [0.08;0.17]	0.1 [0.08;0.17]	0.16 [0.09;0.18]	0.414
C18:1/C18:0	1.58 [1.1;2]	1.53 [1.2;1.9]	1.99 [1.4;2.2]	0.319
C22:5/C18:2	0.01 [0.01;0.02]	0.01 [0.01;0.02]	0.01 [0.01;0.02]	0.162
C22:6/C18:3	0.26 [0.18;0.5]	0.29 [0.19;0.57]	0.53 [0.22;0.55]	0.376
C20:1/C18:1	0.03 [0.03;0.05]	0.04 [0.03;0.04]	0.04 [0.03;0.04]	0.832
C18/C16	0.41 [0.38;0.46]	0.43 [0.4;0.44]	0.43 [0.39;0.44]	0.689

	AD (N = 83)	MCI (N = 92)	CTL (N = 23)	*p**
C20/C18	0.1 [0.08;0.11]	0.09 [0.08;0.11]	0.11 [0.08;0.16]	0.902
C22/C20	0.51 [0.41;0.61]	0.56 [0.44;0.63]	0.42 [0.38;0.59]	0.914
C22:4/C20:4	0.1 [0.08;0.13]	0.11 [0.09;0.12]	0.1 [0.08;0.13]	0.734
C22:5/C20:5	0.72 [0.57;0.95]	0.74 [0.54;1.01]	0.71 [0.51;0.97]	0.5
GSA[£]	5806 [4472;7287]	6189 [4869;7852]	7014 [5035;8589]	0.987
AASA[£]	83 [69;119]	82 [65;99]	87 [75;105]	0.261
CEL[£]	99 [82;128]	106 [81;141]	91 [81;115]	0.259
CML[£]	1115 [949;1310]	1022 [827;1221]	1089 [879;1277]	0.026
MDAL[£]	143 [89;258]	156 [87;244]	200 [90;296]	0.804

*: *p*-value after applying a multinomial regression analysis in which CTL group was set as the reference category[$]**:** values are percentage respect to all measured fatty acids. [£]: values are µmol/moles of lysine. AD: Alzheimer's disease; MCI: mild cognitive impairment; CTL: control; ACL: average chain length; SFA; saturated fatty acids; UFA: unsaturated fatty acids; MUFA: monounsaturated fatty acids; PUFA: polyunsaturated fatty acids; PUFA n-3: polyunsaturated fatty acids from n-3 series; PUFA n-6: polyunsaturated fatty acids from n-6 series; DBI: double bond index; PI; peroxidizability index; GSA: glutamic semialdehyde; AASA: aminoadipic semialdehyde; CEL: carboxyethyl lysine; CML: carboxymethyl lysine; MDAL: malodialdehyde lysine

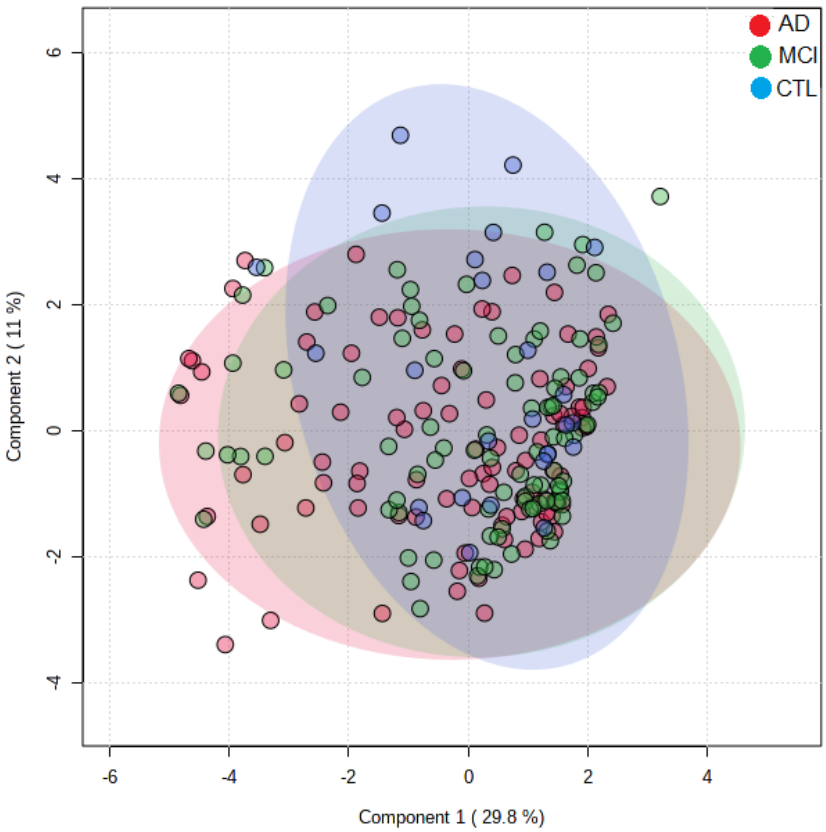

Supplementary Figure 1. Partial least squares-discriminant analysis (PLS-DA) of CSF lipidome profile of patients with AD, MCI and control subjects detected in negative ionization mode.

Supplementary Table 3. Association between lipid features (presented with monoisotopic mass and retention time, Mass@RT), detected after injection of CSF in positive ionization mode, and diagnosis of AD, MCI and control.

Mass@RT	Raw *p*	FDR corrected *p*	Fisher's LSD
874.2736@7.674751	0.0012821	0.22308	AD - MCI; AD - CTL; MCI - CTL
1834.572@10.63213	0.0051397	0.44715	MCI - AD; AD - CTL; MCI - CTL
1316.419@10.07758	0.019161	0.84433	MCI - AD; CTL - AD; CTL - MCI
1760.551@10.58203	0.031578	0.84433	MCI - AD; CTL - AD; CTL - MCI
1127.35@9.837348	0.034209	0.84433	AD - MCI; AD - CTL; MCI - CTL
722.169@5.427679	0.035498	0.84433	MCI - AD; AD - CTL; MCI - CTL
791.7359@6.477523	0.042708	0.84433	MCI - AD; CTL - AD; MCI - CTL
944.898@10.46475	0.043446	0.84433	MCI - AD; CTL - AD; CTL - MCI
776.9137@7.440158	0.043672	0.84433	AD - MCI; CTL - AD; CTL - MCI
952.3084@9.296468	0.048578	0.84526	MCI - AD; AD - CTL; MCI - CTL
757.2425@8.747852	0.060549	0.95777	MCI - AD; AD - CTL; MCI - CTL
1630.516@9.209106	0.086299	0.96947	AD - MCI; AD - CTL; MCI - CTL
1704.532@9.356576	0.09733	0.96947	AD - MCI; CTL - AD; CTL - MCI
708.8482@7.436589	0.098085	0.96947	AD - MCI; AD - CTL; MCI - CTL
1134.433@7.444628	0.1057	0.96947	AD - MCI; CTL - AD; CTL - MCI
765.5786@6.516496	0.11537	0.96947	MCI - AD; CTL - AD; CTL - MCI
965.9515@10.46575	0.11568	0.96947	AD - MCI; AD - CTL; CTL - MCI
1982.614@10.73106	0.11693	0.96947	MCI - AD; AD - CTL; MCI - CTL
390.2925@5.106614	0.12033	0.96947	AD - MCI; AD - CTL; CTL - MCI
478.4672@5.43572	0.13796	0.96947	AD - MCI; CTL - AD; CTL - MCI
1186.386@8.119684	0.14855	0.96947	AD - MCI; AD - CTL; CTL - MCI
1112.365@7.834328	0.15606	0.96947	MCI - AD; CTL - AD; MCI - CTL
1020.334@9.503639	0.1568	0.96947	MCI - AD; CTL - AD; MCI - CTL
785.9034@7.442687	0.15808	0.96947	MCI - AD; CTL - AD; CTL - MCI
980.9518@10.46499	0.1585	0.96947	MCI - AD; CTL - AD; CTL - MCI
1390.441@10.17982	0.16368	0.96947	AD - MCI; CTL - AD; CTL - MCI
908.2835@9.298206	0.16406	0.96947	AD - MCI; CTL - AD; CTL - MCI
375.4032@10.74488	0.1716	0.96947	AD - MCI; CTL - AD; CTL - MCI
1234.878@7.407701	0.1808	0.96947	AD - MCI; CTL - AD; CTL - MCI
834.2629@9.054037	0.18132	0.96947	MCI - AD; CTL - AD; CTL - MCI
197.1304@1.115522	0.18351	0.96947	AD - MCI; AD - CTL; MCI - CTL
977.8707@10.24946	0.19491	0.96947	AD - MCI; AD - CTL; MCI - CTL
1168.376@9.833958	0.20015	0.96947	MCI - AD; CTL - AD; MCI - CTL
1423.433@10.27249	0.21424	0.96947	MCI - AD; CTL - AD; CTL - MCI
659.2367@4.213481	0.21693	0.96947	MCI - AD; CTL - AD; MCI - CTL
566.7156@7.44091	0.22761	0.96947	MCI - AD; CTL - AD; CTL - MCI
2015.61@10.77283	0.24865	0.96947	MCI - AD; CTL - AD; CTL - MCI
772.7728@10.74629	0.25069	0.96947	AD - MCI; CTL - AD; CTL - MCI
1201.37@9.966498	0.25479	0.96947	MCI - AD; CTL - AD; CTL - MCI
831.2641@9.053738	0.25678	0.96947	MCI - AD; CTL - AD; CTL - MCI
932.3507@7.956814	0.25998	0.96947	AD - MCI; AD - CTL; MCI - CTL
533.4287@5.806467	0.26107	0.96947	MCI - AD; AD - CTL; MCI - CTL

Mass@RT	Raw *p*	FDR corrected *p*	Fisher's LSD
1094.355@9.681943	0.26398	0.96947	AD - MCI; AD - CTL; CTL - MCI
1793.544@10.62916	0.26421	0.96947	MCI - AD; AD - CTL; MCI - CTL
1349.411@10.18069	0.27833	0.96947	MCI - AD; CTL - AD; CTL - MCI
317.3089@8.322917	0.27894	0.96947	AD - MCI; CTL - AD; CTL - MCI
1464.461@10.27167	0.28091	0.96947	MCI - AD; CTL - AD; CTL - MCI
1097.356@9.682508	0.2837	0.96947	MCI - AD; AD - CTL; MCI - CTL
663.5911@8.823825	0.29487	0.96947	AD - MCI; CTL - AD; CTL - MCI
954.9352@10.46555	0.29603	0.96947	AD - MCI; CTL - AD; CTL - MCI
732.7834@6.885322	0.3301	0.96947	MCI - AD; CTL - AD; CTL - MCI
545.4296@5.105006	0.33026	0.96947	AD - MCI; CTL - AD; CTL - MCI
686.2217@8.386384	0.33525	0.96947	MCI - AD; CTL - AD; CTL - MCI
587.5138@7.858512	0.33659	0.96947	AD - MCI; CTL - AD; CTL - MCI
185.2218@1.112496	0.33777	0.96947	AD - MCI; AD - CTL; CTL - MCI
631.6144@8.314855	0.34182	0.96947	AD - MCI; CTL - AD; CTL - MCI
576.5338@6.516213	0.3456	0.96947	MCI - AD; CTL - AD; CTL - MCI
364.3928@3.006444	0.36964	0.96947	MCI - AD; AD - CTL; MCI - CTL
1645.496@10.51594	0.37328	0.96947	AD - MCI; CTL - AD; CTL - MCI
1538.482@10.35287	0.37842	0.96947	MCI - AD; AD - CTL; MCI - CTL
760.2427@8.747723	0.38107	0.96947	MCI - AD; AD - CTL; MCI - CTL
567.7215@7.436368	0.38735	0.96947	AD - MCI; CTL - AD; CTL - MCI
629.5292@7.843907	0.39474	0.96947	AD - MCI; AD - CTL; CTL - MCI
1228.433@8.978764	0.39545	0.96947	AD - MCI; AD - CTL; MCI - CTL
129.1563@0.901209	0.39779	0.96947	AD - MCI; CTL - AD; CTL - MCI
547.5167@8.531993	0.40329	0.96947	AD - MCI; CTL - AD; CTL - MCI
1408.449@8.76775	0.4114	0.96947	MCI - AD; CTL - AD; CTL - MCI
862.8504@7.462605	0.41554	0.96947	MCI - AD; CTL - AD; MCI - CTL
1034.999@10.46247	0.41602	0.96947	AD - MCI; CTL - AD; CTL - MCI
994.9706@10.46583	0.41751	0.96947	AD - MCI; CTL - AD; CTL - MCI
724.2482@8.420138	0.42034	0.96947	MCI - AD; AD - CTL; MCI - CTL
733.788@6.88271	0.42452	0.96947	MCI - AD; CTL - AD; CTL - MCI
1482.468@8.933481	0.42816	0.96947	AD - MCI; CTL - AD; CTL - MCI
759.6057@7.840828	0.43177	0.96947	AD - MCI; CTL - AD; CTL - MCI
497.3332@3.654919	0.43285	0.96947	AD - MCI; CTL - AD; CTL - MCI
856.8595@10.46463	0.44437	0.96947	AD - MCI; CTL - AD; CTL - MCI
500.4377@4.431073	0.44942	0.96947	MCI - AD; CTL - AD; CTL - MCI
763.5938@8.03585	0.45881	0.96947	AD - MCI; AD - CTL; CTL - MCI
674.698@10.74442	0.46484	0.96947	AD - MCI; CTL - AD; CTL - MCI
854.2311@6.676765	0.46493	0.96947	AD - MCI; CTL - AD; CTL - MCI
801.2694@8.746971	0.47227	0.96947	MCI - AD; CTL - AD; CTL - MCI
516.4125@5.105329	0.47229	0.96947	AD - MCI; AD - CTL; MCI - CTL
893.3024@6.668782	0.47914	0.96947	AD - MCI; CTL - AD; CTL - MCI
1701.639@10.46622	0.48008	0.96947	AD - MCI; CTL - AD; CTL - MCI
872.2921@9.052311	0.48198	0.96947	MCI - AD; CTL - AD; CTL - MCI
753.5848@6.516179	0.50268	0.96947	MCI - AD; CTL - AD; CTL - MCI
677.5481@8.326365	0.52293	0.96947	AD - MCI; CTL - AD; CTL - MCI

Mass@RT	Raw *p*	FDR corrected *p*	Fisher's LSD
1169.099@8.324103	0.52669	0.96947	AD - MCI; CTL - AD; CTL - MCI
588.5448@8.531194	0.53624	0.96947	AD - MCI; AD - CTL; MCI - CTL
799.5803@8.032224	0.53724	0.96947	AD - MCI; CTL - AD; CTL - MCI
1334.428@8.582393	0.54669	0.96947	AD - MCI; AD - CTL; CTL - MCI
1275.391@10.07966	0.54707	0.96947	AD - MCI; CTL - AD; CTL - MCI
828.8232@10.29756	0.54855	0.96947	AD - MCI; CTL - AD; CTL - MCI
1867.566@10.67709	0.57803	0.96947	AD - MCI; CTL - AD; CTL - MCI
1719.519@10.57721	0.59305	0.96947	MCI - AD; CTL - AD; MCI - CTL
1696.68@10.46615	0.59559	0.96947	AD - MCI; CTL - AD; CTL - MCI
662.4713@8.030101	0.59835	0.96947	AD - MCI; CTL - AD; CTL - MCI
682.8248@7.439494	0.61535	0.96947	AD - MCI; CTL - AD; CTL - MCI
602.1881@4.216712	0.61983	0.96947	MCI - AD; CTL - AD; CTL - MCI
819.6235@8.967945	0.62089	0.96947	AD - MCI; CTL - AD; CTL - MCI
880.6542@8.030765	0.62536	0.96947	AD - MCI; CTL - AD; CTL - MCI
395.403@5.644417	0.62986	0.96947	AD - MCI; CTL - AD; CTL - MCI
627.2645@3.551949	0.63099	0.96947	AD - MCI; CTL - AD; CTL - MCI
979.3072@9.506021	0.64295	0.96947	MCI - AD; CTL - AD; MCI - CTL
625.7757@7.444204	0.64666	0.96947	AD - MCI; AD - CTL; MCI - CTL
688.664@8.322677	0.66009	0.96947	AD - MCI; CTL - AD; CTL - MCI
452.4514@5.64722	0.66029	0.96947	AD - MCI; CTL - AD; CTL - MCI
1023.333@9.503904	0.67128	0.96947	MCI - AD; AD - CTL; MCI - CTL
611.5223@8.322529	0.67557	0.96947	AD - MCI; AD - CTL; CTL - MCI
784.3074@7.135902	0.67743	0.96947	MCI - AD; AD - CTL; MCI - CTL
1686.525@10.52052	0.6827	0.96947	AD - MCI; AD - CTL; MCI - CTL
683.2216@8.396513	0.68709	0.96947	AD - MCI; CTL - AD; CTL - MCI
443.3857@4.20638	0.68736	0.96947	MCI - AD; CTL - AD; CTL - MCI
800.2516@7.225904	0.68839	0.96947	MCI - AD; CTL - AD; MCI - CTL
1994.984@10.74414	0.69337	0.96947	AD - MCI; CTL - AD; CTL - MCI
746.7401@7.47546	0.70197	0.96947	MCI - AD; AD - CTL; MCI - CTL
720.5264@8.025848	0.70288	0.96947	MCI - AD; AD - CTL; MCI - CTL
573.5605@8.325267	0.70313	0.96947	AD - MCI; CTL - AD; CTL - MCI
645.593@8.530423	0.70948	0.96947	AD - MCI; CTL - AD; CTL - MCI
762.8905@7.434217	0.71947	0.96947	AD - MCI; AD - CTL; MCI - CTL
337.3469@5.647639	0.72226	0.96947	AD - MCI; CTL - AD; CTL - MCI
858.3301@7.597923	0.73845	0.96947	MCI - AD; CTL - AD; MCI - CTL
728.696@8.325562	0.73886	0.96947	AD - MCI; CTL - AD; CTL - MCI
905.2851@9.297722	0.74035	0.96947	AD - MCI; CTL - AD; CTL - MCI
500.4373@4.186082	0.74102	0.96947	MCI - AD; CTL - AD; CTL - MCI
1941.583@10.72644	0.74211	0.96947	AD - MCI; AD - CTL; CTL - MCI
829.6085@8.028658	0.74404	0.96947	AD - MCI; AD - CTL; CTL - MCI
868.6885@6.516443	0.74776	0.96947	MCI - AD; CTL - AD; CTL - MCI
857.6391@8.032341	0.75271	0.96947	MCI - AD; CTL - AD; CTL - MCI
817.6105@8.03251	0.75843	0.96947	AD - MCI; CTL - AD; CTL - MCI
798.2711@8.746824	0.76373	0.96947	AD - MCI; CTL - AD; CTL - MCI
1080.394@8.552401	0.76664	0.96947	AD - MCI; AD - CTL; MCI - CTL

Mass@RT	Raw *p*	FDR corrected *p*	Fisher's LSD
959.857@10.6239	0.76697	0.96947	MCI - AD; AD - CTL; MCI - CTL
565.7083@7.442972	0.77311	0.96947	AD - MCI; CTL - AD; CTL - MCI
871.6651@8.032261	0.78164	0.96947	AD - MCI; CTL - AD; CTL - MCI
396.3861@3.923965	0.79047	0.96947	MCI - AD; CTL - AD; CTL - MCI
803.6014@8.029677	0.80083	0.96947	AD - MCI; AD - CTL; CTL - MCI
570.2167@3.553241	0.80343	0.96947	MCI - AD; AD - CTL; MCI - CTL
843.9492@7.442893	0.80568	0.96947	AD - MCI; AD - CTL; MCI - CTL
747.7463@7.47007	0.80823	0.96947	AD - MCI; CTL - AD; CTL - MCI
609.1997@8.02003	0.81331	0.96947	AD - MCI; AD - CTL; CTL - MCI
829.9321@7.442518	0.8142	0.96947	AD - MCI; CTL - AD; CTL - MCI
861.8141@10.46224	0.81504	0.96947	MCI - AD; CTL - AD; MCI - CTL
2089.631@10.81226	0.81518	0.96947	MCI - AD; CTL - AD; CTL - MCI
875.8279@10.33036	0.81808	0.96947	AD - MCI; CTL - AD; CTL - MCI
777.5763@8.032059	0.82068	0.96947	AD - MCI; CTL - AD; CTL - MCI
1612.504@10.4351	0.82419	0.96947	AD - MCI; AD - CTL; MCI - CTL
1571.475@10.43338	0.82905	0.96947	AD - MCI; CTL - AD; CTL - MCI
946.313@9.296309	0.83017	0.96947	AD - MCI; CTL - AD; CTL - MCI
1154.413@8.784649	0.85154	0.97425	MCI - AD; CTL - AD; CTL - MCI
1497.457@10.35496	0.85615	0.97425	AD - MCI; CTL - AD; CTL - MCI
949.3134@9.296863	0.85957	0.97425	AD - MCI; CTL - AD; CTL - MCI
901.8448@10.3349	0.86732	0.97425	AD - MCI; CTL - AD; CTL - MCI
339.3383@3.924562	0.86797	0.97425	MCI - AD; CTL - AD; MCI - CTL
668.5463@8.825511	0.88181	0.97425	AD - MCI; CTL - AD; CTL - MCI
1260.406@8.374403	0.88194	0.97425	MCI - AD; AD - CTL; MCI - CTL
816.2787@6.13488	0.88247	0.97425	MCI - AD; CTL - AD; MCI - CTL
281.2829@3.923809	0.89209	0.97425	AD - MCI; CTL - AD; CTL - MCI
940.9469@10.45823	0.89506	0.97425	MCI - AD; CTL - AD; CTL - MCI
1908.588@10.67772	0.90581	0.97425	AD - MCI; CTL - AD; CTL - MCI
448.3476@5.104986	0.90693	0.97425	MCI - AD; CTL - AD; MCI - CTL
2056.642@10.78238	0.91148	0.97425	AD - MCI; CTL - AD; CTL - MCI
890.3018@6.66968	0.92599	0.97425	MCI - AD; AD - CTL; MCI - CTL
505.3965@5.106026	0.92647	0.97425	MCI - AD; CTL - AD; CTL - MCI
306.3384@3.002841	0.92856	0.97425	MCI - AD; CTL - AD; CTL - MCI
875.2908@9.052464	0.92946	0.97425	MCI - AD; CTL - AD; CTL - MCI
897.8892@10.46549	0.9606	0.99098	MCI - AD; CTL - AD; CTL - MCI
1038.346@7.52279	0.97281	0.99098	AD - MCI; CTL - AD; CTL - MCI
639.5383@7.299686	0.97437	0.99098	AD - MCI; AD - CTL; CTL - MCI
671.5329@8.326734	0.97769	0.99098	MCI - AD; CTL - AD; CTL - MCI
1556.489@9.095047	0.98067	0.99098	MCI - AD; AD - CTL; MCI - CTL
1242.399@9.963441	0.98122	0.99098	AD - MCI; CTL - AD; CTL - MCI
788.5914@8.035072	0.98528	0.99098	MCI - AD; AD - CTL; MCI - CTL
1053.328@9.684236	0.99311	0.99311	AD - MCI; AD - CTL; CTL - MCI

Supplementary Table 4. Association between lipid features (presented with monoisotopic mass and retention time, Mass@RT), detected after injection of CSF in negative ionization mode, and diagnosis of AD, MCI and control.

Mass@RT	Raw *p*	FDR corrected *p*	Fisher's LSD
830.605@9.17506	0.0063281	0.17086	MCI - AD; CTL - AD; MCI - CTL
609.5135@8.215275	0.02071	0.27958	MCI - AD; CTL - AD; MCI - CTL
636.5484@8.21264	0.068496	0.49283	MCI - AD; AD - CTL; MCI - CTL
678.5261@8.384616	0.090133	0.49283	MCI - AD; AD - CTL; MCI - CTL
633.5593@8.213022	0.096779	0.49283	MCI - AD; AD - CTL; MCI - CTL
1265.302@8.288198	0.13879	0.49283	MCI - AD; AD - CTL; MCI - CTL
619.5427@8.210701	0.13908	0.49283	MCI - AD; AD - CTL; MCI - CTL
760.5294@8.73322	0.14861	0.49283	AD - MCI; CTL - AD; CTL - MCI
751.5893@9.164684	0.16428	0.49283	MCI - AD; CTL - AD; MCI - CTL
802.5764@9.165327	0.23475	0.58128	MCI - AD; CTL - AD; MCI - CTL
1339.32@8.500751	0.23682	0.58128	MCI - AD; AD - CTL; MCI - CTL
728.5377@8.735095	0.43529	0.8692	MCI - AD; CTL - AD; CTL - MCI
1299.257@11.36005	0.45688	0.8692	AD - MCI; CTL - AD; CTL - MCI
1312.302@8.500936	0.47194	0.8692	MCI - AD; CTL - AD; MCI - CTL
692.5416@8.729657	0.48289	0.8692	MCI - AD; CTL - AD; CTL - MCI
256.2401@8.213242	0.57791	0.94682	AD - MCI; AD - CTL; MCI - CTL
528.4519@8.591798	0.6265	0.94682	AD - MCI; CTL - AD; CTL - MCI
530.4683@8.423917	0.67957	0.94682	MCI - AD; AD - CTL; MCI - CTL
646.5366@8.731358	0.68365	0.94682	MCI - AD; CTL - AD; CTL - MCI
709.5447@8.73328	0.70135	0.94682	MCI - AD; CTL - AD; CTL - MCI
734.5884@9.155584	0.7474	0.96095	MCI - AD; CTL - AD; MCI - CTL
1090.247@7.754	0.78658	0.96476	AD - MCI; CTL - AD; CTL - MCI
688.5836@9.167139	0.84524	0.96476	MCI - AD; AD - CTL; MCI - CTL
1257.203@11.23158	0.87719	0.96476	MCI - AD; AD - CTL; MCI - CTL
168.9825@0.9102294	0.9096	0.96476	AD - MCI; CTL - AD; CTL - MCI
1257.051@8.729238	0.92921	0.96476	MCI - AD; AD - CTL; MCI - CTL
166.9863@0.9096728	0.96476	0.96476	MCI - AD; CTL - AD; MCI - CTL

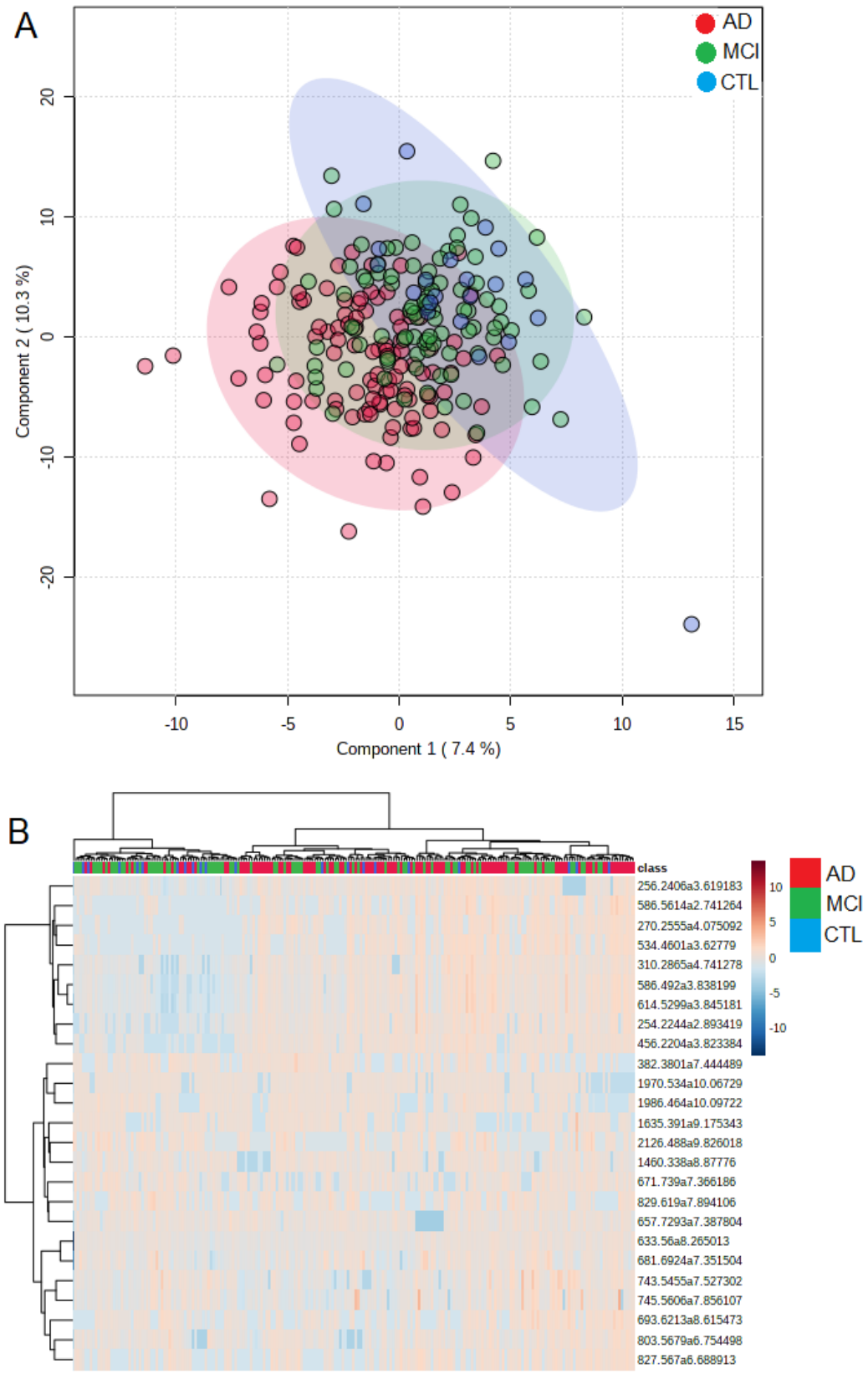

Supplementary Figure 2. Plasma lipidomic profile of patients with AD, MCI, and control subjects detected in negative ionization mode. (A) Partial least squares-discriminant analysis of diagnostic groups. (B) The heat map representation of the top 25 lipids with significantly different (not FDR adjusted) levels between three diagnostic groups.

Spplementary Table 5. Association between lipid features (presented with monoisotopic mass and retention time, Mass@RT), detected after injection of plasma in positive ionization mode, and diagnosis of AD, MCI and control.

Mass@RT	Raw *p*	FDR corrected *p*	Fisher's LSD
948.6996@7.020014	0.0014171	0.33126	AD - CTL; AD - MCI; CTL - MCI
1027.767@7.490652	0.0015287	0.33126	AD - CTL; AD - MCI; CTL - MCI
1362.196@10.40097	0.0016372	0.33126	AD - CTL; AD - MCI; MCI - CTL
730.6385@10.40842	0.0071585	0.74917	AD - CTL; AD - MCI; MCI - CTL
823.7633@10.24519	0.0077986	0.74917	CTL - AD; MCI - AD; MCI - CTL
694.5674@10.39367	0.0092928	0.74917	AD - CTL; AD - MCI; MCI - CTL
1003.843@10.14709	0.010774	0.74917	AD - CTL; AD - MCI; MCI - CTL
967.8199@9.813135	0.011555	0.74917	AD - CTL; AD - MCI; MCI - CTL
1186.342@8.071248	0.012821	0.74917	AD - CTL; MCI - AD; MCI - CTL
1367.371@8.716442	0.014045	0.74917	AD - CTL; MCI - AD; MCI - CTL
929.8393@10.41155	0.015122	0.74917	CTL - AD; MCI - AD; CTL - MCI
950.7167@7.503199	0.016146	0.74917	AD - CTL; AD - MCI; MCI - CTL
809.5922@7.4991	0.01701	0.74917	AD - CTL; AD - MCI; CTL - MCI
689.6126@10.41984	0.017279	0.74917	AD - CTL; AD - MCI; CTL - MCI
1645.438@10.44299	0.021166	0.81809	AD - CTL; AD - MCI; CTL - MCI
429.3348@0.9143981	0.023046	0.81809	CTL - AD; MCI - AD; MCI - CTL
867.6457@7.49806	0.02514	0.81809	AD - CTL; AD - MCI; MCI - CTL
795.7325@10.05771	0.026628	0.81809	CTL - AD; MCI - AD; MCI - CTL
1593.191@7.582058	0.027693	0.81809	AD - CTL; MCI - AD; MCI - CTL
849.7796@10.25691	0.027793	0.81809	CTL - AD; MCI - AD; CTL - MCI
787.6856@10.41144	0.028303	0.81809	AD - CTL; AD - MCI; MCI - CTL
234.1728@0.9119757	0.032967	0.87568	CTL - AD; MCI - AD; MCI - CTL
1021.867@10.05372	0.034426	0.87568	AD - CTL; AD - MCI; CTL - MCI
765.553@7.012727	0.034623	0.87568	CTL - AD; MCI - AD; CTL - MCI
923.7933@10.07447	0.037956	0.91188	AD - CTL; AD - MCI; MCI - CTL
903.8252@10.41869	0.03937	0.91188	CTL - AD; MCI - AD; MCI - CTL
765.5475@6.582529	0.040561	0.91188	AD - CTL; AD - MCI; CTL - MCI
835.6047@7.525056	0.044975	0.94892	AD - CTL; AD - MCI; MCI - CTL
573.5368@8.261002	0.046811	0.94892	CTL - AD; MCI - AD; CTL - MCI
500.4168@4.323842	0.04792	0.94892	AD - CTL; MCI - AD; MCI - CTL
1553.357@10.36816	0.048462	0.94892	AD - CTL; AD - MCI; MCI - CTL
765.6835@9.676582	0.051125	0.9596	CTL - AD; MCI - AD; MCI - CTL
1057.778@6.95536	0.052169	0.9596	AD - CTL; AD - MCI; MCI - CTL
827.7156@10.40082	0.055533	0.96316	AD - CTL; AD - MCI; CTL - MCI
775.2236@6.065872	0.06091	0.96316	AD - CTL; MCI - AD; MCI - CTL
923.258@7.05107	0.061341	0.96316	AD - CTL; AD - MCI; MCI - CTL
907.2325@7.981625	0.065035	0.96316	CTL - AD; MCI - AD; MCI - CTL
1367.152@10.39789	0.066087	0.96316	AD - CTL; AD - MCI; MCI - CTL
793.7153@9.884379	0.068195	0.96316	CTL - AD; MCI - AD; MCI - CTL
727.5517@7.778355	0.07014	0.96316	AD - CTL; MCI - AD; MCI - CTL
922.6617@7.953628	0.070821	0.96316	CTL - AD; AD - MCI; CTL - MCI
741.5653@7.341217	0.072726	0.96316	AD - CTL; MCI - AD; MCI - CTL

Mass@RT	Raw *p*	FDR corrected *p*	Fisher's LSD
889.7731@9.705247	0.075096	0.96316	CTL - AD; MCI - AD; MCI - CTL
868.6527@6.571913	0.08124	0.96316	CTL - AD; AD - MCI; CTL - MCI
826.7044@10.058	0.082394	0.96316	CTL - AD; MCI - AD; CTL - MCI
891.6008@7.958172	0.083514	0.96316	CTL - AD; AD - MCI; CTL - MCI
854.1998@6.588547	0.085266	0.96316	AD - CTL; AD - MCI; MCI - CTL
1275.344@10.02061	0.088028	0.96316	AD - CTL; AD - MCI; CTL - MCI
829.9022@7.321471	0.088873	0.96316	AD - CTL; MCI - AD; MCI - CTL
791.7003@9.707783	0.090087	0.96316	CTL - AD; MCI - AD; MCI - CTL
1343.151@10.44909	0.090318	0.96316	AD - CTL; AD - MCI; MCI - CTL
587.4894@7.787528	0.091079	0.96316	CTL - AD; AD - MCI; CTL - MCI
1538.425@10.30492	0.094458	0.96316	AD - CTL; AD - MCI; CTL - MCI
919.8201@10.06888	0.09668	0.96316	CTL - AD; MCI - AD; CTL - MCI
1005.857@10.28772	0.097423	0.96316	CTL - AD; MCI - AD; CTL - MCI
1020.296@9.451491	0.097827	0.96316	AD - CTL; AD - MCI; MCI - CTL
861.6119@6.596298	0.098407	0.96316	AD - CTL; AD - MCI; CTL - MCI
898.6858@7.036475	0.09883	0.96316	CTL - AD; MCI - AD; MCI - CTL
997.8686@10.13606	0.0998	0.96316	AD - CTL; AD - MCI; MCI - CTL
773.5848@7.700892	0.10023	0.96316	AD - CTL; AD - MCI; CTL - MCI
947.8523@10.25695	0.10268	0.96316	CTL - AD; MCI - AD; CTL - MCI
885.7795@10.03251	0.10654	0.96316	AD - CTL; AD - MCI; MCI - CTL
1023.883@10.17352	0.10847	0.96316	AD - CTL; AD - MCI; MCI - CTL
1397.072@6.988464	0.10856	0.96316	CTL - AD; MCI - AD; MCI - CTL
821.7482@10.07236	0.1102	0.96316	CTL - AD; MCI - AD; MCI - CTL
912.7905@9.966391	0.11517	0.96316	AD - CTL; AD - MCI; MCI - CTL
478.4505@5.36531	0.11623	0.96316	AD - CTL; MCI - AD; MCI - CTL
798.699@10.40433	0.11756	0.96316	AD - CTL; AD - MCI; CTL - MCI
922.6859@6.949636	0.1181	0.96316	AD - CTL; AD - MCI; CTL - MCI
851.595@7.958168	0.11911	0.96316	AD - CTL; AD - MCI; MCI - CTL
1482.414@8.879155	0.12015	0.96316	AD - CTL; MCI - AD; MCI - CTL
1035.883@10.00271	0.1263	0.96316	CTL - AD; MCI - AD; CTL - MCI
878.7359@10.12069	0.13146	0.96316	AD - CTL; AD - MCI; MCI - CTL
1061.901@10.08891	0.13385	0.96316	AD - CTL; AD - MCI; MCI - CTL
1299.228@10.68634	0.13511	0.96316	CTL - AD; AD - MCI; CTL - MCI
743.5748@7.441987	0.13828	0.96316	AD - CTL; MCI - AD; MCI - CTL
1076.263@7.78177	0.13846	0.96316	CTL - AD; MCI - AD; CTL - MCI
835.7639@10.16745	0.13856	0.96316	CTL - AD; MCI - AD; MCI - CTL
1033.778@7.035721	0.1388	0.96316	CTL - AD; MCI - AD; CTL - MCI
1113.34@8.738673	0.14028	0.96316	AD - CTL; AD - MCI; CTL - MCI
941.8055@9.76874	0.14401	0.96316	CTL - AD; MCI - AD; MCI - CTL
798.2399@8.691993	0.14684	0.96316	AD - CTL; AD - MCI; MCI - CTL
1760.479@10.53803	0.1471	0.96316	AD - CTL; AD - MCI; MCI - CTL
925.8082@10.2177	0.14737	0.96316	AD - CTL; AD - MCI; CTL - MCI
1096.298@8.587538	0.14891	0.96316	AD - CTL; AD - MCI; CTL - MCI
849.6643@8.352206	0.15245	0.96316	CTL - AD; AD - MCI; CTL - MCI
872.2592@9.00082	0.15441	0.96316	AD - CTL; AD - MCI; MCI - CTL

Mass@RT	Raw *p*	FDR corrected *p*	Fisher's LSD
1080.35@8.508165	0.15579	0.96316	AD - CTL; AD - MCI; MCI - CTL
839.6129@6.950355	0.16233	0.96316	AD - CTL; AD - MCI; CTL - MCI
1686.466@10.43407	0.16374	0.96316	AD - CTL; AD - MCI; CTL - MCI
985.7211@6.968664	0.16403	0.96316	AD - CTL; AD - MCI; MCI - CTL
854.7351@10.24886	0.1659	0.96316	CTL - AD; MCI - AD; MCI - CTL
1834.505@10.58556	0.16678	0.96316	AD - CTL; AD - MCI; MCI - CTL
911.2401@9.242718	0.1714	0.96316	AD - CTL; AD - MCI; MCI - CTL
819.7318@9.90745	0.17206	0.96316	CTL - AD; MCI - AD; CTL - MCI
852.2402@6.606456	0.17313	0.96316	CTL - AD; AD - MCI; CTL - MCI
773.5553@6.322183	0.17466	0.96316	CTL - AD; AD - MCI; CTL - MCI
1001.897@10.41236	0.17707	0.96316	CTL - AD; MCI - AD; CTL - MCI
975.7362@7.026757	0.17864	0.96316	AD - CTL; MCI - AD; MCI - CTL
657.4971@0.9188228	0.18421	0.96316	AD - CTL; AD - MCI; MCI - CTL
1094.315@9.628272	0.1843	0.96316	AD - CTL; AD - MCI; MCI - CTL
566.6922@7.358762	0.18741	0.96316	CTL - AD; AD - MCI; CTL - MCI
368.3428@6.989621	0.18768	0.96316	AD - CTL; MCI - AD; MCI - CTL
999.8847@10.28044	0.18796	0.96316	CTL - AD; AD - MCI; CTL - MCI
874.7046@9.811177	0.18818	0.96316	AD - CTL; AD - MCI; CTL - MCI
815.6132@7.032407	0.1903	0.96316	CTL - AD; MCI - AD; MCI - CTL
908.2499@9.242761	0.19045	0.96316	AD - CTL; AD - MCI; MCI - CTL
1048.379@9.202257	0.19099	0.96316	AD - CTL; AD - MCI; MCI - CTL
1061.811@7.575009	0.19123	0.96316	CTL - AD; MCI - AD; MCI - CTL
940.9145@10.40436	0.19256	0.96316	AD - CTL; AD - MCI; MCI - CTL
1708.539@10.25833	0.19557	0.96316	CTL - AD; MCI - AD; CTL - MCI
1392.374@9.335585	0.19685	0.96316	AD - CTL; MCI - AD; MCI - CTL
843.9168@7.319713	0.19755	0.96316	CTL - AD; MCI - AD; MCI - CTL
719.5813@7.814231	0.19923	0.96316	CTL - AD; AD - MCI; CTL - MCI
779.5437@6.602743	0.19984	0.96316	CTL - AD; MCI - AD; CTL - MCI
535.1567@7.501583	0.20268	0.96316	AD - CTL; AD - MCI; CTL - MCI
1187.358@8.939273	0.20686	0.96316	AD - CTL; AD - MCI; CTL - MCI
798.6596@8.208514	0.20736	0.96316	AD - CTL; MCI - AD; MCI - CTL
837.6221@7.848754	0.20768	0.96316	CTL - AD; AD - MCI; CTL - MCI
1228.388@8.928229	0.20821	0.96316	AD - CTL; MCI - AD; MCI - CTL
1338.195@10.46311	0.21338	0.96316	AD - CTL; AD - MCI; CTL - MCI
1537.109@7.030225	0.21556	0.96316	CTL - AD; MCI - AD; CTL - MCI
829.5618@6.494051	0.21866	0.96316	CTL - AD; MCI - AD; CTL - MCI
727.221@8.362071	0.2195	0.96316	AD - CTL; AD - MCI; CTL - MCI
349.2733@0.9123762	0.22157	0.96316	CTL - AD; MCI - AD; MCI - CTL
776.7169@10.69225	0.22238	0.96316	CTL - AD; AD - MCI; CTL - MCI
662.4448@7.953356	0.22924	0.96316	CTL - AD; MCI - AD; CTL - MCI
625.7507@7.321451	0.23156	0.96316	CTL - AD; MCI - AD; MCI - CTL
531.4017@5.001466	0.23633	0.96316	AD - CTL; AD - MCI; CTL - MCI
875.6767@8.427777	0.23634	0.96316	AD - CTL; AD - MCI; CTL - MCI
1947.759@10.7235	0.23638	0.96316	CTL - AD; MCI - AD; CTL - MCI
1373.416@10.02484	0.23791	0.96316	CTL - AD; MCI - AD; CTL - MCI

Mass@RT	Raw *p*	FDR corrected *p*	Fisher's LSD
734.8273@7.334836	0.24074	0.96316	CTL - AD; MCI - AD; MCI - CTL
448.3286@5.019092	0.24404	0.96316	CTL - AD; MCI - AD; MCI - CTL
762.8594@7.326734	0.24451	0.96316	AD - CTL; MCI - AD; MCI - CTL
969.8372@9.962495	0.24793	0.96316	AD - CTL; MCI - AD; MCI - CTL
1349.362@10.12826	0.24887	0.96316	AD - CTL; AD - MCI; CTL - MCI
1441.392@8.886689	0.24956	0.96316	CTL - AD; MCI - AD; CTL - MCI
891.7873@9.878552	0.24984	0.96316	CTL - AD; MCI - AD; CTL - MCI
2616.312@10.54081	0.25231	0.96316	CTL - AD; MCI - AD; MCI - CTL
1053.289@9.628531	0.25248	0.96316	AD - CTL; AD - MCI; CTL - MCI
789.5645@7.094165	0.25386	0.96316	CTL - AD; MCI - AD; CTL - MCI
1464.407@10.21943	0.25537	0.96316	AD - CTL; AD - MCI; CTL - MCI
1018.945@10.69091	0.25694	0.96316	CTL - AD; AD - MCI; CTL - MCI
683.195@8.337936	0.25706	0.96316	AD - CTL; AD - MCI; CTL - MCI
639.5121@6.922685	0.25737	0.96316	CTL - AD; MCI - AD; CTL - MCI
687.5956@10.28296	0.25865	0.96316	CTL - AD; MCI - AD; CTL - MCI
917.8048@9.901769	0.25971	0.96316	CTL - AD; MCI - AD; CTL - MCI
867.7313@9.688652	0.2623	0.96316	AD - CTL; MCI - AD; MCI - CTL
831.2331@8.998206	0.26453	0.96316	AD - CTL; AD - MCI; MCI - CTL
1720.548@10.38086	0.26515	0.96316	CTL - AD; MCI - AD; CTL - MCI
1011.886@10.12557	0.26595	0.96316	AD - CTL; AD - MCI; MCI - CTL
814.692@8.932172	0.26706	0.96316	CTL - AD; AD - MCI; CTL - MCI
883.5631@7.593288	0.26742	0.96316	AD - CTL; MCI - AD; MCI - CTL
796.1518@6.060647	0.27012	0.96316	AD - CTL; AD - MCI; MCI - CTL
1466.396@9.480596	0.27099	0.96316	CTL - AD; AD - MCI; CTL - MCI
1663.441@9.297435	0.27267	0.96316	AD - CTL; AD - MCI; CTL - MCI
862.8162@7.305413	0.27511	0.96316	CTL - AD; MCI - AD; MCI - CTL
1709.463@10.10443	0.27592	0.96316	CTL - AD; MCI - AD; CTL - MCI
803.7169@10.5207	0.27678	0.96316	CTL - AD; MCI - AD; MCI - CTL
1334.377@8.533263	0.27714	0.96316	AD - CTL; AD - MCI; MCI - CTL
833.2103@7.616618	0.2801	0.96316	AD - CTL; AD - MCI; MCI - CTL
1085.807@7.496671	0.28338	0.96316	AD - CTL; AD - MCI; CTL - MCI
1493.132@7.399634	0.28355	0.96316	CTL - AD; AD - MCI; CTL - MCI
1293.351@8.526791	0.28377	0.96316	AD - CTL; AD - MCI; CTL - MCI
709.6219@8.294881	0.28432	0.96316	CTL - AD; MCI - AD; CTL - MCI
1059.885@9.989738	0.28671	0.96316	CTL - AD; MCI - AD; CTL - MCI
1302.403@9.113504	0.28797	0.96316	AD - CTL; MCI - AD; MCI - CTL
829.585@7.95167	0.29439	0.96316	AD - CTL; MCI - AD; MCI - CTL
771.5767@7.291079	0.29483	0.96316	AD - CTL; MCI - AD; MCI - CTL
635.62@8.875026	0.29696	0.96316	AD - CTL; MCI - AD; MCI - CTL
681.792@7.336611	0.29909	0.96316	AD - CTL; MCI - AD; MCI - CTL
1006.866@9.994699	0.30095	0.96316	AD - CTL; AD - MCI; MCI - CTL
292.306@2.189239	0.30183	0.96316	AD - CTL; AD - MCI; MCI - CTL
819.2473@6.061583	0.30596	0.96316	CTL - AD; MCI - AD; CTL - MCI
1219.334@8.309442	0.30601	0.96316	AD - CTL; MCI - AD; MCI - CTL
1071.295@7.775069	0.3083	0.96316	CTL - AD; MCI - AD; CTL - MCI

Mass@RT	Raw *p*	FDR corrected *p*	Fisher's LSD
770.5816@6.569112	0.3089	0.96316	CTL - AD; MCI - AD; CTL - MCI
761.6684@10.36372	0.31382	0.96316	AD - CTL; AD - MCI; CTL - MCI
732.7539@6.680182	0.31519	0.96316	AD - CTL; AD - MCI; MCI - CTL
931.8369@10.07288	0.31657	0.96316	CTL - AD; MCI - AD; CTL - MCI
952.7203@7.035904	0.31932	0.96316	CTL - AD; MCI - AD; MCI - CTL
961.719@7.031269	0.3203	0.96316	AD - CTL; AD - MCI; MCI - CTL
841.626@7.123726	0.32386	0.96316	AD - CTL; AD - MCI; CTL - MCI
793.5974@7.782673	0.32529	0.96316	AD - CTL; MCI - AD; MCI - CTL
500.4168@4.076473	0.32745	0.96316	AD - CTL; MCI - AD; MCI - CTL
781.562@6.956029	0.32799	0.96316	AD - CTL; AD - MCI; CTL - MCI
787.6081@7.95678	0.32917	0.96316	CTL - AD; MCI - AD; CTL - MCI
733.7596@6.263375	0.33045	0.96316	CTL - AD; MCI - AD; MCI - CTL
765.7014@10.69182	0.33442	0.96316	CTL - AD; AD - MCI; CTL - MCI
526.4432@4.07226	0.3366	0.96316	AD - CTL; MCI - AD; MCI - CTL
1534.364@10.40481	0.33772	0.96316	AD - CTL; AD - MCI; CTL - MCI
791.7159@10.68125	0.3434	0.96316	AD - CTL; AD - MCI; CTL - MCI
1713.498@10.26141	0.34633	0.96316	CTL - AD; MCI - AD; CTL - MCI
1630.452@9.161541	0.34857	0.96316	AD - CTL; MCI - AD; MCI - CTL
1916.791@10.70516	0.34869	0.96316	AD - CTL; AD - MCI; MCI - CTL
1515.408@9.038616	0.35158	0.96316	AD - CTL; AD - MCI; CTL - MCI
781.5594@6.673632	0.352	0.96316	CTL - AD; MCI - AD; MCI - CTL
1556.43@9.047953	0.35301	0.96316	AD - CTL; MCI - AD; MCI - CTL
980.9143@10.402	0.35329	0.96316	CTL - AD; MCI - AD; CTL - MCI
1028.851@9.833941	0.35404	0.96316	AD - CTL; MCI - AD; MCI - CTL
682.7976@7.335763	0.35413	0.96316	AD - CTL; MCI - AD; MCI - CTL
980.8517@9.964045	0.35673	0.96316	AD - CTL; AD - MCI; CTL - MCI
1053.926@10.26385	0.35714	0.96316	AD - CTL; MCI - AD; MCI - CTL
495.3315@2.736793	0.35854	0.96316	CTL - AD; AD - MCI; CTL - MCI
748.1675@5.352467	0.36232	0.96316	AD - CTL; AD - MCI; MCI - CTL
556.4058@0.9168819	0.36497	0.96316	CTL - AD; AD - MCI; CTL - MCI
708.6551@10.69842	0.36551	0.96316	AD - CTL; AD - MCI; MCI - CTL
2204.596@10.81449	0.36585	0.96316	AD - CTL; AD - MCI; MCI - CTL
887.7948@10.18031	0.36601	0.96316	AD - CTL; AD - MCI; MCI - CTL
2015.524@10.73101	0.3664	0.96316	AD - CTL; MCI - AD; MCI - CTL
1297.168@10.73917	0.36794	0.96316	CTL - AD; AD - MCI; CTL - MCI
1497.401@10.30889	0.36827	0.96316	AD - CTL; AD - MCI; MCI - CTL
395.3859@5.536681	0.36875	0.96316	CTL - AD; MCI - AD; CTL - MCI
848.6881@9.77105	0.36905	0.96316	AD - CTL; MCI - AD; MCI - CTL
1672.487@9.731697	0.37402	0.96316	AD - CTL; AD - MCI; MCI - CTL
894.6772@7.024692	0.37862	0.96316	AD - CTL; MCI - AD; MCI - CTL
1261.378@9.118979	0.37987	0.96316	AD - CTL; AD - MCI; MCI - CTL
917.7563@9.670757	0.38362	0.96316	AD - CTL; AD - MCI; MCI - CTL
775.5565@7.639708	0.38514	0.96316	CTL - AD; MCI - AD; MCI - CTL
745.5939@7.827757	0.38533	0.96316	CTL - AD; AD - MCI; CTL - MCI
1489.108@6.979362	0.38551	0.96316	CTL - AD; MCI - AD; MCI - CTL

Mass@RT	Raw *p*	FDR corrected *p*	Fisher's LSD
824.6885@9.895133	0.3875	0.96316	CTL - AD; MCI - AD; CTL - MCI
739.6858@10.71779	0.38847	0.96316	AD - CTL; AD - MCI; CTL - MCI
633.5321@7.750349	0.38848	0.96316	AD - CTL; AD - MCI; MCI - CTL
708.8235@6.909931	0.39091	0.96316	AD - CTL; MCI - AD; MCI - CTL
789.6999@10.53112	0.39234	0.96316	AD - CTL; AD - MCI; MCI - CTL
682.6391@10.73761	0.39258	0.96316	AD - CTL; AD - MCI; MCI - CTL
811.6842@8.601756	0.39567	0.96316	CTL - AD; AD - MCI; CTL - MCI
2311.602@10.85751	0.39605	0.96316	CTL - AD; AD - MCI; CTL - MCI
984.8828@10.26324	0.39621	0.96316	AD - CTL; AD - MCI; MCI - CTL
1318.227@10.68181	0.39721	0.96316	CTL - AD; AD - MCI; CTL - MCI
421.4204@2.60361	0.39837	0.96316	AD - CTL; AD - MCI; MCI - CTL
1994.558@7.439299	0.39968	0.96316	AD - CTL; MCI - AD; MCI - CTL
915.7888@9.732122	0.40173	0.96316	CTL - AD; MCI - AD; MCI - CTL
776.8855@7.331917	0.40176	0.96316	AD - CTL; AD - MCI; MCI - CTL
763.5182@6.858298	0.40331	0.96316	CTL - AD; AD - MCI; CTL - MCI
855.5336@7.039243	0.40478	0.96316	AD - CTL; MCI - AD; MCI - CTL
1760.574@10.27352	0.40509	0.96316	CTL - AD; MCI - AD; CTL - MCI
1967.734@10.5466	0.4058	0.96316	AD - CTL; MCI - AD; MCI - CTL
979.2697@9.449753	0.40712	0.96316	AD - CTL; AD - MCI; CTL - MCI
717.5663@7.739121	0.40984	0.96316	AD - CTL; MCI - AD; MCI - CTL
924.7227@9.828918	0.41097	0.96316	CTL - AD; MCI - AD; CTL - MCI
1145.314@8.061877	0.41137	0.96316	CTL - AD; AD - MCI; CTL - MCI
667.6281@10.68883	0.41301	0.96316	CTL - AD; AD - MCI; CTL - MCI
1465.434@8.719833	0.41439	0.96316	CTL - AD; AD - MCI; CTL - MCI
1447.428@10.12928	0.41771	0.96316	AD - CTL; AD - MCI; MCI - CTL
757.5627@7.028447	0.41842	0.96316	CTL - AD; MCI - AD; MCI - CTL
833.748@10.00517	0.41913	0.96316	AD - CTL; MCI - AD; MCI - CTL
843.6443@7.575299	0.41919	0.96316	CTL - AD; MCI - AD; MCI - CTL
751.5497@7.735329	0.41946	0.96316	AD - CTL; MCI - AD; MCI - CTL
991.8196@9.744276	0.41957	0.96316	CTL - AD; MCI - AD; MCI - CTL
1696.616@10.40914	0.42167	0.96316	AD - CTL; MCI - AD; MCI - CTL
1941.511@10.67711	0.4217	0.96316	AD - CTL; AD - MCI; MCI - CTL
841.7153@9.6387	0.42216	0.96316	CTL - AD; MCI - AD; MCI - CTL
1497.072@6.996967	0.42346	0.96316	AD - CTL; MCI - AD; MCI - CTL
873.7813@10.11875	0.42659	0.96316	AD - CTL; AD - MCI; MCI - CTL
1288.179@10.49738	0.42665	0.96316	CTL - AD; MCI - AD; CTL - MCI
735.6372@8.352237	0.42707	0.96316	CTL - AD; AD - MCI; CTL - MCI
699.5201@7.298812	0.43124	0.96316	AD - CTL; MCI - AD; MCI - CTL
497.3141@3.540539	0.43127	0.96316	AD - CTL; AD - MCI; MCI - CTL
612.1749@7.967497	0.43343	0.96316	AD - CTL; AD - MCI; CTL - MCI
1275.184@10.70342	0.43584	0.96316	AD - CTL; MCI - AD; MCI - CTL
852.7203@10.08004	0.43853	0.96316	AD - CTL; MCI - AD; MCI - CTL
755.7361@6.677587	0.43946	0.96316	AD - CTL; MCI - AD; MCI - CTL
850.7035@9.922549	0.43959	0.96316	CTL - AD; MCI - AD; CTL - MCI
875.7964@10.26718	0.44214	0.96316	CTL - AD; MCI - AD; CTL - MCI

Mass@RT	Raw *p*	FDR corrected *p*	Fisher's LSD
861.7829@10.38621	0.44521	0.96316	CTL - AD; MCI - AD; MCI - CTL
635.5473@8.057007	0.44721	0.96316	AD - CTL; AD - MCI; CTL - MCI
743.5447@6.741745	0.4484	0.96316	AD - CTL; MCI - AD; MCI - CTL
813.6276@8.037707	0.44904	0.96316	CTL - AD; MCI - AD; CTL - MCI
786.6604@8.423006	0.45067	0.96316	CTL - AD; MCI - AD; CTL - MCI
733.7593@6.67848	0.45373	0.96316	CTL - AD; MCI - AD; CTL - MCI
724.2209@8.36776	0.45472	0.96316	CTL - AD; AD - MCI; CTL - MCI
876.7198@9.959331	0.45514	0.96316	CTL - AD; AD - MCI; CTL - MCI
1445.066@6.882811	0.45537	0.96316	AD - CTL; AD - MCI; CTL - MCI
901.8116@10.2829	0.45583	0.96316	CTL - AD; AD - MCI; CTL - MCI
973.8682@10.26877	0.45884	0.96316	CTL - AD; MCI - AD; CTL - MCI
364.3772@2.599141	0.45918	0.96316	AD - CTL; MCI - AD; MCI - CTL
645.5711@8.474198	0.46128	0.96316	AD - CTL; AD - MCI; MCI - CTL
833.5919@7.378052	0.46154	0.96316	CTL - AD; AD - MCI; CTL - MCI
801.2377@8.691717	0.46156	0.96316	AD - CTL; AD - MCI; CTL - MCI
519.3299@2.334037	0.46176	0.96316	CTL - AD; MCI - AD; MCI - CTL
1715.581@10.38285	0.46342	0.96316	AD - CTL; AD - MCI; MCI - CTL
1701.574@10.40784	0.46429	0.96316	AD - CTL; MCI - AD; MCI - CTL
980.7527@7.557303	0.46489	0.96316	CTL - AD; AD - MCI; CTL - MCI
1719.455@10.5333	0.46604	0.96316	AD - CTL; AD - MCI; MCI - CTL
785.5932@7.58003	0.46612	0.96316	CTL - AD; MCI - AD; MCI - CTL
706.6397@10.54552	0.46623	0.96316	CTL - AD; MCI - AD; MCI - CTL
893.2652@6.587764	0.46848	0.96316	AD - CTL; AD - MCI; MCI - CTL
900.3438@8.747513	0.47024	0.96316	AD - CTL; AD - MCI; CTL - MCI
129.1502@0.8239806	0.47024	0.96316	CTL - AD; AD - MCI; CTL - MCI
758.6278@7.916036	0.47253	0.96316	CTL - AD; MCI - AD; CTL - MCI
822.6724@9.731529	0.47284	0.96316	CTL - AD; MCI - AD; MCI - CTL
880.7506@10.26717	0.47436	0.96316	AD - CTL; AD - MCI; CTL - MCI
940.8204@10.14813	0.47444	0.96316	CTL - AD; AD - MCI; CTL - MCI
1216.055@8.32154	0.47561	0.96316	CTL - AD; AD - MCI; CTL - MCI
352.3304@3.821818	0.48001	0.96316	CTL - AD; AD - MCI; CTL - MCI
726.5643@6.412218	0.48113	0.96316	AD - CTL; AD - MCI; CTL - MCI
914.8057@10.12705	0.48253	0.96316	AD - CTL; AD - MCI; MCI - CTL
1059.793@7.099659	0.48444	0.96316	CTL - AD; MCI - AD; CTL - MCI
707.6037@7.992209	0.48836	0.96316	CTL - AD; AD - MCI; CTL - MCI
1390.39@10.12638	0.48995	0.96316	CTL - AD; AD - MCI; CTL - MCI
1391.419@8.525249	0.49213	0.96316	CTL - AD; MCI - AD; CTL - MCI
805.561@6.835739	0.49336	0.96316	CTL - AD; AD - MCI; CTL - MCI
1409.413@9.412878	0.49495	0.96316	AD - CTL; AD - MCI; CTL - MCI
1508.123@6.80953	0.49504	0.96316	CTL - AD; AD - MCI; CTL - MCI
672.5194@5.5559	0.49525	0.96316	AD - CTL; AD - MCI; MCI - CTL
637.5631@8.356158	0.49571	0.96316	CTL - AD; AD - MCI; CTL - MCI
847.7639@10.09175	0.49819	0.96316	CTL - AD; MCI - AD; CTL - MCI
819.5921@8.912476	0.50104	0.96316	AD - CTL; AD - MCI; MCI - CTL
1761.498@10.13398	0.5019	0.96316	CTL - AD; AD - MCI; CTL - MCI

Mass@RT	Raw *p*	FDR corrected *p*	Fisher's LSD
843.7316@9.775476	0.50213	0.96316	AD - CTL; MCI - AD; MCI - CTL
811.6077@7.716831	0.50304	0.96316	CTL - AD; AD - MCI; CTL - MCI
642.5185@8.360685	0.50661	0.96316	CTL - AD; AD - MCI; CTL - MCI
831.5754@6.903709	0.51008	0.96316	CTL - AD; AD - MCI; CTL - MCI
1299.398@9.909835	0.51063	0.96316	AD - CTL; MCI - AD; MCI - CTL
565.6858@7.360398	0.51193	0.96316	AD - CTL; AD - MCI; CTL - MCI
1097.314@9.628453	0.51193	0.96316	CTL - AD; MCI - AD; MCI - CTL
1336.178@10.38227	0.51271	0.96316	AD - CTL; AD - MCI; MCI - CTL
1006.332@8.20305	0.51389	0.96316	CTL - AD; MCI - AD; CTL - MCI
774.7006@10.52784	0.514	0.96316	CTL - AD; MCI - AD; MCI - CTL
674.5344@6.128766	0.51414	0.96316	CTL - AD; MCI - AD; CTL - MCI
817.5929@7.235104	0.51532	0.96316	CTL - AD; MCI - AD; CTL - MCI
2163.563@10.79941	0.5206	0.96316	AD - CTL; MCI - AD; MCI - CTL
1510.365@10.45408	0.5212	0.96316	AD - CTL; AD - MCI; MCI - CTL
965.8049@9.685646	0.5221	0.96316	CTL - AD; MCI - AD; CTL - MCI
819.6103@7.756669	0.52657	0.96316	AD - CTL; AD - MCI; MCI - CTL
663.5648@8.76145	0.52948	0.96316	AD - CTL; AD - MCI; MCI - CTL
1734.557@10.26479	0.53059	0.96316	CTL - AD; MCI - AD; CTL - MCI
543.331@2.272861	0.53065	0.96316	AD - CTL; AD - MCI; MCI - CTL
609.1753@7.966011	0.53253	0.96316	AD - CTL; AD - MCI; CTL - MCI
511.4058@0.9201053	0.53815	0.96316	AD - CTL; MCI - AD; MCI - CTL
946.6861@6.834289	0.5384	0.96316	CTL - AD; AD - MCI; CTL - MCI
1973.777@10.67922	0.54034	0.96316	CTL - AD; AD - MCI; CTL - MCI
611.5334@8.300722	0.54142	0.96316	AD - CTL; MCI - AD; MCI - CTL
791.7058@6.435223	0.5428	0.96316	CTL - AD; MCI - AD; CTL - MCI
859.7635@10.02417	0.54319	0.96316	AD - CTL; AD - MCI; MCI - CTL
805.5594@6.615555	0.54453	0.96316	AD - CTL; AD - MCI; MCI - CTL
756.6108@7.452854	0.54628	0.96316	CTL - AD; AD - MCI; CTL - MCI
669.5871@8.722047	0.5467	0.96316	AD - CTL; AD - MCI; CTL - MCI
783.5767@7.134716	0.54791	0.96316	CTL - AD; MCI - AD; CTL - MCI
705.545@6.807164	0.54951	0.96316	AD - CTL; AD - MCI; MCI - CTL
760.2114@8.6943	0.55382	0.96316	CTL - AD; MCI - AD; CTL - MCI
677.522@8.260931	0.55618	0.96316	AD - CTL; AD - MCI; MCI - CTL
948.677@7.954051	0.55624	0.96316	AD - CTL; MCI - AD; MCI - CTL
653.4716@8.255313	0.55715	0.96316	AD - CTL; AD - MCI; MCI - CTL
1043.85@9.859391	0.55736	0.96316	CTL - AD; AD - MCI; CTL - MCI
707.6873@9.040414	0.56015	0.96316	CTL - AD; AD - MCI; CTL - MCI
817.5796@7.949477	0.56078	0.96316	CTL - AD; MCI - AD; CTL - MCI
763.6856@10.5257	0.56185	0.96316	AD - CTL; MCI - AD; MCI - CTL
688.637@8.258913	0.565	0.96316	CTL - AD; MCI - AD; MCI - CTL
1908.521@10.61434	0.56563	0.96316	AD - CTL; MCI - AD; MCI - CTL
1025.9@10.27795	0.5658	0.96316	CTL - AD; MCI - AD; CTL - MCI
331.3221@2.450209	0.56643	0.96316	AD - CTL; MCI - AD; MCI - CTL
713.6121@10.34604	0.56663	0.96316	AD - CTL; AD - MCI; CTL - MCI
521.3469@2.898388	0.56826	0.96316	CTL - AD; AD - MCI; CTL - MCI

Mass@RT	Raw *p*	FDR corrected *p*	Fisher's LSD
909.6457@7.95547	0.57983	0.96316	CTL - AD; MCI - AD; CTL - MCI
516.3903@5.020352	0.58951	0.96316	CTL - AD; MCI - AD; MCI - CTL
902.7374@9.993323	0.58973	0.96316	AD - CTL; MCI - AD; MCI - CTL
2534.658@10.93703	0.59207	0.96316	CTL - AD; AD - MCI; CTL - MCI
708.8237@7.311582	0.59256	0.96316	CTL - AD; MCI - AD; CTL - MCI
765.5653@7.235921	0.59332	0.96316	CTL - AD; AD - MCI; CTL - MCI
780.179@6.052964	0.59356	0.96316	CTL - AD; MCI - AD; MCI - CTL
889.81@10.32954	0.59377	0.96316	AD - CTL; AD - MCI; CTL - MCI
871.7638@9.965164	0.59677	0.96316	AD - CTL; AD - MCI; MCI - CTL
747.7162@7.307392	0.59694	0.96316	CTL - AD; MCI - AD; CTL - MCI
861.7795@10.17774	0.59845	0.96316	CTL - AD; MCI - AD; CTL - MCI
1316.37@10.02441	0.59916	0.96316	CTL - AD; MCI - AD; CTL - MCI
949.2759@9.244714	0.59924	0.96316	AD - CTL; AD - MCI; CTL - MCI
718.5592@6.490638	0.59962	0.96316	AD - CTL; MCI - AD; MCI - CTL
1017.834@9.827017	0.60764	0.96316	CTL - AD; MCI - AD; CTL - MCI
227.2602@1.704457	0.60773	0.96316	CTL - AD; MCI - AD; CTL - MCI
1008.882@10.14056	0.60778	0.96316	CTL - AD; MCI - AD; CTL - MCI
613.4732@0.9206858	0.60975	0.96316	CTL - AD; MCI - AD; MCI - CTL
185.2128@0.9858018	0.60988	0.96316	CTL - AD; AD - MCI; CTL - MCI
687.5089@0.9127401	0.61051	0.96316	AD - CTL; AD - MCI; MCI - CTL
954.9001@10.40785	0.61525	0.96316	AD - CTL; MCI - AD; MCI - CTL
1030.867@9.971003	0.61525	0.96316	CTL - AD; MCI - AD; CTL - MCI
826.689@8.525631	0.61612	0.96316	AD - CTL; MCI - AD; MCI - CTL
1013.901@10.26652	0.61676	0.96316	AD - CTL; MCI - AD; MCI - CTL
1242.352@9.90887	0.61905	0.96316	CTL - AD; AD - MCI; CTL - MCI
1023.295@9.451741	0.62258	0.96316	AD - CTL; MCI - AD; MCI - CTL
1243.383@8.063785	0.62265	0.96316	CTL - AD; AD - MCI; CTL - MCI
1421.07@6.93314	0.62371	0.96316	AD - CTL; AD - MCI; CTL - MCI
978.7357@7.054719	0.62475	0.96316	CTL - AD; MCI - AD; CTL - MCI
1349.254@7.402835	0.62747	0.96316	CTL - AD; AD - MCI; CTL - MCI
743.5808@7.751631	0.62795	0.96316	AD - CTL; MCI - AD; MCI - CTL
857.6063@7.953896	0.62894	0.96316	AD - CTL; AD - MCI; CTL - MCI
767.58@7.354791	0.6328	0.96316	AD - CTL; AD - MCI; CTL - MCI
759.5776@7.429874	0.63381	0.96316	CTL - AD; MCI - AD; CTL - MCI
952.7308@7.675968	0.63484	0.96316	AD - CTL; AD - MCI; CTL - MCI
1134.389@7.353609	0.64365	0.96316	CTL - AD; AD - MCI; CTL - MCI
974.7156@7.400927	0.64425	0.96316	AD - CTL; AD - MCI; CTL - MCI
926.2587@7.056248	0.64711	0.96316	CTL - AD; MCI - AD; CTL - MCI
699.6196@9.860396	0.64716	0.96316	CTL - AD; MCI - AD; CTL - MCI
696.5068@6.126513	0.64746	0.96316	AD - CTL; AD - MCI; MCI - CTL
1201.325@9.906036	0.64993	0.96316	AD - CTL; AD - MCI; CTL - MCI
985.2581@9.450237	0.65354	0.96316	AD - CTL; MCI - AD; MCI - CTL
890.2674@6.58766	0.65581	0.96316	AD - CTL; AD - MCI; CTL - MCI
771.8517@7.320538	0.65607	0.96316	AD - CTL; MCI - AD; MCI - CTL
982.2672@9.450147	0.65701	0.96316	AD - CTL; AD - MCI; MCI - CTL

Mass@RT	Raw *p*	FDR corrected *p*	Fisher's LSD
1319.153@10.54677	0.65749	0.96316	AD - CTL; AD - MCI; CTL - MCI
900.7016@7.438399	0.65828	0.96316	CTL - AD; MCI - AD; CTL - MCI
2237.574@10.82829	0.65828	0.96316	CTL - AD; AD - MCI; CTL - MCI
856.8277@10.40762	0.65886	0.96316	AD - CTL; MCI - AD; MCI - CTL
674.6725@10.6776	0.6625	0.96316	AD - CTL; MCI - AD; MCI - CTL
753.5538@6.568918	0.66657	0.96316	AD - CTL; AD - MCI; MCI - CTL
693.8093@7.336282	0.66692	0.96316	CTL - AD; MCI - AD; MCI - CTL
863.6124@6.840269	0.67376	0.96316	CTL - AD; AD - MCI; CTL - MCI
1010.544@9.079222	0.67387	0.96316	AD - CTL; AD - MCI; MCI - CTL
1122.4@9.381156	0.6767	0.96316	CTL - AD; AD - MCI; CTL - MCI
1852.504@9.513699	0.67945	0.96316	AD - CTL; AD - MCI; MCI - CTL
993.8372@9.85586	0.67962	0.96316	AD - CTL; MCI - AD; MCI - CTL
480.4604@5.98914	0.68006	0.96316	AD - CTL; AD - MCI; MCI - CTL
897.8532@10.40786	0.68025	0.96316	AD - CTL; AD - MCI; MCI - CTL
1571.418@10.37642	0.68032	0.96316	CTL - AD; AD - MCI; CTL - MCI
875.2573@9.001309	0.68042	0.96316	AD - CTL; AD - MCI; CTL - MCI
849.242@6.605921	0.68167	0.96316	AD - CTL; AD - MCI; CTL - MCI
745.5577@7.163082	0.68212	0.96316	AD - CTL; AD - MCI; CTL - MCI
588.521@8.491263	0.6843	0.96316	CTL - AD; AD - MCI; CTL - MCI
621.6048@8.711067	0.68502	0.96316	AD - CTL; MCI - AD; MCI - CTL
1739.514@10.27073	0.68627	0.96316	CTL - AD; MCI - AD; MCI - CTL
1735.482@10.12215	0.68645	0.96316	CTL - AD; AD - MCI; CTL - MCI
368.3442@10.702	0.68806	0.96316	CTL - AD; AD - MCI; CTL - MCI
954.7367@7.436397	0.68857	0.96316	CTL - AD; MCI - AD; CTL - MCI
705.8029@7.330953	0.68893	0.96316	AD - CTL; MCI - AD; MCI - CTL
817.7152@9.73625	0.68973	0.96316	CTL - AD; MCI - AD; MCI - CTL
816.2496@6.052661	0.69012	0.96316	AD - CTL; MCI - AD; MCI - CTL
1043.763@6.966658	0.69267	0.96316	CTL - AD; MCI - AD; CTL - MCI
772.7448@10.6759	0.69567	0.96316	AD - CTL; MCI - AD; MCI - CTL
793.596@7.370205	0.69598	0.96316	CTL - AD; MCI - AD; MCI - CTL
1765.53@10.28371	0.69791	0.96316	AD - CTL; AD - MCI; MCI - CTL
946.2775@9.244238	0.69991	0.96316	AD - CTL; AD - MCI; MCI - CTL
977.829@10.13722	0.70002	0.96316	CTL - AD; AD - MCI; CTL - MCI
3052.216@7.030312	0.70483	0.96316	CTL - AD; AD - MCI; CTL - MCI
631.5899@8.253419	0.70691	0.96316	AD - CTL; MCI - AD; MCI - CTL
1039.916@10.28265	0.70789	0.96316	CTL - AD; MCI - AD; MCI - CTL
857.7473@9.873384	0.70878	0.96316	AD - CTL; AD - MCI; MCI - CTL
1317.403@8.303732	0.71426	0.96316	CTL - AD; MCI - AD; CTL - MCI
1154.37@8.736567	0.71471	0.96316	CTL - AD; MCI - AD; CTL - MCI
739.5113@6.95502	0.71475	0.96316	CTL - AD; AD - MCI; CTL - MCI
906.7682@10.29223	0.71608	0.96316	CTL - AD; AD - MCI; CTL - MCI
965.9152@10.4031	0.71697	0.96316	CTL - AD; MCI - AD; MCI - CTL
1598.476@9.643834	0.71759	0.96316	CTL - AD; MCI - AD; CTL - MCI
784.6436@7.977169	0.71769	0.96316	CTL - AD; AD - MCI; CTL - MCI
643.4828@0.9145122	0.71989	0.96316	AD - CTL; AD - MCI; CTL - MCI

Mass@RT	Raw *p*	FDR corrected *p*	Fisher's LSD
1009.869@9.968734	0.72114	0.96316	CTL - AD; AD - MCI; CTL - MCI
723.5188@7.253028	0.72199	0.96316	AD - CTL; MCI - AD; MCI - CTL
710.2606@6.480101	0.72206	0.96316	CTL - AD; MCI - AD; MCI - CTL
1545.165@7.508879	0.72276	0.96316	CTL - AD; AD - MCI; CTL - MCI
791.5792@7.277426	0.72344	0.96316	CTL - AD; AD - MCI; CTL - MCI
1778.491@9.393716	0.72361	0.96316	CTL - AD; MCI - AD; MCI - CTL
1513.103@6.921723	0.72378	0.96316	AD - CTL; AD - MCI; CTL - MCI
647.6204@8.717925	0.72516	0.96316	CTL - AD; AD - MCI; CTL - MCI
924.7008@7.118914	0.72801	0.96316	AD - CTL; AD - MCI; CTL - MCI
761.5953@7.935157	0.72927	0.96316	CTL - AD; MCI - AD; CTL - MCI
1743.604@10.41227	0.7301	0.96316	CTL - AD; MCI - AD; MCI - CTL
926.7178@7.579635	0.7331	0.96316	CTL - AD; MCI - AD; CTL - MCI
772.643@8.185639	0.73345	0.96316	CTL - AD; MCI - AD; CTL - MCI
729.5294@6.441341	0.73547	0.96316	CTL - AD; MCI - AD; MCI - CTL
691.6275@10.56128	0.7376	0.96316	AD - CTL; AD - MCI; CTL - MCI
847.6446@8.18031	0.7386	0.96316	AD - CTL; AD - MCI; MCI - CTL
1015.822@9.66031	0.74054	0.96316	CTL - AD; MCI - AD; CTL - MCI
1150.281@8.067189	0.74165	0.96316	CTL - AD; MCI - AD; CTL - MCI
945.8375@10.08881	0.74397	0.96316	CTL - AD; MCI - AD; CTL - MCI
733.6206@8.058771	0.74479	0.96316	CTL - AD; AD - MCI; CTL - MCI
764.7362@9.036797	0.74549	0.96316	CTL - AD; AD - MCI; CTL - MCI
900.7209@9.862691	0.74689	0.96316	AD - CTL; MCI - AD; MCI - CTL
763.569@7.951186	0.74919	0.96316	CTL - AD; AD - MCI; CTL - MCI
730.5975@7.352081	0.74923	0.96316	CTL - AD; MCI - AD; CTL - MCI
418.3072@5.721759	0.74982	0.96316	AD - CTL; MCI - AD; MCI - CTL
1376.421@9.277494	0.75423	0.96316	AD - CTL; AD - MCI; CTL - MCI
1112.323@7.780697	0.75778	0.96316	AD - CTL; MCI - AD; MCI - CTL
1704.509@10.10644	0.75782	0.96316	CTL - AD; MCI - AD; CTL - MCI
1730.527@10.12213	0.75811	0.96316	CTL - AD; AD - MCI; CTL - MCI
910.7711@9.826213	0.75849	0.96316	AD - CTL; AD - MCI; CTL - MCI
971.8532@10.11854	0.76104	0.96316	AD - CTL; AD - MCI; CTL - MCI
640.5042@8.061189	0.76121	0.96316	AD - CTL; AD - MCI; CTL - MCI
728.6673@8.262896	0.76173	0.96316	AD - CTL; MCI - AD; MCI - CTL
902.8486@7.308088	0.76626	0.96316	CTL - AD; AD - MCI; CTL - MCI
897.7788@9.998964	0.76961	0.96316	AD - CTL; AD - MCI; MCI - CTL
720.4992@7.952013	0.77147	0.96316	CTL - AD; AD - MCI; CTL - MCI
869.7478@9.820498	0.77352	0.96316	AD - CTL; AD - MCI; MCI - CTL
1942.805@10.68841	0.77485	0.96316	AD - CTL; AD - MCI; MCI - CTL
877.6908@8.807655	0.77643	0.96316	AD - CTL; AD - MCI; CTL - MCI
728.5807@6.880475	0.77662	0.96316	CTL - AD; AD - MCI; CTL - MCI
810.6576@7.962715	0.77867	0.96316	CTL - AD; AD - MCI; CTL - MCI
749.5347@7.310224	0.77926	0.96316	AD - CTL; MCI - AD; MCI - CTL
1081.778@6.844794	0.7812	0.96316	CTL - AD; AD - MCI; CTL - MCI
916.8221@10.27371	0.7829	0.96316	CTL - AD; AD - MCI; CTL - MCI
1168.334@9.779051	0.7834	0.96316	AD - CTL; MCI - AD; MCI - CTL

Mass@RT	Raw *p*	FDR corrected *p*	Fisher's LSD
942.8386@10.29269	0.7838	0.96316	AD - CTL; MCI - AD; MCI - CTL
699.6504@8.261372	0.78385	0.96316	AD - CTL; MCI - AD; MCI - CTL
994.9322@10.40212	0.78863	0.96572	CTL - AD; MCI - AD; MCI - CTL
795.6105@7.87375	0.78912	0.96572	CTL - AD; MCI - AD; CTL - MCI
747.5236@7.123257	0.79337	0.96806	CTL - AD; MCI - AD; MCI - CTL
777.5451@7.953998	0.79527	0.96806	CTL - AD; AD - MCI; CTL - MCI
943.8204@9.924993	0.79707	0.96806	AD - CTL; MCI - AD; MCI - CTL
523.3624@3.635846	0.79742	0.96806	AD - CTL; AD - MCI; MCI - CTL
999.7372@6.958735	0.80436	0.96997	CTL - AD; MCI - AD; CTL - MCI
1529.398@10.40945	0.80541	0.96997	CTL - AD; MCI - AD; CTL - MCI
609.5283@7.98348	0.80734	0.96997	AD - CTL; MCI - AD; MCI - CTL
337.3323@5.539873	0.8075	0.96997	CTL - AD; MCI - AD; CTL - MCI
977.749@7.43601	0.80915	0.96997	CTL - AD; AD - MCI; CTL - MCI
893.7472@9.755979	0.81437	0.96997	CTL - AD; MCI - AD; MCI - CTL
932.3137@7.890954	0.81474	0.96997	AD - CTL; AD - MCI; CTL - MCI
545.4076@5.016461	0.81528	0.96997	AD - CTL; AD - MCI; CTL - MCI
567.6978@7.356551	0.81684	0.96997	AD - CTL; AD - MCI; MCI - CTL
663.5947@10.36814	0.81913	0.96997	AD - CTL; AD - MCI; CTL - MCI
688.5492@6.449206	0.82293	0.96997	CTL - AD; MCI - AD; MCI - CTL
306.3254@2.596773	0.8242	0.96997	CTL - AD; MCI - AD; MCI - CTL
1921.746@10.74484	0.82484	0.96997	CTL - AD; MCI - AD; CTL - MCI
1127.307@9.779261	0.82689	0.96997	CTL - AD; MCI - AD; CTL - MCI
733.5607@7.381152	0.82801	0.96997	CTL - AD; AD - MCI; CTL - MCI
491.3938@5.020523	0.82997	0.96997	AD - CTL; MCI - AD; MCI - CTL
1249.17@10.72123	0.83	0.96997	CTL - AD; AD - MCI; CTL - MCI
790.8984@7.32809	0.83124	0.96997	CTL - AD; AD - MCI; CTL - MCI
443.3681@4.072941	0.83182	0.96997	AD - CTL; MCI - AD; MCI - CTL
866.645@7.730146	0.83315	0.96997	AD - CTL; AD - MCI; MCI - CTL
919.7651@9.832148	0.83404	0.96997	CTL - AD; MCI - AD; MCI - CTL
585.4376@5.016397	0.83414	0.96997	CTL - AD; MCI - AD; CTL - MCI
803.5703@7.950968	0.83797	0.9704	CTL - AD; MCI - AD; CTL - MCI
903.5824@6.561565	0.84001	0.9704	CTL - AD; AD - MCI; CTL - MCI
1035.793@7.429593	0.84182	0.9704	AD - CTL; AD - MCI; MCI - CTL
905.2516@9.242067	0.84222	0.9704	AD - CTL; MCI - AD; MCI - CTL
899.7956@10.13728	0.8425	0.9704	CTL - AD; AD - MCI; CTL - MCI
957.8557@10.08375	0.85592	0.98335	AD - CTL; AD - MCI; MCI - CTL
547.4938@8.480261	0.85858	0.98335	AD - CTL; AD - MCI; CTL - MCI
1260.361@8.311184	0.85861	0.98335	AD - CTL; AD - MCI; MCI - CTL
753.5289@6.369004	0.86426	0.98796	AD - CTL; AD - MCI; MCI - CTL
1345.162@10.57774	0.87216	0.99195	AD - CTL; MCI - AD; MCI - CTL
722.1365@5.347299	0.87451	0.99195	CTL - AD; MCI - AD; CTL - MCI
666.4942@5.00766	0.87739	0.99195	AD - CTL; MCI - AD; MCI - CTL
817.6255@7.432163	0.87897	0.99195	CTL - AD; AD - MCI; CTL - MCI
921.7795@9.972382	0.88029	0.99195	CTL - AD; MCI - AD; CTL - MCI
702.5659@6.758093	0.88255	0.99195	CTL - AD; MCI - AD; MCI - CTL

Mass@RT	Raw *p*	FDR corrected *p*	Fisher's LSD
762.7197@8.713416	0.88281	0.99195	CTL - AD; MCI - AD; MCI - CTL
845.7476@9.930879	0.88299	0.99195	CTL - AD; MCI - AD; CTL - MCI
1505.402@10.46347	0.88341	0.99195	CTL - AD; MCI - AD; MCI - CTL
807.5754@7.015933	0.88497	0.99195	AD - CTL; AD - MCI; CTL - MCI
390.2755@5.021452	0.88573	0.99195	AD - CTL; MCI - AD; MCI - CTL
927.8241@10.29996	0.88854	0.99326	CTL - AD; AD - MCI; CTL - MCI
641.6121@10.71867	0.89145	0.99469	AD - CTL; AD - MCI; MCI - CTL
1408.191@8.314888	0.89421	0.99593	CTL - AD; AD - MCI; CTL - MCI
812.676@8.375509	0.89657	0.99673	CTL - AD; AD - MCI; CTL - MCI
1612.445@10.37781	0.90019	0.99673	CTL - AD; AD - MCI; CTL - MCI
995.8529@9.989904	0.90148	0.99673	AD - CTL; AD - MCI; MCI - CTL
1016.928@10.51097	0.90542	0.99673	AD - CTL; AD - MCI; MCI - CTL
608.4493@5.011184	0.90665	0.99673	AD - CTL; AD - MCI; MCI - CTL
1589.427@9.174856	0.91181	0.99673	AD - CTL; MCI - AD; MCI - CTL
1524.46@9.528401	0.91181	0.99673	CTL - AD; MCI - AD; MCI - CTL
731.5454@6.899851	0.91346	0.99673	CTL - AD; AD - MCI; CTL - MCI
800.6758@8.657833	0.91419	0.99673	CTL - AD; AD - MCI; CTL - MCI
649.6361@9.038178	0.91619	0.99673	CTL - AD; MCI - AD; CTL - MCI
979.8424@10.26374	0.9177	0.99673	AD - CTL; AD - MCI; CTL - MCI
559.4329@5.753519	0.91894	0.99673	CTL - AD; MCI - AD; MCI - CTL
750.7203@8.876523	0.92324	0.99673	AD - CTL; AD - MCI; MCI - CTL
1423.38@10.21456	0.9237	0.99673	AD - CTL; AD - MCI; MCI - CTL
891.6419@7.381134	0.92729	0.99673	CTL - AD; MCI - AD; MCI - CTL
791.5414@6.555255	0.92768	0.99673	CTL - AD; MCI - AD; MCI - CTL
1290.194@10.66004	0.93394	0.99673	CTL - AD; AD - MCI; CTL - MCI
1704.467@9.305242	0.93397	0.99673	AD - CTL; MCI - AD; MCI - CTL
716.5779@7.055906	0.93517	0.99673	AD - CTL; MCI - AD; MCI - CTL
982.8687@10.11996	0.93648	0.99673	AD - CTL; MCI - AD; MCI - CTL
1527.142@7.425088	0.93673	0.99673	CTL - AD; MCI - AD; CTL - MCI
757.2134@8.692929	0.93754	0.99673	AD - CTL; AD - MCI; MCI - CTL
987.8869@10.27398	0.9391	0.99673	AD - CTL; AD - MCI; MCI - CTL
1045.868@9.995921	0.94055	0.99673	AD - CTL; MCI - AD; MCI - CTL
2089.545@10.76857	0.94103	0.99673	AD - CTL; AD - MCI; CTL - MCI
686.1929@8.336611	0.9411	0.99673	AD - CTL; AD - MCI; MCI - CTL
1019.851@9.965627	0.94155	0.99673	AD - CTL; MCI - AD; MCI - CTL
714.6589@8.251107	0.94238	0.99673	AD - CTL; MCI - AD; MCI - CTL
533.4062@5.725878	0.94364	0.99673	CTL - AD; MCI - AD; CTL - MCI
1023.735@6.847432	0.95023	0.99673	CTL - AD; MCI - AD; MCI - CTL
978.8313@9.818647	0.95345	0.99673	CTL - AD; MCI - AD; CTL - MCI
2294.667@7.031036	0.95591	0.99673	CTL - AD; MCI - AD; CTL - MCI
258.3036@2.592687	0.95745	0.99673	AD - CTL; AD - MCI; MCI - CTL
1037.901@10.1413	0.95818	0.99673	AD - CTL; AD - MCI; MCI - CTL
505.3756@5.019604	0.96004	0.99673	CTL - AD; MCI - AD; CTL - MCI
452.4326@5.539625	0.96122	0.99673	CTL - AD; AD - MCI; CTL - MCI
1450.438@9.397492	0.96378	0.99673	AD - CTL; AD - MCI; CTL - MCI

Mass@RT	Raw *p*	FDR corrected *p*	Fisher's LSD
700.5498@6.248382	0.96876	0.99673	CTL - AD; AD - MCI; CTL - MCI
1731.449@9.966222	0.96878	0.99673	AD - CTL; AD - MCI; MCI - CTL
900.6525@7.95111	0.96879	0.99673	CTL - AD; MCI - AD; CTL - MCI
1793.473@10.58367	0.96896	0.99673	AD - CTL; MCI - AD; MCI - CTL
777.5288@6.252894	0.96961	0.99673	CTL - AD; MCI - AD; MCI - CTL
704.5802@6.983054	0.9698	0.99673	AD - CTL; MCI - AD; MCI - CTL
834.2306@8.999018	0.96999	0.99673	AD - CTL; MCI - AD; MCI - CTL
959.872@10.24321	0.97061	0.99673	CTL - AD; MCI - AD; CTL - MCI
1335.392@9.278417	0.97492	0.99673	CTL - AD; MCI - AD; CTL - MCI
1617.162@7.517326	0.97552	0.99673	AD - CTL; AD - MCI; MCI - CTL
1067.76@6.849758	0.97672	0.99673	AD - CTL; MCI - AD; MCI - CTL
964.2856@7.088918	0.97724	0.99673	CTL - AD; MCI - AD; CTL - MCI
1705.439@9.94414	0.97811	0.99673	CTL - AD; MCI - AD; CTL - MCI
303.2903@1.774941	0.97897	0.99673	CTL - AD; AD - MCI; CTL - MCI
895.7636@9.874258	0.98248	0.99673	CTL - AD; MCI - AD; CTL - MCI
665.6131@10.51491	0.9829	0.99673	AD - CTL; MCI - AD; MCI - CTL
1746.562@10.39784	0.98562	0.99673	AD - CTL; MCI - AD; MCI - CTL
1004.85@9.870429	0.98612	0.99673	CTL - AD; AD - MCI; CTL - MCI
729.5682@8.084014	0.98865	0.99673	CTL - AD; MCI - AD; CTL - MCI
599.458@0.9162689	0.98898	0.99673	AD - CTL; AD - MCI; CTL - MCI
1408.396@8.719361	0.9905	0.99673	AD - CTL; AD - MCI; MCI - CTL
2385.612@10.88552	0.99436	0.99673	CTL - AD; AD - MCI; CTL - MCI
1521.076@6.984597	0.99445	0.99673	CTL - AD; MCI - AD; CTL - MCI
985.8698@10.09436	0.99509	0.99673	AD - CTL; AD - MCI; MCI - CTL
1867.494@10.61951	0.99692	0.99692	CTL - AD; AD - MCI; CTL - MCI

Supplementary Table 6. Association between lipid features (presented with monoisotopic mass and retention time, Mass@RT), detected after injection of plasma in negative ionization mode, and diagnosis of AD, MCI and control.

Mass@RT	Raw p	FDR corrected p	Fisher's LSD
270.2555@4.075092	0.002472	0.30337	AD - MCI; AD - CTL; MCI - CTL
586.492@3.838199	0.0026264	0.30337	AD - MCI; AD - CTL; MCI - CTL
803.5679@6.754498	0.0035082	0.30337	AD - MCI; AD - CTL; MCI - CTL
827.567@6.688913	0.0037097	0.30337	AD - MCI; AD - CTL; MCI - CTL
254.2244@2.893419	0.0040649	0.30337	AD - MCI; AD - CTL; CTL - MCI
1635.391@9.175343	0.0053701	0.30337	MCI - AD; CTL - AD; CTL - MCI
614.5299@3.845181	0.0057653	0.30337	AD - MCI; AD - CTL; MCI - CTL
586.5614@2.741264	0.0062592	0.30337	AD - MCI; AD - CTL; MCI - CTL
693.6213@8.615473	0.0073112	0.30337	AD - MCI; AD - CTL; MCI - CTL
310.2865@4.741278	0.0075766	0.30337	AD - MCI; AD - CTL; MCI - CTL
256.2406@3.619183	0.0079643	0.30337	AD - MCI; AD - CTL; MCI - CTL
1970.534@10.06729	0.010555	0.34866	MCI - AD; CTL - AD; MCI - CTL
743.5455@7.527302	0.010817	0.34866	MCI - AD; AD - CTL; MCI - CTL
829.619@7.894106	0.012786	0.38268	MCI - AD; AD - CTL; MCI - CTL

Mass@RT	Raw p	FDR corrected p	Fisher's LSD
671.739@7.366186	0.016448	0.45946	AD - MCI; AD - CTL; CTL - MCI
1986.464@10.09722	0.018859	0.47741	MCI - AD; AD - CTL; MCI - CTL
456.2204@3.823384	0.020909	0.47741	AD - MCI; AD - CTL; MCI - CTL
633.56@8.265013	0.021351	0.47741	AD - MCI; AD - CTL; MCI - CTL
2126.488@9.826018	0.021648	0.47741	AD - MCI; CTL - AD; CTL - MCI
657.7293@7.387804	0.025156	0.52701	MCI - AD; CTL - AD; MCI - CTL
534.4601@3.62779	0.026998	0.53868	AD - MCI; AD - CTL; MCI - CTL
382.3801@7.444489	0.029683	0.56533	MCI - AD; AD - CTL; MCI - CTL
745.5606@7.856107	0.035774	0.61476	MCI - AD; CTL - AD; MCI - CTL
1460.338@8.87776	0.036779	0.61476	MCI - AD; CTL - AD; CTL - MCI
681.6924@7.351504	0.039208	0.61476	MCI - AD; AD - CTL; MCI - CTL
282.2566@3.825725	0.041045	0.61476	AD - MCI; AD - CTL; MCI - CTL
729.5663@8.117242	0.042748	0.61476	MCI - AD; AD - CTL; MCI - CTL
1080.781@10.23194	0.043457	0.61476	MCI - AD; CTL - AD; MCI - CTL
338.2427@3.633484	0.04371	0.61476	AD - MCI; AD - CTL; CTL - MCI
466.3116@0.9092885	0.047405	0.61476	MCI - AD; AD - CTL; MCI - CTL
713.7467@7.843049	0.048155	0.61476	AD - MCI; AD - CTL; MCI - CTL
1209.88@10.92099	0.048158	0.61476	MCI - AD; AD - CTL; MCI - CTL
766.5294@8.699066	0.048418	0.61476	AD - MCI; AD - CTL; MCI - CTL
308.2708@4.06351	0.051993	0.62764	AD - MCI; AD - CTL; CTL - MCI
869.6153@7.530498	0.052428	0.62764	AD - MCI; AD - CTL; MCI - CTL
1534.355@9.030187	0.058526	0.62901	AD - MCI; CTL - AD; CTL - MCI
537.509@7.4428	0.061285	0.62901	MCI - AD; CTL - AD; CTL - MCI
1090.25@7.778246	0.06186	0.62901	MCI - AD; CTL - AD; CTL - MCI
1304.368@9.115836	0.062511	0.62901	MCI - AD; CTL - AD; MCI - CTL
362.2429@3.159128	0.063053	0.62901	AD - MCI; AD - CTL; CTL - MCI
715.4966@7.016564	0.063141	0.62901	MCI - AD; CTL - AD; MCI - CTL
734.5885@9.165747	0.063189	0.62901	AD - MCI; CTL - AD; CTL - MCI
430.2058@3.629293	0.064553	0.62901	AD - MCI; AD - CTL; MCI - CTL
392.295@0.9487602	0.069499	0.63634	MCI - AD; AD - CTL; MCI - CTL
1174.294@8.046156	0.070042	0.63634	MCI - AD; AD - CTL; MCI - CTL
2118.562@10.18498	0.071078	0.63634	MCI - AD; AD - CTL; MCI - CTL
1156.334@8.734098	0.07138	0.63634	AD - MCI; AD - CTL; CTL - MCI
284.2716@4.616582	0.075932	0.64206	AD - MCI; AD - CTL; MCI - CTL
628.5783@9.456162	0.077513	0.64206	MCI - AD; CTL - AD; MCI - CTL
1174.765@7.247752	0.081683	0.64206	AD - MCI; AD - CTL; MCI - CTL
1852.494@10.06151	0.081884	0.64206	MCI - AD; CTL - AD; CTL - MCI
366.3483@6.407446	0.082365	0.64206	AD - MCI; AD - CTL; MCI - CTL
676.5267@7.73108	0.083901	0.64206	AD - MCI; AD - CTL; MCI - CTL
944.797@10.28032	0.084626	0.64206	MCI - AD; CTL - AD; CTL - MCI
477.2857@0.9114354	0.086906	0.64206	MCI - AD; CTL - AD; MCI - CTL
304.2396@3.046623	0.087872	0.64206	AD - MCI; AD - CTL; MCI - CTL
366.274@4.614098	0.089051	0.64206	AD - MCI; AD - CTL; CTL - MCI
823.9373@7.350907	0.089424	0.64206	MCI - AD; AD - CTL; MCI - CTL
1206.877@10.91919	0.091817	0.64206	MCI - AD; AD - CTL; MCI - CTL

Mass@RT	Raw p	FDR corrected p	Fisher's LSD
1682.385@9.282221	0.094479	0.64206	MCI - AD; CTL - AD; MCI - CTL
1009.62@7.652688	0.094716	0.64206	MCI - AD; AD - CTL; MCI - CTL
1561.374@9.034982	0.095006	0.64206	AD - MCI; CTL - AD; CTL - MCI
617.5584@3.820866	0.10518	0.69952	AD - MCI; AD - CTL; MCI - CTL
803.6012@7.459167	0.10692	0.69997	MCI - AD; AD - CTL; MCI - CTL
380.2599@4.61507	0.11015	0.71004	AD - MCI; AD - CTL; MCI - CTL
791.5655@6.914985	0.11212	0.71177	MCI - AD; AD - CTL; MCI - CTL
899.5815@7.078151	0.11687	0.72887	MCI - AD; AD - CTL; MCI - CTL
845.6151@7.624812	0.11829	0.72887	MCI - AD; AD - CTL; MCI - CTL
878.768@10.41518	0.12228	0.73393	MCI - AD; AD - CTL; MCI - CTL
280.2405@3.163136	0.12261	0.73393	AD - MCI; AD - CTL; MCI - CTL
1203.255@3.826806	0.12509	0.73821	AD - MCI; AD - CTL; CTL - MCI
624.5774@8.173498	0.13068	0.75666	AD - MCI; AD - CTL; CTL - MCI
2282.527@10.31235	0.13539	0.75666	MCI - AD; CTL - AD; CTL - MCI
861.8805@7.35106	0.13824	0.75666	MCI - AD; AD - CTL; MCI - CTL
665.6293@8.770185	0.13863	0.75666	MCI - AD; AD - CTL; MCI - CTL
1655.206@7.58398	0.14228	0.75666	AD - MCI; AD - CTL; MCI - CTL
609.4629@7.820113	0.14943	0.75666	MCI - AD; CTL - AD; CTL - MCI
306.2546@3.488815	0.1505	0.75666	AD - MCI; AD - CTL; MCI - CTL
466.3121@4.061674	0.15183	0.75666	MCI - AD; AD - CTL; MCI - CTL
741.5285@7.083037	0.1527	0.75666	MCI - AD; AD - CTL; MCI - CTL
880.6083@9.658386	0.15571	0.75666	MCI - AD; CTL - AD; CTL - MCI
898.2097@6.584642	0.15772	0.75666	AD - MCI; CTL - AD; CTL - MCI
1257.015@11.26142	0.15809	0.75666	MCI - AD; AD - CTL; MCI - CTL
966.7821@10.08707	0.15836	0.75666	MCI - AD; AD - CTL; MCI - CTL
938.7385@9.88793	0.15902	0.75666	MCI - AD; CTL - AD; CTL - MCI
1011.636@8.022781	0.15959	0.75666	MCI - AD; AD - CTL; MCI - CTL
1020.804@10.20426	0.16033	0.75666	MCI - AD; CTL - AD; MCI - CTL
314.0855@7.050134	0.16428	0.75666	AD - MCI; AD - CTL; MCI - CTL
1020.225@7.076828	0.16462	0.75666	MCI - AD; CTL - AD; MCI - CTL
1579.175@7.46394	0.16671	0.75666	MCI - AD; CTL - AD; CTL - MCI
588.5131@3.639651	0.16741	0.75666	MCI - AD; AD - CTL; MCI - CTL
567.7004@7.360743	0.1693	0.75666	MCI - AD; AD - CTL; MCI - CTL
775.5511@7.627165	0.17087	0.75666	MCI - AD; CTL - AD; MCI - CTL
1062.838@10.40199	0.17759	0.75666	AD - MCI; CTL - AD; CTL - MCI
800.1028@6.760911	0.17778	0.75666	MCI - AD; CTL - AD; CTL - MCI
1056.851@10.96285	0.17856	0.75666	AD - MCI; AD - CTL; MCI - CTL
1386.32@8.711142	0.17886	0.75666	AD - MCI; CTL - AD; CTL - MCI
927.6163@7.639467	0.17997	0.75666	MCI - AD; AD - CTL; MCI - CTL
853.6183@7.833375	0.1806	0.75666	MCI - AD; AD - CTL; MCI - CTL
928.7665@10.10364	0.1834	0.75666	AD - MCI; CTL - AD; CTL - MCI
418.3287@4.748488	0.18439	0.75666	MCI - AD; CTL - AD; CTL - MCI
646.5373@8.773251	0.18807	0.75666	AD - MCI; AD - CTL; CTL - MCI
886.7095@8.611621	0.18813	0.75666	AD - MCI; AD - CTL; CTL - MCI
1575.136@7.060055	0.18905	0.75666	MCI - AD; CTL - AD; MCI - CTL

Mass@RT	Raw p	FDR corrected p	Fisher's LSD
862.557@6.534954	0.19232	0.75666	MCI - AD; CTL - AD; MCI - CTL
649.6346@9.047277	0.19355	0.75666	MCI - AD; AD - CTL; MCI - CTL
609.5139@8.260134	0.194	0.75666	MCI - AD; AD - CTL; MCI - CTL
767.5452@7.494052	0.19503	0.75666	AD - MCI; AD - CTL; MCI - CTL
406.2298@3.413454	0.19735	0.75864	MCI - AD; CTL - AD; MCI - CTL
868.1904@6.58529	0.20528	0.77652	AD - MCI; CTL - AD; CTL - MCI
748.6034@9.200956	0.20876	0.77652	MCI - AD; AD - CTL; MCI - CTL
795.9053@7.356886	0.20901	0.77652	AD - MCI; AD - CTL; MCI - CTL
886.5541@6.527361	0.20995	0.77652	AD - MCI; AD - CTL; MCI - CTL
340.2389@2.514799	0.21359	0.77652	MCI - AD; AD - CTL; MCI - CTL
2134.502@10.21573	0.21544	0.77652	MCI - AD; CTL - AD; CTL - MCI
664.5283@8.041248	0.21602	0.77652	AD - MCI; AD - CTL; CTL - MCI
364.2588@3.830391	0.2193	0.77652	AD - MCI; AD - CTL; MCI - CTL
1605.186@7.565443	0.22328	0.77652	MCI - AD; CTL - AD; CTL - MCI
474.4067@7.450848	0.22459	0.77652	AD - MCI; AD - CTL; MCI - CTL
727.5503@7.806191	0.22473	0.77652	MCI - AD; AD - CTL; MCI - CTL
1904.43@9.589234	0.22529	0.77652	AD - MCI; CTL - AD; CTL - MCI
825.5862@7.275902	0.2261	0.77652	MCI - AD; AD - CTL; MCI - CTL
604.6778@7.328922	0.23907	0.81438	MCI - AD; CTL - AD; MCI - CTL
1316.3@8.306988	0.24199	0.8177	AD - MCI; CTL - AD; CTL - MCI
1004.67@8.508281	0.24447	0.81946	AD - MCI; CTL - AD; CTL - MCI
2060.492@10.15548	0.24777	0.82392	MCI - AD; CTL - AD; CTL - MCI
564.5106@3.838582	0.25063	0.82687	AD - MCI; AD - CTL; MCI - CTL
613.7045@7.377222	0.25781	0.83143	MCI - AD; AD - CTL; MCI - CTL
888.7081@9.934292	0.25794	0.83143	MCI - AD; AD - CTL; MCI - CTL
1168.264@7.773187	0.25796	0.83143	AD - MCI; CTL - AD; CTL - MCI
952.234@7.066471	0.26044	0.83301	MCI - AD; CTL - AD; CTL - MCI
1896.504@9.995	0.26724	0.83955	MCI - AD; CTL - AD; MCI - CTL
266.1552@0.917104	0.27165	0.83955	MCI - AD; CTL - AD; CTL - MCI
382.372@6.993882	0.27183	0.83955	MCI - AD; CTL - AD; CTL - MCI
775.6063@8.856654	0.27193	0.83955	AD - MCI; AD - CTL; MCI - CTL
565.6872@7.36455	0.2725	0.83955	AD - MCI; CTL - AD; CTL - MCI
1468.34@9.462811	0.27548	0.84252	AD - MCI; AD - CTL; CTL - MCI
679.6441@8.95453	0.27929	0.84387	MCI - AD; AD - CTL; MCI - CTL
593.5717@8.349791	0.27995	0.84387	MCI - AD; CTL - AD; CTL - MCI
817.5813@7.077917	0.28346	0.84836	MCI - AD; CTL - AD; MCI - CTL
816.6329@7.497834	0.28842	0.8549	AD - MCI; AD - CTL; CTL - MCI
1230.351@8.937416	0.29201	0.8549	AD - MCI; AD - CTL; MCI - CTL
855.6337@7.911394	0.29741	0.8549	AD - MCI; CTL - AD; CTL - MCI
1014.059@7.342006	0.2986	0.8549	AD - MCI; AD - CTL; MCI - CTL
788.604@6.890119	0.3011	0.8549	AD - MCI; AD - CTL; MCI - CTL
940.7619@10.01659	0.30139	0.8549	MCI - AD; AD - CTL; MCI - CTL
168.9827@0.8980215	0.30282	0.8549	AD - MCI; AD - CTL; CTL - MCI
330.2552@3.269598	0.30398	0.8549	AD - MCI; AD - CTL; MCI - CTL
1248.915@11.0106	0.30401	0.8549	AD - MCI; AD - CTL; MCI - CTL

Mass@RT	Raw p	FDR corrected p	Fisher's LSD
298.0548@7.588399	0.30855	0.85719	AD - MCI; AD - CTL; MCI - CTL
635.619@8.892027	0.30912	0.85719	AD - MCI; AD - CTL; MCI - CTL
1838.443@9.956767	0.31297	0.85719	MCI - AD; CTL - AD; MCI - CTL
565.5412@7.914079	0.31301	0.85719	AD - MCI; CTL - AD; CTL - MCI
528.4528@8.62726	0.31664	0.85852	AD - MCI; AD - CTL; MCI - CTL
990.7796@10.02497	0.31807	0.85852	MCI - AD; CTL - AD; MCI - CTL
831.5991@7.322594	0.32219	0.85852	MCI - AD; AD - CTL; MCI - CTL
802.5753@9.19616	0.32612	0.85852	AD - MCI; AD - CTL; MCI - CTL
972.827@10.43404	0.32657	0.85852	MCI - AD; CTL - AD; CTL - MCI
851.9697@7.355388	0.32682	0.85852	MCI - AD; AD - CTL; MCI - CTL
946.2062@6.596558	0.32859	0.85852	AD - MCI; CTL - AD; CTL - MCI
872.1889@6.051651	0.33073	0.85852	AD - MCI; CTL - AD; CTL - MCI
246.1977@3.156233	0.33614	0.85852	MCI - AD; AD - CTL; MCI - CTL
255.9198@0.8787619	0.33969	0.85852	AD - MCI; AD - CTL; MCI - CTL
626.5163@7.923781	0.34091	0.85852	MCI - AD; CTL - AD; CTL - MCI
942.7818@10.14162	0.34114	0.85852	MCI - AD; CTL - AD; MCI - CTL
1044.837@10.82677	0.34556	0.85852	MCI - AD; CTL - AD; CTL - MCI
868.7177@10.27373	0.3456	0.85852	MCI - AD; CTL - AD; MCI - CTL
603.352@2.278469	0.34623	0.85852	AD - MCI; AD - CTL; CTL - MCI
875.768@10.41772	0.34915	0.85852	MCI - AD; AD - CTL; MCI - CTL
805.6179@7.887004	0.35254	0.85852	AD - MCI; AD - CTL; MCI - CTL
793.7811@6.702332	0.35364	0.85852	MCI - AD; AD - CTL; MCI - CTL
951.6164@7.535073	0.3541	0.85852	AD - MCI; AD - CTL; MCI - CTL
1608.371@9.166328	0.3556	0.85852	AD - MCI; CTL - AD; CTL - MCI
1912.457@10.03214	0.35652	0.85852	MCI - AD; CTL - AD; MCI - CTL
396.3938@7.772253	0.36563	0.87471	AD - MCI; AD - CTL; CTL - MCI
929.633@8.022272	0.36824	0.87471	MCI - AD; AD - CTL; MCI - CTL
899.9721@7.341887	0.37852	0.87471	MCI - AD; AD - CTL; MCI - CTL
1010.686@8.508702	0.37968	0.87471	MCI - AD; CTL - AD; CTL - MCI
871.6288@7.76492	0.38135	0.87471	AD - MCI; AD - CTL; MCI - CTL
298.0545@7.079425	0.3825	0.87471	MCI - AD; AD - CTL; MCI - CTL
262.2289@3.899446	0.38257	0.87471	AD - MCI; AD - CTL; MCI - CTL
150.0172@7.447442	0.38473	0.87471	AD - MCI; AD - CTL; MCI - CTL
1526.412@9.538194	0.38496	0.87471	AD - MCI; CTL - AD; CTL - MCI
606.4899@7.807484	0.38673	0.87471	MCI - AD; CTL - AD; MCI - CTL
1339.322@8.526498	0.39098	0.87471	AD - MCI; CTL - AD; CTL - MCI
878.2196@6.614951	0.39107	0.87471	MCI - AD; CTL - AD; CTL - MCI
956.7125@9.0611	0.39128	0.87471	MCI - AD; CTL - AD; MCI - CTL
555.3516@2.74756	0.39369	0.87471	AD - MCI; AD - CTL; MCI - CTL
660.4572@7.812515	0.39656	0.87471	MCI - AD; CTL - AD; MCI - CTL
278.2241@2.625063	0.39664	0.87471	AD - MCI; CTL - AD; CTL - MCI
751.5501@7.747551	0.39975	0.87694	MCI - AD; AD - CTL; MCI - CTL
667.6649@7.335101	0.40296	0.87739	AD - MCI; AD - CTL; MCI - CTL
875.7804@6.704637	0.40414	0.87739	MCI - AD; CTL - AD; MCI - CTL
538.4952@3.646798	0.40678	0.87857	AD - MCI; AD - CTL; CTL - MCI

Mass@RT	Raw p	FDR corrected p	Fisher's LSD
767.3818@8.431698	0.40954	0.87998	AD - MCI; AD - CTL; CTL - MCI
1100.277@7.760468	0.41182	0.88037	MCI - AD; CTL - AD; MCI - CTL
1857.441@9.50781	0.42107	0.88992	AD - MCI; CTL - AD; CTL - MCI
1339.012@11.26437	0.42327	0.88992	MCI - AD; AD - CTL; MCI - CTL
352.3302@2.737242	0.42715	0.88992	AD - MCI; AD - CTL; CTL - MCI
841.5792@6.967369	0.42808	0.88992	MCI - AD; AD - CTL; MCI - CTL
2074.536@10.24164	0.42856	0.88992	MCI - AD; CTL - AD; CTL - MCI
579.3521@2.34216	0.43075	0.88992	MCI - AD; AD - CTL; MCI - CTL
422.2314@0.8994756	0.43219	0.88992	AD - MCI; AD - CTL; MCI - CTL
530.4687@8.465807	0.43434	0.88992	AD - MCI; AD - CTL; MCI - CTL
1132.379@7.362415	0.4354	0.88992	MCI - AD; CTL - AD; MCI - CTL
786.5869@6.421164	0.44113	0.89563	AD - MCI; AD - CTL; MCI - CTL
166.0482@7.446527	0.443	0.89563	AD - MCI; AD - CTL; MCI - CTL
1783.422@9.407887	0.44682	0.89563	AD - MCI; AD - CTL; MCI - CTL
416.3556@6.945403	0.44733	0.89563	MCI - AD; CTL - AD; CTL - MCI
166.0482@7.049704	0.44888	0.89563	MCI - AD; AD - CTL; MCI - CTL
918.7763@10.27377	0.45382	0.90119	MCI - AD; CTL - AD; CTL - MCI
678.5429@8.048443	0.45624	0.90172	AD - MCI; AD - CTL; MCI - CTL
773.5349@7.207838	0.46282	0.91043	MCI - AD; CTL - AD; MCI - CTL
795.4152@8.808328	0.47305	0.92521	AD - MCI; AD - CTL; MCI - CTL
687.7425@7.354784	0.47595	0.92521	AD - MCI; AD - CTL; MCI - CTL
952.6829@8.021495	0.47696	0.92521	MCI - AD; AD - CTL; MCI - CTL
1134.391@7.359352	0.48086	0.92726	AD - MCI; AD - CTL; MCI - CTL
224.0352@7.080448	0.48846	0.92726	MCI - AD; CTL - AD; CTL - MCI
749.5353@7.331657	0.48864	0.92726	MCI - AD; AD - CTL; MCI - CTL
841.5801@6.689997	0.48958	0.92726	MCI - AD; AD - CTL; MCI - CTL
923.5816@6.95791	0.4926	0.92726	MCI - AD; AD - CTL; MCI - CTL
583.3841@3.648111	0.49268	0.92726	AD - MCI; AD - CTL; CTL - MCI
337.3336@5.531845	0.49443	0.92726	AD - MCI; AD - CTL; MCI - CTL
430.3797@7.280397	0.49572	0.92726	AD - MCI; AD - CTL; MCI - CTL
372.0742@8.28294	0.499	0.92925	AD - MCI; AD - CTL; CTL - MCI
925.6004@7.207539	0.50344	0.93337	AD - MCI; AD - CTL; MCI - CTL
1117.267@7.7818	0.50631	0.93455	AD - MCI; AD - CTL; MCI - CTL
949.2057@6.59614	0.51436	0.93904	MCI - AD; AD - CTL; MCI - CTL
1822.494@9.923573	0.51705	0.93904	MCI - AD; CTL - AD; MCI - CTL
1630.434@9.820328	0.51851	0.93904	AD - MCI; AD - CTL; MCI - CTL
801.7437@8.263937	0.52343	0.93904	MCI - AD; AD - CTL; MCI - CTL
844.5903@6.774294	0.52395	0.93904	MCI - AD; CTL - AD; CTL - MCI
240.067@7.049735	0.52436	0.93904	MCI - AD; AD - CTL; MCI - CTL
749.6112@8.884564	0.52443	0.93904	MCI - AD; AD - CTL; MCI - CTL
1378.386@9.273844	0.52821	0.93918	MCI - AD; CTL - AD; MCI - CTL
968.7972@10.23271	0.52899	0.93918	MCI - AD; CTL - AD; MCI - CTL
627.3526@2.178736	0.54069	0.95177	AD - MCI; CTL - AD; CTL - MCI
820.6399@9.67819	0.54294	0.95177	MCI - AD; CTL - AD; CTL - MCI
1713.205@7.625144	0.54425	0.95177	MCI - AD; CTL - AD; CTL - MCI

Mass@RT	Raw p	FDR corrected p	Fisher's LSD
1704.454@9.910536	0.54739	0.95177	AD - MCI; AD - CTL; MCI - CTL
895.2104@6.584989	0.55009	0.95177	MCI - AD; CTL - AD; CTL - MCI
899.8139@10.43862	0.55535	0.95177	AD - MCI; AD - CTL; MCI - CTL
762.5864@6.768826	0.55573	0.95177	MCI - AD; AD - CTL; MCI - CTL
916.7682@10.1203	0.55959	0.95177	AD - MCI; CTL - AD; CTL - MCI
846.6806@8.505761	0.56	0.95177	MCI - AD; AD - CTL; MCI - CTL
1180.397@7.379596	0.56781	0.95177	AD - MCI; AD - CTL; MCI - CTL
1764.419@9.883121	0.56964	0.95177	MCI - AD; CTL - AD; CTL - MCI
793.5824@7.429101	0.57458	0.95177	MCI - AD; AD - CTL; MCI - CTL
481.3153@2.747491	0.57793	0.95177	AD - MCI; AD - CTL; CTL - MCI
302.26@4.624677	0.58172	0.95177	AD - MCI; AD - CTL; MCI - CTL
695.6136@7.330896	0.58575	0.95177	MCI - AD; AD - CTL; MCI - CTL
928.6832@8.507815	0.58692	0.95177	MCI - AD; CTL - AD; MCI - CTL
805.5788@7.217164	0.58921	0.95177	MCI - AD; AD - CTL; MCI - CTL
695.6743@9.338923	0.58979	0.95177	MCI - AD; CTL - AD; CTL - MCI
860.6958@8.777534	0.59417	0.95177	MCI - AD; AD - CTL; MCI - CTL
1038.717@9.061782	0.59458	0.95177	MCI - AD; AD - CTL; MCI - CTL
1164.263@8.06108	0.5946	0.95177	MCI - AD; CTL - AD; CTL - MCI
962.7523@9.840564	0.5947	0.95177	MCI - AD; AD - CTL; MCI - CTL
747.7182@7.327138	0.59814	0.95177	AD - MCI; AD - CTL; MCI - CTL
1094.246@7.445204	0.60069	0.95177	MCI - AD; CTL - AD; CTL - MCI
760.5705@6.26726	0.60543	0.95177	AD - MCI; AD - CTL; CTL - MCI
446.0922@7.130357	0.60795	0.95177	MCI - AD; AD - CTL; MCI - CTL
1616.381@9.698575	0.60967	0.95177	AD - MCI; AD - CTL; MCI - CTL
564.6806@7.363884	0.61037	0.95177	AD - MCI; AD - CTL; MCI - CTL
747.6001@8.589078	0.61228	0.95177	AD - MCI; AD - CTL; CTL - MCI
712.6336@9.048402	0.61299	0.95177	AD - MCI; CTL - AD; CTL - MCI
326.1911@0.9177756	0.61407	0.95177	MCI - AD; CTL - AD; CTL - MCI
663.6497@9.173032	0.61569	0.95177	AD - MCI; AD - CTL; CTL - MCI
1314.412@7.351956	0.61595	0.95177	MCI - AD; CTL - AD; MCI - CTL
669.5845@8.587976	0.61806	0.95177	AD - MCI; CTL - AD; CTL - MCI
932.7923@10.36507	0.62329	0.95177	AD - MCI; AD - CTL; CTL - MCI
874.7027@9.059296	0.62449	0.95177	MCI - AD; CTL - AD; MCI - CTL
739.6632@9.042378	0.62531	0.95177	AD - MCI; AD - CTL; MCI - CTL
777.5732@7.761169	0.63066	0.95177	AD - MCI; CTL - AD; CTL - MCI
567.6964@7.020106	0.63153	0.95177	AD - MCI; AD - CTL; MCI - CTL
501.285@0.9115115	0.63318	0.95177	AD - MCI; AD - CTL; MCI - CTL
1265.304@8.317414	0.64083	0.95177	AD - MCI; CTL - AD; CTL - MCI
953.6318@7.773795	0.64109	0.95177	AD - MCI; AD - CTL; MCI - CTL
914.7498@9.970864	0.6425	0.95177	MCI - AD; CTL - AD; MCI - CTL
853.6181@7.391542	0.64305	0.95177	AD - MCI; CTL - AD; CTL - MCI
721.5862@8.550552	0.64487	0.95177	MCI - AD; AD - CTL; MCI - CTL
1003.604@7.638888	0.64549	0.95177	AD - MCI; AD - CTL; MCI - CTL
858.6828@8.295018	0.64579	0.95177	MCI - AD; AD - CTL; MCI - CTL
803.6018@7.811677	0.64635	0.95177	AD - MCI; AD - CTL; MCI - CTL

Mass@RT	Raw p	FDR corrected p	Fisher's LSD
630.7059@7.338646	0.64738	0.95177	MCI - AD; CTL - AD; CTL - MCI
294.1846@0.9122928	0.66394	0.9652	MCI - AD; AD - CTL; MCI - CTL
839.5648@6.619895	0.66623	0.9652	MCI - AD; CTL - AD; CTL - MCI
790.6189@7.390762	0.66705	0.9652	MCI - AD; AD - CTL; MCI - CTL
723.5192@7.263705	0.66771	0.9652	MCI - AD; AD - CTL; MCI - CTL
843.5981@7.203787	0.66804	0.9652	MCI - AD; AD - CTL; MCI - CTL
759.5973@8.425959	0.67077	0.96581	AD - MCI; AD - CTL; CTL - MCI
832.6607@8.265459	0.67853	0.97095	MCI - AD; AD - CTL; MCI - CTL
1690.398@9.793382	0.6805	0.97095	MCI - AD; AD - CTL; MCI - CTL
328.2396@2.811327	0.68129	0.97095	MCI - AD; AD - CTL; MCI - CTL
306.3258@2.738293	0.68689	0.97562	MCI - AD; AD - CTL; MCI - CTL
372.0745@7.97957	0.69062	0.9776	MCI - AD; CTL - AD; CTL - MCI
789.5503@6.459791	0.69301	0.97768	MCI - AD; AD - CTL; MCI - CTL
683.2847@6.986095	0.6966	0.97945	MCI - AD; AD - CTL; MCI - CTL
753.5549@0.9127842	0.70294	0.98173	MCI - AD; AD - CTL; MCI - CTL
937.7109@8.902461	0.70614	0.98173	AD - MCI; CTL - AD; CTL - MCI
765.5316@7.033838	0.70644	0.98173	MCI - AD; AD - CTL; MCI - CTL
842.5747@6.266425	0.7076	0.98173	AD - MCI; AD - CTL; MCI - CTL
566.4404@8.473511	0.7154	0.98726	AD - MCI; AD - CTL; MCI - CTL
1242.283@8.059021	0.71649	0.98726	AD - MCI; CTL - AD; CTL - MCI
1600.43@9.651221	0.71865	0.98726	MCI - AD; AD - CTL; MCI - CTL
830.6038@9.228494	0.72792	0.98904	AD - MCI; AD - CTL; MCI - CTL
699.5242@6.976769	0.72838	0.98904	MCI - AD; CTL - AD; CTL - MCI
378.2797@7.001453	0.73165	0.98904	AD - MCI; CTL - AD; CTL - MCI
821.1918@6.053569	0.7331	0.98904	MCI - AD; CTL - AD; MCI - CTL
844.6654@8.036557	0.73792	0.98904	AD - MCI; AD - CTL; MCI - CTL
930.78@10.22842	0.74057	0.98904	MCI - AD; CTL - AD; CTL - MCI
901.6012@7.469654	0.74685	0.98904	MCI - AD; CTL - AD; MCI - CTL
904.7653@10.23203	0.74722	0.98904	MCI - AD; AD - CTL; MCI - CTL
897.6443@7.893804	0.75069	0.98904	AD - MCI; CTL - AD; CTL - MCI
582.4445@7.825049	0.75415	0.98904	MCI - AD; CTL - AD; CTL - MCI
717.5297@7.395051	0.75631	0.98904	MCI - AD; CTL - AD; MCI - CTL
862.5464@9.187845	0.75752	0.98904	AD - MCI; AD - CTL; CTL - MCI
1413.339@8.710682	0.76083	0.98904	AD - MCI; CTL - AD; CTL - MCI
954.6995@8.449994	0.76489	0.98904	MCI - AD; AD - CTL; MCI - CTL
1674.449@9.752429	0.76648	0.98904	MCI - AD; AD - CTL; MCI - CTL
827.6031@7.379742	0.76833	0.98904	AD - MCI; AD - CTL; CTL - MCI
2340.6@10.3331	0.7686	0.98904	MCI - AD; CTL - AD; MCI - CTL
1599.131@7.024176	0.77332	0.98904	AD - MCI; AD - CTL; MCI - CTL
2266.596@10.28768	0.77508	0.98904	MCI - AD; CTL - AD; CTL - MCI
2192.572@10.2401	0.77519	0.98904	MCI - AD; CTL - AD; CTL - MCI
621.6035@8.719591	0.77582	0.98904	AD - MCI; AD - CTL; CTL - MCI
1778.469@9.984798	0.7785	0.98904	AD - MCI; CTL - AD; CTL - MCI
870.6816@8.015265	0.77894	0.98904	MCI - AD; AD - CTL; MCI - CTL
829.7762@8.264398	0.78592	0.98904	MCI - AD; CTL - AD; CTL - MCI

Mass@RT	Raw p	FDR corrected p	Fisher's LSD
698.617@8.884568	0.79146	0.98904	AD - MCI; CTL - AD; CTL - MCI
739.5125@6.985776	0.79278	0.98904	MCI - AD; AD - CTL; MCI - CTL
791.7052@6.414154	0.79433	0.98904	MCI - AD; CTL - AD; CTL - MCI
895.6289@7.639768	0.79989	0.98904	MCI - AD; AD - CTL; MCI - CTL
388.1052@7.438978	0.80237	0.98904	MCI - AD; AD - CTL; MCI - CTL
727.5389@6.454489	0.80312	0.98904	AD - MCI; CTL - AD; CTL - MCI
833.6003@7.754013	0.80398	0.98904	AD - MCI; AD - CTL; MCI - CTL
422.3068@6.979189	0.80824	0.98904	AD - MCI; CTL - AD; CTL - MCI
872.6971@8.444492	0.81012	0.98904	MCI - AD; AD - CTL; MCI - CTL
940.6828@8.302088	0.81499	0.98904	MCI - AD; CTL - AD; CTL - MCI
1542.36@9.586532	0.81777	0.98904	AD - MCI; CTL - AD; CTL - MCI
1082.319@8.491274	0.81852	0.98904	MCI - AD; CTL - AD; CTL - MCI
891.5955@6.909632	0.81891	0.98904	MCI - AD; CTL - AD; CTL - MCI
737.5363@7.512155	0.81942	0.98904	AD - MCI; CTL - AD; CTL - MCI
1191.286@8.062442	0.8208	0.98904	AD - MCI; CTL - AD; CTL - MCI
654.5447@8.319116	0.82143	0.98904	MCI - AD; CTL - AD; CTL - MCI
166.9864@0.8975194	0.8219	0.98904	AD - MCI; AD - CTL; MCI - CTL
1978.45@9.675071	0.82233	0.98904	MCI - AD; CTL - AD; CTL - MCI
1709.406@9.296441	0.82417	0.98904	AD - MCI; CTL - AD; CTL - MCI
1095.061@0.891619	0.82471	0.98904	MCI - AD; CTL - AD; CTL - MCI
1756.401@9.394732	0.83381	0.98904	AD - MCI; AD - CTL; MCI - CTL
1748.469@9.840881	0.83437	0.98904	MCI - AD; AD - CTL; MCI - CTL
829.7152@7.326677	0.83767	0.98904	MCI - AD; CTL - AD; CTL - MCI
2356.554@10.35842	0.83986	0.98904	AD - MCI; CTL - AD; CTL - MCI
1120.717@9.060571	0.84477	0.98904	AD - MCI; CTL - AD; CTL - MCI
1390.317@8.520737	0.84893	0.98904	AD - MCI; CTL - AD; CTL - MCI
801.5872@7.386083	0.85347	0.98904	AD - MCI; AD - CTL; MCI - CTL
535.6401@6.836503	0.85394	0.98904	AD - MCI; AD - CTL; MCI - CTL
1042.104@7.397967	0.85482	0.98904	AD - MCI; CTL - AD; CTL - MCI
847.6302@8.015558	0.85632	0.98904	MCI - AD; AD - CTL; MCI - CTL
662.7532@7.845572	0.85773	0.98904	MCI - AD; AD - CTL; MCI - CTL
368.3627@7.147114	0.86001	0.98904	MCI - AD; AD - CTL; MCI - CTL
734.5556@6.148917	0.86334	0.98904	MCI - AD; AD - CTL; MCI - CTL
649.6342@6.834196	0.86357	0.98904	AD - MCI; AD - CTL; MCI - CTL
1631.205@7.618723	0.86551	0.98904	MCI - AD; CTL - AD; MCI - CTL
1312.3@8.523244	0.86623	0.98904	MCI - AD; AD - CTL; MCI - CTL
946.8123@10.43749	0.87373	0.98904	MCI - AD; CTL - AD; CTL - MCI
650.5149@7.654854	0.87687	0.98904	AD - MCI; CTL - AD; CTL - MCI
2000.523@10.18557	0.87758	0.98904	MCI - AD; CTL - AD; CTL - MCI
709.7241@7.356794	0.87896	0.98904	AD - MCI; AD - CTL; MCI - CTL
688.5894@9.185258	0.8791	0.98904	MCI - AD; AD - CTL; MCI - CTL
735.5974@8.724844	0.88237	0.98904	AD - MCI; AD - CTL; MCI - CTL
566.6944@7.362887	0.88313	0.98904	MCI - AD; AD - CTL; MCI - CTL
914.6711@8.25771	0.88316	0.98904	AD - MCI; AD - CTL; MCI - CTL
947.5843@6.857738	0.8867	0.98904	MCI - AD; CTL - AD; CTL - MCI

Mass@RT	Raw p	FDR corrected p	Fisher's LSD
651.7253@7.355584	0.88684	0.98904	MCI - AD; CTL - AD; CTL - MCI
964.7638@9.97777	0.888	0.98904	AD - MCI; CTL - AD; CTL - MCI
424.4268@8.324709	0.8899	0.98904	MCI - AD; AD - CTL; MCI - CTL
1002.801@10.56875	0.89367	0.9906	AD - MCI; AD - CTL; CTL - MCI
1487.352@8.88495	0.89828	0.99309	AD - MCI; CTL - AD; CTL - MCI
751.5919@9.199992	0.90095	0.99341	AD - MCI; AD - CTL; MCI - CTL
865.5806@6.626831	0.90712	0.99453	MCI - AD; CTL - AD; MCI - CTL
753.5551@6.541616	0.90957	0.99453	MCI - AD; AD - CTL; MCI - CTL
573.536@8.263888	0.91091	0.99453	MCI - AD; CTL - AD; MCI - CTL
791.6548@9.056418	0.91146	0.99453	AD - MCI; AD - CTL; CTL - MCI
2052.465@9.754786	0.91812	0.99716	AD - MCI; CTL - AD; CTL - MCI
1026.258@7.454004	0.92108	0.99716	AD - MCI; AD - CTL; MCI - CTL
1452.398@9.414979	0.92393	0.99716	AD - MCI; CTL - AD; CTL - MCI
747.5182@7.124533	0.92567	0.99716	MCI - AD; AD - CTL; MCI - CTL
652.5278@7.998206	0.92931	0.99716	AD - MCI; AD - CTL; MCI - CTL
794.1722@6.05669	0.93367	0.99716	MCI - AD; CTL - AD; MCI - CTL
1830.421@9.496582	0.9343	0.99716	AD - MCI; AD - CTL; CTL - MCI
893.6143@7.404487	0.93534	0.99716	AD - MCI; AD - CTL; MCI - CTL
865.5828@6.847401	0.93559	0.99716	MCI - AD; CTL - AD; CTL - MCI
693.6587@9.082807	0.94078	0.99716	MCI - AD; CTL - AD; CTL - MCI
1036.703@8.452739	0.94588	0.99716	MCI - AD; CTL - AD; CTL - MCI
1118.703@8.455143	0.94941	0.99716	AD - MCI; AD - CTL; MCI - CTL
2208.54@10.26592	0.95513	0.99716	AD - MCI; AD - CTL; CTL - MCI
819.5987@7.467992	0.95529	0.99716	MCI - AD; CTL - AD; CTL - MCI
927.521@6.536581	0.95605	0.99716	MCI - AD; CTL - AD; MCI - CTL
811.7525@9.698566	0.95632	0.99716	MCI - AD; CTL - AD; CTL - MCI
763.6281@9.046785	0.95851	0.99716	AD - MCI; AD - CTL; MCI - CTL
739.355@8.015241	0.95915	0.99716	AD - MCI; CTL - AD; CTL - MCI
1629.191@7.506148	0.9605	0.99716	MCI - AD; AD - CTL; MCI - CTL
637.354@2.747553	0.96164	0.99716	MCI - AD; AD - CTL; MCI - CTL
372.0741@7.133225	0.9666	0.99716	MCI - AD; CTL - AD; MCI - CTL
674.5972@8.909329	0.96755	0.99716	MCI - AD; CTL - AD; CTL - MCI
680.5593@8.355327	0.9686	0.99716	AD - MCI; CTL - AD; CTL - MCI
1556.414@9.724865	0.98193	0.99832	AD - MCI; AD - CTL; CTL - MCI
1659.355@8.475827	0.98425	0.99832	AD - MCI; AD - CTL; MCI - CTL
446.0925@7.592075	0.98833	0.99832	MCI - AD; AD - CTL; MCI - CTL
733.5833@8.419053	0.99044	0.99832	MCI - AD; CTL - AD; CTL - MCI
372.0744@7.592812	0.99174	0.99832	MCI - AD; CTL - AD; CTL - MCI
815.565@6.626442	0.99185	0.99832	MCI - AD; CTL - AD; CTL - MCI
314.0859@7.445667	0.99202	0.99832	AD - MCI; CTL - AD; CTL - MCI
790.6472@9.698031	0.99474	0.99832	MCI - AD; CTL - AD; CTL - MCI
1014.809@10.89464	0.99803	0.99832	MCI - AD; CTL - AD; MCI - CTL
702.5433@7.975122	0.99826	0.99832	AD - MCI; AD - CTL; CTL - MCI
818.6499@7.971651	0.99827	0.99832	MCI - AD; AD - CTL; MCI - CTL
581.3681@2.906709	0.99832	0.99832	MCI - AD; AD - CTL; MCI - CTL

RELATED ARTICLE

The experimental part of the following article was partially carried out by Faridé Dakterzada during the performance of her Ph.D. research work, and it contains a part of the results presented in this thesis.

SLEEPJ, 2021, 1–9

doi: 10.1093/sleep/zsaa147
Advance Access Publication Date: 7 August 2020
Original Article

ORIGINAL ARTICLE

Decrease in sleep depth is associated with higher cerebrospinal fluid neurofilament light levels in patients with Alzheimer's disease

Adriano Targa[1,2,†], Faride Dakterzada[3,†], Ivan Benítez[1,2], Ricard López[3], Montserrat Pujol[1], Mireia Dalmases[1,2], Alfonso Arias[3], Manuel Sánchez-de-la-Torre[1,2], Henrik Zetterberg[4,5,6], Kaj Blennow[6,7], Reinald Pamplona[8], Mariona Jové[8], Ferran Barbé[1,2] and Gerard Piñol-Ripoll[3,*]

[1]Translational Research in Respiratory Medicine, Hospital Universitari Arnau de Vilanova-Santa Maria, IRBLleida, Lleida, Spain, [2]Centro de Investigación Biomédica en Red de Enfermedades Respiratorias (CIBERES), Madrid, Spain, [3]Unitat Trastorns Cognitius, Clinical Neuroscience Research, Santa Maria University Hospital, IRBLleida, Lleida, Spain, [4]Department of Molecular Neuroscience, UCL Institute of Neurology, Queen Square, London, UK, [5]UK Dementia Research Institute, London, UK, [6]Department of Psychiatry and Neurochemistry, Institute of Neuroscience and Physiology, Sahlgrenska University Hospital, University of Gothenburg, Mölndal, Sweden, [7]Clinical Neurochemistry Laboratory, Sahlgrenska University Hospital, Mölndal, Sweden and [8]Experimental Medicine Department, IRBLleida, University of Lleida, Lleida, Spain

[†]Co-first authors. A.T. and F.D. contributed equally to this study.

[*]Corresponding author. Gerard Piñol-Ripoll, Cognitive Disorders Unit, Hospital Universitari Santa Maria, Rovira Roure no. 44, 25198 Lleida, Spain. Email: gerard_437302@hotmail.com.

Abstract

Study Objectives: The majority of studies investigating the association between sleep and Alzheimer's disease (AD) biomarkers have been performed in healthy participants. Our objective was to investigate the association between sleep and several biomarkers that reflect distinct aspects of AD physiopathology.

Methods: The cohort included 104 individuals with mild-moderate AD. The participants were submitted to one-night polysomnography, and cerebrospinal fluid was collected in the following morning to measure the selected biomarkers associated with amyloid deposition, tau pathology, neurodegeneration, axonal damage, synaptic integrity, neuroinflammation, and oxidative damage.

Results: There was a positive correlation between neurofilament light (NF-L) and the time spent in stage 1 of non-rapid eyes movement (NREM) (N1) sleep and a negative correlation between this marker and the time spent in stage 3 of NREM (N3) sleep. Accordingly, we observed that deep sleep was associated with lower levels of NF-L, whereas light sleep increased the probability of having higher levels of this marker. Furthermore, chitinase-3-like-1 (YKL-40) was negatively correlated with sleep efficiency, the time spent in stage 2 of NREM (N2) sleep, and the time spent in N3 sleep. Conversely, there was a positive correlation between N3 sleep and the oxidative protein damage markers N-ε-(carboxyethyl)lysine and N-ε-(malondialdehyde)lysine.

Conclusions: There were significant correlations between sleep parameters and AD biomarkers related to axonal damage and neuroinflammation, such as NF-L and YKL-40. A lack of deep sleep was associated with higher levels of NF-L. This highlights a potential role for NF-L as a biomarker of sleep disruption in patients with mild-moderate AD in addition to its role in predicting neurodegeneration and cognitive decline.

Statement of Significance

This study is the first to report an association between sleep and several biomarkers that reflect distinct aspects of Alzheimer's disease (AD) physiopathology in a population of patients with AD. Such investigation addressed the importance of sleep depth in maintaining lower levels of neurofilament light (NF-L), a marker for axonal damage that also predicts the cognitive decline of patients with AD. Further studies using different approaches and performed in distinct cohorts of patients will be necessary to confirm the potential role of NF-L as a marker for sleep disruption. In case of a positive outcome, sleep-based interventions could be considered to prevent the axonal damage and possibly the cognitive decline.

Key words: Alzheimer's disease; biomarkers; sleep; NF-L; YKL-40

Submitted: 28 February, 2020; **Revised:** 16 July, 2020

Introduction

Alzheimer's disease (AD) is a highly incapacitating and prevalent neurodegenerative disorder considered one of the largest public health and economic challenges of this century [1]. The main hallmarks of this disease are the deposition of amyloid-beta (Aβ) protein, the formation of tau protein neurofibrillary tangles (NFTs), and neurodegeneration [2]. These events precede the loss of cognitive function by years or decades. In addition, noncognitive signs, such as anxiety, depression, olfactory dysfunction, and sleep disturbances, which drastically affect patients' quality of life, may appear before cognitive symptoms [3–6].

The levels of AD biomarkers measured by positron emission tomography (PET) or assessed in cerebrospinal fluid (CSF), especially Aβ42 protein, total-tau (T-tau), and phospho-tau (P-tau), are strongly correlated with the levels in the brain [7–9]. Such assessments increase the possibility of an early diagnosis [10]. Accordingly, studies have suggested that biomarkers should be used to classify patients regardless of clinical symptoms or disease stage [11]. In addition, the study of biomarkers in recent years has shed light on distinct physiological events associated with the progression of the disease, such as disrupted sleep [10]. During the sleep–wake cycle, Aβ levels fluctuate in a circadian pattern such that there is an increase in the Aβ concentration during wakefulness and a decrease during sleep [12, 13]. Furthermore, animal studies have shown that Aβ levels are increased after acute sleep deprivation and infusion of orexin, a neurotransmitter that improves wakefulness [14]. This has been confirmed by some studies in humans [15], whereas others have failed to demonstrate the same results [16]. Nevertheless, Aβ clearance is demonstrably increased during sleep, especially in slow-wave sleep (SWS) [17]. A similar relationship between sleep and tau protein accumulation, the second pathological hallmark of AD, was recently proposed [18, 19]. However, studies on patients with AD are needed given that the above-mentioned investigations were predominantly performed in cognitively normal participants. In addition, a variety of molecules have recently emerged as potential AD biomarkers, but their relationship with sleep remains to be fully elucidated [20–23]. Furthermore, considering the modifiable nature of sleep and its influence on memory consolidation, the identification of markers for sleep disruption at the early stages of the disease could contribute to the implementation of sleep-based strategies aiming to prevent the cognitive decline.

Based on this, we investigated the association between sleep and several CSF biomarkers in patients with mild-moderate AD. The investigated markers reflect different aspects of AD physiopathology: amyloid deposition (Aβ42), tau pathology (P-tau), neurodegeneration (T-tau), axonal damage (neurofilament light [NF-L]), synaptic integrity (neurogranin), microglial activation (soluble variant of the triggering receptor expressed on myeloid cells 2 [sTREM2]), neuroinflammation (chitinase-3-like-1 [YKL-40]), other types of neuronal injury (orexin and leptin), and protein oxidative damage (glutamic semialdehyde [GSA], aminoadipic semialdehyde [AASA], N-ε-(carboxyethyl)lysine [CEL], N-ε-(malondialdehyde)lysine [MDAL], and N-ε-(carboxymethyl)lysine [CML]).

Methods

Study population

This was an ancillary study of a prospective trial designed to evaluate the influence of obstructive sleep apnea on the cognitive evolution of patients with AD after a 1-year follow-up (NCT02814045). Patients were recruited from the Cognitive Disorders Unit at the Hospital Universitari Santa Maria (Lleida, Spain) for 4 years (2014–2018). Eligibility criteria included drug-naïve participants aged above 60 years who were diagnosed with AD according to the National Institute on Aging and Alzheimer's Association criteria [24]. Additionally, only patients with mild-moderate cognitive impairment (mini-mental state examination [MMSE]≥20) were included. The patient, the responsible caregiver, and the legal representative (when different from the responsible caregiver) signed an informed consent form.

The exclusion criteria were as follows: (1) the presence of visual and/or communication problems that could make adherence with the study procedures difficult; (2) the presence of a previously diagnosed sleep disorder; (3) the presence of excessive somnolence for unknown reasons; (4) comorbidities, such as cancer, severe depression, severe renal or hepatic insufficiency, severe cardiac, or respiratory failure; (5) excessive alcohol intake (>280 g/week); (6) MRI evidence of hydrocephalus, stroke, a space-occupying lesion, or any clinically relevant central nervous system disease other than AD; (7) the presence of mental disorders according to DSM-V-TR criteria; (8) any-time use of medication under investigation or the use of beta-blockers, antidepressants, neuroleptics, or hypnotics fewer than 15 days before the conduction of polysomnography (PSG); (9) the presence of untreated (or treated for less than 3 months prior to the screening visit) vitamin B12 or folate deficiency; and (10) the presence of untreated thyroid disease.

Study design

The patients arrived at the Cognitive Disorders Unit of Hospital Universitari Santa Maria (Lleida, Spain) and were assessed for eligibility. Eligible patients were submitted to overnight PSG, and in the following morning, CSF and blood were collected to determine the levels of the biomarkers. Only patients who underwent PSG and from whom CSF was collected were included in the study.

Neuropsychological assessment

The MMSE was used to include only patients with mild-moderate cognitive impairment. The MMSE includes questions to evaluate different domains, such as attention, time and place orientation, and word recall. The scores of this test range from 0 to 30, and a higher score indicates better cognitive function [25, 26].

Clinical variables

The following variables were collected: age, sex, years of education, toxic habits (alcohol consumption and smoking), vascular risk factors (hypertension, diabetes mellitus, dyslipidemia, stroke, and cardiopathy), personal psychiatric history, and family psychiatric and neurological history. Body mass index (BMI) was calculated as body weight (in kg)/height (in m^2).

Polysomnography

To assess sleep–wake parameters, we performed a PSG during the night (Philips Respironics Alice 6 LDx, Somnomedics, Somnoscreen plus Versión 2.7.0, and ApneaLink Resmed). The measured PSG variables were sleep efficiency (in %, defined as the ratio between total sleep time and the time spent in bed), latency to stage 1 of non-rapid eyes movement (NREM) sleep (N1) (in minutes, defined as the time spent awake until the first sleep episode while in bed), latency to rapid eyes movement (REM) sleep (in minutes, defined as the time until the first REM sleep episode while in bed), the time spent in N1 stage (%, defined as the percentage of time spent in N1 while sleeping), the time spent in stage 2 of NREM sleep (N2) (%, defined as the percentage of time spent in N2 while sleeping), the time spent in stage 3 of NREM sleep (N3) (also known as SWS) (%, defined as the percentage of time spent in N3 while sleeping), the time in REM sleep (%, defined as the percentage of time spent in REM sleep while sleeping), and the apnea-hypopnea index (AHI) (defined as the number of apnea and hypopnea events per hour during the time spent sleeping).

CSF biomarkers

CSF samples were collected between 8:00 am and 10:00 am to avoid variations related to the circadian rhythm. The samples were collected in polypropylene tubes, centrifuged at 2000 × *g* for 10 min at 4°C, immediately frozen, and stored within 4 hours in a –80°C freezer. Later, they were used for biomarkers analysis.

The concentration of neurogranin was measured using an in-house enzyme-linked immunosorbent assay (ELISA) as previously described in detail [27]. The CSF sTREM2 concentration was measured using an in-house immunoassay with electrochemiluminescent detection on a Meso Scale Discovery instrument (MSD, Rockville, MD) as previously described in detail [28]. The orexin concentration was measured using an in-house radioimmunoassay as previously described [29]. YKL-40, NF-L, and leptin were measured by commercial ELISA kits (Quidel, San Diego, CA; UmanDiagnostics, Sweden; and R&D Systems, Minneapolis, MN, respectively). The core AD biomarkers (Aβ42, T-tau, and P-tau) were measured using commercial kits (Innotest β-Amyloid1-42; Innotest hTAU Ag; and Innotest Phospho-TAU181P, Fujirebio-Europe, Gent, Belgium). All measurements were performed in one round of experiments using one batch of reagents by board-certified laboratory technicians who were blinded to the clinical data. The intra-assay coefficients of variation were lower than 10% for internal quality control samples (two per plate).

We measured five protein oxidation-derived markers. Two of them, GSA and AASA, are markers of direct oxidative damage to proteins, whereas CEL is a marker of indirect protein oxidation derived from carbohydrate oxidation/glycolysis. CML is a mixed oxidation marker derived from the oxidation of carbohydrates and lipids, and MDAL is a marker of indirect protein oxidation derived from the oxidation of lipids.

The concentration of these markers was measured as trifluoroacetic acid methyl ester derivates in acid hydrolyzed delipidated and reduced protein samples using gas chromatography/mass spectrometry as previously described [30].

Genetic analysis

DNA was extracted from buffy coat cells using a Maxwell RCS blood DNA kit (Promega, USA). Twenty microliters of DNA were used for apolipoprotein E (ApoE) genotyping by a polymerase chain reaction.

Statistical analysis

Descriptive statistics of the mean (standard deviation of the mean [SD]) and median (interquartile range [IQR]) were estimated for normally distributed and nonnormally distributed quantitative data, respectively. The absolute and relative frequencies were used for qualitative variables. The normality of the distribution was analyzed using the Shapiro–Wilk test. Associations between biomarkers and sleep parameters were assessed by Spearman's rank test. Partial correlations controlling for age, sex, and ApoE4 status were calculated. Principal component analysis (PCA) is a technique used to reduce the number of variables without losing information [31]. We performed this technique using the percentage of time on different sleep stages (N1, N2, N3, and REM) to characterize the sleep architecture of our cohort. The results indicated that the variability of our sample was mainly defined by the sleep depth. Accordingly, there were three main profiles of patients in terms of sleep architecture: (1) deep sleepers (individuals with a propensity to deepen their sleep, reaching the later stages of sleep [N3 and REM sleep]); (2) moderate sleepers (individuals who exhibited intermediate sleep); and (3) light sleepers (individuals who spent most of the time in the lighter sleep stage [N1]). The probability of having high values of biomarkers (using the median as the cutoff) was assessed in relation to sleep depth using logistic regression models. R statistical software version 3.3.1 was used for all analyses [32]. All the tests were two-tailed, and p-values < 0.05 were considered statistically significant.

Results

Cohort characteristics

The cohort included 104 participants, most of whom were women (56.7%), with a median [IQR] age of 76 [72.0;80.0] years and a BMI of 27.8 [25.6; 31.2]. The most frequently associated comorbidities were hypertension (63.5%), dyslipidemia (42.3%), diabetes mellitus (19.2%), and heart diseases (19.2%). Fifty percent of the participants were ApoE4-positive. Table 1 shows all of the demographic characteristics, including sample characteristics, cognitive status, and self-reported and objective sleep measurements.

Correlations between sleep parameters and CSF biomarkers

Unadjusted and adjusted correlations between sleep parameters and all of the studied CSF biomarkers are presented in Table 2. The majority of these correlations were related to NF-L and YKL-40. Sleep efficiency and the percentage of time spent in N2 and N3 were negatively correlated with the levels of YKL-40 (rho = –0.287, p = 0.006; rho = –0.240, p = 0.022; rho = –0.254, p = 0.015, respectively). In addition, there was a positive correlation between NF-L and the percentage of time spent in N1 (rho = 0.253, p = 0.016) and a negative correlation between this marker and the percentage of time spent in N3 (rho = –0.268, p = 0.010). Aβ42 was negatively correlated with N1 latency only

(rho = –0.221, p = 0.039) and demonstrated a tendency to be related to REM sleep latency (rho = –0.214, p = 0.056) that was lost after adjusting for age, sex and ApoE4 status. No correlation was observed with T-tau, P-Tau, neurogranin, or sTREM2. Regarding oxidative damage markers, there was a positive correlation between CML and REM sleep latency (rho = 0.242, p = 0.040) and a negative correlation between this marker and the percentage of time spent in REM sleep (rho = –0.240, p = 0.029). In addition, CEL showed a negative correlation with N1 duration (rho = –0.266, p = 0.016).

After adjusting all the parameters for age, sex, and ApoE4 status, there was a similar pattern of correlations in relation to YKL-40, NF-L, and CML. Sleep efficiency (rho = –0.298, p = 0.003), the percentage of time spent in N2 (rho = –0.245, p = 0.018), and the percentage of time spent in N3 (rho = –0.277, p = 0.007) remained negatively correlated with YKL-40. Additionally, NF-L was positively correlated with the percentage of time spent in N1 (rho = 0.240, p = 0.021) and was negatively correlated with the percentage of time spent in N3 (rho = –0.266, p = 0.010), as previously demonstrated. In addition, there was a positive correlation between CML and REM sleep latency (rho = 0.272, p = 0.019) and a negative correlation between this marker and the percentage of time spent in REM sleep (rho = –0.240, p = 0.028). The percentage of time spent in N3 was positively correlated with CEL (rho = 0.226, p = 0.039) and MDAL (rho = 0.243, p = 0.025).

Table 1. Descriptive characteristics of patients with mild-moderate AD

	Global
	n (%), mean (SD), or median [IQR]
Sociodemographic data	
Women	59 (56.7%)
Age, years	76.0 [72.0;80.0]
BMI, kg·m^{-2}	27.8 [25.6;31.2]
Comorbidities	
Hypertension	66 (63.5%)
Diabetes mellitus	20 (19.2%)
Dyslipidemia	44 (42.3%)
Heart diseases	20 (19.2%)
Stroke	4 (3.85%)
AD parameters	
MMSE	23.5 [22.0;25.0]
Aβ42	69 (75.0%)
T-tau	55 (59.8%)
P-tau	62 (67.4%)
ApoE4	52 (50.0%)
PSG parameters	
Epworth sleepiness scale	5.00 [2.00;8.00]
Time in bed, minutes	412 (47.2)
Total sleep time, minutes	266 (81.8)
Sleep efficiency, %	67.3 [53.9;78.2]
N1 stage, %	11.6 [7.14;18.4]
N2 stage, %	23.0 [16.6;31.1]
N3 stage, %	17.5 [9.15;25.2]
REM sleep, %	6.99 [2.98;11.4]
Latency to N1, minutes	32.1 (36.7)
Latency to REM sleep, minutes	171 (84.1)
AHI	30.1 (22.8)
Arousal index	39.8 [26.2;51.3]

Biomarker levels as a function of sleep depth

To evaluate the relationship between sleep structure and CSF biomarkers in more detail, we first selected the biomarkers that correlated with at least one sleep stage (the percentage of time spent in N1, N2, N3, and/or REM sleep) (see Table 2). We performed a PCA, which indicated that N1 and N3 stages were the sleep variables that most captured the total variability of the data (Figure 1). Based on this, we observed that our population was distributed according to the sleep depth, as deep sleepers (Figure 1, right side), moderate sleepers (Figure 1, middle), and light sleepers (Figure 1, left side). The cluster that represented the light sleepers exhibited an increased percentage of time in the N1 stage, whereas the deep sleepers cluster exhibited an increased percentage of time in N3 (p < 0.001 for both) (Supplementary Table S1).

The evaluation of biomarker levels as a function of sleep depth is presented in Table 3 (for the analysis performed exclusively with Aβ42 positive individuals, see Supplementary Table S2). CSF levels of NF-L increased as the depth of sleep decreased (Figure 2). Accordingly, moderate sleep increased the probability

Table 2. Correlations between sleep parameters and CSF biomarkers

	Sleep efficiency		N1 stage		N2 stage		N3 stage	
Biomarkers	Rho	Rho adjusted	Rho	Rho adjusted	Rho	Rho adjusted	Rho	Rho adjusted
Aβ42	0.173	0.194	0.047	–0.033	0.173	0.171	0.097	0.172
T-Tau	–0.124	–0.112	–0.019	–0.056	–0.151	–0.152	–0.109	–0.060
P-Tau	–0.107	–0.079	–0.044	–0.088	–0.111	–0.091	–0.070	0.001
NF-L	–0.182	–0.190	**0.253***	**0.240***	–0.003	–0.022	**–0.268***	**–0.266***
YKL-40	**–0.287****	**–0.298****	0.096	0.123	**–0.240***	**–0.245***	**–0.254***	**–0.277****
Leptin	0.109	0.136	–0.071	**–0.211***	0.045	0.019	0.054	0.193
Orexin	0.100	0.131	0.096	–0.087	–0.009	–0.025	–0.003	0.167
Neurogranin	–0.107	–0.086	0.073	0.003	–0.057	–0.056	–0.122	–0.041
sTREM2	0.001	–0.005	0.056	0.049	–0.014	–0.032	–0.037	–0.045
AASA	–0.045	–0.014	–0.044	–0.144	–0.120	–0.119	0.069	0.179
CEL	0.016	0.027	**–0.266***	**–0.295****	–0.137	–0.141	0.191	**0.226***
CML	0.034	0.040	–0.182	–0.191	–0.035	–0.035	0.120	0.134
GSA	0.036	0.056	–0.174	**–0.243***	0.050	0.040	0.076	0.160
MDAL	0.042	0.063	–0.087	–0.149	–0.083	–0.080	0.179	**0.243***

Spearman correlations between sleep parameters and CSF biomarkers. The represented values are unadjusted (Rho) or adjusted for age, sex, and ApoE4 status (Rho adjusted). The values in bold represent statistically significant correlations: $^{*}p < 0.05$ and $^{"}p < 0.01$.

of higher levels of NF-L with an odds ratio (OR) of 1.694 (95% confidence interval (CI): 0.609 to 4.857), but this relationship did not reach statistical significance (p = 0.316). However, light sleepers presented an OR of 3.273 (95% CI: 1.150 to 9.845; p = 0.029), which was maintained after adjusting for age, sex, and ApoE4 status (OR: 3.125; 95% CI: 0.992 to 10.442; p = 0.056). Considering that the apnea-hypopnea index was different among the groups (Supplementary Table S1), we performed an additional model including OSA as a possible confounding factor (Supplementary Table S3). Similarly, due to the influence of cardiovascular risk factors on the biomarkers herein studied, we included a model considering cardiovascular disease-associated variables (hypertension, heart disease, and stroke). Both models generated similar outcomes compared with the previous ones, with light sleepers presenting an increased risk of higher levels of NF-L (OR: 3.171; 95% CI: 0.986 to 10.847; p = 0.057, with OSA as a confounding factor; and OR: 3.485; 95% CI: 0.991 to 13.262; p = 0.057, with cardiovascular disease-associated variables as a confounding factor).

Regarding YKL-40, there was also a progressive increase in the CSF levels as the depth of sleep decreased (Figure 2). Moderate sleepers presented an OR of 1.343 (95% CI: 0.475 to 3.872), and deep sleepers presented an OR of 1.850 (95% CI: 0.598 to 5.910) after adjustment. However, none of these relationships reached statistical significance (p = 0.579 and p = 0.289, respectively). A similar outcome was observed for the marker GSA. In moderate sleepers (OR: 0.822; 95% CI: 0.260 to 2.578; p = 0.736) and light sleepers (OR: 1.320; 95% CI: 0.381 to 4.784; p = 0.664) the OR increased as GSA levels rose, but this relationship did not reach statistical significance after adjusting for the conditional factors. No significant differences were observed for leptin, CEL, CML, or MDAL.

Discussion

In the present study, we investigated the relationship between sleep structure and several CSF biomarkers that reflect distinct aspects of AD pathophysiology. Our findings suggest significant correlations between sleep and molecules such as NF-L and YKL-40. We observed that this cohort of patients exhibited three different profiles according to the sleep depth, which we classified as light, moderate, and deep sleep. Interestingly, light sleepers demonstrated an increased probability of high levels of NF-L, a marker that predicts cognitive decline and is strongly correlated with T-tau. Despite the reduced statistical power, a similar outcome was observed for YKL-40 levels.

Several CSF and plasma biomarkers have been studied in recent years to achieve early and/or accurate diagnosis of the disease. Among these biomarkers, NF-L, a biomarker of axonal damage and neurodegeneration, plays a prominent role in AD as well as in other neurodegenerative and nondegenerative diseases [33, 34]. In AD, this molecule is also a marker of cognitive decline and predicts clinical progression [35]. In the present study, we observed a positive correlation between CSF NF-L levels and N1 sleep and a negative correlation between this marker and N3 sleep. Furthermore, individuals who spent more time in the lighter phases of sleep (light sleepers) had an increased probability of having high NF-L levels compared with that of individuals who spent more time in N3 sleep (deep sleepers). This is in line with studies reporting the importance of SWS for different biological processes, including Aβ42 clearance [17, 36]. Based on this, it can be speculated that a decrease in the time spent in N3 affects the elimination of NF-L in a similar manner as that demonstrated for Aβ42. In addition, the decreased clearance of toxic metabolites due to poor sleep quality leads to neuronal damage and axonal injury, which in turn can increase NF-L levels [37]. Regardless, our findings suggest a possible role for NF-L as a marker of sleep disruption in AD. Accordingly, Zhang and collaborators [38] reported an important role for NF-L in predicting both self-reported and objective sleep quality in a non-AD population with chronic insomnia disorder.

We demonstrated associations between sleep structure and other biomarkers, such as YKL-40, that were not observed when we stratified our population into three clusters according to sleep profiles. This suggests that the relationship between these markers and sleep may be particular to specific sleep stages. In fact, the YKL-40 level is negatively correlated with the percentage of time spent in N2 and N3. YKL-40 has been reported to be a promising indicator of glial inflammation in AD [39], and

Table 2. Continued

REM sleep		Latency to N1 stage		Latency to REM sleep		Arousal index	
Rho	Rho adjusted	Rho	Rho adjusted	Rho	Rho adjusted	Rho	Rho adjusted
0.051	0.051	**−0.221***	−0.179	−0.214	−0.133	0.177	0.090
0.087	0.086	−0.001	0.018	−0.029	0.005	0.032	−0.003
0.049	0.053	−0.022	−0.001	0.163	0.209	0.033	−0.030
−0.079	−0.083	−0.117	−0.112	−0.205	**−0.223***	0.035	0.057
−0.019	−0.022	0.064	0.048	−0.083	−0.108	−0.013	0.027
0.083	0.069	−0.160	−0.068	0.110	0.200	0.085	−0.049
0.165	0.139	**−0.211***	−0.098	**−0.227***	−0.066	0.074	−0.079
0.043	0.041	−0.031	0.002	0.009	0.055	0.094	0.027
−0.002	−0.006	0.021	0.027	0.023	0.013	−0.031	−0.013
−0.095	−0.089	−0.011	0.065	0.109	0.187	−0.049	−0.140
−0.003	−0.001	0.185	0.213	0.045	0.106	−0.075	−0.113
−0.240*	**−0.240***	0.168	0.179	**0.242***	**0.272***	−0.126	−0.139
−0.140	−0.131	0.144	0.194	0.079	0.137	−0.187	**−0.247***
−0.063	−0.063	0.068	0.106	−0.024	0.046	0.011	−0.056

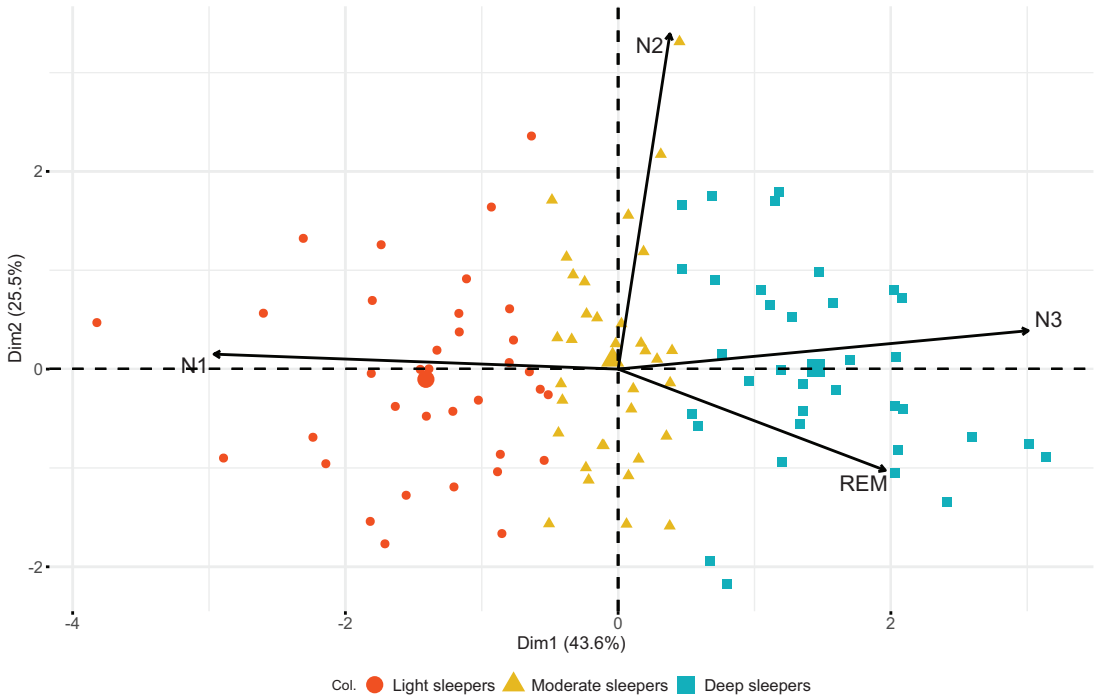

Figure 1. Distribution of patients with mild-moderate AD according to the PCA. The PCA indicated that time in the N1 and N3 stages were the sleep variables that most captured the total variability of the data. Based on this, the participants were distributed in three different populations defined by tertiles: individuals who exhibited lighter sleep (light sleepers), individuals who exhibited intermediate sleep (moderate sleepers), and individuals who exhibited deep sleep (deep sleepers).

Table 3. Biomarker levels according to sleep depth

	Model 1		Model 2		Model 3	
Biomarkers	OR (95% CI)	P	OR (95% CI)	P	OR (95% CI)	P
NF-L						
Moderate sleep	1.694 (0.609 to 4.857)	0.316	1.847 (0.646 to 5.479)	0.257	1.855 (0.646 to 5.533)	0.256
Light sleep	3.273 (1.15 to 9.845)	0.029	3.165 (1.008 to 10.552)	0.053	3.125 (0.992 to 10.442)	0.056
YKL-40						
Moderate sleep	1.255 (0.456 to 3.498)	0.66	1.34 (0.477 to 3.838)	0.58	1.343 (0.475 to 3.872)	0.579
Light sleep	1.846 (0.662 to 5.294)	0.245	1.885 (0.613 to 5.993)	0.272	1.85 (0.598 to 5.91)	0.289
Leptin						
Moderate sleep	0.609 (0.215 to 1.678)	0.341	0.841 (0.273 to 2.594)	0.762	0.843 (0.272 to 2.608)	0.766
Light sleep	0.409 (0.14 to 1.149)	0.094	0.825 (0.244 to 2.864)	0.757	0.839 (0.246 to 2.942)	0.78
CEL						
Moderate sleep	0.643 (0.212 to 1.892)	0.426	0.71 (0.229 to 2.149)	0.546	0.705 (0.227 to 2.138)	0.539
Light sleep	0.454 (0.144 to 1.368)	0.166	0.478 (0.138 to 1.582)	0.231	0.469 (0.135 to 1.561)	0.222
CML						
Moderate sleep	0.872 (0.293 to 2.563)	0.803	0.854 (0.281 to 2.563)	0.779	0.859 (0.282 to 2.579)	0.786
Light sleep	0.543 (0.175 to 1.63)	0.28	0.524 (0.154 to 1.718)	0.29	0.531 (0.155 to 1.749)	0.302
GSA						
Moderate sleep	0.679 (0.227 to 1.987)	0.481	0.807 (0.256 to 2.519)	0.711	0.822 (0.26 to 2.578)	0.736
Light sleep	0.718 (0.235 to 2.152)	0.555	1.25 (0.365 to 4.451)	0.725	1.32 (0.381 to 4.784)	0.664
MDAL						
Moderate sleep	0.989 (0.332 to 2.922)	0.984	1.056 (0.344 to 3.237)	0.923	1.022 (0.324 to 3.205)	0.971
Light sleep	0.47 (0.15 to 1.417)	0.184	0.623 (0.184 to 2.079)	0.44	0.553 (0.157 to 1.897)	0.347

Logistic regression models assessing the probability of having high levels of biomarkers based on sleep depth. Model 1, unadjusted analysis; model 2, adjusted for age and sex; model 3, adjusted for age, sex, and ApoE4 status.

poor-quality sleep is associated with an increase in microglial activation and neuroinflammation [40, 41]. Accordingly, previous studies have reported that CSF YKL-40 levels predict poor sleep in Aβ-positive older adults [42]. Similarly, worse self-reported sleep quality is associated with higher levels of this marker in non-AD participants with and without a family history of AD [43]. This may explain the negative association between the time spent in N3 and YKL-40 levels observed in the current study.

Studies have reported that Aβ levels decrease due to an increased rate of metabolite clearance during sleep and that this event is especially dependent on SWS [17, 36]. Accordingly, sleep deprivation and chronic sleep restriction increase the

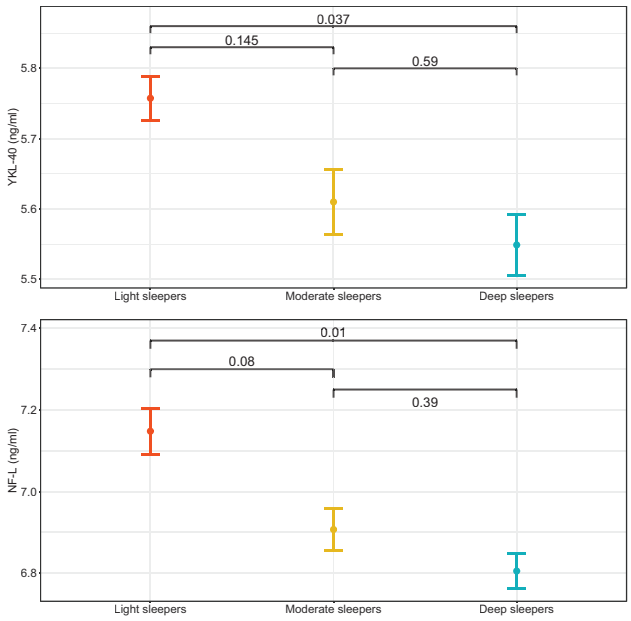

Figure 2. Biomarker levels according to sleep profile. The data are represented as the mean ± standard error of the mean.

levels of this marker [14]. Similarly, specific sleep events, such as sleep spindles, are able to predict T-tau concentrations in healthy individuals [19, 44]. Despite this, we did not observe the expected association between sleep and the classical biomarkers of AD (Aβ, T-tau, and P-Tau). In fact, such association was not observed in a study with patients with AD [45]. Based on this, we hypothesize that the relationship between sleep and AD classical biomarkers is present up to a specific point of the disease's progression. However, as the levels of these markers increase, such correlation is no longer observed. At this stage, other markers, such as NF-L, may better represent sleep quality.

Evidence from both animal and human studies have linked sleep deprivation to increased oxidative stress and reduced antioxidant defenses [46, 47]. In addition, studies have suggested that diverse oxidative pathways contribute to AD pathogenesis [48, 49]. In fact, Pamplona and collaborators [30] reported increased levels of the same oxidative stress markers that we measured in this study in postmortem tissue from patients with AD. However, whether sleep disturbances and poor sleep quality increase oxidative damage in patients with AD is unknown. Here, we observed that all oxidative damage markers, with the exception of AASA and CML, demonstrated an unexpected association with sleep variables. Both CEL and MDAL were positively correlated with the time spent in N3, whereas GSA was negatively correlated with the time spent in N1. Accordingly, we observed correlations with specific sleep stages but failed to observe an association with sleep depth. Further studies using oxidative damage-related approaches will improve our understanding and elucidate the relationship between oxidative stress and sleep structure in patients with AD.

It is important to address some limitations of our study. First, the patients were enrolled from a cognitive unit, not from a population-based community. Second, patients with severe AD were not included. Also, due to the sample size, the data herein presented were not adjusted for multiple comparisons. In addition, although statistically significant, the observed correlations were relatively weak and the sleep–wake schedule was not monitored in the days before the study. Considering this, our findings should be carefully considered. Furthermore, it is not possible to establish whether there was a causal relationship between sleep parameters and biomarker levels due to the cross-sectional design of the study. On the other hand, this study has some strengths. All sleep data were generated by PSG in a population of patients with mild-moderate AD, which has been accomplished in very few studies. To our knowledge, this is the first time that the association between sleep and several AD biomarkers that reflect distinct aspects of the disease has been investigated in individuals with AD.

In conclusion, we demonstrated significant correlations between different sleep parameters and AD biomarkers, such as NF-L and YKL-40. In addition, we observed that our population of patients with mild-moderate AD is divided into three different clusters according to their sleep profiles: light, moderate, and deep sleepers. Furthermore, a lack of sleep depth was associated with higher levels of NF-L, a marker of neurodegeneration that demonstrably predicts cognitive decline. This highlights the potential role of NF-L as a marker of sleep disruption in patients with mild-moderate AD. Further studies using different approaches and performed in distinct cohorts of patients will be necessary to confirm this. In case of a positive outcome, sleep-based interventions could be considered to prevent the axonal damage and possibly the cognitive decline.

Supplementary Material

Supplementary material is available at *SLEEP* online.

Funding

This study was supported by the Generalitat of Catalonia, Department of Health (PERIS 2019 SLT008/18/00050) and "Fundació La Marató TV3" (464/C/2014) to G.P.R.; by the Spanish Ministry of Economy and Competitiveness, Institute of Health Carlos III (grant number P114/00328), the Spanish Ministry of Science, Innovation and University (RTI 2018–099) of Catalonia, and Agency for Management of University and Research grants (2017 SGR696) to R.P. This study has been co-financed by FEDER funds from the European Union ("A way to build Europe"). IRBLleida is a CERCA Programme/Generalitat of Catalonia. F.D. was supported by the Agency for Management of University and Research grants (FI_B100153).

Acknowledgments

We would like to express our sincere gratitude to all the patients and to all the members of the Sleep and Dementia Unit at the Hospital Universitari Santa Maria. We were also supported by the IRBLleida Biobank (B.0000682) and PLATAFORMA BIOBANCOS PT17/0015/0027/. Author's contributions: G.P., F.B., and M.S. designed the study. A.T., F.D., and G.P. searched the literature. R.L., M.P., M.D., A.A., H.Z., K.B., R.P., and F.D. collected the data. I.B. and A.T. analyzed the data. A.T., F.D., I.B., F.B., R.P., M.J., and G.P. interpreted the data. A.T., F.D., and G.P. wrote the manuscript draft. All authors revised the manuscript and approved it for submission.

Conflict of interest statement. All authors declare that they have no conflict of interest.

References

1. Salthouse TA. What and when of cognitive aging. *Curr Dir Psychol Sci*. 2004;**13**(4):140–144.
2. Masters CL, *et al*. Alzheimer's disease. *Nat Rev Dis Primers*. 2015;**1**:15056.
3. Caraci F, *et al*. Depression and Alzheimer's disease: neurobiological links and common pharmacological targets. *Eur J Pharmacol*. 2010;**626**(1):64–71.
4. Ferretti L, *et al*. Anxiety and Alzheimer's disease. *J Geriatr Psychiatry Neurol*. 2001;**14**(1):52–58.
5. Peter-Derex L, *et al*. Sleep and Alzheimer's disease. *Sleep Med Rev*. 2015;**19**:29–38.
6. Zou Y, *et al*. Olfactory dysfunction in Alzheimer's disease. *Neuropsychiatr Dis Treat*. 2016;**12**:869.
7. Clark CM, *et al*.; AV-45-A16 Study Group. Cerebral PET with florbetapir compared with neuropathology at autopsy for detection of neuritic amyloid-β plaques: a prospective cohort study. *Lancet Neurol*. 2012;**11**(8):669–678.
8. Smith PLP, *et al*. Neonatal peripheral immune challenge activates microglia and inhibits neurogenesis in the developing murine hippocampus. *Dev Neurosci*. 2014;**36**(2):119–31. doi:10.1159/000359950.
9. Buerger K, *et al*. CSF phosphorylated tau protein correlates with neocortical neurofibrillary pathology in Alzheimer's disease. *Brain*. 2006;**129**(Pt 11):3035–3041.
10. Albert MS, *et al*. The diagnosis of mild cognitive impairment due to Alzheimer's disease: recommendations from the National Institute on Aging-Alzheimer's Association workgroups on diagnostic guidelines for Alzheimer's disease. *Alzheimers Dement*. 2011;**7**(3):270–279.
11. Jack CR Jr, *et al*.; Contributors. NIA-AA Research Framework: toward a biological definition of Alzheimer's disease. *Alzheimers Dement*. 2018;**14**(4):535–562.
12. Spira AP, *et al*. Self-reported sleep and β-amyloid deposition in community-dwelling older adults. *JAMA Neurol*. 2013;**70**(12):1537–1543.
13. Sprecher KE, *et al*. Amyloid burden is associated with self-reported sleep in nondemented late middle-aged adults. *Neurobiol Aging*. 2015;**36**(9):2568–2576.
14. Kang JE, *et al*. Amyloid-beta dynamics are regulated by orexin and the sleep-wake cycle. *Science*. 2009;**326**(5955):1005–1007.
15. Shokri-Kojori E, *et al*. β-Amyloid accumulation in the human brain after one night of sleep deprivation. *Proc Natl Acad Sci U S A*. 2018;**115**(17):4483–4488.
16. Olsson M, *et al*. Sleep deprivation and cerebrospinal fluid biomarkers for Alzheimer's disease. *Sleep*. 2018;**41**(5). doi:10.1093/sleep/zsy025
17. Ju Y-ES, *et al*. Slow wave sleep disruption increases cerebrospinal fluid amyloid-β levels. *Brain*. 2017;**140**(8):2104–2111. doi:10.1093/brain/awx148
18. Wang C, *et al*. Bidirectional relationship between sleep and Alzheimer's disease: role of amyloid, tau, and other factors. *Neuropsychopharmacology*. 2020;**45**(1):104–120.
19. Winer JR, *et al*. Sleep as a potential biomarker of tau and β-amyloid burden in the human brain. *J Neurosci*. 2019;**39**(32):6315–6324.
20. Janelidze S, *et al*. CSF biomarkers of neuroinflammation and cerebrovascular dysfunction in early Alzheimer disease. *Neurology*. 2018;**91**(9):e867–e877.
21. Lieb W, *et al*. Association of plasma leptin levels with incident Alzheimer disease and MRI measures of brain aging. *JAMA*. 2009;**302**(23):2565–2572.
22. Liguori C. Orexin and Alzheimer's disease. *Curr Top Behav Neurosci*. 2017;**33**:305–322.
23. Mattsson N, *et al*. Association between longitudinal plasma neurofilament light and neurodegeneration in patients with Alzheimer disease. *JAMA Neurol*. 2019;**76**(7):791–799.
24. McKhann GM, *et al*. The diagnosis of dementia due to Alzheimer's disease: recommendations from the National Institute on Aging-Alzheimer's Association workgroups on diagnostic guidelines for Alzheimer's disease. *Alzheimers Dement*. 2011;**7**(3):263–269.
25. Folstein MF, *et al*. "Mini-mental state." A practical method for grading the cognitive state of patients for the clinician. *J Psychiatr Res*. 1975;**12**(3):189–98.
26. Lobo A, *et al*. Revalidación y normalización del mini-examen cognoscitivo (primera version en castellano del mini-mental status examination) en la población general geriátrica. *Med Clin (Barc)*. 1999;**112**(20):767–74.
27. Nazir FH, *et al*. Expression and secretion of synaptic proteins during stem cell differentiation to cortical neurons. *Neurochem Int*. 2018;**121**:38–49.
28. Gisslén M, *et al*. CSF concentrations of soluble TREM2 as a marker of microglial activation in HIV-1 infection. *Neurol Neuroimmunol Neuroinflamm*. 2019;**6**(1):e512.
29. Portelius E, *et al*. Exploring Alzheimer molecular pathology in Down's syndrome cerebrospinal fluid. *Neurodegener Dis*. 2014;**14**(2):98–106.
30. Pamplona R, *et al*. Proteins in human brain cortex are modified by oxidation, glycoxidation, and lipoxidation. Effects of Alzheimer disease and identification of lipoxidation targets. *J Biol Chem*. 2005;**280**(22):21522–21530.
31. Jolliffe IT, *et al*. Principal component analysis: a review and recent developments. *Philos Trans A Math Phys Eng Sci*. 2016;**374**(2065):20150202.
32. R Core Team. R: A language and environment for statistical computing. Vienna, Austria: R Foundation for Statistical Computing; 2013. http://www.R-project.org/.
33. Bridel C, *et al*. Diagnostic value of cerebrospinal fluid neurofilament light protein in neurology: a systematic review and meta-analysis. *JAMA Neurol*. 2019;**76**(9):1035–1048.
34. Alcolea D, *et al*. CSF sAPPβ, YKL-40, and neurofilament light in frontotemporal lobar degeneration. *Neurology*. 2017;**89**(2):178–188.
35. Preische O, *et al*.; Dominantly Inherited Alzheimer Network. Serum neurofilament dynamics predicts neurodegeneration and clinical progression in presymptomatic Alzheimer's disease. *Nat Med*. 2019;**25**(2):277–283.
36. Xie L, *et al*. Sleep drives metabolite clearance from the adult brain. *Science*. (80). 2013;**342**(6156):373–7.
37. Hickman S, *et al*. Microglia in neurodegeneration. *Nat Neurosci*. 2018;**21**(10):1359–1369.
38. Zhang P, *et al*. Patients with chronic insomnia disorder have increased serum levels of neurofilaments, neuron-specific enolase and S100B: does organic brain damage exist? *Sleep Med*. 2018;**48**:163–171.
39. Wang L, *et al*. Cerebrospinal fluid levels of YKL-40 in prodromal Alzheimer's disease. *Neurosci Lett*.. 2020;**715**(2019):134658.
40. Bellesi M, *et al*. Sleep loss promotes astrocytic phagocytosis and microglial activation in mouse cerebral cortex. *J Neurosci*. 2017;**37**(21):5263–5273.

41. Atienza M, *et al*. Low-grade inflammation in the relationship between sleep disruption, dysfunctional adiposity, and cognitive decline in aging. *Sleep Med Rev*. 2018;**42**:171–183.
42. Fjell AM, *et al*. Neuroinflammation and tau interact with amyloid in predicting sleep problems in aging independently of atrophy. *Cereb Cortex*. 2018;**28**(8):2775–2785.
43. Sprecher KE, *et al*. Poor sleep is associated with CSF biomarkers of amyloid pathology in cognitively normal adults. *Neurology*. 2017;**89**(5):445–453.
44. Kam K, *et al*. Sleep oscillation-specific associations with Alzheimer's disease CSF biomarkers: novel roles for sleep spindles and tau. *Mol Neurodegener*. 2019;**14**(1):10.
45. Bubu OM, *et al*. Obstructive sleep apnea and longitudinal Alzheimer's disease biomarker changes. *Sleep*. 2019;**42**(6). doi:10.1093/sleep/zsz048
46. Kumar A, *et al*. Possible nitric oxide modulation in protective effect of (*Curcuma longa*, Zingiberaceae) against sleep deprivation-induced behavioral alterations and oxidative damage in mice. *Phytomedicine*. 2008;**15**(8):577–86.
47. Teixeira KRC, *et al*. Night workers have lower levels of antioxidant defenses and higher levels of oxidative stress damage when compared to day workers. *Sci Rep*. 2019;**9**(1):4455.
48. Butterfield DA, *et al*. Oxidative stress, dysfunctional glucose metabolism and Alzheimer disease. *Nat Rev Neurosci*. 2019;**20**(3):148–160.
49. Tönnies E, *et al*. Oxidative stress, synaptic dysfunction, and Alzheimer's disease. *J Alzheimer's Dis*. 2017. doi:10.3233/JAD-161088

CERTIFICATE OF ETHICAL APPROVAL

Institut Català de la Salut
Hospital Universitari
Arnau de Vilanova

El Comité Ético de Investigación Clínica en la reunión de 28 de abril de 2016, acta 5/2016, informó favorablemente la solicitud de enmienda **"Biomarkers of Alzheimer disease progression in patients with mild cognitive impairment: a lipidomic approach"** al proyecto de investigación titulado: **"Identificación de biomarcadores en plasma y líquido cefalorraquídeo como predictores del desarrollo de la enfermedad de Alzheimer en pacientes con deterioro cognitivo leve utilizando técnicas metabolómicas"** propuesto por la Dra. Alba Naudí como investigadora principal en el IRBLleida, esta enmienda y consideró que:

- Se cumplen los requisitos necesarios de idoneidad del protocolo en relación a los objetivos del estudio y que están justificados los riesgos y molestias previsibles para los sujetos participantes.
- La capacitad del investigador y los medios de que dispone son apropiados para llevar a cabo el estudio.
- Las muestras biológicas solicitadas y los datos asociados a las mismas son adecuadas para el cumplimiento de los objetivos de dicho proyecto.
- Es adecuado el procedimiento para obtener el consentimiento informado de los sujetos que participan en el estudio.

Lleida, 23 de mayo de 2016

Joan Antoni Schoenenberger
Presidente

Informe del Comité de Ética de Investigación con Medicamentos

Don **Eduard Solé Mir**, presidente del Comité de Ética de Investigación con Medicamentos del Hospital Universitari Arnau de Vilanova de la Gerència Territorial de Lleida – GSS,

CERTIFICA

Que este Comité ha evaluado la enmienda por cambio de investigador principal del estudio titulado "**Biomarcadores lipídicos y de daño oxidativo como indicadores de la progresión de la Enfermedad de Alzheimer en pacientes con deterioro cognitivo"**.

Tal y como figura en el acta 6/2020, de 25 de marzo de 2021, este Comité considera que:

La capacidad del equipo investigador y los medios disponibles son apropiados para llevar a cabo el estudio, siempre que el procedimiento se adapte a los protocolos asistenciales del centro.

El alcance de las compensaciones económicas previstas no interfiere con el respeto a los postulados éticos.

Que este Comité acepta los aspectos locales de este estudio CEIC-1374, con el Dr. Gerard Piñol Ripoll como investigador principal en el Institut de Recerca Biomèdica de Lleida (IRBLleida).

Que el CEIm del Hospital Universitari Arnau de Vilanova de la Gerència Territorial de Lleida – GSS, tanto en su composición como en sus procedimientos, cumple con las normas de BPC (CPMP/ICH/135/95) y con la legislación vigente que regula su funcionamiento, y que la composición del CEIm del Hospital Universitari Arnau de Vilanova de la Gerència Territorial de Lleida – GSS citada a continuación, teniendo en cuenta que en el caso de que algún miembro participe en el ensayo o declare algún conflicto de interés, se ausentará durante la evaluación.

Que la composición actual del CEIm es la siguiente:

Dr. Eduard Solé Mir, presidente, médico asistencial
Dr. Xavier Gómez Arbonés, vicepresidente, médico.
Sra. Núria Badia Sanmartín, secretaria técnica, no sanitario
Dr. Joan Antoni Schoenenberger Arnaiz, farmacéutico hospital
Dr. Juan Costa Pagès, médico farmacólogo
Sra. Montse Solanilla Puértolas, no sanitario
Dr. Xavier Galindo Ortego, médico asistencial
Dra. Marta Ortega Bravo, médico asistencial
Dr. Eugeni Joan Paredes Costa, médico asistencial
Dr. Manel Portero Otín, médico
Dr. Francesc Purroy García, médico asistencial
Dr. Oriol Yuguero Torres, médico asistencial
Sr. Raül Llevot Pérez, jurista y experto con conocimientos suficientes en protección de datos
Sra. Cristina Casas Pi, no sanitario
Dra. Juana Inés García Soler, farmacéutica atención primaria
Dr. Robert Montal Roure, médico asistencial
Sra. Maria Teresa Grau Armengol, unidad atención al usuario
Sr. Josep Maria Gutiérrez Vilaplana, enfermero
Sra. Efthymia Ktistaki, representante de pacientes

EDUARDO SOLE MIR / num:2502376

Firmado digitalmente por EDUARDO SOLE MIR / num:2502376
Fecha: 2021.03.29 11:56:46 +02'00'

Fdo. Dr. Eduard Solé Mir
Presidente del CEIm.